91600
new 82-10

COMPLIMENTARY COPY
Please Credit Ontario Hydro Research if
Reproduced in Whole or in Part.

ontario hydro
research division

MIRAMICHI EPICENTRAL AREA - IN SITU STRESS PILOT PROJECT

Report No: 85-185-K

D.A. McKay & J.B. Williams
Civil Research Department
J.R. Bowlby & J.D. Grass
Design and Development Division

ABSTRACT

In situ stress measurements were performed in six separate boreholes in the epicentral area of the 1982 Miramichi, N.B. earthquakes to confirm a thrust fault mechanism as the source of this seismic activity. The test results indicate that a complex series of inter-related factors caused this series of earthquakes.

job	file	date	report no.
740644-709-400	844.33	July 26, 1985	85-185-K

TABLE OF CONTENTS

Page No

1. INTRODUCTION 1

2. PURPOSE 2

3. GEOLOGY 3

   3.1 Faults 3
   3.2 Joint Patterns 3

4. FIELD TESTING 5

   4.1 Test Method 6
   4.3 Temperature 8

5. FIELD TEST RESULTS 9

   5.1 Summary of Test Results 9

6. TREMORS, ROCKBURSTS AND POP-UPS 11

7. STRESS DROP 13

8. INCLINED HOLES 14

9. RELATIONSHIP OF STRESSES TO EARTHQUAKES 14

10. CONCLUSIONS 18

REFERENCES 20

TABLES 2-10 23-31

DISTRIBUTION - last page -

LIST OF APPENDICES

		Page No
APPENDIX 1	UNITED STATES BUREAU OF MINES BOREHOLE DEFORMATION GAUGE TEST METHOD	61
APPENDIX 2	DETAILED TEST RESULTS	79
APPENDIX 3	GEOLOGIC BOREHOLE LOGS	85
APPENDIX 4	ENGINEERING BOREHOLE LOGS	88
APPENDIX 5	PHOTOGRAPHIC RECORD OF CORE FROM TEST HOLES	96
APPENDIX 6	FIELD TEST CURVES	103
APPENDIX 7	BIAXIAL TEST CURVES	164
APPENDIX 8	ROCKBURST PHOTOGRAPHIC RECORD	216
APPENDIX 9	PHOTOGRAPHIC RECORD OF CORE FROM INCLINED HOLES	228
APPENDIX 10	BRUNSWICK MINING AND SMELTING, BATHRUST MINE STRESS DATA	233
APPENDIX 11	GENERATION OF FIGURE 20a	236

LIST OF FIGURES

Page No

FIGURE 1 LOCATION OF STUDY AREA 32

FIGURE 2 LOCATION MAP OF STUDY AREA 33

FIGURE 3 LOCATION OF OBSERVED GROUND BREAK AND SURFACE PROJECTIONS OF RUPTURE PLANES OF PRINCIPAL JANUARY AND MARCH EARTHQUAKES 34

FIGURE 4 THEORETICAL FAULT PLANE STRUCTURE BASED ON ANALYSIS OF SEISMIC RECORDS 35

FIGURE 5 SURFACE DISPLACEMENT ALONG PRE-EXISTING JOINT ON MAIN OUTCROP LOOKING SOUTH 36

FIGURE 6 GEOLOGY OF THE MIRAMICHI EPICENTRAL REGION 37

FIGURE 7 FRACTURE ORIENTATIONS ON THE MAIN OUTCROP AS MAPPED BY FYFFE, 1983 38

FIGURE 8 CROSS SECTIONAL VIEW OF U.S. BUREAU OF MINES OVERCORING TECHNIQUE BEFORE AND AFTER OVER-CORING 39

FIGURE 9 ORIENTATIONS OF P, BOREHOLE 1 40

FIGURE 10 ORIENTATIONS OF P, BOREHOLE 2 41

FIGURE 11 ORIENTATIONS OF P, BOREHOLE 3 42

FIGURE 12 ORIENTATIONS OF P, BOREHOLE 4 43

FIGURE 13 ORIENTATIONS OF P, BOREHOLE 5 44

FIGURE 14 ORIENTATIONS OF P, BOREHOLE 6 45

FIGURE 15 AVERAGE ORIENTATIONS OF P FOR ALL BOREHOLES 46

FIGURE 16 SECONDARY PRINCIPAL STRESS ORIENTATIONS EPICENTRAL AREA, MIRAMICHI EARTHQUAKE SEQUENCE 47

FIGURE 17a MIRAMICHI P STRESS ORIENTATIONS ROLLING MEAN AVERAGES 48

FIGURE 17b MIRAMICHI P STRESS ORIENTATIONS HISTOGRAM OF TEST RESULTS 48

LIST OF FIGURES (continued)

		Page No
FIGURE 18	NEW ENGLAND - NEAR SURFACE STRESS ORIENTATIONS, From Plumb et al, 1984	49
FIGURE 19	SAN ANGREAS FAULT - NEAR SURFACE STRESS ORIENTATIONS From Tullis, 1981	50
FIGURE 20	STRUCTURAL FEATURES ON MAIN OUTCROP	51
FIGURE 20a	ELEVATION CHANGES ON MAIN OUTCROP	52
FIGURE 21	STRESS TRAJECTORIES IN A HILL DUE TO GRAVITY (From Jaeger and Cook, 1979)	53
FIGURE 22	COMPARISON OF MEASURED STRESS AND INFERRED STRESS FROM FAULT PLANE SOLUTIONS, From Plumb et al, 1984a	54
FIGURE 23	DIRECTION OF MAJOR PRINCIPAL STRESS PRIOR TO THE MAGNITUDE 7.8 TANGSHAN EARTHQUAKE From Wang and Wei, 1984	55
FIGURE 24	MAJOR PRINCIPAL STRESS ORIENTATIONS AFTER THE MAGNITUDE 7.8 TANGSHAN EARTHQUAKE, From Wang and Wei, 1984	56
FIGURE 25	MEASURED ORIENTATIONS OF MAJOR PRINCIPAL IN-SITU STRESSES PRIOR TO THE TANGSHAN EARTHQUAKE, From Wang and Wei, 1984	57
FIGURE 26	MEASURED ORIENTATIONS OF MAJOR PRINCIPAL IN-SITU STRESS AFTER THE TANGSHAN EARTHQUAKE, From Wang and Wei, 1984	57
FIGURE 27	PATTERN OF FAULT MOTIONS IN PROVINCES OF KANSU, TSINGHAI, SZECHWAN AND YUNNAN, From Zhin, 1984	58
FIGURE 28	STRESS CHANGES AT SOME STATIONS IN NORTH CHINA REGION, From Yi and Ge 1984	59
FIGURE 29	STRESS CHANGES AT SOME STATIONS IN THE SOUTH-WESTERN REGION, From Yi and Ge, 1984	59
FIGURE 30	SCHEMATIC DIAGRAM SHOWING THE UNUSUAL CHANGES IN STRESS (Jinshu Station), From Yi and Ge, 1984	60
FIGURE 31	RELATIONSHIP BETWEEN EPICENTRAL DISTANCE AND RATE OF STRESS CHANGE, From Yi and Ge, 1984	60

LIST OF TABLES

		Page No
TABLE 1	MAIN OUTCROP JOINT SETS	4
TABLE 2	SUMMARY OF TEST RESULTS - BOREHOLE 1	23
TABLE 3	SUMMARY OF TEST RESULTS - BOREHOLE 2	24
TABLE 4	SUMMARY OF TEST RESULTS - BOREHOLE 3	25
TABLE 5	SUMMARY OF TEST RESULTS - BOREHOLE 4	26
TABLE 6	SUMMARY OF TEST RESULTS - BOREHOLE 5	27
TABLE 7	SUMMARY OF TEST RESULTS - BOREHOLE 6	28
TABLE 8	SUMMARY OF TEST RESULTS - BOREHOLES 1 TO 6	29
TABLE 9	AVERAGE P STRESS ORIENTATIONS	30
TABLE 10	SUMMARY OF ROCKBURST OCCURRENCES	31

91601
new 82-10

ontario hydro
research division

To Mr. Ivan C. MacFarlane
National Research Council
Division of Building Research
Bldg M-20, Room 205
Ottawa, Ontario
K1A OR6

Attn: Dr. H. Wallace

MIRAMICHI EPICENTRAL AREA - IN SITU STRESS PILOT PROJECT

1. INTRODUCTION

On January 9, 1982 at 12:53 U.T., an earthquake of magnitude 5.7 occurred in the Miramichi Region of New Brunswick as shown in Figure 1. This event was followed by a complex series of aftershocks (Wetmiller et al 1984) with the principal aftershocks occurring on:

January 9 at 16:36 U.T. Mb 5.1
January 11 at 21:41 U.T. Mb 5.4
March 31 at 21:02 U.T. Mb 5.0
June 16 at 11:43 U.T. Mb 4.7

The June 1982 event occurred in a different area than the earlier activity and may have occurred independently (Wetmiller et al, 1984).

Analysis of the seismicity records (Choy et al, 1983; Wetmiller et al, 1984) determined that the activity was centered in the Indian Lake area (Figure 2) of the Miramichi Region. The results of the seismic analysis were used as a guide for the location of the boreholes used for the stress measurements in this study.

The Miramichi earthquakes are of great scientific interest for several reasons.

1) They included the largest earthquakes in eastern North America since the Cornwall-Massena earthquake of 1944,

2) The main shock was the first earthquake in eastern North America that was large enough to be recorded on modern worldwide seismograph networks (Choy et al, 1983) and so the source parameters can be determined by many techniques,

3) The aftershock sequence has been unusually long (continuing to the present) and complex and has allowed the compilation of

the most complete seismicity record for an event in eastern North America.

This stress measurement project has been a co-operative venture involving the following agencies: the United States Nuclear Regulatory Commission (USNRC) the Atomic Energy Control Board (AECB), the National Research Council of Canada (NRCC), the Earth Physics Branch of the federal Department of Energy Mines and Resources (EMR), the New Brunswick Department of Natural Resources (NBDNR) and Ontario Hydro (OH).

2. PURPOSE

The purpose of this was to measure the near (within 30m) surface stresses using the USBM technique. These results would determine whether or not the measured stresses agreed with the depth stresses inferred from the seismic data and from the surface pop-up and reverse fault type structure on the outcrop that had been cleared the previous year.

Analysis of the seismicity records has led to the construction of Figure 3 (Wetmiller et al, 1984) and has given rise to the theory that the seismic events occurred on two parallel thrust faults such as those shown in Figure 4 (Wetmiller et al, 1984). A "thrust joint" (Wetmiller et al, 1984) was found on an outcrop in the epicentral area as shown in Figure 5. This outcrop was later cleared and became the main outcrop where boreholes 1 and 2 were located. This surface feature would have gone unnoticed in the rough terrain of the Miramichi except that the rupture traversed an outcrop on a logging road and, as such, the rupture was visible. From the results of the analysis of the earthquake records, it is believed that there are two rupture planes that strike 005°, along which, thrusting has occurred (Wetmiller et al, 1984). This would result from an essentially east-west trending principal stress. To this end then, this study was undertaken in order to make sufficient in situ stress measurements in the rock mass in order to outline the general horizontal stress field and to relate these findings to the thrust fault theory. This project was used as a guide for more detailed stress studies that will be carried out in the future.

3. GEOLOGY

The epicentral area is located in the northern part of the Appalachian Mountains and lies along the axis of a structure known as the Miramichi Geanticline or Massif. A detailed description of the geology of the area is contained in Fyffe (1983, 1982) and Rogers (1970) and only a brief description is given here. The oldest rocks in the area are Cambro-Ordovician quartz wackes, quartzites and slates which are overlain by predominantly felsic volcanic rocks followed by a sequence of mafic volcanic rocks and greywackes. This structure is locally intruded by granitoids of Ordovician age. This complex was deformed and metamorphosed during the Taconic Orogeny. In Devonian times, during the Acadian Orogeny, the Massif was intruded by large volumes of mainly granitic magma producing the plutons in which the earthquakes occurred and the stress measurements were made (Lyons and Faul, 1968).

Post-Acadian faulting oriented east to north-east and exhibiting dextral strike slip offsets has occurred in the area (Burke and Chandra, 1983). Subsequent differential uplift and erosion have led to the present pluton exposure. The region has been glaciated in the recent past and it is believed that the area may be experiencing post-glacial rebound of a few tens of millimeters per year (Vanicek 1976). A prominent fault in the area is the Catamaran fault which offsets, by several kilometers, the granite pluton to the south of the epicentral area. No evidence has been found to indicate recent movement on the Catamaran fault or similar faults (Fyffe, 1982). The Catamaran fault was not involved in the 1982 earthquake activity (Wetmiller et al, 1984) and detailed geological and geophysical surveys of the main shock epicentral area have to this point failed to associate the earthquake activity with any known pre-existing faults.

Detailed information on the fault and jointing patterns in the epicentral area are contained in Fyffe (1983, 1982). A summary of these patterns is given below.

3.1 Faults

There are two zones of intense shearing as shown in the area geology map (Figure 6). These zones strike between 95° and 115°. In one outcrop, a red microgranite dyke is sheared and contains a mylonitic structure which is linked by small folds trending 150°. Along strike to the south-east, there is a local occurrence of tectonic breccia (Fyffe, 1982).

3.2 Joint Patterns

Fyffe (1983) mapped the joint orientations on the main outcrop where boreholes 1 and 2 are located and defined the 6 distinct joint sets which are described in Table 1. The joint set strikes are shown in Figure 7.

TABLE 1

MAIN OUTCROP JOINT SETS

Set	Strike	Dip/Dip Direction	Spacing	Description
1	350°-10°	30°-70°/W mostly 40°-50°W	Rare	Surfaces epidote covered, slickensides rake 75°S
2	120°	vertical	2-3m	filled with quartz stringer and aplite dykes, space between quartz veins and hanging wall
3	20°-50°	vertical	1-4m	Some open 1-2mm
4	345°-0°	50°-80°/E mostly 60°-70°/E	2-6m	Epidote and chlorite filled slickensides rake 25°S
5	60°-70°	55°-65°/NW	Rare	
6	E-W	5°-18°/N	10cm	Subhorizontal, approximately parallel to slope surface

In sequence of joint formation as postulated by Fyffe (1983) the oldest joint set is Set 1 and Set 6 is the youngest. The thrust joint on the main outcrop is a member of set 1. This offset could be attributed to glacial unloading, frost heave or post-glacial tectonic stress (Fyffe, 1983, p4). Set 2 offsets Set 1 by 1cm of left lateral movement but only one example of this was observed. Set 2 is displaced by Set 3 in a right lateral sense by 1cm. Set 4 consistently offsets Set 2 and 3 in a right lateral sense. Displacements of Set 2 range from 35cm at the north end of the outcrop to 6cm at the joint terminus at the south end of the outcrop. This change in displacement occurs over a distance of 55m and is attributed to bifurcation of the fracture (Fyffe, 1983). About 4cm of post glacial upthrusting occurs on a 3m section of the northern part of this fracture. Tension gashes consistent with right lateral movement along this fracture were also observed. Set 5 offsets a Set 2 joint 1cm left laterally but does not affect Set 4 joints. For this reason, it is believed that Sets 4 and 5 formed at the same time. Set 6 joints are subhorizontal sheeting joints which form approximately parallel to the outcrop surface and are thought to result from erosional unloading. Fyffe (1983) further postulates that Sets 1,2 and 3 were formed under the stress regime with the maximum compression parallel to Set 2. Sets 4 and 5 are believed to have formed as the result of a major compressive force which was aligned slightly east of north.

4. FIELD TESTING

In order to investigate the principal stress orientation that had been deduced from analysis of the seismicity records, it was decided by the joint committee of agencies interested in this earthquake sequence (USNRC, AECB, NRCC, EMR, NBDNR, and OH) to determine the rock stress in the epicentral area. It was decided to use the U.S. Bureau of Mines borehole deformation gauge to determine the in situ rock stress. The field testing was to be carried out by the Civil Research Department of Ontario Hydro with support for the drilling being provided by NRCC and the AECB. The New Brunswick Department of Natural Resources was to log the drill core and provide logistical assistance in the field.

The locations of the test sites (Figure 6) were selected from the available (December, 1983) geologic data. In order to minimize the physical dissimilarities between rocks at the widely separated sites, it was decided to place as many boreholes as possible in the diorite and yet not compromise the borehole pattern which was laid out to cover directions parallel and perpendicular to the trend of the postulated structure. Boreholes 1,2,3 and 4 were located in the diorite while boreholes 5 and 6 were located in granite. The reasoning behind the locations of these boreholes is as follows: boreholes 1 and 2 were placed on either side of the surface thrust feature on the outcrop to determine the rock stresses in the hanging wall and footwall blocks of the thrust type structure located on the main outcrop; borehole 3 was located in the center of the epicentral area in order to assess the conditions at the center of the seismic activity; borehole 4 was located outside the epicentral block to determine if there was an observable change in stress levels outside of the epicentral area; borehole 5 was chosen in an area away from the epicentral area in order to measure the background stress field. Borehole 6 was added to the program in the field when there was sufficient time available to drill this hole which, in conjunction with boreholes 4 and 5, would complete a line of holes perpendicular to the line formed by boreholes 1,2,3 and 4 and parallel to the postulated fault structure.

The test depths that were originally selected were at 3.0m, 6.1m, 10.7m, and 15.2m, with additional tests at 22.9m and 30.5m to be carried out in borehole 1. These depths were chosen for convenience of drilling and not because of geological constraints. Additional funding made available by AECB enabled the program to be expanded from 5 to 6 boreholes and for all six boreholes to be extended to a depth of 30.5m. Boreholes 3 and 6 have tests only at depths of 7.6m, 15.2m, 22.9m and 30.5m due to time constraints. These two holes were the last drilled and it was apparent from the earlier holes that the shallower test depths of 3.0m and 6.1m could be dispensed with because of the high probability of encountering unsuitable rock for testing. At each test depth in all holes, a second overcoring test was performed approximately 40cm below the first test to confirm the results of the first test. If the two tests disagreed, a third was performed to determine which test was in error. This situation occurred only once in the case of tests 39,40 and 41.

4.1 Test Method

The United States Bureau of Mines Borehole Deformation measures the deformation of a 3.81cm diameter borehole while it is overcored by a 9.75cm diameter thinwall bit. This is shown in Figure 8. Strain relief measurements are made along three axes which form a 60° strain rosette in a plane perpendicular to the borehole axis. After the downhole testing is completed, the overcore is recovered and subjected to testing in a biaxial chamber to determine the Young's modulus of the material. This result is combined with the downhole strain relief measurements to calculate the secondary principal stresses existing in the plane perpendicular to the borehole axis. The maximum secondary principal stress (P) and the minimum secondary principal stress (Q) are termed secondary because they represent the maximum and minimum stress in one plane within the three-dimensional stress tensor. Three non-parallel boreholes would be required to completely define the three dimensional primary stress field using this test method. A detailed description of the testing procedure is presented in Appendix 1.

The analytical method used to calculate the stresses is based on elastic thick wall cylinder theory using a 60° strain rosette solution. The equations used are:

$$P = \frac{E}{(1-\nu^2)d} \left[U_1+U_2+U_3+\frac{1}{\sqrt{2}} \left[(U_1-U_2)^2 + (U_2-U_3)^2 + (U_3-U_1)^2\right]^{1/2}\right]$$

$$Q = \frac{E}{(1-\nu^2)d} \left[U_1+U_2+U_3-\frac{1}{\sqrt{2}} \left[(U_1-U_2)^2 + (U_2-U_3)^2 + (U_3-U_1)^2\right]^{1/2}\right]$$

$$\theta = 1/2 \tan^{-1} \frac{\sqrt{3}\,(U_2-U_3)}{2U_1-U_2-U_3}$$

where P is the major secondary principal stress

Q is the minor secondary principal stress

θ is the angle measured from gauge axis U_1 to P in a counter-clockwise direction

E is the Young's Modulus of elasticity of the rock in which the measurement was made

ν is the Poisson's ratio of the rock

d is the diameter of the borehole in which the gauge was placed

U_1, U_2, U_3 - are the strains measured along the three gauge axes and are positive for an increasing diameter

The value of Young's Modulus of Elasticity (E) is calculated using the formula:

$$E = \frac{4ab^2Po}{(b^2-a^2)U}$$

where a = inner radius of overcore

b = outer radius of overcore

P_0 = applied hydraulic pressure

U = diametral borehole deformation

When the overcore is tested, the E value is determined along each of the three axes and if it is found that the three values E_1, E_2 or E_3 vary by more than 25% from the average value of the three E values, then it is necessary to apply an anisotropic solution to the field test data.

Only two anisotropic elastic constants of the material are necessary for the plane strain evaluation of secondary stresses (Hooker & Johnson, 1969). These parameters are:

$$\alpha_{11} = \frac{1 - \gamma_{13}\gamma_{31}}{E_1}$$

$$\alpha_{22} = \frac{1 - \gamma_{23}\gamma_{32}}{E_2}$$

where E_i = Young's modulus in the i direction

γ_{ij} = Poisson's ratio in the ij plane

The above subscripts refer to the orthogonal coordinate system defined by the axis of the core and the directions of maximum and minimum Young's modulus in the plane perpendicular to the axis of the core. This procedure avoids errors in the field data that are due to elastic non-linearity in the rock. This method involves many calculations and subsequent laboratory tests. Tullis (1981) found that, by using what he termed an "approximate" anisotropic solution, it was possible to obtain results that varied little from the Hooker and Johnson (1969) solution and yet avoided the cumbersome analysis and testing. This method was applied to all of the test results to correct for the effect of rock anisotropy. The equation is:

$$U_i^m = U_i(E_i/E) \quad i = 1,2,3$$

where E_i = Young's modulus for axis i

E = is the average Young's modulus for the three axes

U_i = is the deformation measured on axis i

U_i^m = is the modified deformation on axis i

The modified deformations are then substituted into the original equations, (1), (2) and (3), for P,Q and θ. At the conclusion of the re-calculation, it was determined that the stress magnitudes and directions were not greatly affected by rock anisotropy in this case.

4.2 Temperature

The USBM gauge is relatively insensitive to thermal changes. However, as part of the standard test procedure, the gauge is allowed to stabilize downhole for approximately 15 minutes prior to testing to remove this thermal effect from the test results. The thermal difference between the rock and the drill water is not of concern as long as the temperature difference between the two is within 3°C (Hooker and Duval, 1971). During early testing at Miramichi, the drill water met this criteria. As the project progressed and the weather became warmer, it became a concern. There were no facilities available to cool the drill water. Thermal tests were undertaken to correct for this imbalance.

5. FIELD TEST RESULTS

The results of the field tests are presented in Tables 2-7 and Figures 9-14. A detailed discussion of the test results from each borehole are contained in Appendix 2. The geologic logs of the boreholes were provided by Mr. L. Fyffe of NBDNR and are contained in Appendix 3. The engineering logs were prepared by Mr. D.A. McKay of OH and are contained in Appendix 4. The photographic record of the core from each hole is in Appendix 5. The field test curves are in Appendix 6 and the biaxial test curves are in Appendix 7. A record of observed rock bursts is contained in Appendix 8 while a record of the core recovered from three short inclined holes on the main outcrop is given in Appendix 9. A brief summary of the test results is given below.

5.1 Summary Of Test Results

In situ rock stress measurements were made in six separate boreholes at the Miramichi site with 57 tests out of 64 attempts being successful. A summary of the test results is given in Table 8. The average maximum secondary principal stress orientations for each hole are given in Table 9 and Figures 15 and 16. The average azimuths, calculated as arithmetic means, given in Table 9 have been rounded off to the nearest degree.

For holes 2,3 and 6 the tests were broken into subsets so as not to obscure stress trends in a particular section of the hole. In borehole 2, tests 35a, 35b, and 36, are grouped together as the average P orientation is nearly perpendicular to the average P direction for the rest of the borehole. Borehole 3 has only 4 successful tests, the results of which fall into two groups. The effect of the very competent zone of rock between the two upper test zones and the lower test zone in an area of otherwise well jointed rock cannot at present be properly accounted for. Borehole 6 was divided into two groups because test 63 was below a second fault and seemed to be separate from the other tests because of its P orientation as well as its P/Q ratio. It should be noted that the P stress from test 63 is of the same magnitude as tests 51 and 52 while tests 54,55,58 and 59 all measured tension and may all be influenced by the large fault. The average P orientations for each borehole are shown in Figure 16 along with the known faults and the projected thrust structures in the epicentral area.

The results from all tests were subjected to a rolling mean average analysis, the results are shown in Figure 17a. The rolling mean average was applied to all test results in two ways. The first result used a 20° window ±10° plotted on 5° centers while the second used a 10° window ±5° plotted on 5° centers. The resulting plots, given in Figure 17a, indicate that the 20° window shows broad trends with a peak at 055° and the 10° window similarly shows a peak at 055°. A histogram of P orientations for all tests is shown in Figure 17b. The results collected by Plumb et al (1984b) from several studies in the New England area are shown in Figure 18. The similarity between these results and the results of this study are readily apparent. This seems to indicate that for the near-surface region in the New England/Maritime Canada area, the principal secondary stress, P, has an azimuth of approximately 055°. This does not agree with data from the Bathurst Mine (Appendix 10) but this data comes from deeper depths (475-1000m) than this study and may be controlled by other local structures. These studies are only two cases and as more stress measurements are made in the New England/Maritime Canada area, it will become apparent as to how representative of the area are these studies. The consistent northeast trend of the stress measurements is not what would be expected of an area with thrust faults that are supposed to strike 005°. Only the results from borehole 4 which have an average orientation of 274° seem to agree with the postulated thrust faults. The fact that the borehole 4 results are different from the other boreholes suggests that a subsurface structure of greater complexity may exist in this area than is presently postulated.

The magnitudes of the stresses measured in this study are the same as those reported by Plumb (1984a) which seems to indicate that these stress magnitudes and orientations may be common near faults oriented NNE in the New England/Maritime Canada area although local conditions such as topography and weathering will influence the stress levels measured. The amount of crustal decoupling and fault plane characteristics will also influence the stress test results. Tullis (1981) and Raleigh et al (1972) report in situ stress results made near strike slip faults in California and Colorado which, although consistent with stress orientations derived from fault plane solutions as shown in Figure 19, are quite small being on the order of 1 to 4 MPa in compression. Tullis (1981) reported measuring tension at one site in his study, as was the case with several tests in the Miramichi study, but the results were anomalous with the P stresses being oriented at nearly 90° to each other and were attributed to several possible causes: 1) residual stress and not regional stresses, 2) gauge movement, 3) strain relief on macrofractures or 4) thermal effects. Causes 1 and 4 would be very near surface affect which is not expected at the depths of some of the tensile stress measured at Miramichi. No gauge slippage occurred during any test. The two tests in Tullis' study were separated by 0.31m but were carried out at very shallow depths of 0.25m and 0.56m while deepest depth at which tension was measured in the Miramichi study was 29.86m (test 49, BH2 Figure 20) and only strain relief on macrofractures may be a possible cause. The possibility that the tensile stresses are in response to uplift must also be considered as a possible explanation in this case. Uplift is known to have occurred on the main outcrop because of levelling data gathered by Mr. J. Chandra of NBDNR has shown (Figure 20a) upward movement of some survey points on the outcrop. An explanation of how Figure 20a was generated ~~and~~ is contained in Appendix 11. This data is discussed more fully in the following section on tremors, rockbursts and popups. The possibility of uplift occurring elsewhere in the epientral block is quite high. Raleigh et al (1972) stated that the assumed stress orientation of 45° to the fault plane as determined by the fault plane solution for the major principal stress could be in error by as much as 40° if sliding has occurred along an existing fault in an otherwise intact rock and caused the earthquake. However, an error of only 20° could be achieved if the nodal plane corresponding to the fault is known. At present it is not certain whether sliding has occurred along the structures at the Miramichi site.

6. TREMORS, ROCKBURSTS AND POP-UPS

A series of rockbursts occurred and two tremors were felt during the drilling of boreholes 1 and 2 on the main outcrop. Photographs of afterburst fragments are in Appendix 8. An account of the rockbursts was kept although accurate crack measurements were not made due to the fact that these occurrences were totally unexpected and no provision for suitable measuring had been made.

The first series of rockbursts that were personally witnessed occurred on Sunday May 20. The weather was warm (air temperature 20°C) and sunny. The drill water was drawn from a sump which was fed by springs in the area and had a temperature of 19°C. It is interesting to note that after the first rockburst, a previously dry fracture located on the outcrop map (Figure 20) at grid coordinates (L5.0, R3.2) produced water with a temperature of 4°C and in quantities of 1-2 L/min. During the afternoon of May 20 this fracture alternately produced water and was dry or nearly dry following succeeding rockbursts. The description of the series of rock bursts is given in Table 10.

Following the activity of May 27, there was a 5 day period of steady rainfall during which only one small rockburst was observed on the outcrop by the drill crew. This burst occurred during the early afternoon of June 1. Although no daytime rockbursts were observed during the May 20 - June 1 period except where noted above, it was not uncommon to find evidence of overnight rockbursts on returning to the outcrop the following morning. Mr. J. Chandra of the New Brunswick Department of Natural Resources plotted these bursts on a surface map of the outcrop (Figure 20). A series of diagrams showing the relationship of the P stress orientation and the differential vertical displacements measured on the main outcrop are shown in Figure 20a.

The location of the bursts defined a line which approximately parallels the orientation of the P stress as determined in boreholes 1 and 2. The bursts were of two types. The first type is the explosive burst usually of areas not more than 0.20m and are accompanied by a sharp audible pop and sometimes small fragments of flyrock. The fragments involved in this type are lenticular and are not more than 2-3 cm thickness. The second type of burst is larger covering an area of several square meters and is accompanied by a tearing sound not unlike the sound made by lake ice when it breaks up. There is no flyrock associated with this type of burst. The first type of burst seems mainly confined to the western part of the outcrop although areas in the southeast part of the outcrop probably formed in a similar method. The second type of burst occurred mainly on the eastern side of the outcrop. One of these bursts (marked #3 in Figure 20) did occur on the western side of the outcrop although the failure was a tensile failure with clean vertical fracture faces. On the eastern side, the fractures were inclined to the surface and had sharp edges. Photographs of the various bursts are contained in Appendix 8.

Two pop-ups existed on the main outcrop at the time of this project (May-June 1984). The pop-up, marked as area 11 in Figure 20, occurred not long after the outcrop was cleared in September 1983. This pop-up grew after the initial sequence of rockbursts and then seemed to become stable until the May 27 bursts when it grew approximately 21mm and then stabilized again. A second pop-up developed in area 5 after the first series of rockbursts and it was noted that the two pop-ups had three things in common:

1) both are located on the surface of the footwall block of the thrust fault structure on the main outcrop,

2) both are located near the visible end point of the thrust fault structure,

3) both indicate a compressive stress oriented at approximately 290°.

The rockbursts trace out a line bearing approximately 050° which is subparallel to the P stresses in boreholes 1 and 2 (excluding 2b) and forms an angle of approximately 60° with the line defined by rock pop-ups. This suggests that significant shear stresses exist near the outcrop surface and that sufficient testing would have to be performed in order to determine the shear components of the three dimensional stress tensor before the principal stresses could be determined. A bulging of a rock layer was observed in area 3 but it was not certain whether this disturbance was due to the rockbursts on either side of area 3 or the beginning of another pop-up. The photographs of this structure are contained in Appendix 8 as well.

On June 2, 1984, a small tremor with an accompanying audible boom sound was experienced. The event occurred at 16:07:40 local time and was accompanied by a slight surface vibration which lasted from 1 to 2 seconds. At 16:18:45 a second smaller audible boom was detected but there was no accompanying surface vibration. Dr. J. Adams (1985) checked records of seismometer KLN which showed that the first event occurred at 16:07:13 local time and was of approximately magnitude 1. The time difference between the site time and recorded time is probably due to an error in the watch time at the site. No motion of the second event was recorded. It is possible that these two events are aftershocks of the 1982 series of earthquakes which are being recorded by station KLN (Adams, 1985).

The failure mode for all of the observed rockbursts was that of a very thin layer popping off the main outcrop much like an onion skin peeling off. Approximate measurements were made on some of the fractures with the tools that were at hand. These measurements are contained in Appendix 8.

7. STRESS DROP

Burst 1 occurred immediately after overcore test 7 was completed at 16:35:45 on May 20. Test 8 was started at 17:37:20 and finished at 18:20:35. It was physically impossible to reset the gauge for another test any sooner after the occurrence of burst No 1. The results for these tests are:

Test 7	P = 3.93 MPa	Test 8	P = 2.71 MPa
	Q = -1.47 MPa		Q = 0.12 MPa
	P Azimuth 058°		P Azimuth 050°

There was a stress change between the two tests but in view of the variance between other pairs of tests, the significance of this stress change is uncertain. The times of these three events are known very accurately because the bit advance rate was monitored during the test with the reading times being recorded to verify that a constant downfeed rate was maintained by the drill crew during a test.

8. INCLINED HOLES

After the completion of the overcoring testing, three short inclined holes were drilled on the main outcrop to examine the near surface fracture patterns. The locations and orientations of these holes are shown in Figure 20. The photographic record made of the core from these holes is given in Appendix 9. The first hole was drilled at a plunge of 45° and to a depth of 2.75m while holes 2 and 3 were drilled at 60° to depths of 3.66m and 4.88m respectively. The three holes trend 030°.

The most notable things about the core recovered were the number of shallow dipping joints in the rock and how the frequency of joints decreases with depth. In a zone of rockbursts, this greater density of near surface joints may be the result of stress relief. Another thing worth noting, is that even though the surface layer of rock is well jointed, there is sufficient stress being transmitted through the rock mass to generate these surface bursts.

9. RELATIONSHIP OF STRESSES TO EARTHQUAKES

The mechanism causing the Miramichi earthquakes is thought to be thrust faulting, based on the analysis of earthquake records to derive the fault plane solutions for this sequence of events (Wetmiller et al, 1984). The hypocentres for these events are believed to be situated at a depth of approximately 0-7km relative to sea level. The deepest test overcoring stress measurement in this study is at a depth of 31m. The relationship between near-surface measurements and deep stress conditions is not well known although attempts have been made to correlate the two. Studies by Tullis (1981), Zoback (1980), Haimson (1978) and Raleigh et al (1972) show that near surface stress measurements (depths less than 60m) and deep stress tests (depths greater than 300m) do seem to correlate fairly well for stress orientation. The relationship of near surface and deep stress magnitudes is as yet not clearly defined. If the mechanism in the Miramichi earthquake sequence is a thrust type with a fault trace estimated to have a strike of approximately 005° then the maximum stress measured in the horizontal plane should have a bearing of approximately 095° rather than the 055° bearing which was measured. This 055° orientation appears to be similar to a situation reported by Tullis (1981) (Figure 19) from his study of the San Andreas fault where slip movement has caused a deflection of the P stress from the perpendicular direction to the strike of the fault plane. Tullis (1981) believed that inhomogeneities on the fault plane surfaces caused stress deflections which when taken into consideration could explain a situation which did not agree with the observed fault mechanism. The P stress alignments determined in Miramichi are in agreement with measurements in New England as given in Plumb et al (1984a,b) and shown in Figure 18. These P orientations were obtained with overcoring techniques but are at 90° to those derived by fault plane solutions given in Zoback and Zoback (1980) and Yang and Aggarwal (1981). The two cases quoted in Zoback and Zoback (1980) which are located in the New England area are Block et al (1979) and Oliver, Johnson and Dorman (1970). The common factor in these three cases (Block et al, 1979; Oliver et al, 1970; and Yang and Aggarwal, 1981) is that all three involve thrust faults. This suggests that perhaps:

1) stress orientations vary along a thrust fault as it approaches the surface; ie the conditions change from a solid body to half space,

2) other conditions such as topography, glacial rebound, jointing patterns, and weathering are the dominant factors rather than the thrust fault stress field at the surface. The works by Zoback and Zoback (1980) and Yang and Aggarwal (1981) are presently under review due to more recent data which has come to light and so this problem of differing P stress orientations may be resolved (Adams, 1985).

Adams (1985) stated that stress measurements at the Brunswick Mining and Smelting Bathurst mine approximately 75km from the site and at 1km. depth, gave major stress magnitudes of approximately 55 MPa in an ESE-WNW direction. This information, a copy of which was supplied by Dr. Adams, is contained in Appendix 10. Yang and Aggarwal (1981) noted that, east of the Appalachians, σ_1 was parallel to the age gradient as delineated from offshore magnetic anomalies. The magnetic anomalies are aligned perpendicular to the age gradient. These σ_1 orientations were determined from fault plane solutions. Toward the interior of the continent, σ_1 is nearly parallel to the direction of absolute motion of the North American plate. The general stress orientations obtained from the fault plane solutions would seem to further support the hypothesis of an essentially north-south striking thrust fault in the Miramichi area. However, the test results from the six borings do not agree with this hypothesis, except in the case of borehole 4, and the upper part of borehole 3. The major secondary principal (P) stress direction appears to be aligned in a north-easterly direction and, depending on the boring, forms an angle of from 2° to 64° with the calculated strike of the thrust structure. The larger angles would tend to indicate a strike-slip movement along this fault structure. An estimate of the vertical stress that can be made assuming straight gravimetric loading:

$$\sigma_v = \int_0^z \rho g dz$$

where σ_v = is stresss due to the overburden
ρ = is the density of material
g = is the gravimetric constant
z = is the vertical depth

assuming $\rho = 2.70$ g/cc
$g = 9.81$ m/sec
$z = 30$m

would yield a

$$\sigma_z = 0.795 \text{ MPa}$$

This estimate of vertical stress indicates that for the most part σ_3 is in the vertical direction which would tend to support a thrust fault mechanism theory. This gravimetric estimate of the vertical stress may not be correct however, because of three conditions: 1) the area has been glaciated, 2) the study area has a complex structure and 3) the area has had a history of igneous intrusion, that is not completely known at present and this could influence the present in situ stress field. Glaciation has affected the stress field in other areas such as southern Ontario (McKay 1981) and may have modified the stress field in the Miramichi Region as well. Superimposed on this glacial influence will be the effect of the tectonic movements. The sum total of these stress generating factors cannot be fully estimated until sufficient stress measurements are made to calculate the full three dimensional stress tensor.

For example, Serafim (1961) performed stress measurements on opposite sides of a fault in a jointed, unaltered granite rock mass in the Picote powerplant in Portugal. The vertical stress measured within 5m of the fault was a maximum of 45.60 MPa while there was only 80m of overburden at the site which would create a load of 1.96 MPa assuming gravimetric loading. On the opposite side of the fault the maximum vertical stress was 20.59 MPa but two other tests on the same side of the fault gave vertical stresses that were tensile (1.47 MPa and 19.61 MPa respectively). The type of fault at the site was not mentioned, nor were corrections made for the stress concentrations due to the geometry of the opening. This example does, however, show that stress conditions near a fault may be complex and variable as has been found at the Miramichi site.

Jaeger and Cook (1979), stated that there is a topographic control of the concentration of stresses near the surface. Their information was based on analytical methods employing photoelastic or finite element methods. The problem with this, as the authors have stated, is that boundary conditions are applied to arbitrary surfaces bounding the area of interest. These boundary conditions will control the computed stresses in the body but it is not clear at present what these conditions should be. The stress trajectories shown in Figure 21 are based on finite element calculations which assume that the stresses on planes AB and CD are normal and that there is no displacement on BC. These conditions would not be applicable in an area of faulting where there is a possibility of some or none of the above conditions being true. Studies in the area of a well known topographic feature, the Niagara Falls Gorge (McKay 1983), show that although measurements prove there is a topographic stress concentration present, analytical techniques are not yet sufficiently developed to accurately forecast stress concentrations due to this topographic effect with a 100% confidence level.

Myrvang and Grimstad (1984) in dealing with a problem of rockbursts in tunnels driven in gneisses have found that changes in the topography such as valleys can generate very large stress concentrations which they named "valley side stresses". The result of these "valley side stresses" is to cause the maximum stress to be aligned parallel to the slope surface. This would be the expected case in borehole 5 which was located on the side of a hill that had a 10-15° slope. The strike of the hillside was approximately N60E. The average P stress orientation for borehole 5 is N37E. The influence of topography on stress measurements is expected in the very near surface as shown in Figure 22 from Plumb et al (1984a) but the test results from borehole 5 show little variation in the direction of P throughout the hole. The lowest test, test 48, was done at a depth of 31.00m and approximately 176m from the valley side. There could be two explanations for this: 1) the effect of topography is more extensive than first thought, 2) by coincidence the regional stress is in the same direction as the topographic effect in this case.

Recent studies of in situ stresses near faults in China (Wang and Wei, 1984; Zhin, 1984 and Yi and Ge 1984) are shown in Figures 23-31 and indicate that depending on when a stress measurement is made after an earthquake, the stress field orientation and magnitude vary greatly. Figures 28-31 are taken from Yi and Ge (1984) and show how the in situ stress can drop after an earthquake and may become tensile. The stress can then increase with time before being released by another earthquake. This behaviour, if true for all environments, could explain some of the unexpectedly high and low stress levels measured at the Miramichi site.

Park (1983) described the manner in which different methods of igneous emplacement can modify the local stress field to the extent that the principal stress, σ_1, would be vertical or nearly so at near-surface with the intermediate and minor principal stresses σ_2 and σ_3, in the horizontal plane. This again points out the limits to which interpretation of the area structure can be made without obtaining information on the three dimensional stress field.

The reason that the above factors have been brought into consideration is that, although the Miramichi series of stress measurements indicate a near surface fault mechanism other than pure thrusting, until the complete three dimensional stress field has been determined in the Miramichi area, the results of this study do not conclusively disprove a thrust mechanism. The stress field at a depth of 6-7km may be different than the near surface stress field and could be, as the seismic records indicate a thrust fault mechanism. Hydraulic fracturing measurements would be required to determine the in situ stresses at depth of 1km or more in order to define these deep stresses. However, this was not the aim of this pilot project. The aim of this project was to provide a direction for discussion and for future work. This aim has been met.

10. CONCLUSIONS

The results from five of the six borings in the Miramichi Region epicentral area indicate that the principal secondary stress in the horizontal plane has a north-easterly 055° to 095° orientation. This does not agree with a pure thrust fault mechanism obtained from the fault plane solutions derived from seismicity records. The results from one boring do agree with this structural orientation indicating that a very complex structure exists in the area that may be better understood as work in the area proceeds. The fact that the earthquake with an accompanying release of the crustal stresses occurred approximately 2.25 years prior to these measurements must be considered. The post-earthquake stress field could be indicative of a more relaxed condition of the rock mass under which local structural features would be the dominant influence on the post-quake stress field.

ACKNOWLEDGEMENTS

This project was made possible through the co-operation of several agencies. The National Research Council of Canada and the Atomic Energy Control Board provided funds to cover the drilling costs for the project. The New Brunswick Department of Natural Resources provided excellent logistical support throughout the project which was greatly appreciated. Grateful thanks are extended to all the individuals who took the time and trouble to review this report and make several valuable suggestions on how to improve it.

Approved by:

T.G. Cormick

for T.W. Klym
Manager
Civil Research Dept

Prepared by:

D.A. McKay

D.A. McKay
Geotechnical Engineer
Rock Sciences Section

and

JB Williams

J.B. Williams
Technician
Rock Sciences Section

and

JR Bowlby

J.R. Bowlby
Senior Engineering Geologist -
Geotechnical Development
Geotechnical & Hydraulic Engineering Dept

and

JD Grass

J.D. Grass
Senior Engineering Geologist
Geotechnical & Hydraulic Engineering Dept

REFERENCES

1. Adams, J. Personal communication, Earth Physics Branch, Dept of Energy, Mines and Resources, 1985.

2. Block, J.W., Clement, R.C., Lew, L.R. and de Boer J. "Recent Thrust Faulting in Southeastern Connecticut" Geology, vol 7, pp 79-82, 1979.

3. Burke, K.B.S. and Chandra, J.J. "Gravity Survey of the Epicentral Area of the Main Sequence of 1982 Miramichi Earthquakes", New Brunswick Department of Natural Resources open file report 83-3.

4. Choy, G.L., Boatwright, J., Dewey, J.W. and Sipkin, S.A. "A Teleseismic Analysis of the New Brunswick Earthquake of January 9, 1982" J. Geophys Res, vol 88 pp 2199-2212, 1983.

5. Fyffe, L.R. "Joint Patterns Within the Epicentral Area of the 1982 Miramichi Earthquake", New Brunswick Department of Natural Resources Open File Report 83-13, 1983.

6. Fyffe, L.R. "Geology in the Vicinity of the 1982 Miramichi Earthquake Northumberland County, New Brunswick", New Brunswick Department of Natural Resources, Open File Report 82-27, 1982.

7. Haimson, B.C. "Hydrofracturing Stress Measurements Hole UN-1 Darlington Generating Station", Ontario Hydro Design and Development Division Report No 78250, 1978.

8. Hooker, V.E. and Duval, W.I. "In Situ Rock Temperature Stress Investigations in Rock Quarries", Rep Invest U.S. Bur Mines 7578 12pp, 1971.

9. Hooker, V.E. and Johnson, C.F. "Near Surface Horizontal Stresses, Including the Effects of Rock Anisotropy", Rep Invest U.S. Bur Mines 7224, 29 pp 1969.

10. Jaeger, J.C. and Cook, N.G.W. "Fundamentals of Rock Mechanics", Chapman and Hall, London, 3 ed, 1979.

11. Lyons, J.B. and H. Faul. "Isotope Geochronology of the Northern Appalachians in Studies of Appalachian Geology: Northern and Maritime", E-an Zen, White, W.S., Hadley, J.B., Thompson Jr, J.B., Editors pp 305-318, 1968.

12. McKay, D.A. "Sir Adam Beck GS No 3 Preliminary Study - In Situ Rock Stress Measurements", Ontario Hydro Civil Research Department Report No 83-493-K, 1983.

13. McKay, D.A. "Darlington GS Rock Stress Measurements Forebay Area", Ontario Hydro Civil Research Department Report No 81-375-

H, 1981.

14. Myrvang, A.M. and Grimstad, E. "Coping with the Problem of Rockbursts in Hard Rock Tunnelling", Tunnels and Tunnelling vol 16 no 7 pp 13-15, July 1984.

15. Oliver, J., Johnson, T., and Dorman, J. "Postglacial Faulting and Seismicity in New York and Quebec", Can J of Earth Sci, vol 7 pp 579-590, 1970.

16. Park, R.G. "Foundations of Structural Geology", Chapman and Hall, New York, NY 1983.

17. Plumb, R., Engelder, T., and Sbar, M. "Near-Surface In Situ Stress-2 A Comparison with Stress Directions Inferred from Earthquakes, Joints, Topography Near Blue Mountain Lake, New York" J Geophys Res vol 89 no B11 pp 9333-9349, 1984(a).

18. Plumb, R., Engelder, R., and Yale, D. "Near-Surface In Situ Stress-3 Correlation with Microcrack Fabric within the New Hampshire Granites" J Geophys Res, vol 89 no B11 pp 9350-9364, 1984(b).

19. Raleigh, C.B., Healy, J.H., and Brederhoft, J.D. "Faulting and Crustal Stress at Rangely Colorado" in "Flow and Fracture of Rocks" Geophys Monogr Ser vol 16 ed HC Heard et al pp 275-284 AGU Washington, DC, 1972.

20. Rogers, J. "The Tectonics of the Appalachians", Wiley Interscience, NY, 277 pp 1970.

21. Serafim, J.L. "Internal Stresses in Galleries" Seventh International Congress on Large Dams, Rome 1961 pp 141-165.

22. Tullis, T.E. "Stress Measurements Via Shallow Overcoring Near the San Andreas Fault", in Mechanical Behaviour of Crustal Rocks, The Handin Volume, Geophysical Monograph 24, American Geophysical Union, 1981.

23. Vanicek, P. "Pattern of Recent Crustal Movements in Maritime Canada", Can J Earth Sci vol 13 pp 661-667, 1976.

24. Wang, E.F. and Wei, C.U. "In-Situ Stress Characteristics in the Tang Shan Region Before and After the 1976 Earthquake" in "A Study of Stresses in the Earth's Crust" S.C.Li ed, Earthquake and Geology Information Office, National Earthquake Authorities, Earthquake Publications Ltd, Bejing, China, pp71-76, 1984.

25. Wetmiller, R.J., Adams, J., Anglin, F.M., Hasegawa, H.S. and Stevens, A.E. "Aftershock Sequences of 1982 Miramichi, New Brunswick Earthquakes", Bulletin of the Seismological Society of

America vol 74 no 2 pp 621-653, April 1984.

26. Yang, J.P. and Aggarwal, Y.P. "Seismotectonics of Northeastern United States and Adjacent Canada", J Geophys Res, vol 86 no B6 pp 4981-4998, June 10, 1981.

27. Yi, Z.G. and Ge, L.M. "A Preliminary Examination of the Relationship Between Epicentral Location and Variations in the In-Situ Stress Field" in "A Study of Stresses in the Earth's Crust" S.C.Li, ed, Earthquake and Geology Information Office National Earthquake Authorities, Earthquake Publications ltd, Bejing, China, pp 105-109, 1984.

28. Zhin, C. "Regional Stress Fields and Structural Geology in China" in "A Study of Stresses in the Earth's Crust" S.C.Li ed, Earthquake and Geology Information Office, National Earthquake Authorities, Earthquake Publications Ltd, Bejing, China, pp 81-84, 1984.

29. Zoback, M.D., Tsukahara, H., and Hickman, S. "Stress Measurements at Depth in the Vicinity of the San Andreas Fault: Implications for the Magnitude of Shear Stress at Depth", Journal of Geophysical Research, vol 85, no B11 pp 6157-6173, Nov 10, 1980.

30. Zoback, M.L. and Zoback, M. "State of Stress in Conterminous United States", J of Geophys Res, vol 85, no B11 pp 6113-6156, Nov 10, 1980.

TABLE 2

SUMMARY OF TEST RESULTS

BOREHOLE 1 (BH 1)

Test No	Depth m	Elev m	P MPa	Azimuth of P	Q MPa	P/Q	Young's Modulus (E) MPa
3	3.07	391.01	10.91	088	3.98	2.74	55369
4	3.47	390.61	12.19	076	5.68	2.15	49404
7	7.63	386.45	3.94	058	-1.47	-2.68	58186
8	8.08	386.00	2.71	050	0.12	22.6	60540
11	11.67	382.41	7.48	049	2.41	3.10	52056
12	12.07	382.01	7.72	062	3.15	2.45	54627
15	15.60	378.48	5.89	042	0.93	6.33	55602
16	15.96	378.12	CORE BROKE		-	-	-
18	23.15	370.93	CORE BROKE		-	-	-
21	23.48	370.60	16.41	074	6.89	2.38	62901
22	23.86	370.22	22.74	051	7.61	2.99	64831
23	30.46	363.22	12.78	020	2.54	5.04	50465
24	30.86	363.62	9.82	020	1.55	6.34	50465

TABLE 3

SUMMARY OF TEST RESULTS

BOREHOLE 2 (BH2)

Test No	Depth m	Elev m	P MPa	Azimuth of P	Q MPa	P/Q	Young's Modulus(E) MPa
27	3.02	384.98	CORE BROKE-			-	-
28	3.38	384.62	3.21	105	0.87	3.68	50318
31	6.30	381.70	11.20	061	3.45	3.23	70094
32	6.68	381.32	9.46	058	5.78	1.63	66093
35a	8.93	379.07	8.13	357	5.34	1.52	57913
35b	10.91	377.09	10.89	344	8.22	1.32	57913
36	11.31	376.69	7.58	346	4.80	1.58	57501
39	15.88	372.12	0.16	069	0.07	2.16	59056
40	16.32	371.68	7.39	074	5.50	1.34	54031
41	16.60	371.40	7.64	085	6.45	1.18	56825
44	22.98	365.02	CORE BROKE-			-	-
45	24.78	363.22	6.50	093	5.95	1.09	62684
46	25.10	362.90	6.21	005	5.96	1.04	65352
49	29.86	358.14	7.30	064	-8.21	-0.89	65090
50	30.17	357.83	5.35	058	1.09	3.12	70813

TABLE 4

SUMMARY OF TEST RESULTS

BOREHOLE 3 (BH3)

Test No	Depth m	Elev m	P MPa	Azimuth of P	Q MPa	P/Q	Young's Modulus(E) MPa
53	7.49	392.25	3.11	303	0.06	47.6	52897
56	16.29	383.45	-0.04	304	-3.41	0.01	54626
57	16.47	383.27	CORE	BROKE	-	-	-
60	22.85	376.89	-0.04	009	-0.54	0.07	58651
61	23.26	376.58	-4.89	004	-5.33	0.92	56517

TABLE 5

SUMMARY OF TEST RESULTS

BOREHOLE 4 (BH4)

Test No	Depth m	Elev m	P MPa	Azimuth of P	Q MPa	P/Q	Young's Modulus(E) MPa
1	4.58	322.45	6.31	285	1.20	5.25	44861
2	4.98	322.05	CORE	BROKE	-	-	-
5	8.68	318.35	17.92	268	5.85	3.06	55000
6	9.03	318.00	5.57	258	-2.49	-2.24	55000
9	10.59	316.44	2.18	276	-2.39	-0.91	56978
10	10.99	316.04	1.96	276	-2.19	-0.89	62467
13	15.74	311.29	0.30	316	-1.73	-0.17	46729
14	16.14	310.89	6.87	275	1.45	4.73	46729
17a	23.17	303.86	6.57	354	2.97	2.22	73445
17b	23.57	303.46	CORE	BROKE	-	-	-
19	29.31	297.72	7.21	266	2.15	3.34	59101
20	29.69	297.34	7.74	268	2.50	3.10	55976

TABLE 6

SUMMARY OF TEST RESULTS

BOREHOLE 5 (BH5)

Test No	Depth m	Elev m	P MPa	Azimuth of P	Q MPa	P/Q	Young's Modulus (E) MPa
25	3.56	358.00	8.89	344	5.11	1.74	42895
26	3.92	357.64	6.30	029	2.86	2.20	40546
29	8.16	353.40	20.62	051	6.45	3.19	50029
30	8.60	352.96	17.54	051	11.18	1.57	48477
33	10.65	350.91	18.42	032	11.59	1.59	44911
34	11.13	350.43	19.44	033	14.85	1.31	44911
37	15.45	346.11	16.43	032	12.06	1.36	46162
38	15.85	345.71	16.31	046	10.52	1.55	47318
42	22.83	338.73	15.58	038	8.06	1.93	50071
43	23.23	338.33	18.39	064	11.07	1.66	50071
47	30.58	330.98	15.32	026	10.74	1.43	49987
48	31.00	330.56	15.79	029	10.50	1.50	51855

TABLE 7
SUMMARY OF TEST RESULTS

BOREHOLE 6 (BH6)

Test No	Depth m	Elev m	P MPa	Azimuth of P	Q MPa	P/Q	Young's Modulus(E) MPa
51	7.18	344.26	9.06	052	5.58	1.62	40642
52	7.58	343.76	7.11	043	5.60	1.27	44841
54	15.17	336.27	4.69	069	-0.23	-20.49	36004
55	15.44	336.00	4.27	079	-1.25	-3.42	36004
58	22.82	328.62	-0.08	039	-2.43	0.03	31442
59	23.18	328.26	3.30	052	-0.05	-66.00	31539
62	30.44	321.00	CORE	BROKE	-	-	-
63	30.83	320.61	7.87	012	2.40	3.28	37266

TABLE 8

SUMMARY OF TEST RESULTS BOREHOLES 1 TO 6

Borehole	P Stress MPa		Azimuth of P		Q Stress MPa	
	Max	Min	Max	Min	Max	Min
1	22.74	2.71	088	020	7.61	-1.47
2	11.20	0.16	105	344	8.22	-8.21
3	3.11	-4.89	009	303	0.06	-5.33
4	17.92	0.30	268	354	5.85	-2.49
5	20.62	6.30	064	344	14.85	2.86
6	9.62	-0.08	079	012	5.60	-1.25

TABLE 9

AVERAGE P STRESS ORIENTATIONS

Borehole No	Average Azimuth of P	No of Tests
1	054	11
2a	074	9
2b	353	4
3a	303	2
3b	007	2
4	274	10
5	037	12
6a	056	6
6b	012	1

TABLE 10

SUMMARY OF ROCKBURST OCCURRENCES

Burst No	Date	Local Time	Comments
1	20/5/84	16:36:00	- area 1 on outcrop map - 15 to 20 sec prior to burst there was a loud pop - water flow started from joint on topographic rise at grid co-ordinates L5.0, R3.2 - water temp of flow from joint was 4°C, air temp 19°C
2	20/5/84	16:52:20	- area 2 on map
3	20/5/84	17:17	- burst near drill, area 6 on outcrop map
4	20/5/84	17:22	- burst occurred under rear tire of truck, small rock fragment (50gm) thrown 2.5m from area 4 on map
5	20/5/84	17:36	area 1
6	20/5/84	17:57:50	area 3
7	20/5/84	18:23	area 7
8	20/5/84	18:35	area 8
9	27/5/84	15:21:30	area 9
10	27/5/84	15:28:30	- heard but not seen immediately area 10

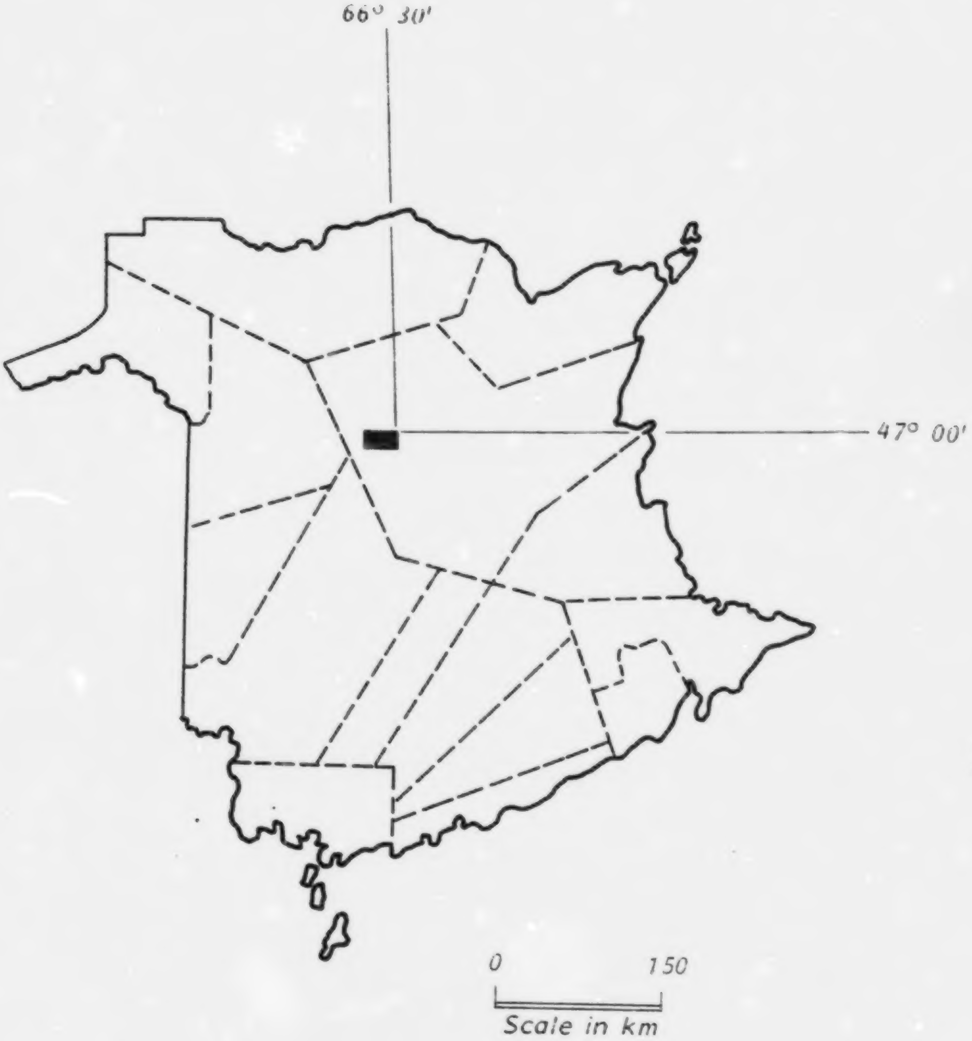
66° 30'
47° 00'
0
150
Scale in km

FIGURE 1
LOCATION OF STUDY AREA

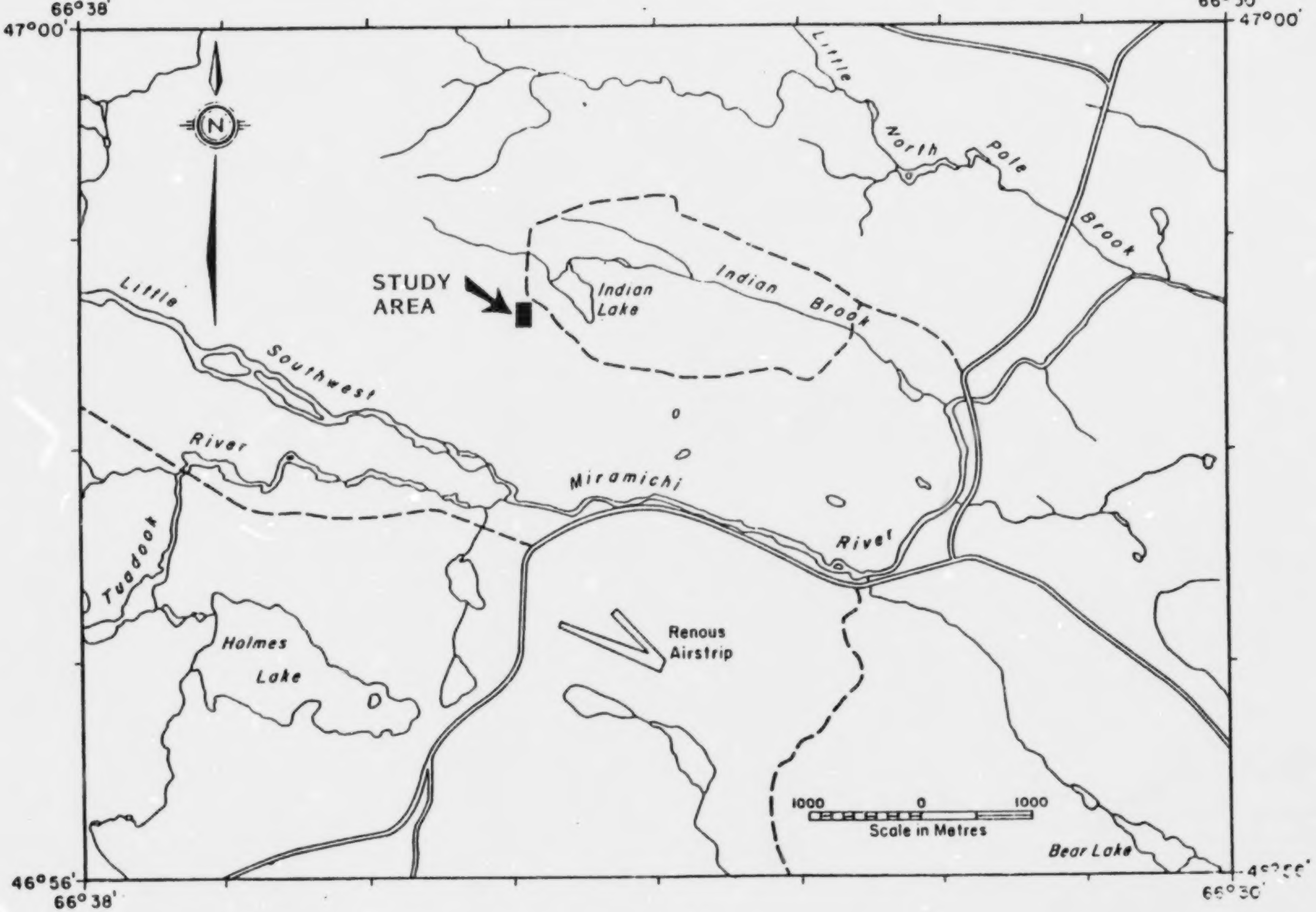
66°38'
47°00'
66°30'
47°00'
N
STUDY
AREA
Little North Pole Brook
Indian Lake
Indian Brook
Little Southwest
River
Miramichi
River
Tuadook
Holmes
Lake
Renous
Airstrip
1000
0
1000
Scale in Metres
Bear Lake
46°56'
66°38'
46°56'
66°30'

FIGURE 2

LOCATION MAP OF STUDY AREA

Figure 6 is the detailed map of this area)

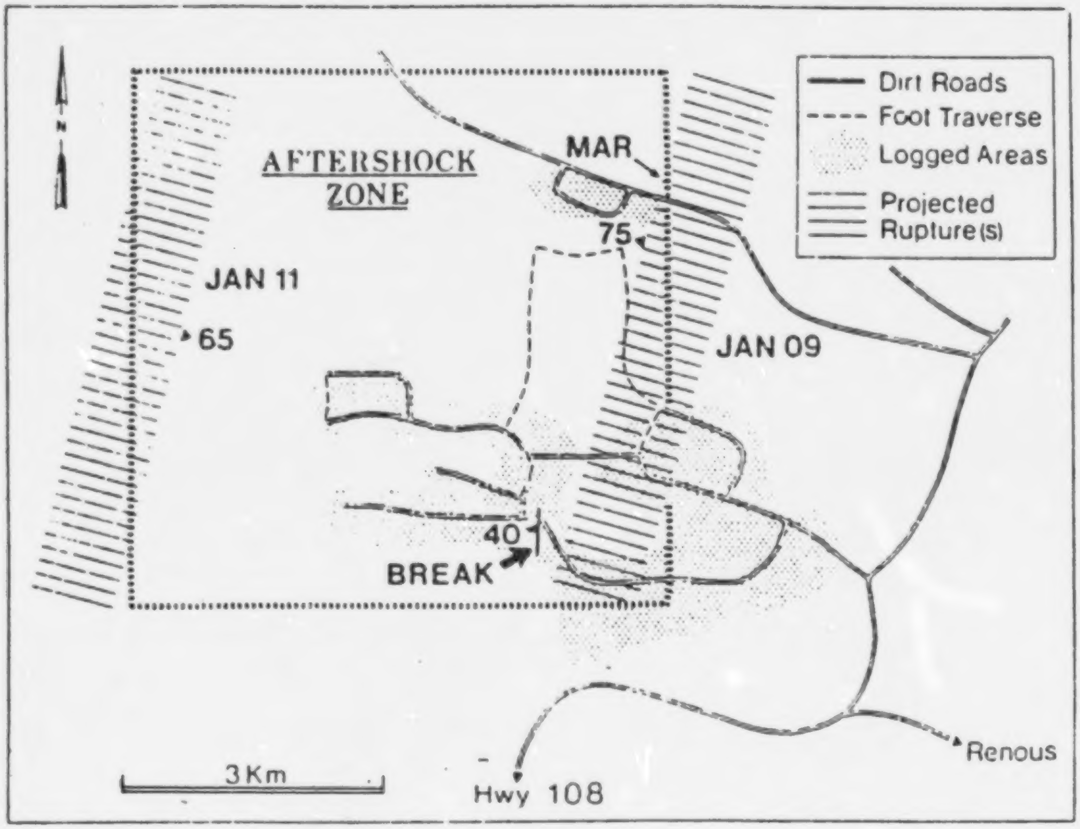

N
AFTERSHOCK ZONE
MAR
75
JAN 11
65
JAN 09
40
BREAK
3Km
Hwy 108
Renous
Dirt Roads
Foot Traverse
Logged Areas
Projected Rupture(s)

FIGURE 3

LOCATION OF OBSERVED GROUND BREAK
AND SURFACE PROJECTIONS OF RUPTURE PLANES
OF PRINCIPAL JANUARY AND MARCH EARTHQUAKES
(FROM WETMILLER et al 1984)

POSSIBLE MIRAMICHI FAULT PLANES

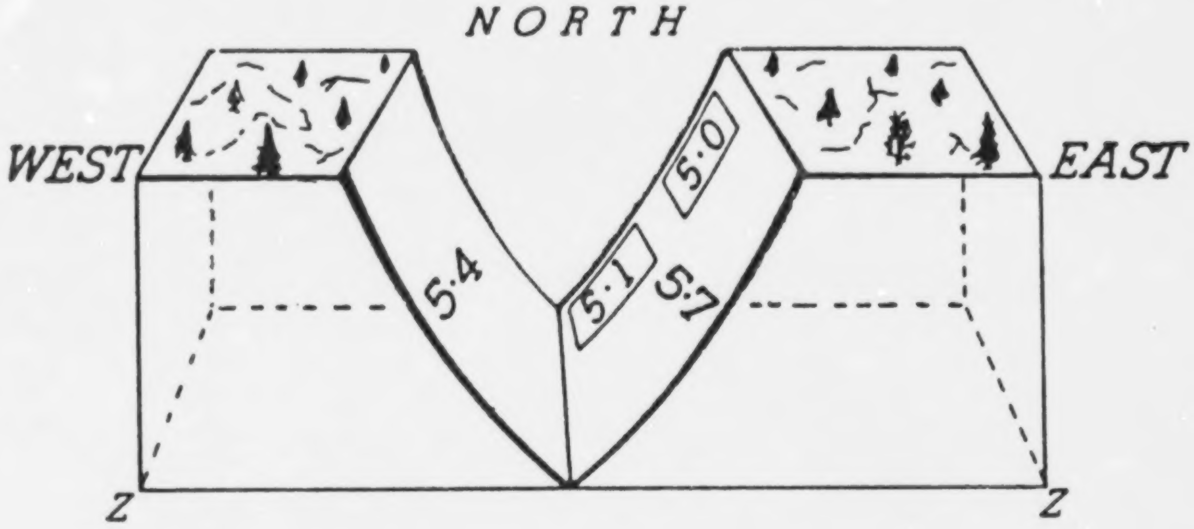
NORTH
WEST
EAST
5.4
5.0
5.1
5.7
Z
Z

5.7 Jan 9 12^h
5.1 Jan 9 16^h
5.4 Jan 11 21^h
5.0 Mar 31 21^h

FIGURE 4

THEORETICAL FAULT PLANE STRUCTURE BASED ON ANALYSIS OF SEISMIC RECORDS (FROM WETMILLER et al 1984)

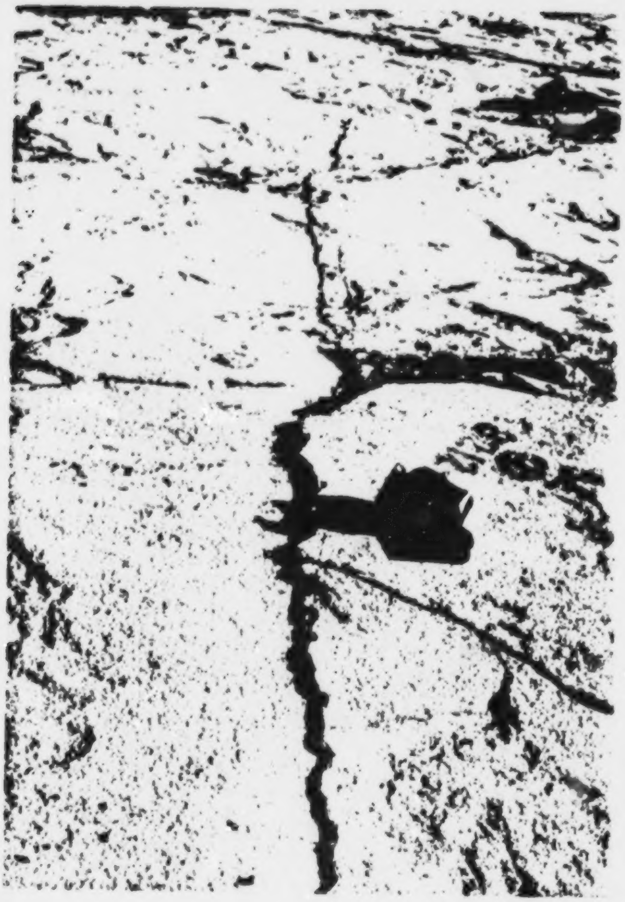

FIGURE 5
SURFACE DISPLACEMENT ALONG PRE-EXISTING JOINT
ON MAIN OUTCROP LOOKING SOUTH
(NOTE: THIS STRUCTURE DIPS WEST)

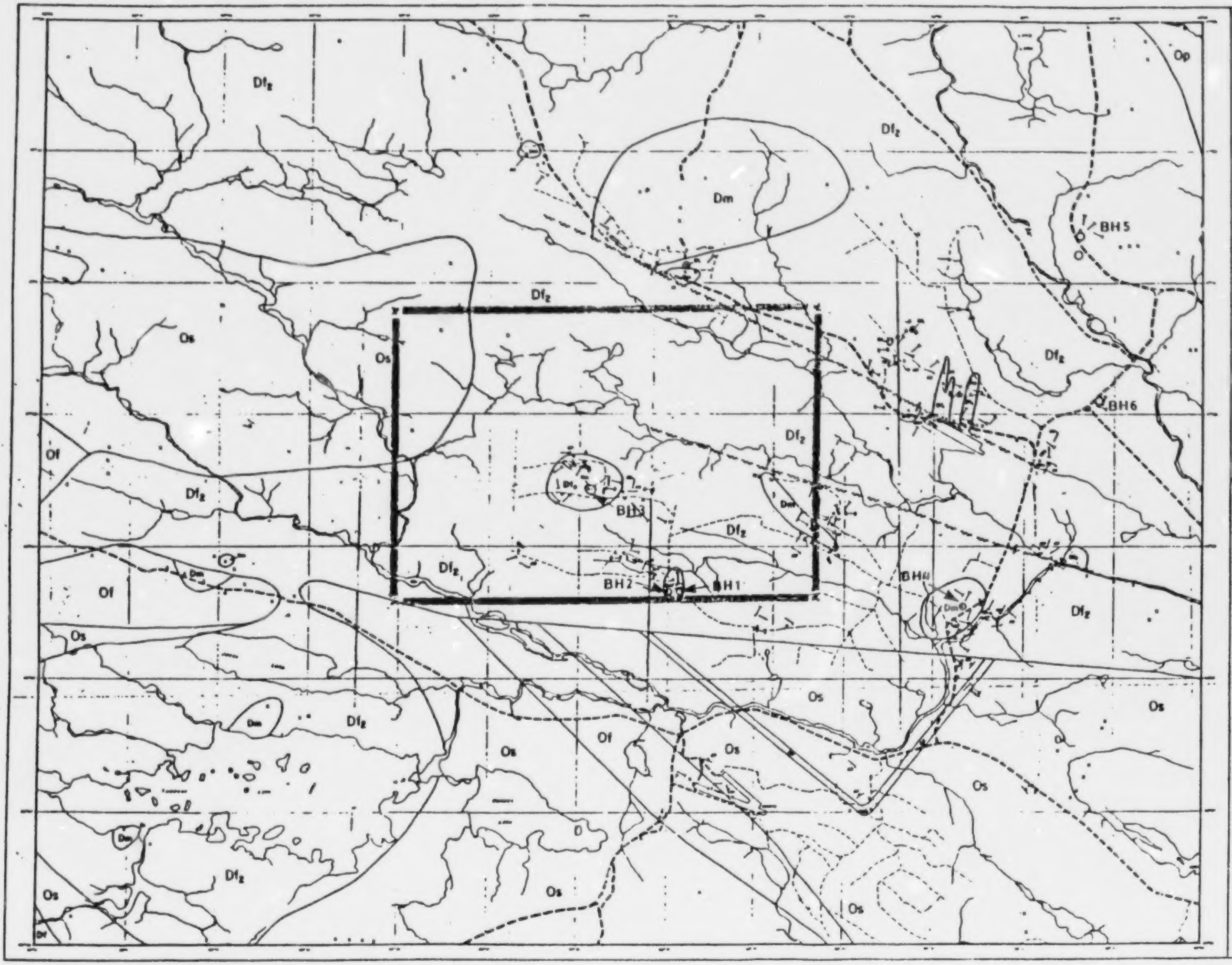
Df2
Dm
Op
BH5
BH6
Os
Of
Df2
BH3
BH2
BH1
BH4
Dm
Df2
Os
Of
Os
Dm
Os
Os
Os
Os

GEOLOGY
of the
MIRAMICHI EPICENTRAL
REGION

After L.R.Fyffe, 1982, 1979, 1972; G.W. Crouse, 1979

FIG. 6
(OPEN FILE REPORT 83-31
PLATE 83-5

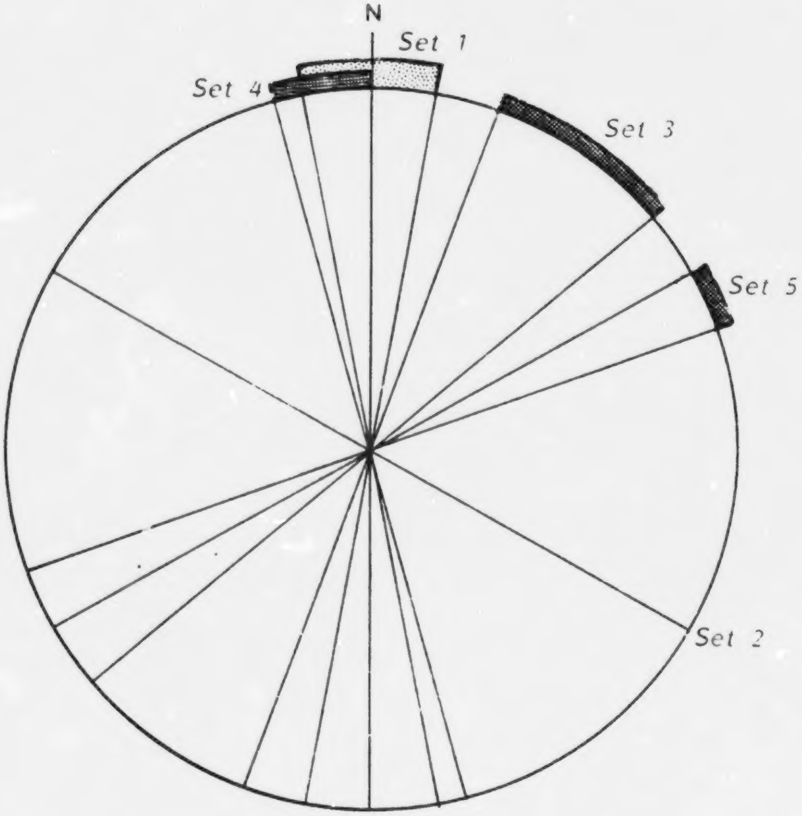
N
Set 1
Set 4
Set 3
Set 5
Set 2

FIGURE 7
FRACTURE ORIENTATIONS ON THE MAIN OUTCROP
AS MAPPED BY FYFFE, 1983

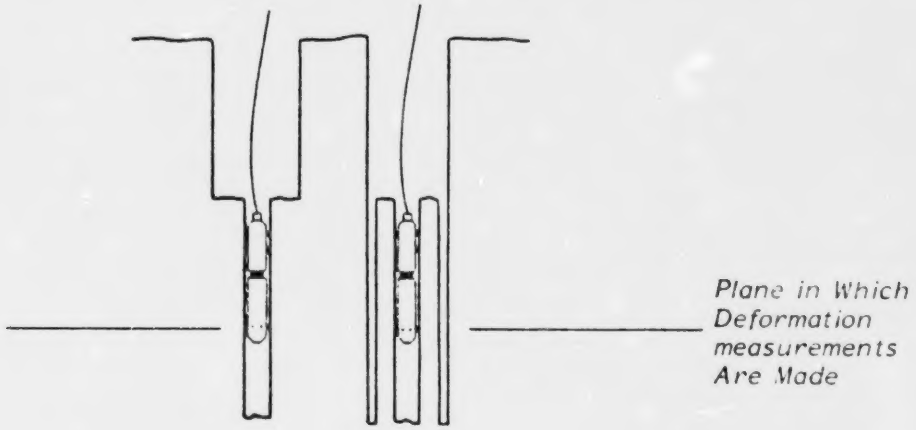
Plane in Which
Deformation
measurements
Are Made

OVERCORING A
BUREAU OF MINES
GAUGE

FIGURE 8

CROSS-SECTIONAL VIEW OF U.S. BUREAU OF MINES OVERCORING TECHNIQUE BEFORE AND AFTER OVERCORING

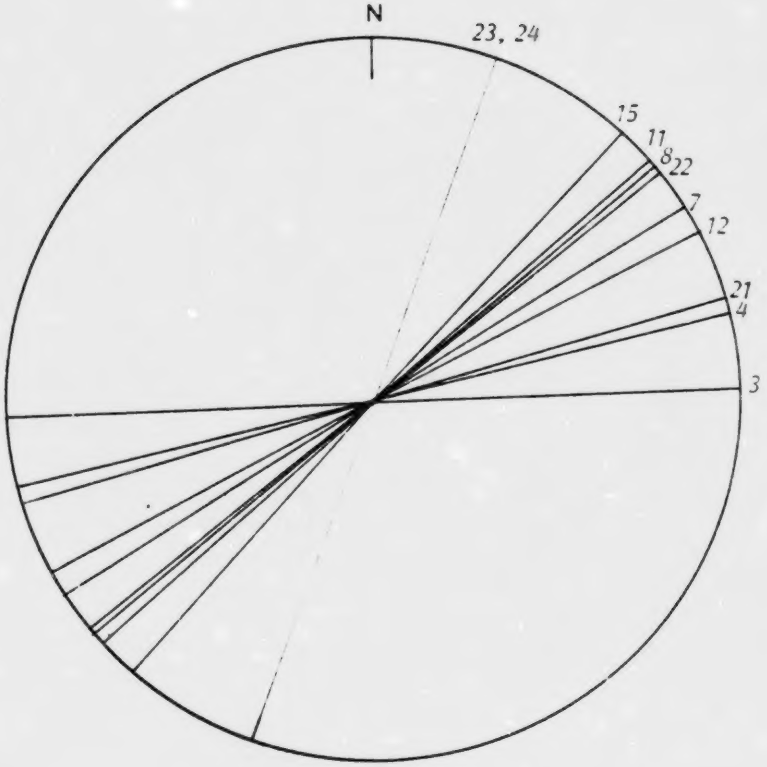
N
23, 24
15
11
8
22
7
12
21
4
3

FIGURE 9

ORIENTATIONS OF P
BOREHOLE 1

Note: Numbers are the Overcoring Test Numbers

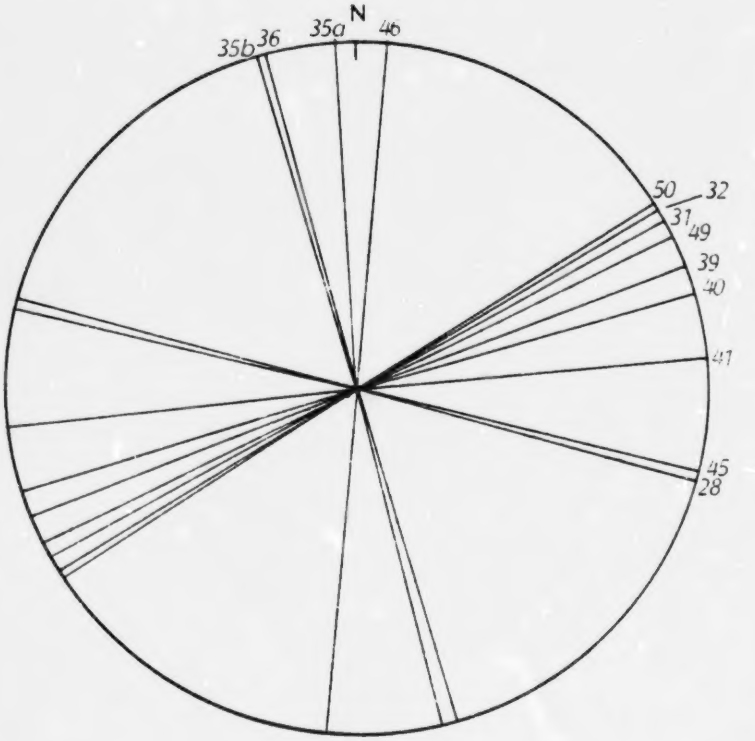
35b
36
35a
N
46
50
32
31
49
39
40
41
45
28

FIGURE 10

ORIENTATIONS OF P
BOREHOLE 2

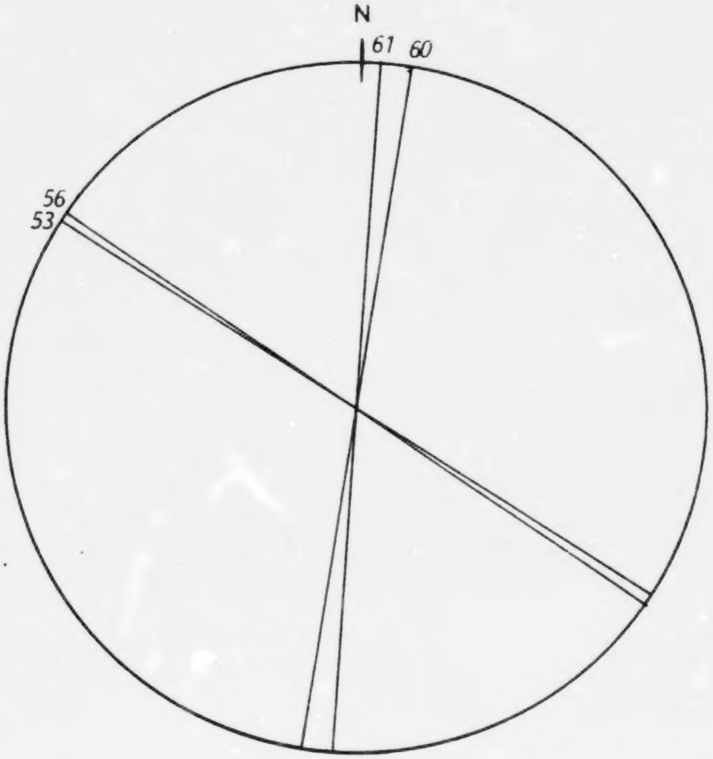

FIGURE 11

ORIENTATIONS OF P
BOREHOLE 3

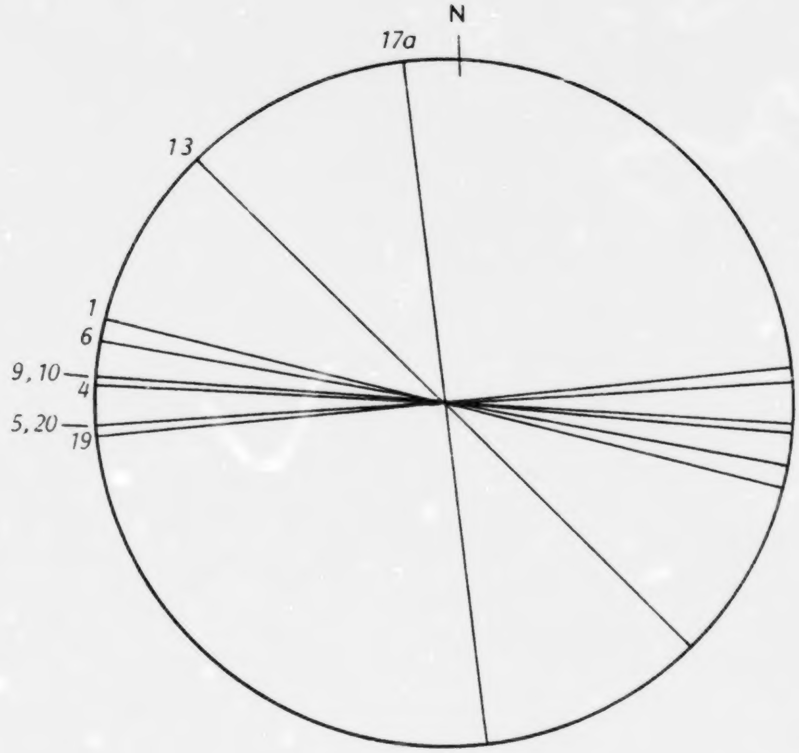
N
17a
13
1
6
9, 10
4
5, 20
19

FIGURE 12
ORIENTATIONS OF P
BOREHOLE 4

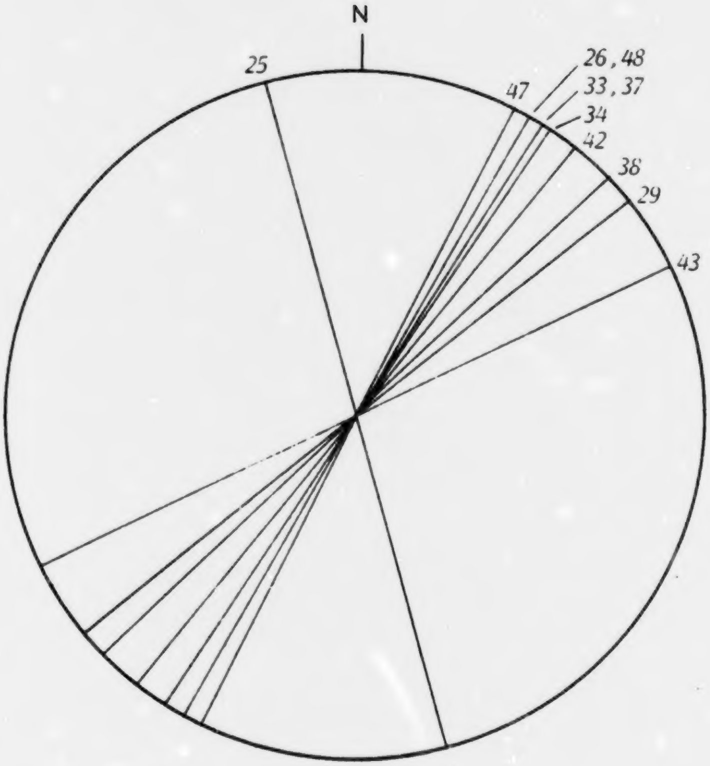
N
25
47
26, 48
33, 37
34
42
38
29
43

FIGURE 13
ORIENTATIONS OF P
BOREHOLE 5

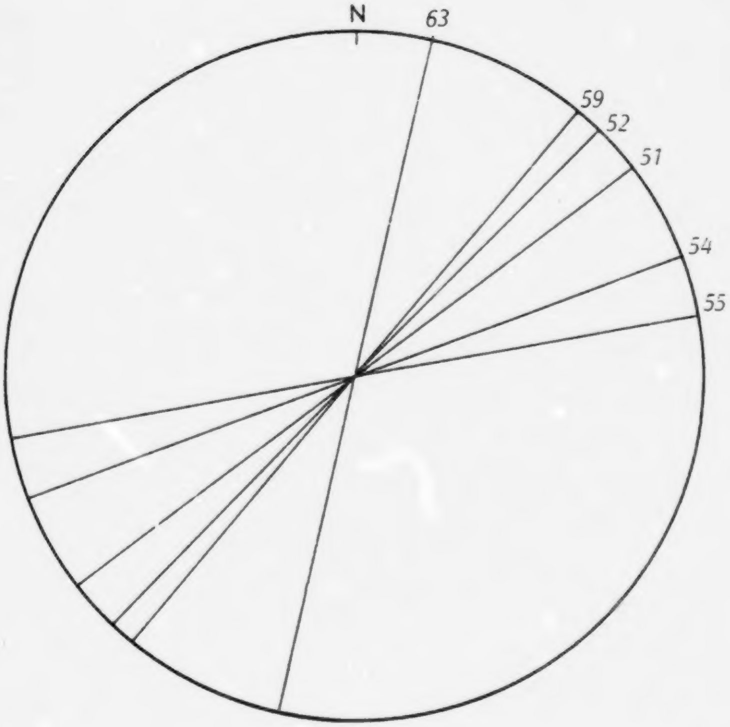
N
63
59
52
51
54
55

FIGURE 14

ORIENTATIONS OF P
BOREHOLE 6

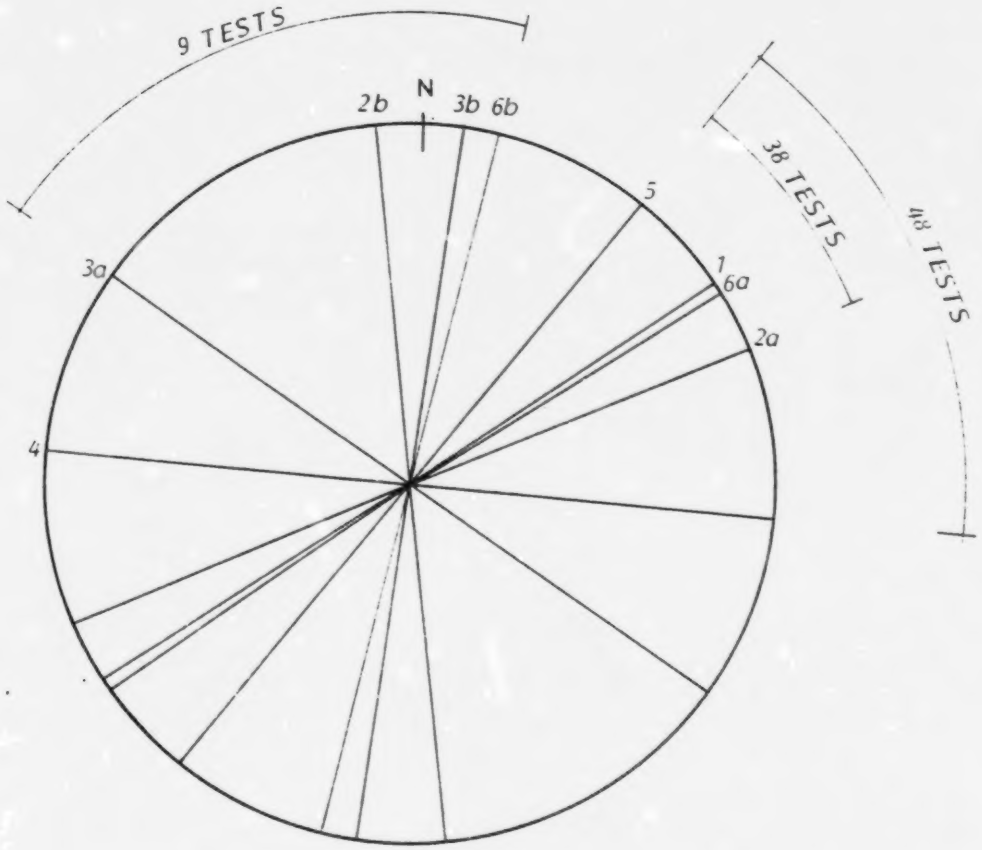
9 TESTS
N
2b
3b
6b
5
1
6a
2a
3a
4
38 TESTS
48 TESTS

FIGURE 15

AVERACE ORIENTATIONS
OF P FOR ALL BOREHOLES

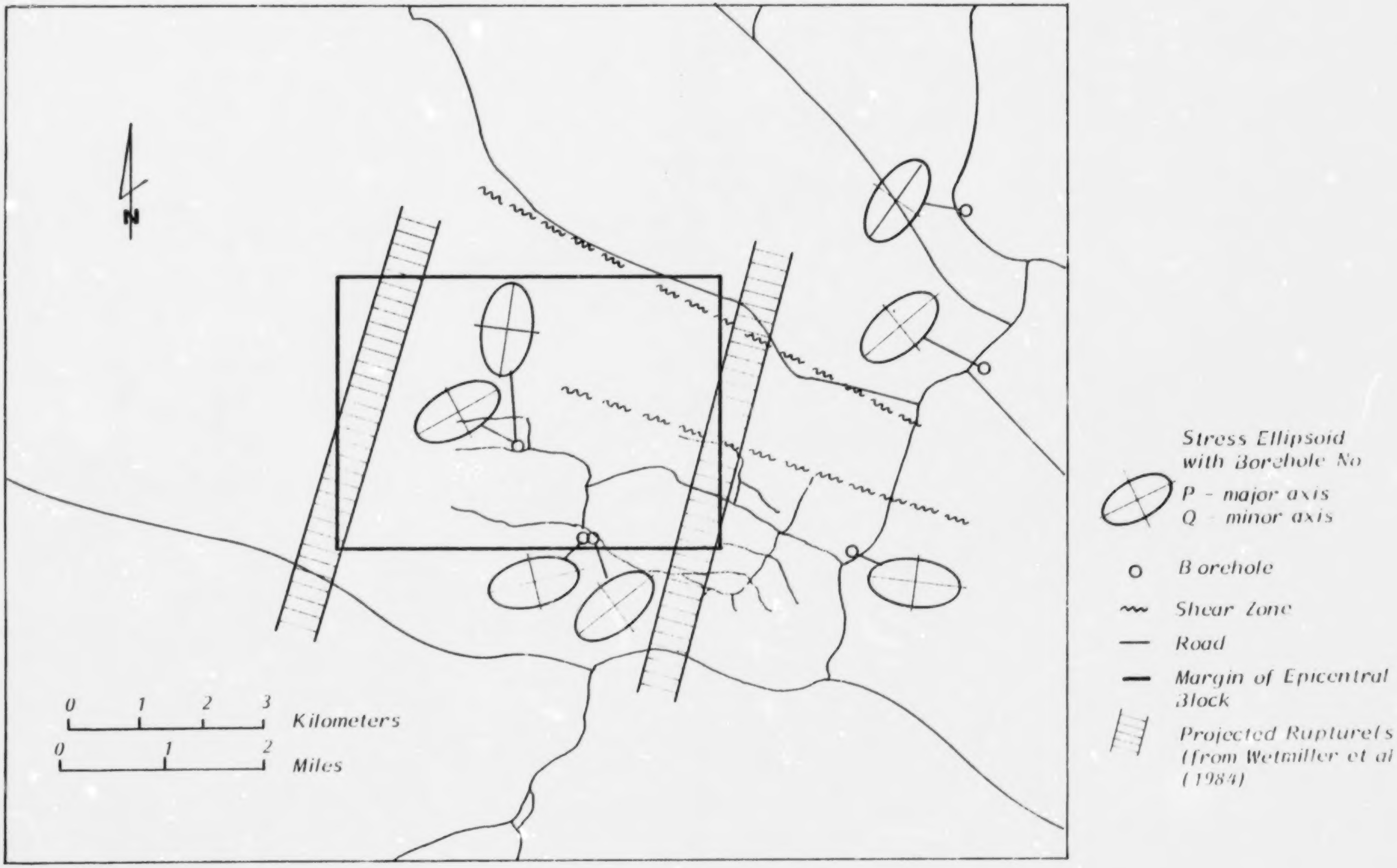
N
0 1 2 3 Kilometers
0 1 2 Miles
Stress Ellipsoid with Borehole No
P - major axis
Q - minor axis
B orehole
Shear Zone
Road
Margin of Epicentral Block
Projected Rupture(s) (from Wetmiller et al. (1984)

FIGURE 16

SECONDARY PRINCIPAL STRESS ORIENTATIONS EPICENTRAL AREA
MIRAMICHI EARTHQUAKE SEQUENCE
(REF: NEW BRUNSWICK DEPT OF NATURAL RESOURCES PLATE 83-5)

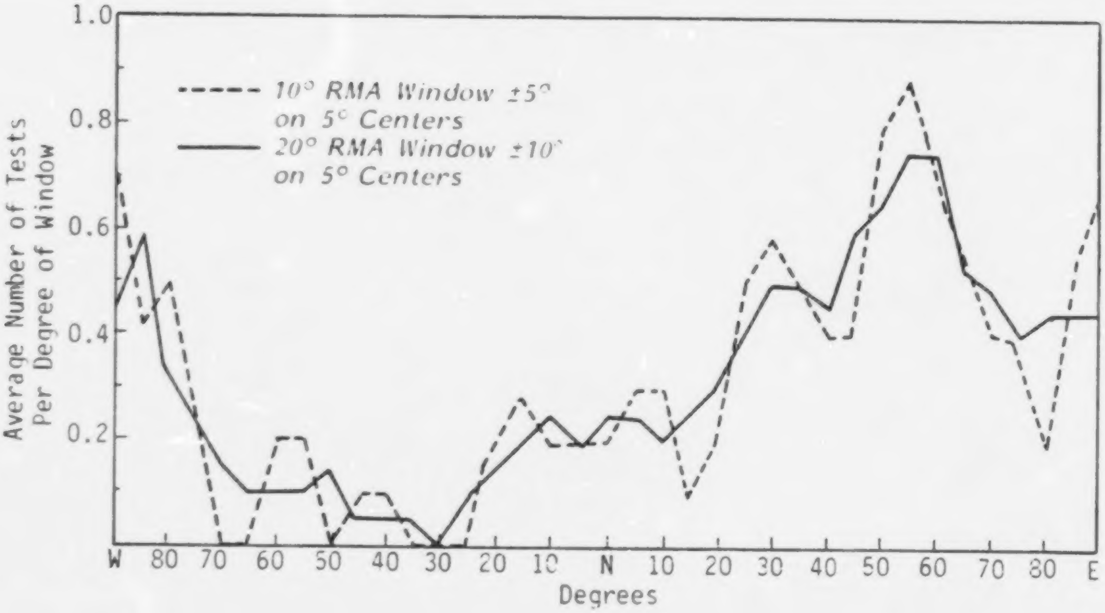

FIGURE 17a

MIRAMICHI P STRESS ORIENTATIONS
ROLLING MEAN AVERAGES

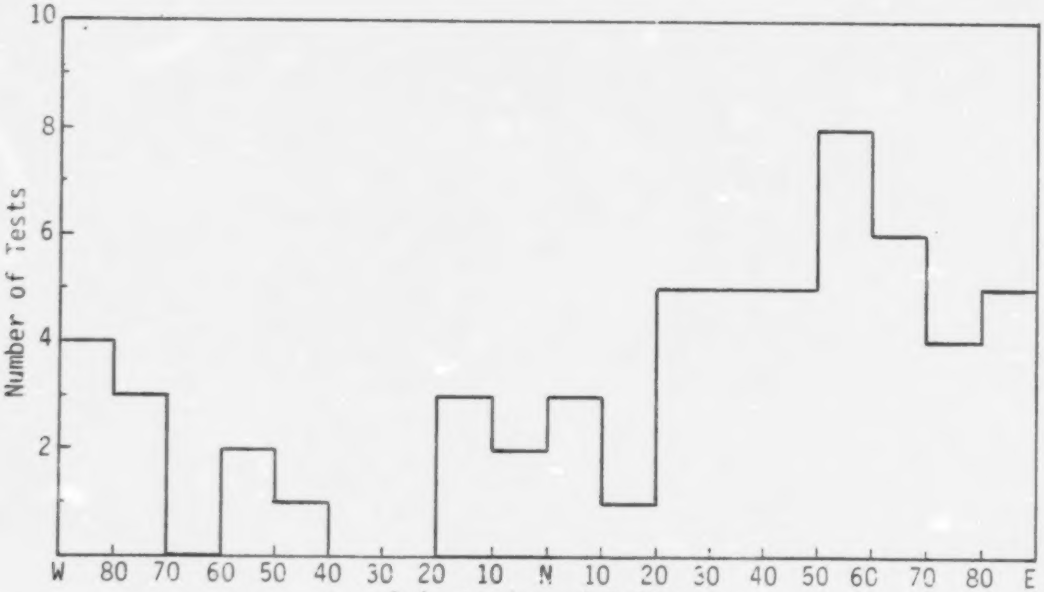

FIGURE 17b

MIRAMICHI P STRESS ORIENTATION
HISTOGRAM OF TEST RESULTS

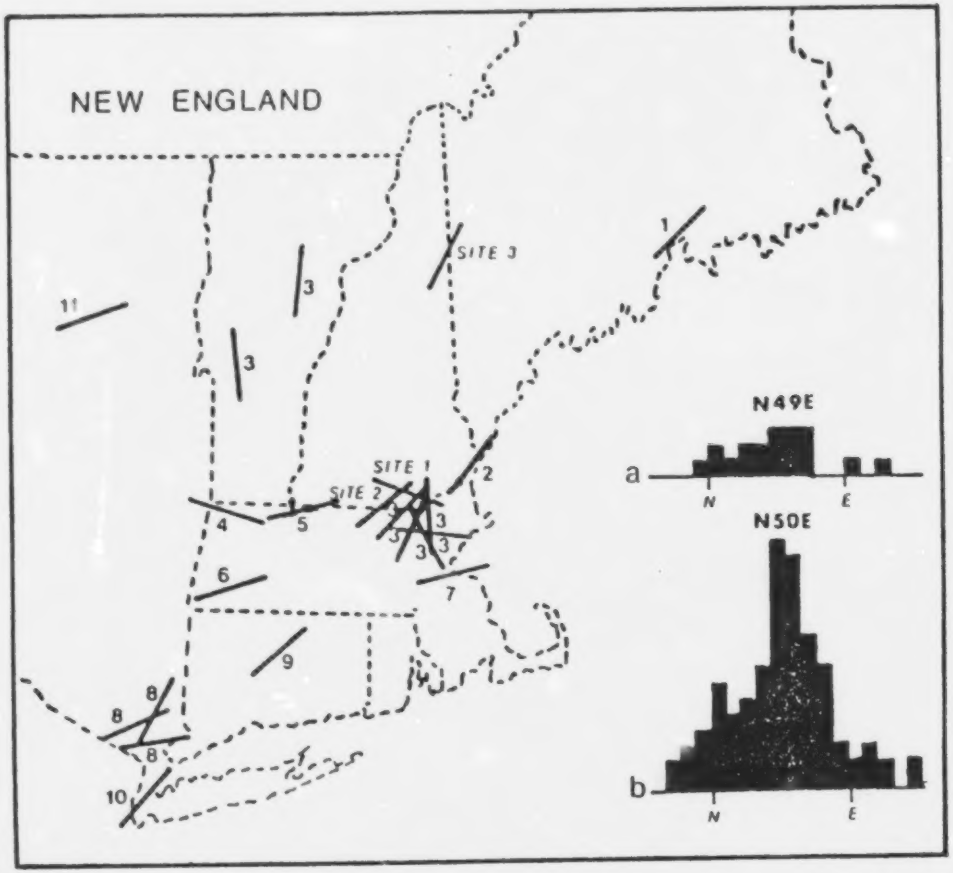

Map of near-surface maximum compressive stress for New England and eastern New York. All data come from overcoring measurements. Inset histograms: (*a*) site average data and (*b*) all measurement regardless of site locations. The statistical orientation of near-surface stress is N50° E. Data sources are 1, *Lee et al.* [1979]; 2, *Lindner and Halpern* [1978]; 3, *Hooker and Johnson* [1969]; 4, *Foundation Sciences, Inc.* [1971]; 5, *Northeast Nuclear Energy Co.* [1974]; 6, *Engelder* [1984]; 7, R. Plumb (unpublished data, 1979); 8, *Dames and Moore* [1977]; 9, *Nataraja* [1977]; and 10, *Ciancia et al.* [1979].

FIGURE 18

NEW ENGLAND - NEAR SURFACE STRESS ORIENTATIONS
(NOTE: STANDARD DEVIATIONS OF MEASUREMENT IS 33°)
FROM PLUMB et al, 1984

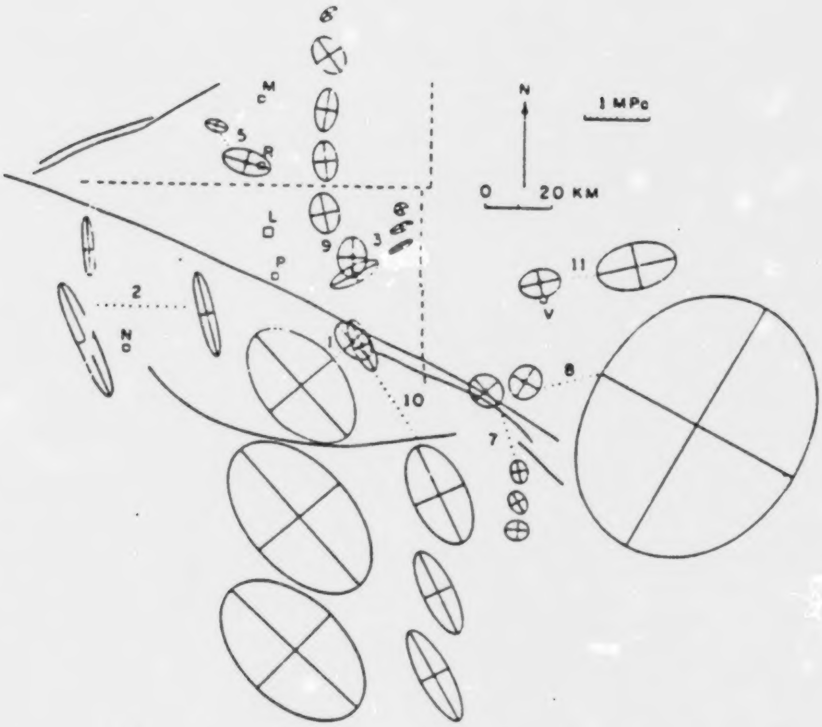

Map of a portion of the southern California uplift, showing all of the data and the averages of the stress directions and aspect ratios of the stress ellipses. The location of each site is shown by a dot in the center of the average stress ellipse axes. The site numbers are shown adjacent to the dotted line that connects the average measurement to the individual ones that contribute to it. For each site the individual measurements are arranged with the one closest to the top of the hole above the ones that were successively below it. The scale for the magnitudes of the stress applies to the individual measurements, but the average measurements have been scaled so all the average ellipses would have the same area. The towns of Newhall, Palmdale, Lancaster, Rosemond, Mojave, and Victorville are shown, as are the county lines (dashed) that separate Los Angeles, Kern, and San Bernadino counties. The San Andreas and associated faults trend WNW across the center of the figure, and a portion of the Garlock fault is in the northwest corner.

FIGURE 19

SAN ANDREAS FAULT - NEAR SURFACE STRESS ORIENTATIONS FROM TULLIS, 1981

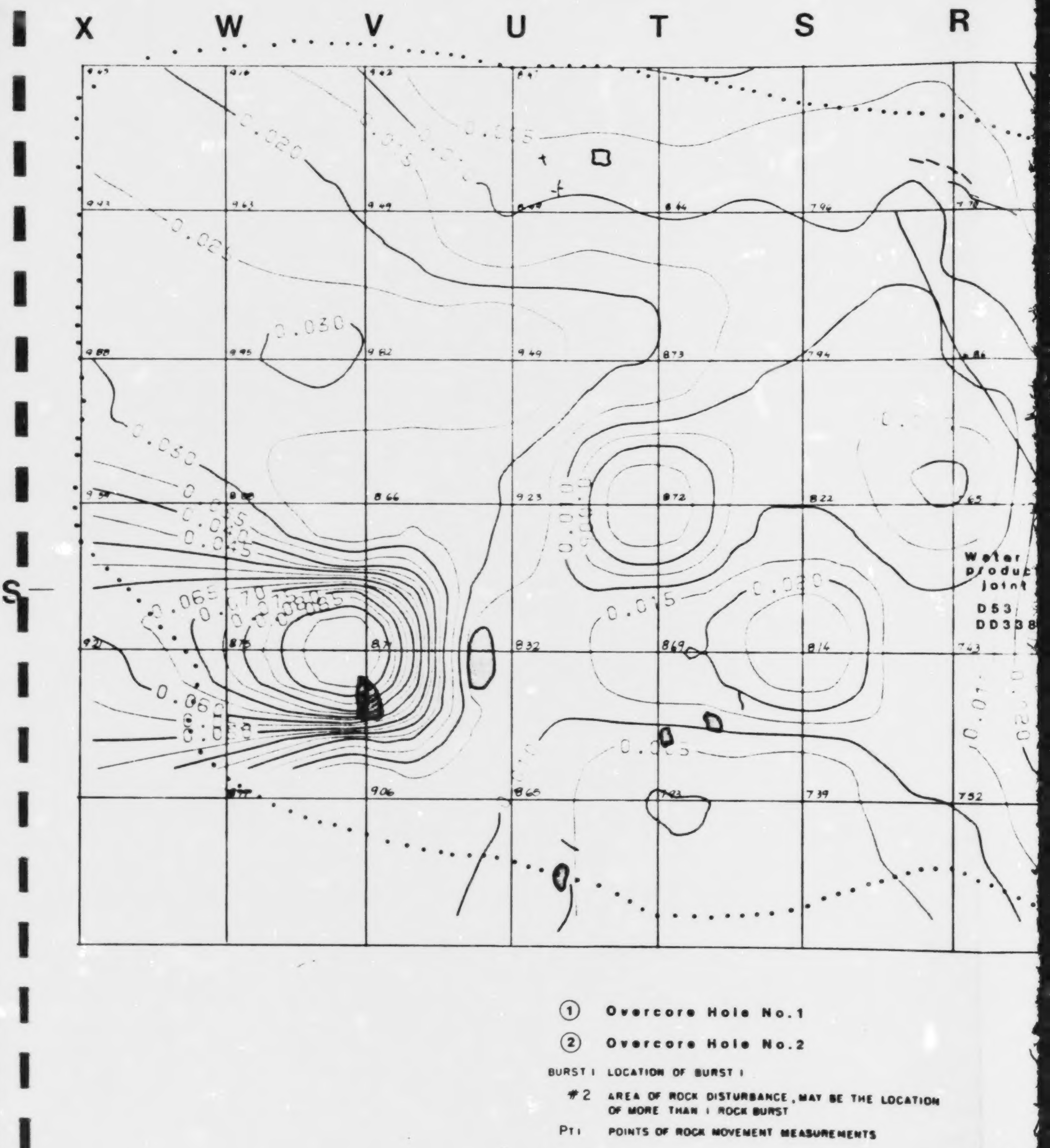
X
W
V
U
T
S
R
S
0.020
0.015
0.015
0.025
0.030
0.030
0.035
0.040
0.045
0.065
0.070
0.075
0.080
0.085
0.060
0.010
0.015
0.030
0.005
0.020
949
916
942
943
963
949
864
796
988
995
982
949
873
794
866
923
872
822
765
875
871
832
869
814
743
906
865
739
752
Water
product
joint
D53
DD338

① Overcore Hole No.1

② Overcore Hole No.2

BURST 1 LOCATION OF BURST 1

#2 AREA OF ROCK DISTURBANCE, MAY BE THE LOCATION OF MORE THAN 1 ROCK BURST

PT1 POINTS OF ROCK MOVEMENT MEASUREMENTS

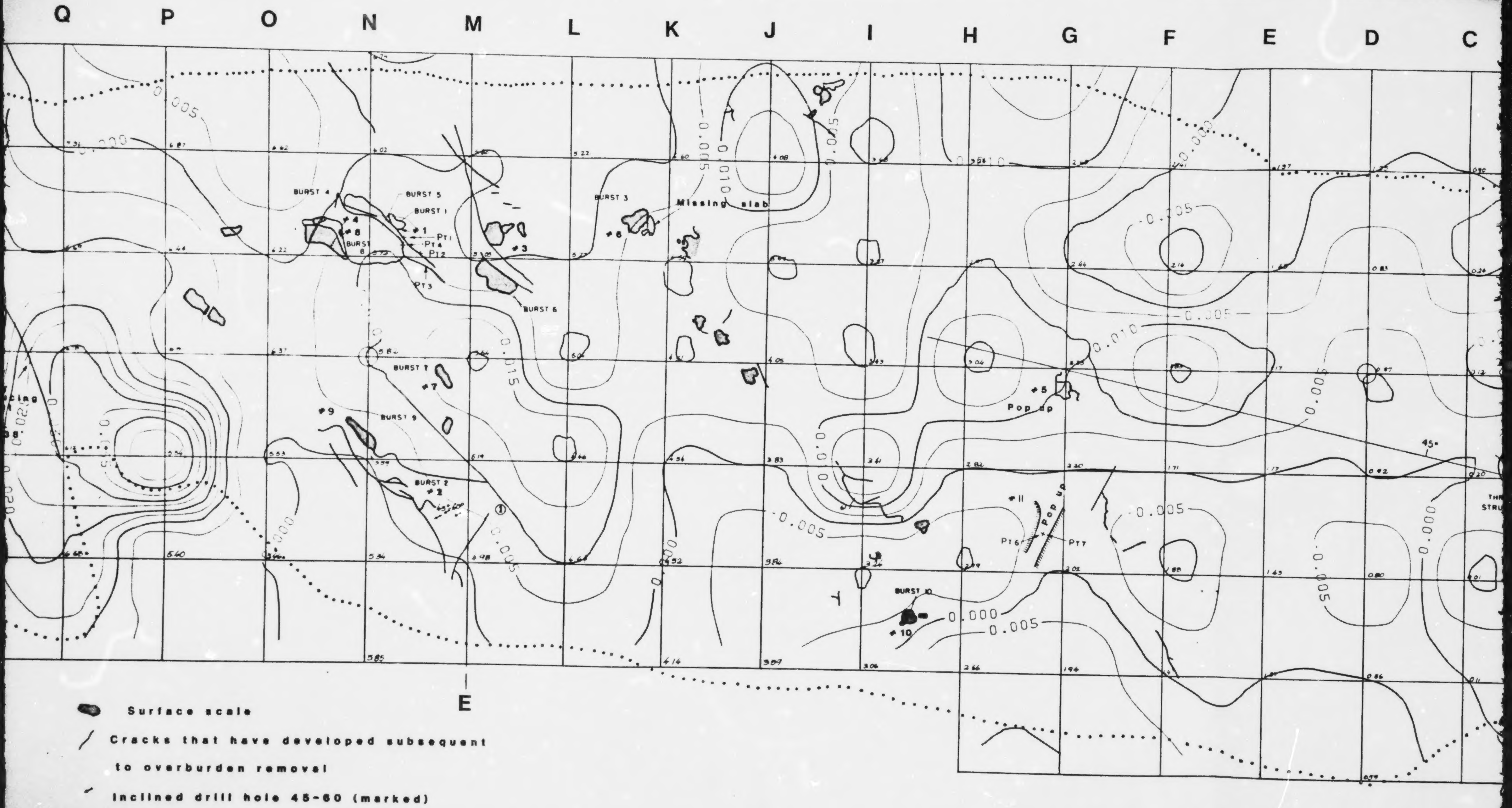
Q P O N M L K J I H G F E D C
BURST 1
BURST 2
BURST 3
BURST 4
BURST 5
BURST 6
BURST 7
BURST 8
BURST 9
BURST 10
#1
#2
#3
#4
#5
#6
#7
#8
#9
#10
#11
PT1
PT2
PT3
PT4
PT6
PT7
Missing slab
Pop up
Pop up
45°
0.000
0.005
0.010
0.015
0.020
-0.005
E
Surface scale
Cracks that have developed subsequent to overburden removal
Inclined drill hole 45-60 (marked)

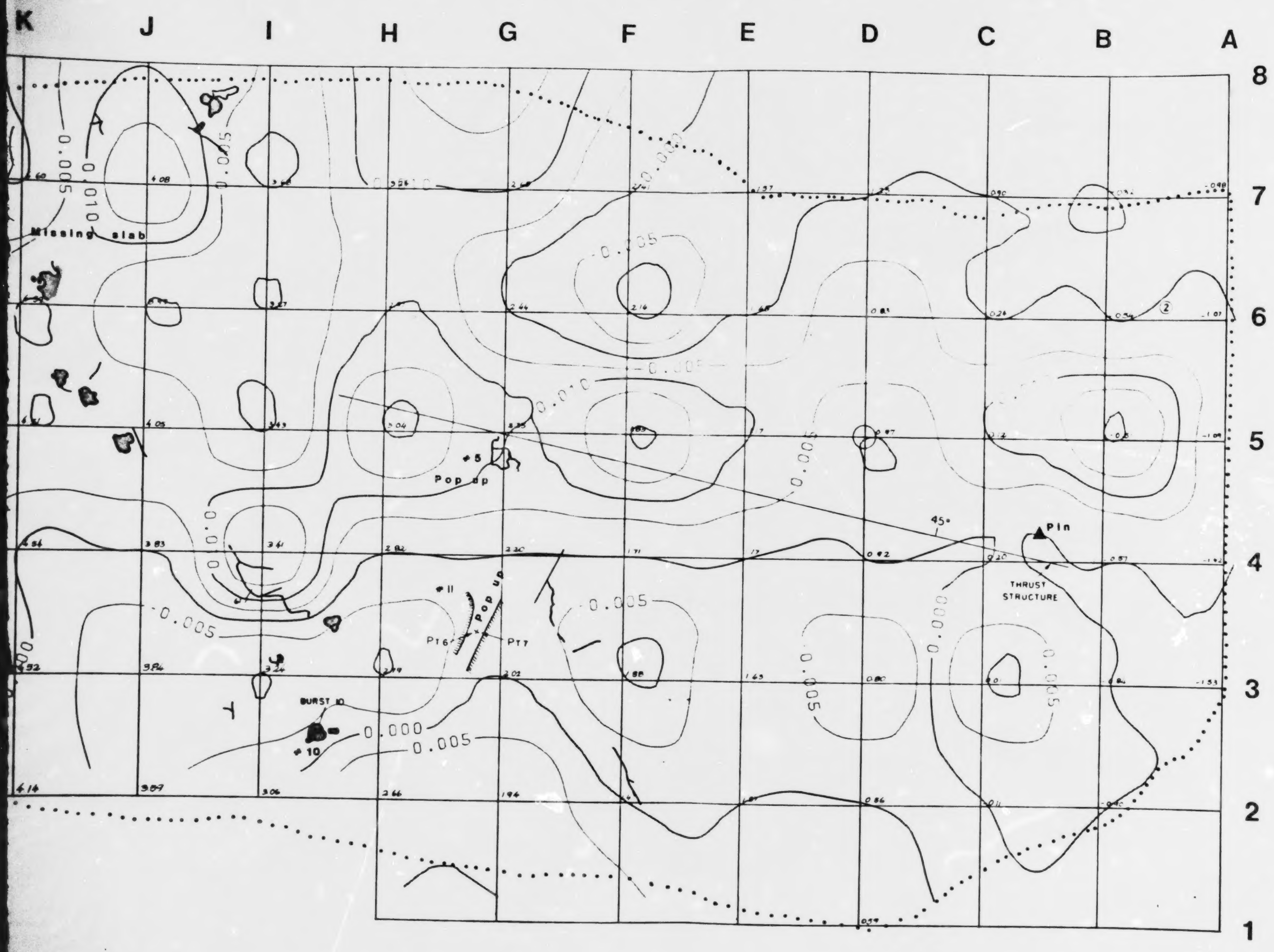
K
J
I
H
G
F
E
D
C
B
A
8
7
6
5
4
3
2
1
Missing slab
0.005
0.010
0.005
-0.005
-0.005
-0.010
0.010
0.000
-0.005
0.005
0.000
0.005
Pop up
#5
#11
Pop up
PT6
PT7
BURST 10
#10
45°
Pin
THRUST STRUCTURE
②

NOTE:CONTOURS REPRESENT ELEVATION CHANGE

BETWEEN JUNE 1983 AND AUGUST 1984

— N

FIGURE 20

MIRAMICHI

EARTHQUAKE PROJECT

MAP OF MAIN OUTCROP

0 5
SCALE(m)

ELEVATION IN METERS RELATIVE TO PIN.

· · · · · APPROXIMATE OUTCROP BOUNDARY.

As observed July 5&6 and August 1 1984

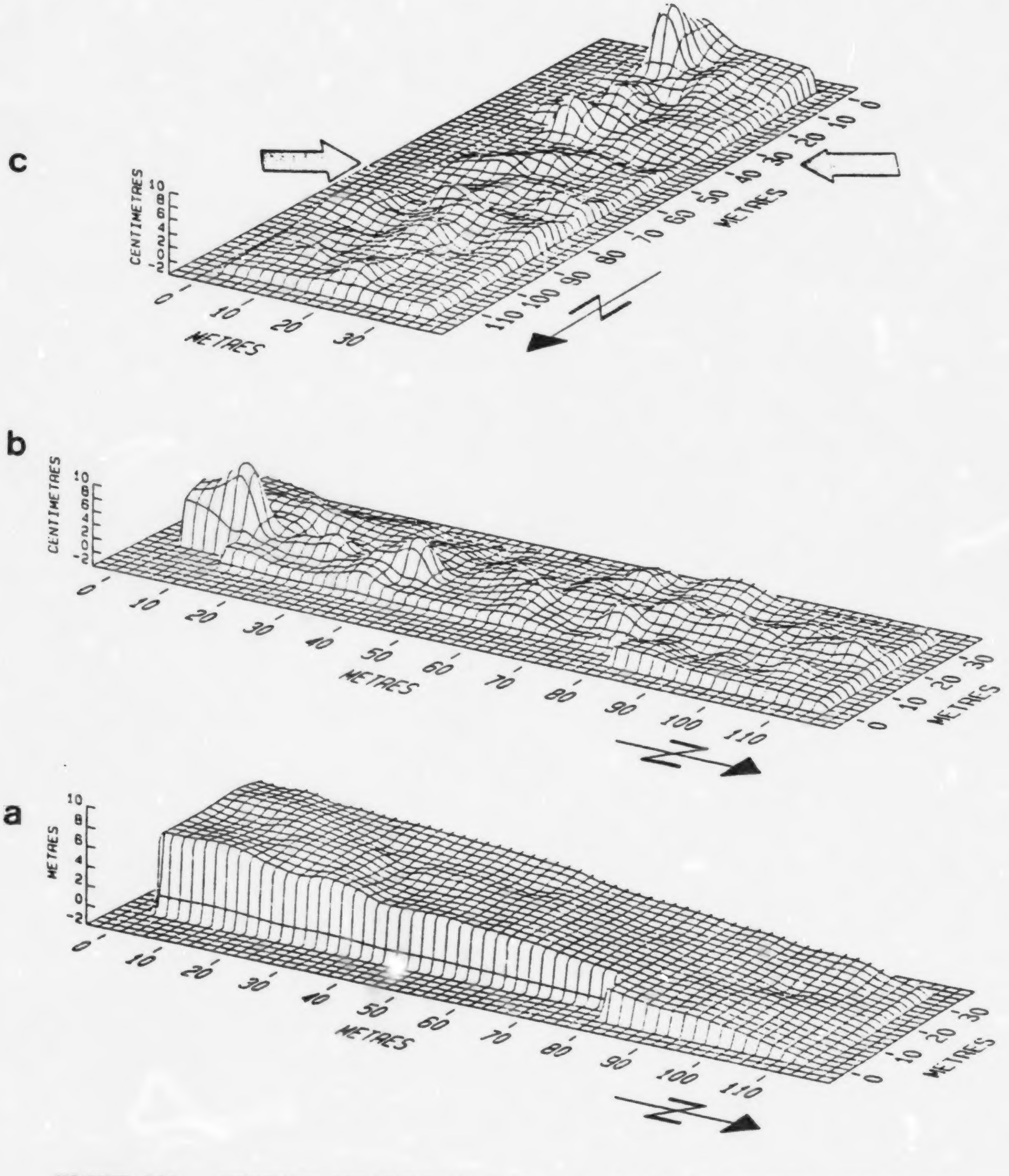

FIGURE 20A: SURVEYED DEFORMATION OF THE INDIAN LAKE OUTCROP, MIRAMICHI, NEW BRUNSWICK. The trend surface indicated in 'a' is modelled on elevations in metres from the 1983 survey data points located on the outcrop. The surface illustrated in 'b' is on the differential values in centimetres determined from 1984 relevelling, viewed from 050°. The same surface is shown in 'c', viewed from 330°. The general orientation of the measured maximum horizontal compressive stress, P, is shown by broad arrows in 'c'. (Survey data provided by J.J. Chandra, NBDNR).

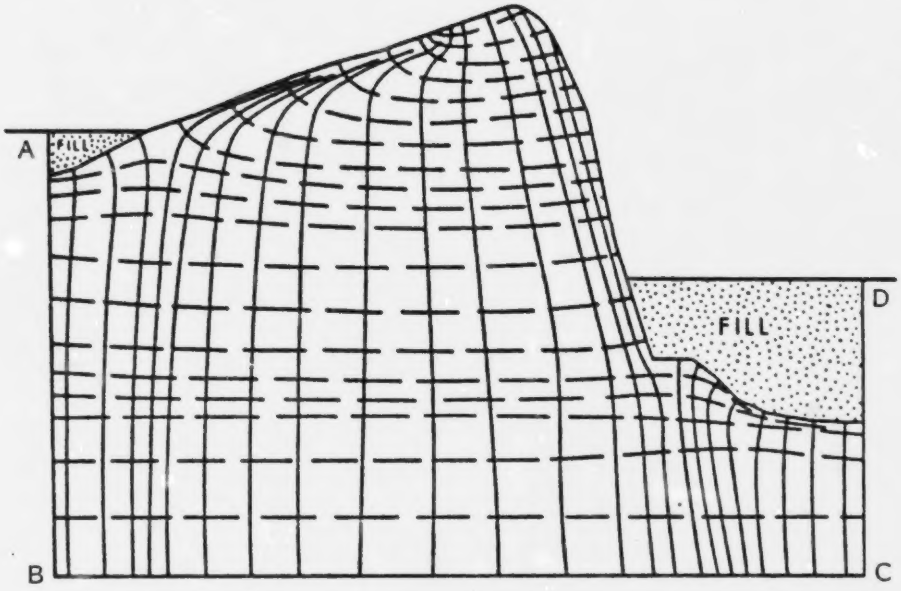

A
FILL
B
D
FILL
C

FIGURE 21

STRESS-TRAJECTORIES IN A HILL DUE TO GRAVITY
(FROM JAEGERAND COOK, 1979)

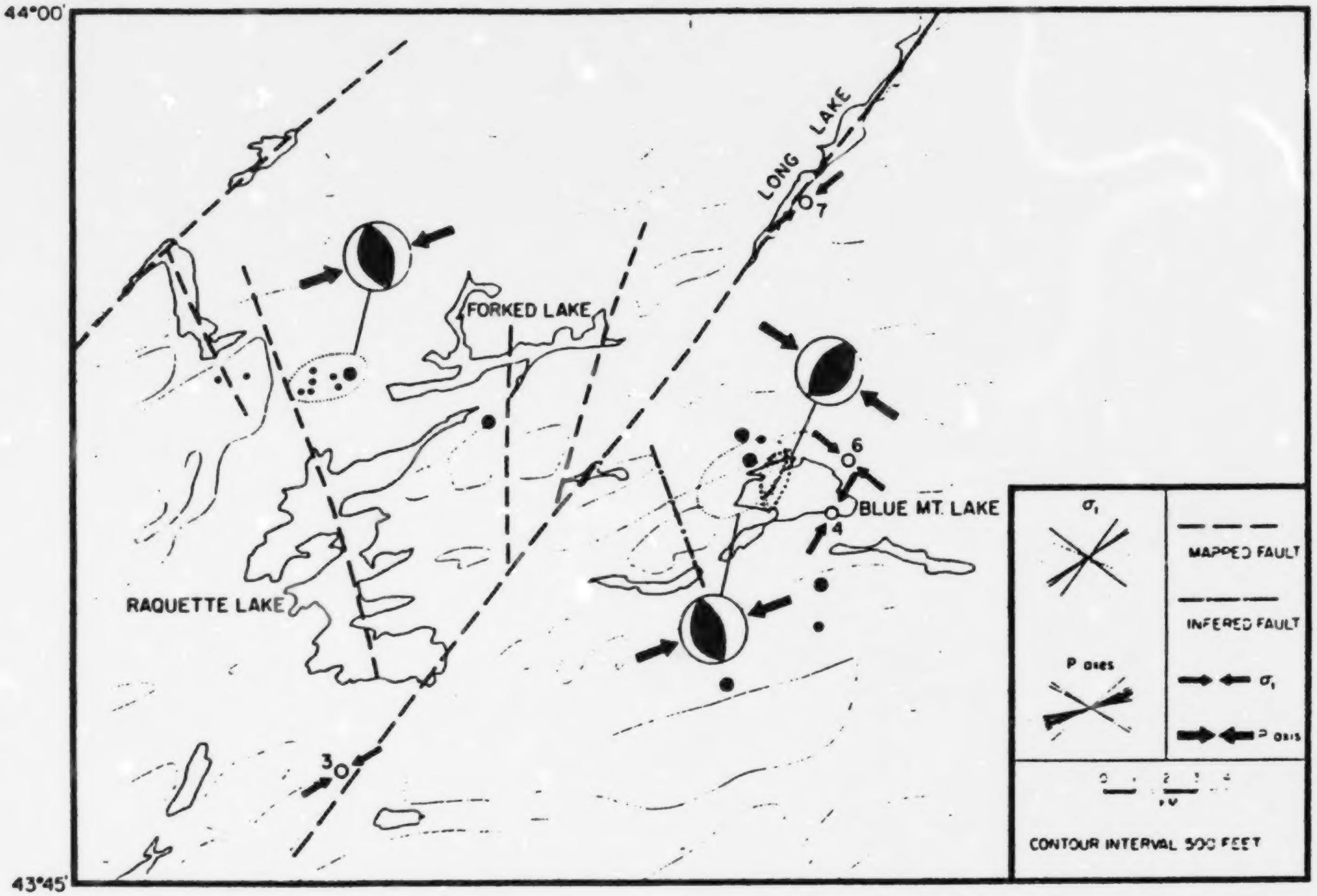
74°45'
74°30'
74°5
44°00'
43°45'
LONG LAKE
FORKED LAKE
RAQUETTE LAKE
BLUE MT. LAKE
7
6
4
3
σ_1
P axes
MAPPED FAULT
INFERED FAULT
σ_1
P axis
CONTOUR INTERVAL 500 FEET

Comparison of measured stress (small arrows) and inferred stress from fault plane solutions (FPS, larger arrows) superimposed on a map showing all events located by the New York State array between December 1971 and October 1980; large dots $m_b > 3$, medium dots m_b 2.0–3.0, smaller dots $m_b < 2$; epicentral zones of swarm activity and associated composite FPS near Blue Mountain Lake (dotted outline and hatched zone) [*Sbar et al.*, 1972]; an aftershock zone of the 1975 Raquette Lake earthquake (dotted outline) and associated FPS [*Yang and Aggarwal*, 1981]; mapped faults; and simplified topography (compare with Figure 9). The inset rose diagrams show the azimuthal distribution of σ_1 and p axes for this region. The dotted lines in the σ_1 rose diagram are sites 1, 2, 5, and 9, whereas the solid lines are sites 3, 4, 6, and 7. Notice the similar azimuthal distribution of σ_1 observed by more than one method (solid lines) and that of the p axes. Note also the multiple FPS observed at Blue Mountain Lake.

FIGURE 22

FROM PLUMB ET AL (1984a)

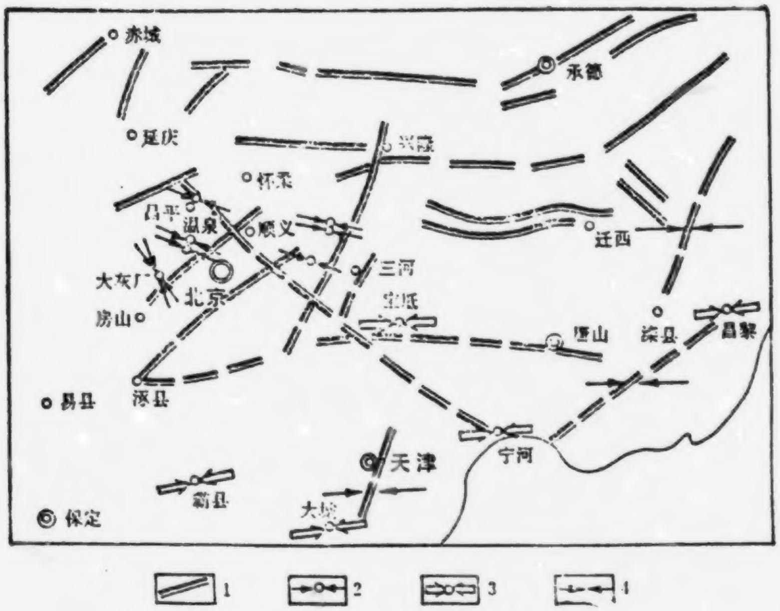
赤城
承德
延庆
兴隆
怀柔
昌平
温泉
顺义
迁西
三河
大灰厂
北京
宝坻
房山
唐山
滦县
昌黎
易县
涿县
宁河
天津
霸县
大城
保定
1
2
3
4

图 1 唐山7.8级地震前主应力方向

1——新生代以来有过活动的断裂；2——实测最大主应力方向；3——释放主应力方向；4——应变主轴方向

FIGURE 23

FROM WANG AND WEI (1984)

Direction of Major Principal Stress Prior to the Magnitude 7.8 Tangshan Earthquake

1. *Faults which have Experience Activity Since the Paleozoic*
2. *Measured Direction of Major Principal Stress*
3. *Direction of Major Principal Stress Relief*
4. *Direction of Major Principal Strain*

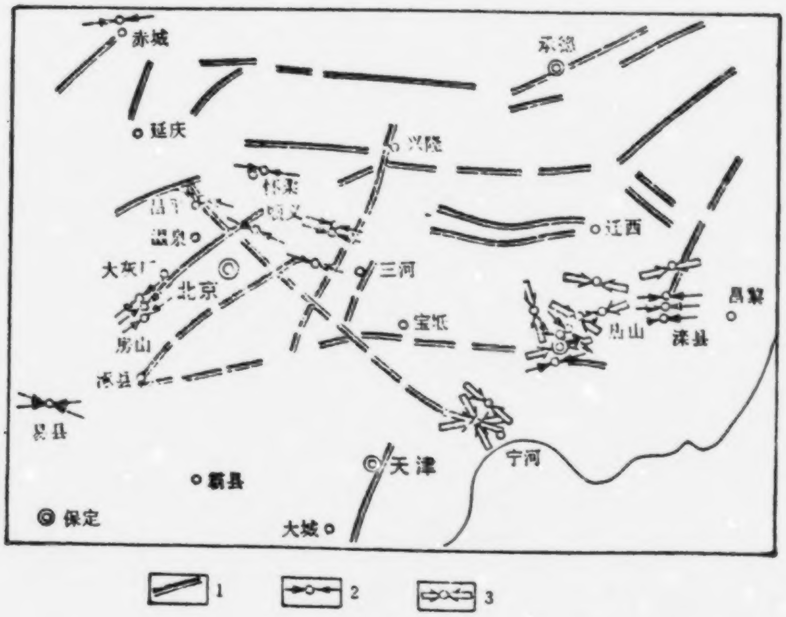
赤城
承德
延庆
兴隆
怀来
昌平
顺义
温泉
迁西
大灰厂
北京
三河
昌黎
宝坻
唐山
滦县
房山
涿县
易县
宁河
天津
霸县
保定
大城
1
2
3

图 2 唐山7.8级地震后主应力方向图
1——新生代以来有过活动的断裂；2——实测最大主应力方向；3——释放主应力方向

FIGURE 24

FROM WANG AND WEI (1984)

Major Principal Stress Orientations After the Magnitude 7.8 Tangshan Earthquake

1. *Faults which have Experienced Activity Since the Paleozoic*
2. *Measured Direction of Major Principal Stress*
3. *Direction of Major Principal Stress Relief*

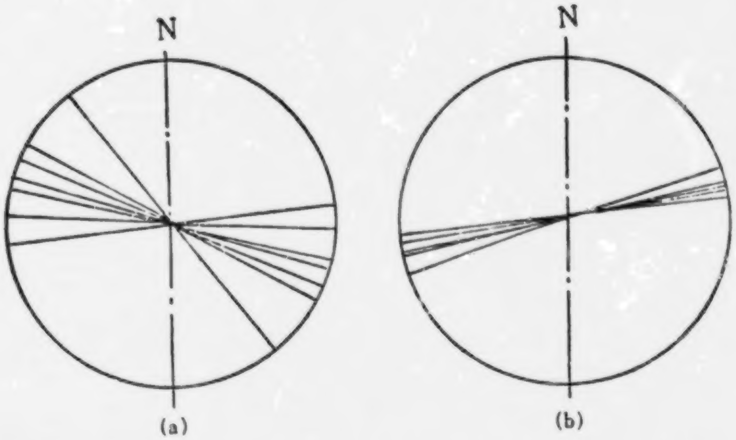

图 3 唐山7.8级地震前京津唐地区原地应力测量最大主应力方向(a)与地震释放主压应力方向(b)的对比

FIGURE 25

FROM WANG AND WEI (1984)

a) Measured Orientations of the Major Principal In-Situ Stresses in the Beijing-Tientsin-Tangshan Region Prior to the Magnitude 7.8 Tangshan Earthquake

b) Orientations of Principal Stress Relief Due to the Earthquake

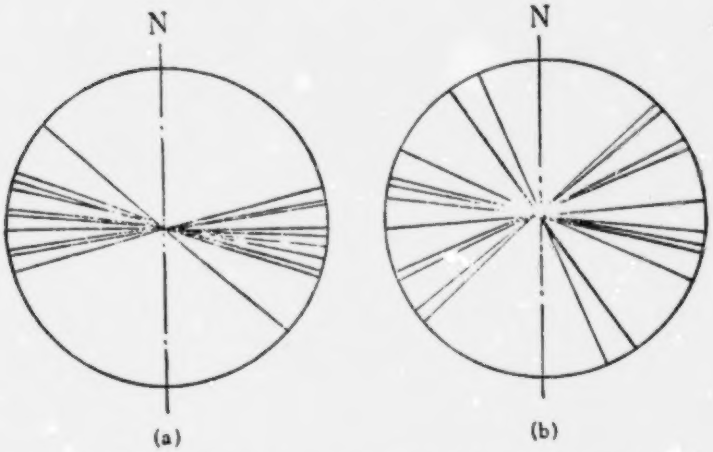

图 4 唐山7.8级地震后原地应力测量最大主应力方向(a)与余震释放主应力方向(b)的对比

FIGURE 26

FROM WANG AND WEI (1984)

a) Measured Orientations of the Major Principal In-Situ Stresses After the Magnitude 7.8 Tangshan Earthquake

b) Orientations of Principal Stress Relief Due to the Aftershocks

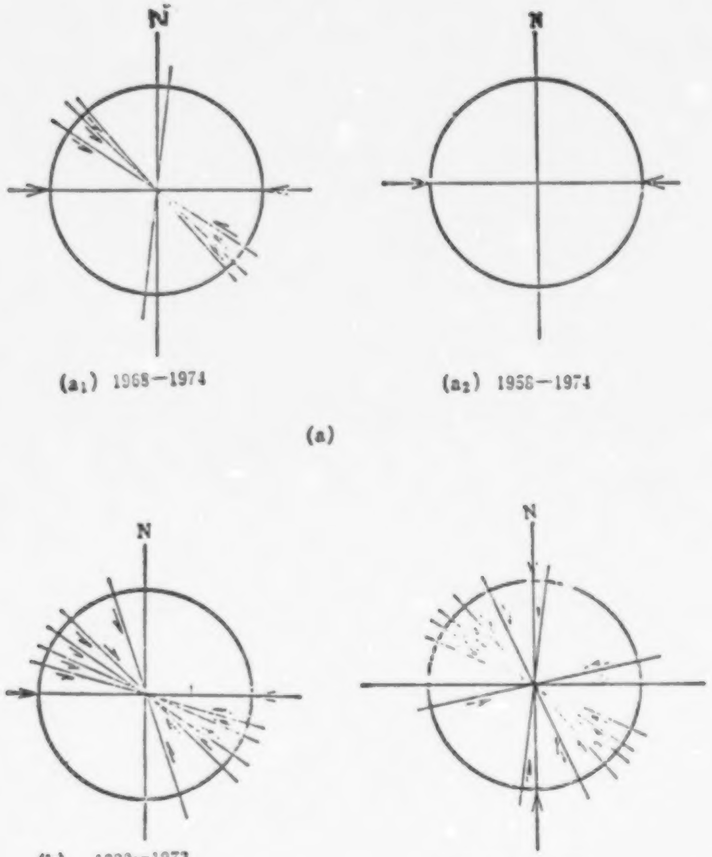

(a_1) 1968—1974

(a_2) 1958—1974

(a)

(b) 1920—1973

(c) 1971—1979

图 4

a_1——甘、青、川、滇断层扭动组合关系；a_2——主压应变方向；b——甘、青、川、滇地震形变带扭动组合关系；c——甘、青、川、滇断层扭动组合关系

FIGURE 27

FROM ZHIN (1984)

- *a1. Pattern of Fault Motion in the Provinces of Kansu, Tsinghai, Szechwan and Yunnan 1968-1974*
- *a2. Direction of Principal Strain 1958-1974*
- *b. Pattern of Fault Motion in the Earthquake Deformation Zone in the Provinces of Kansu, Tsinghai, Szechwan and Yunnan 1920-1973*
- *c. Pattern of Fault Motion in the Provinces of Kansu, Tsinghai, Szechwan, and Yunnan 1971-1979*

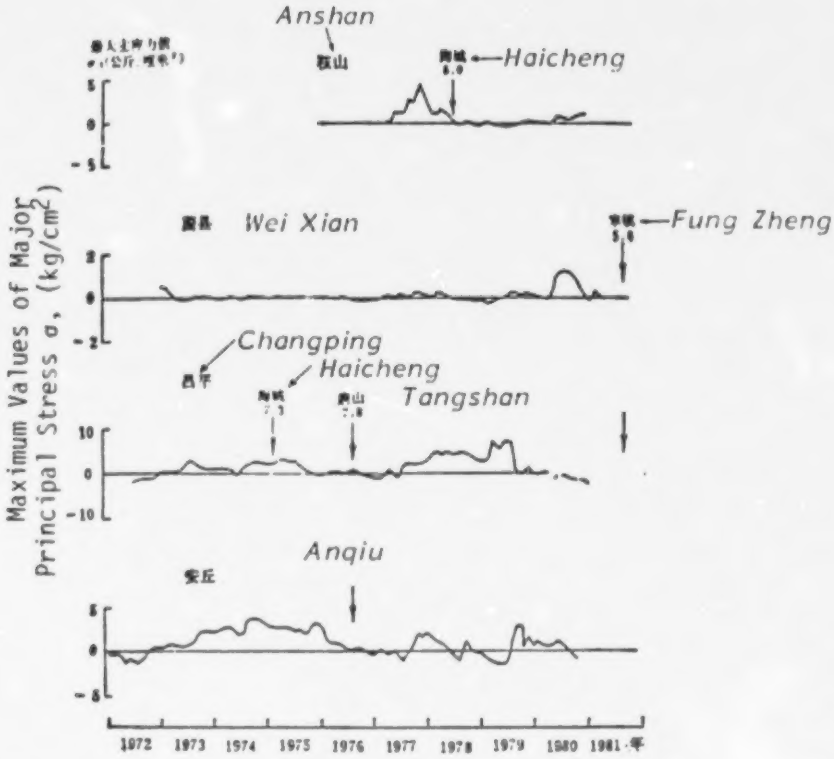

图 1 华北地区部分台站应力曲线

FIGURE 28

FROM YI AND GE (1984)

Stress Changes at Some Stations in North China Region

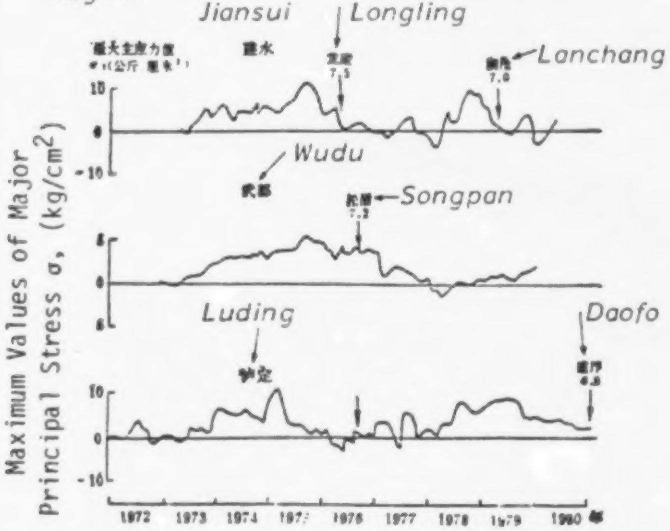

图 2 西南地区部分台站应力曲线

FIGURE 29

FROM YI AND GE (1984)

Stress Changes at Some Stations in the South-Western Region

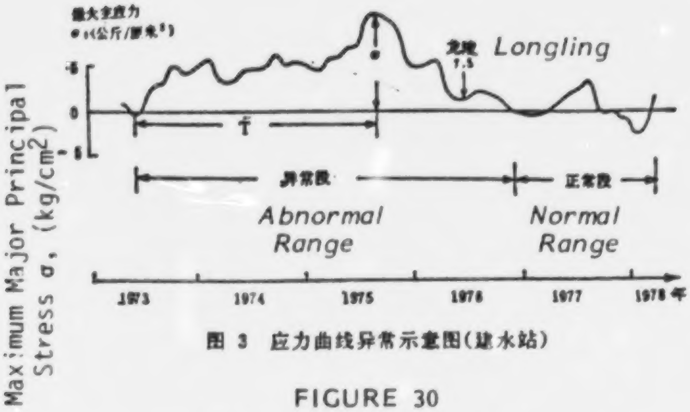

FIGURE 30

FROM YI AND GE (1984)

Schematic Diagram Showing the Unusual Change in Stress (Jinshu Station)

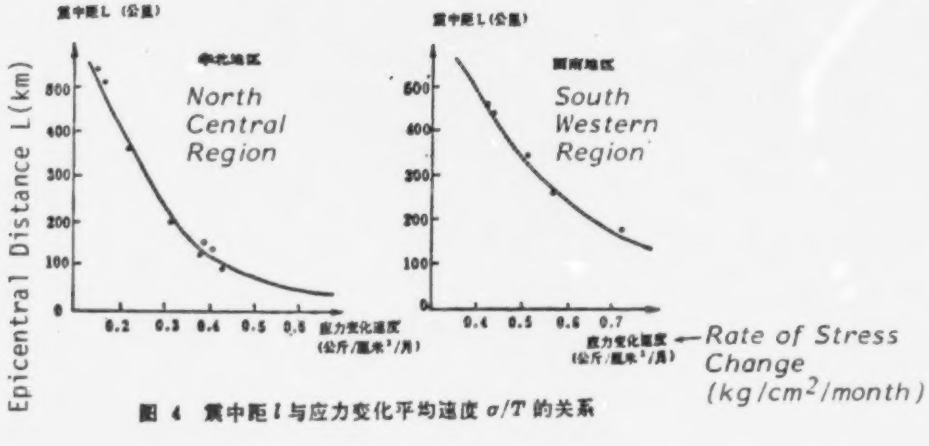

FIGURE 31

FROM YI AND GE (1984)

Relationship Between Epicentral Distance (L) and Rate of Stress Change (σ/T)

APPENDIX 1

UNITED STATES BUREAU OF MINES BOREHOLE DEFORMATION GAUGE TEST METHOD

THE UNITED STATES BUREAU OF MINES BOREHOLE DEFORMATION GAUGE TEST METHOD

The United States Bureau of Mines Borehole Deformation Gauge (USBM gauge) was chosen to measure the stresses existing in rock masses and concrete structures because past experience has shown it to be a reliable instrument. The method consists of drilling an HQ hole (diameter 97.5 mm), drilling a 10 cm long E pilot hole (diameter 38.1 mm), extending the E hole to approximately 60 cm in length, placing the USBM gauge into the hole and then overcoring the gauge with a thin wall bit. Strain readings are taken during this overcoring for each 13 mm of bit advance.

The accuracy for this test method claimed by the US Bureau of Mines is that the stresses measured are within 15% of actual stresses in concrete and slightly better in rock.

TEST THEORY

Strain relief measurements are made along three separate axes which form a 60° strain rosette. After the downhole testing is completed, the overcore is recovered and subjected to testing in a biaxial chamber to determine the Young's modulus of the material. This result is combined with the downhole strain relief measurements to calculate the secondary principal stresses existing in the plane perpendicular to the borehole axis. The maximum secondary principal stress (P) and the minimum secondary principal stress (Q) are termed secondary because they represent the maximum and minimum stress in one plane within a three dimensional rock mass. The relationship of P,Q and θ is shown in Figure 1. Three non-parallel boreholes would be required to completely define the three dimensional stress field using this test method.

The analytical method used to calculate the stresses is based on elastic thick wall cylinder theory using a 60° strain rosette solution. The equations used are:

$$P = \frac{E}{(1-\nu^2)d} \quad [U_1+U_2+U_3+\frac{1}{\sqrt{2}}\ [(U_1-U_2)^2 + (U_2-U_3)^2+(U_3-U_1)^2]^{1/2}]$$

$$Q = \frac{E}{(1-\nu^2)d} \quad [U_1+U_2+U_3-\frac{1}{\sqrt{2}}\ [(U_1-U_2)^2 + (U_2-U_3)^2+(U_3-U_1)^2]^{1/2}]$$

$$\theta = 1/2 \tan^{-1} \frac{\sqrt{3}\ (U_2-U_3)}{2U_1-U_2-U_3}$$

where P is the major secondary principal stress
Q is the minor secondary principal stress
θ is the angle measured from gauge axis U_1 to P in a counter-clockwise direction
E is the Young's Modulus of elasticity of the rock in which the measurement was made (Note: refer to Biaxial Testing Section for a description of this test method)
ν is the Poisson's ratio of the rock
d is the diameter of the borehole in which the gauge was placed
U_1, U_2, U_3 - are the strains measured along the three gauge axes and are positive for an increasing diameter

Deformation Curves

Prior to the computation of the stresses, the test data is plotted to ensure that no unusual downhole behaviour such as drill vibration is misinterpreted as actual strain relief. An example of these curves which plot deformation versus the depth of bit is given in Figure 2.

GAUGE PLACEMENT AND ORIENTATION

The placement of the gauge is accomplished by means of a series of keyed aluminum rods that attach to a placing tool (Figure 3). The gauge is fastened to the placing tool and lowered into the HQ hole until just above the E hole. Prior to the placement of the gauge the wall of the E pilot is scribed using the scribing tool shown in Figure 4. The hardened steel point is aligned with a scope mounted on top of the rods before it is pushed into the hole as shown in Figure 4. The mark enables proper orientation of the gauge in the core during the biaxial test to determine the Young's Modulus of Elasticity of the core in the same directions as the downhole strain readings were made. The scope, as shown in Figure 5, is used to sight a predetermined reference point so that the azimuth of P can be calculated. The gauge is aligned in the same manner.

Drilling Procedure

The drilling procedure for this test makes use of a modified wire line system that was developed by Longyear Canada during several projects at or near the Darlington NGS site. A crawler mounted CME drill equipped with a hydraulic chuck is used as this requires a drill set up time of less than one half day. The hydraulic chuck enables the rods to be easily centered in the hole each time. The drill set up is shown in Figure 6.

The procedure used in preparing the hole for an overcore test is outlined below. The sequence of operations is shown in Figure 7.

1) The hole is advanced to a depth that is 20cm above the predetermined test depth by normal wire line drilling practice using an HQ bit.

2) The HQ standard HQ inner barrel assembly is removed and replaced by a modified assembly that is shown in Figures 8-11. The barrel does not rotate and enables this barrel to be used to drill the E hole.

3) A 10 cm (4 in) E starter barrel is attached to the inner tube and lowered into the hole. A 10 cm starter hole is drilled after the H rods are pulled back approximately 15 cm to ensure the core barrel dogs are engaged.

4) The inner barrel assembly is removed and the starter barrel is replaced by a 60 cm E core barrel. After encountering difficulty in obtaining E core that indicated natural discontinuities and breaks in the rock as opposed to breaks that are caused by drilling, it was decided to switch from a single barrel E core to an IEWS barrel that is shown in Figures 10 and 11. The IEWS barrel has an inner tube that is free to swivel and greatly reduces core breakage due to vibration during drilling and enabled a truer estimation of rock conditions to be made. This improvement enables the avoidance of zones of poor rock which would have jeopardized the gauge with a core breakage during the test. In this step, as in step 3, the H rods are raised to engage the dogs on the core barrel to enable drilling of the E hole.

5) The E core is carefully inspected to ensure that it is possible to carry out a test. It is necessary to have at least 20 cm of solid rock below the buttons. These lengths of rock are necessary to ensure that the complete stress relief action of the core can be monitored during the test.

6) The HQ rods are pulled and the HQ bit is replaced by the thin wall industrial core bit.

7) The E hole is scribed with the scriber shown in Figure 4.

8) The gauge is lowered through the water swivel and drive rod, then attached to the placement tool, lowered down the hole, oriented and then pushed into the E hole.

9) The end plug, through which the electrical readout cable is run, is screwed into the water swivel. The readout cable is then connected to the Vishay strainmeters.

10) The gauge is allowed to thermally stabilize in the E hole for five minutes.

11) The drill water pressure and drill speed are adjusted.

12) The overcoring begins with strain readings taken for every 1.27 cm (0.5 in) of bit advance.

13) At the completion of the overcoring the gauge is removed.

14) The H rods are pulled from the hole and the core breaker is lowered down the hole.

15) The core breaker is removed from the hole and the core catcher is lowered to retrieve the core.

16) The overcore is removed and prepared for biaxial testing.

17) The HQ bit and rods are lowered down the hole and the hole is extended down to the next test horizon.

Biaxial Testing

After completion of the down hole overcoring, the core is prepared for testing in the biaxial chamber. The chamber which is shown in Figure 12 consists of a hollow aluminum cylinder lined with a rubber membrane. A known hydraulic pressure is applied with a hand operated hydraulic pump. The pressure in the system is monitored by means of a gauge attached to the pump.

Once the core has been placed into the chamber and the gauge is inserted into the overcore using the scribe mark as an orientation guide, the system is bled of air bubbles. The core is cycled three times and the strains measured by the gauge monitored on the Vishay readouts. This enables the value of Young's modulus of the core to be determined.

The Young's Modulus of Elasticity (E) is calculated using the formula:

$$E = \frac{4ab^2P_0}{(b^2-a^2)U}$$

where a = inner radius of overcore
b = outer radius of overcore
P_0 = applied hydraulic pressure
U = diametral borehole deformation

When the overcore is tested, the E value is determined along each of the three axes and if it is found that the three values E_1, E_2 and E_3 vary by more than 25%, then it is necessary to apply an anisotropic solution to the field test data.

Only two anisotropic elastic constants of the material are necessary for the plane strain evaluation of secondary stresses (Hooker & Johnson, 1969). These parameters are:

$$\alpha_{11} = \frac{1 - \gamma_{13}\ \gamma_{31}}{E_1}$$

$$\alpha_{22} = \frac{1 - \gamma_{23}\ \gamma_{32}}{E_2}$$

where E_i = Young's modulus in the i direction
γ_{ij} = Poisson's ratio in the ij plane

The above subscripts refer to the orthogonal coordinate system defined by the axis of the core and the directions of maximum and minimum Young's modulus in the plane perpendicular to the axis of the core. This procedure avoids errors in the field data that are due to elastic non-linearity in the rock. This method involves many calculations and subsequent laboratory tests. Tullis (1981) found that, by using what he termed an "approximate" anisotropic solution, it was possible to obtain results that varied little from the Hooker and Johnson (1969) solution and yet avoided the cumbersome analysis and testing. This method was applied to all of the tests results to correct for the effect of rock anisotropy. The equation is:

where $U_i^m = U_i(E_i/E)$ i = 1,2,3
E_i = is Young's modulus for each axis
E = is the average Young's modulus for the three axes
U_i = is the deformation for measured on axis i
U_i^m = is the modified deformation on axis i

The modified deformations are then substituted into the original equations, (1), (2) and (3), for P,Q and θ and new values of P,Q and θ are calculated. The results of the biaxial tests are plotted as load versus deformation such as those shown in Figure 13, to ensure that the rock material is behaving elastically. Readings are taken during the loading and unloading portion of each of the three load-unload cycles. The unloading cycle E value is used in stress calculations because this simulates the downhole stress relief of the rock core as it is overcored.

REFERENCES

1. Hooker, V.E. and C.F. Johnson. "Near Surface Horizontal Stresses, Including the Effects of Rock Anisotropy", Rep Invest US Bur Mines 7224, pp 29, 1969.

2. Tullis, T.E. "Stress Measurements Via Shallow Overcoring Near the San Andreas Fault" in "The Mechanical Behaviour of Crustal Rocks, The Handin Volume", Geophysical Monograph 24, American Geophysical Union, 1981.

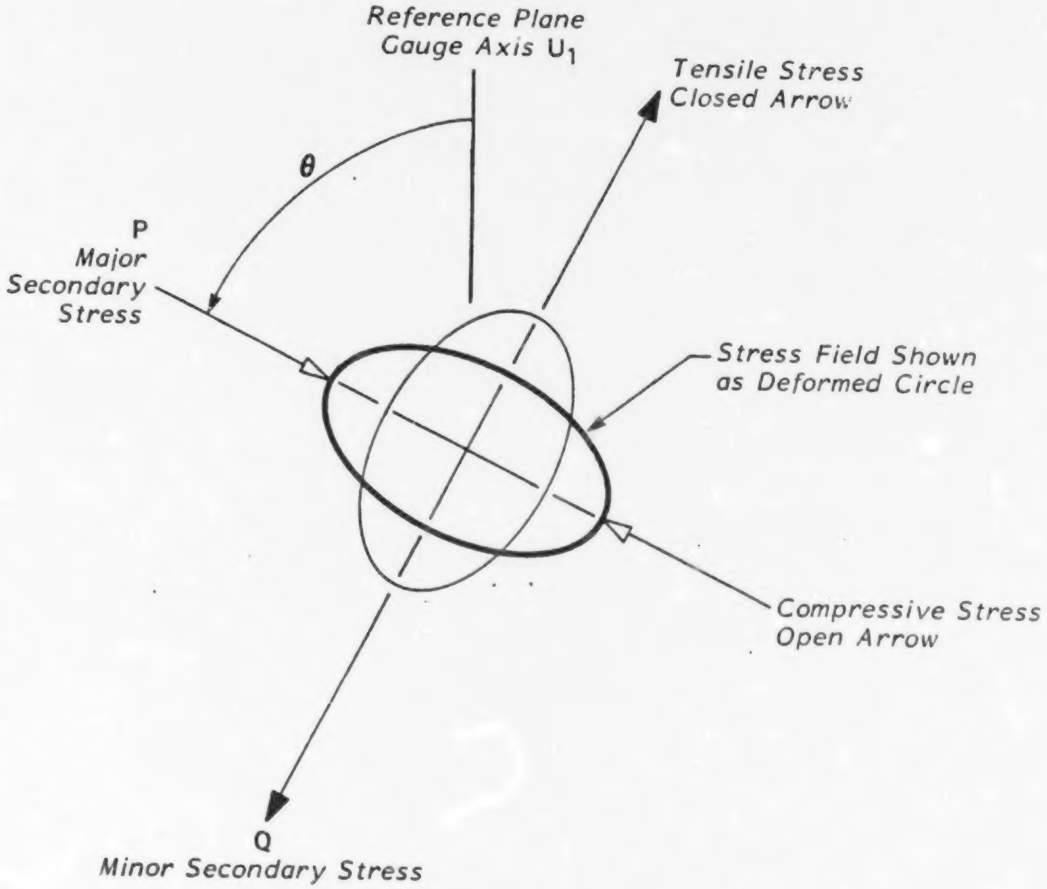
Reference Plane
Gauge Axis U_1
Tensile Stress
Closed Arrow
θ
P
Major
Secondary
Stress
Stress Field Shown
as Deformed Circle
Compressive Stress
Open Arrow
Q
Minor Secondary Stress

FIGURE 1

IN SITU STRESS TERMINOLOGY

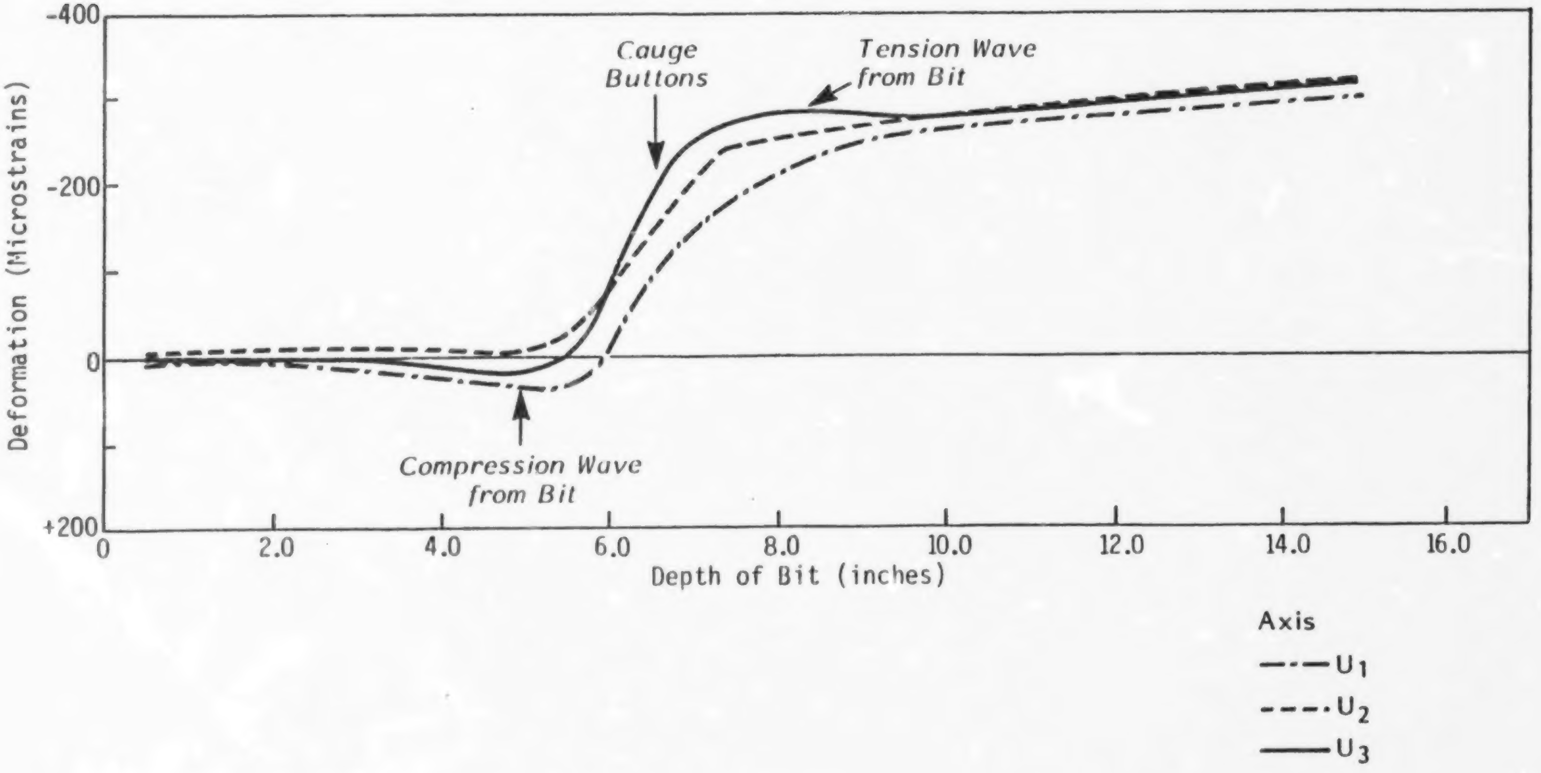

FIGURE 2

TYPICAL DEFORMATION CURVES FROM OVERCORING TEST

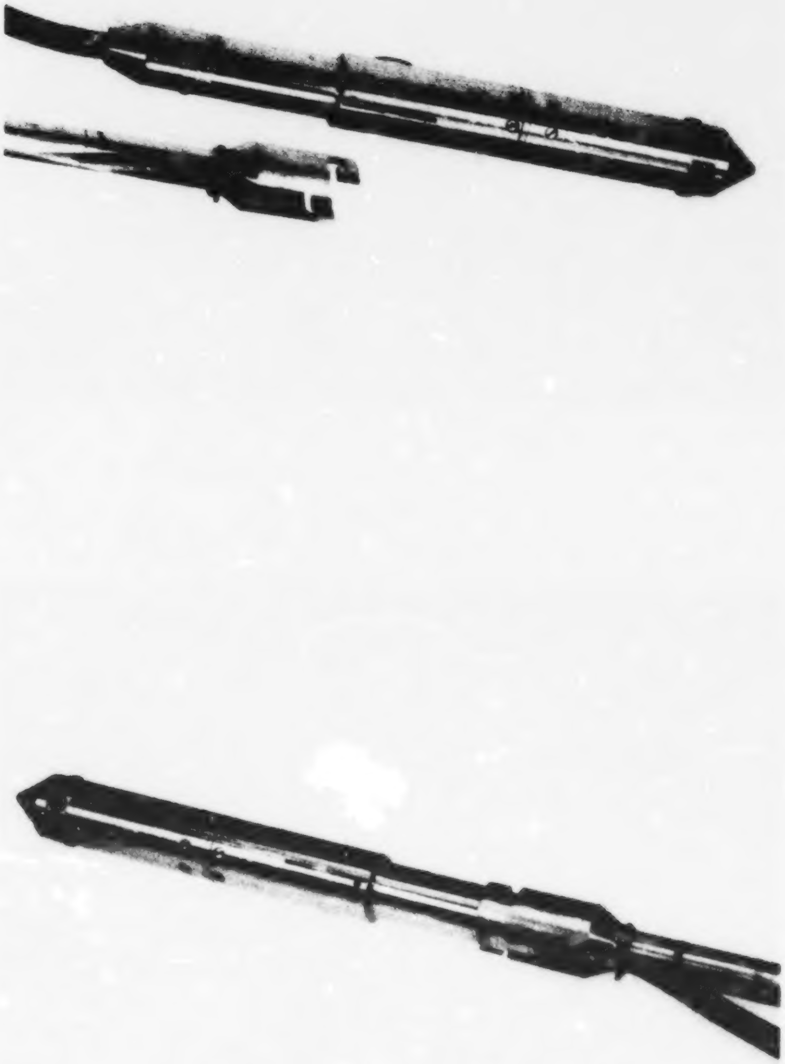

FIGURE 3
PLACING TOOL FOR USBM GAUGE

154528-RD

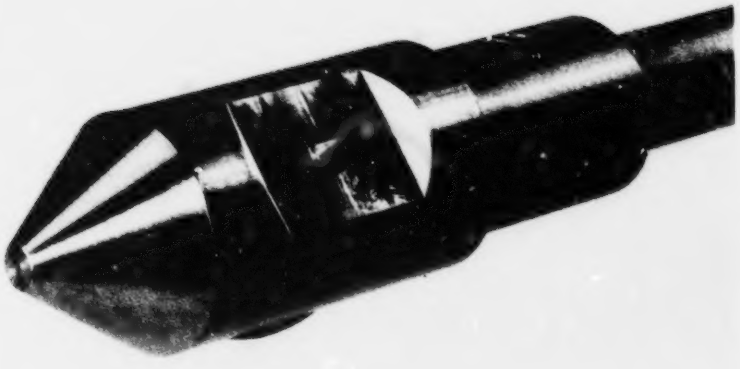

FIGURE 4
STEEL SCRIBING POINT

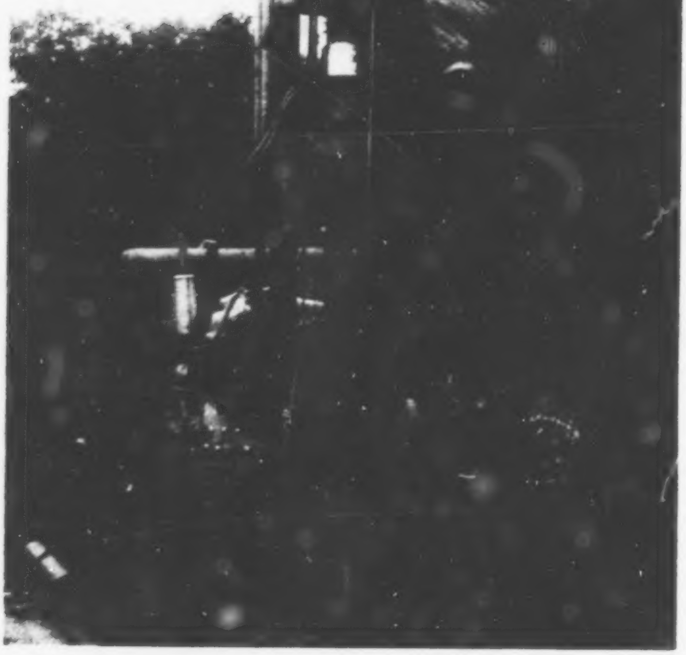

FIGURE 5
ORIENTATION OF THE GAUGE

FIGURE 6

DRILL RIG SET UP FOR OVERCORING

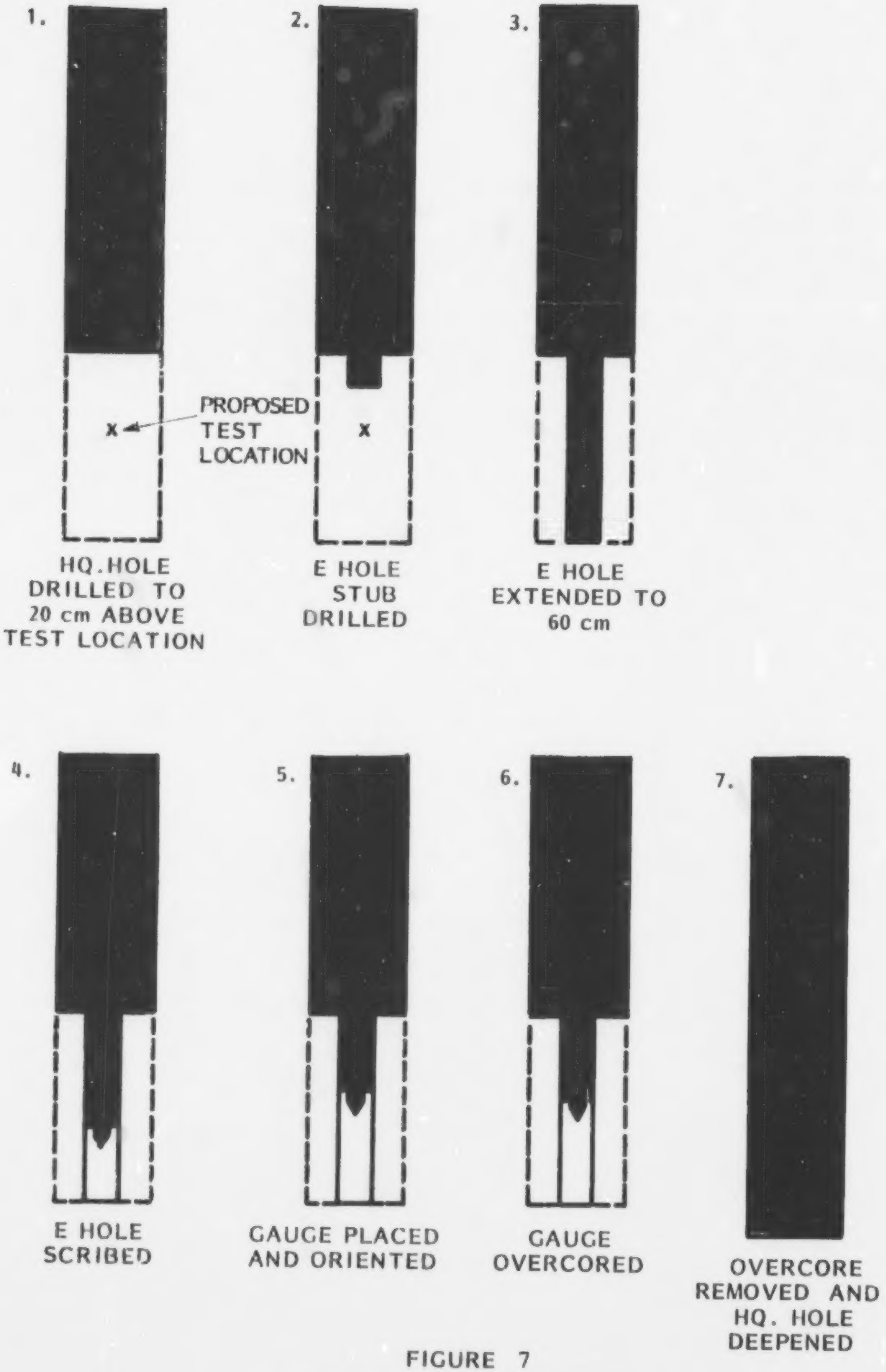
1.
PROPOSED TEST LOCATION
x
HQ.HOLE DRILLED TO 20 cm ABOVE TEST LOCATION
2.
x
E HOLE STUB DRILLED
3.
E HOLE EXTENDED TO 60 cm
4.
E HOLE SCRIBED
5.
GAUGE PLACED AND ORIENTED
6.
GAUGE OVERCORED
7.
OVERCORE REMOVED AND HQ. HOLE DEEPENED

FIGURE 7

SEQUENCE FOR OVERCORE TEST USING HQ. WIRELINE SYSTEM

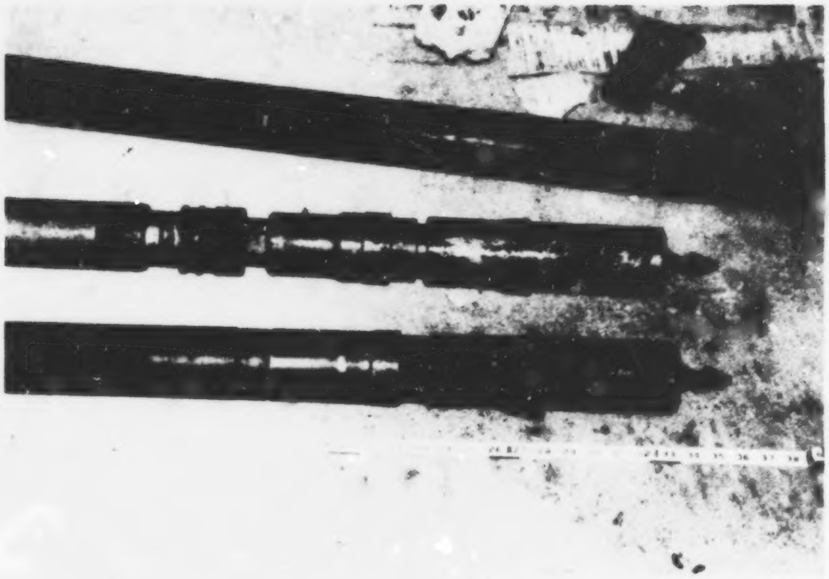

FIGURE 8

TOP STANDARD INNER BARREL ASSEMBLY
BOTTOM MODIFIED INNER BARREL ASSEMBLY

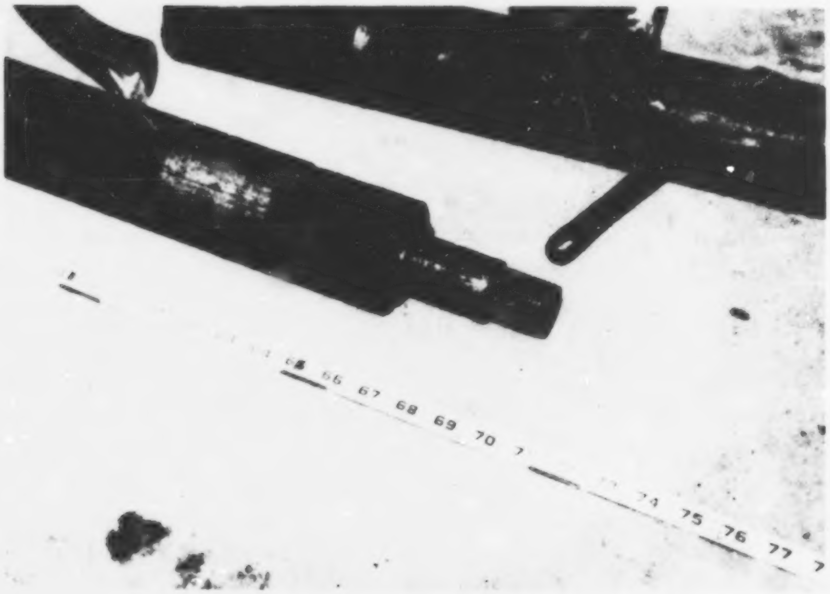

65
66
67
68
69
70
74
75
76
77

FIGURE 9

LOWER END OF MODIFIED INNER
BARREL ASSEMBLY WITH E BARREL
ADAPTOR IN PLACE

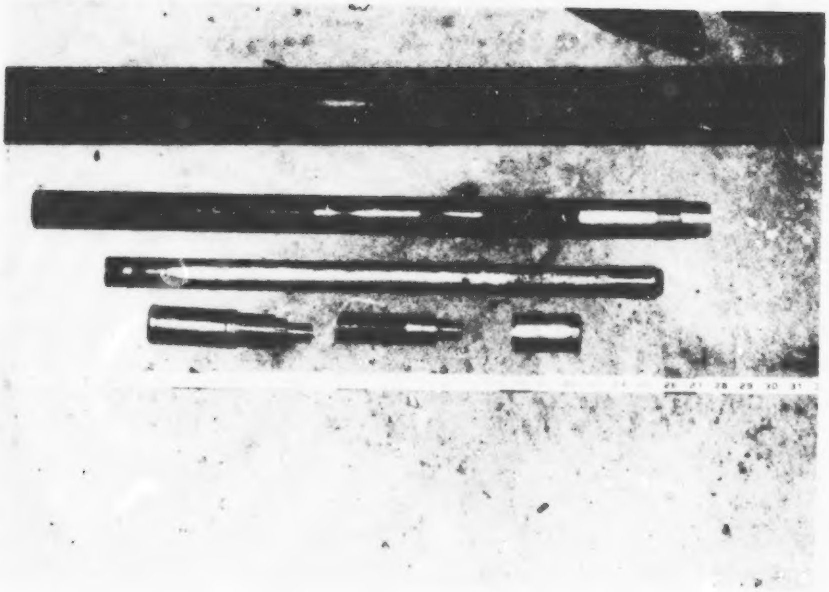

FIGURE 10

DISASSEMBLED IEWS CORE BARREL

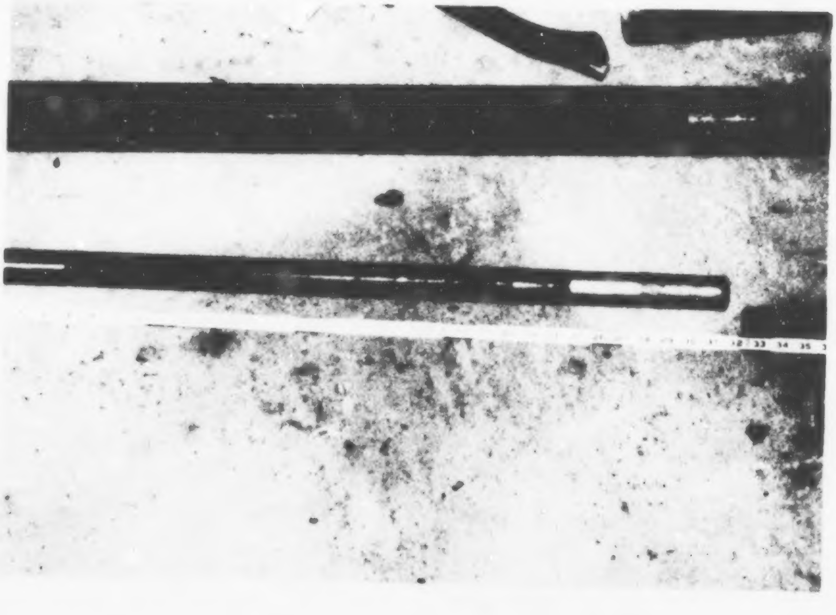

FIGURE 11

ASSEMBLED IEWS CORE BARREL

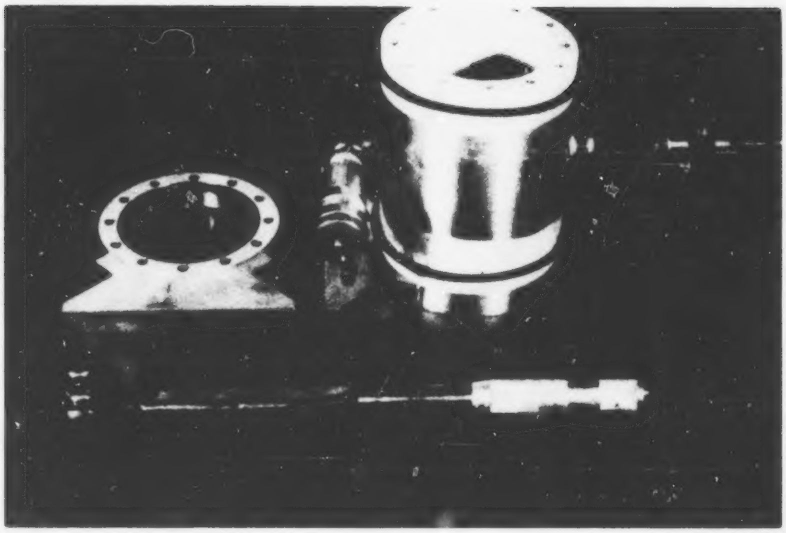

FIGURE 12

BIAXIAL CELL FOR YOUNG'S MODULUS DETERMINATION

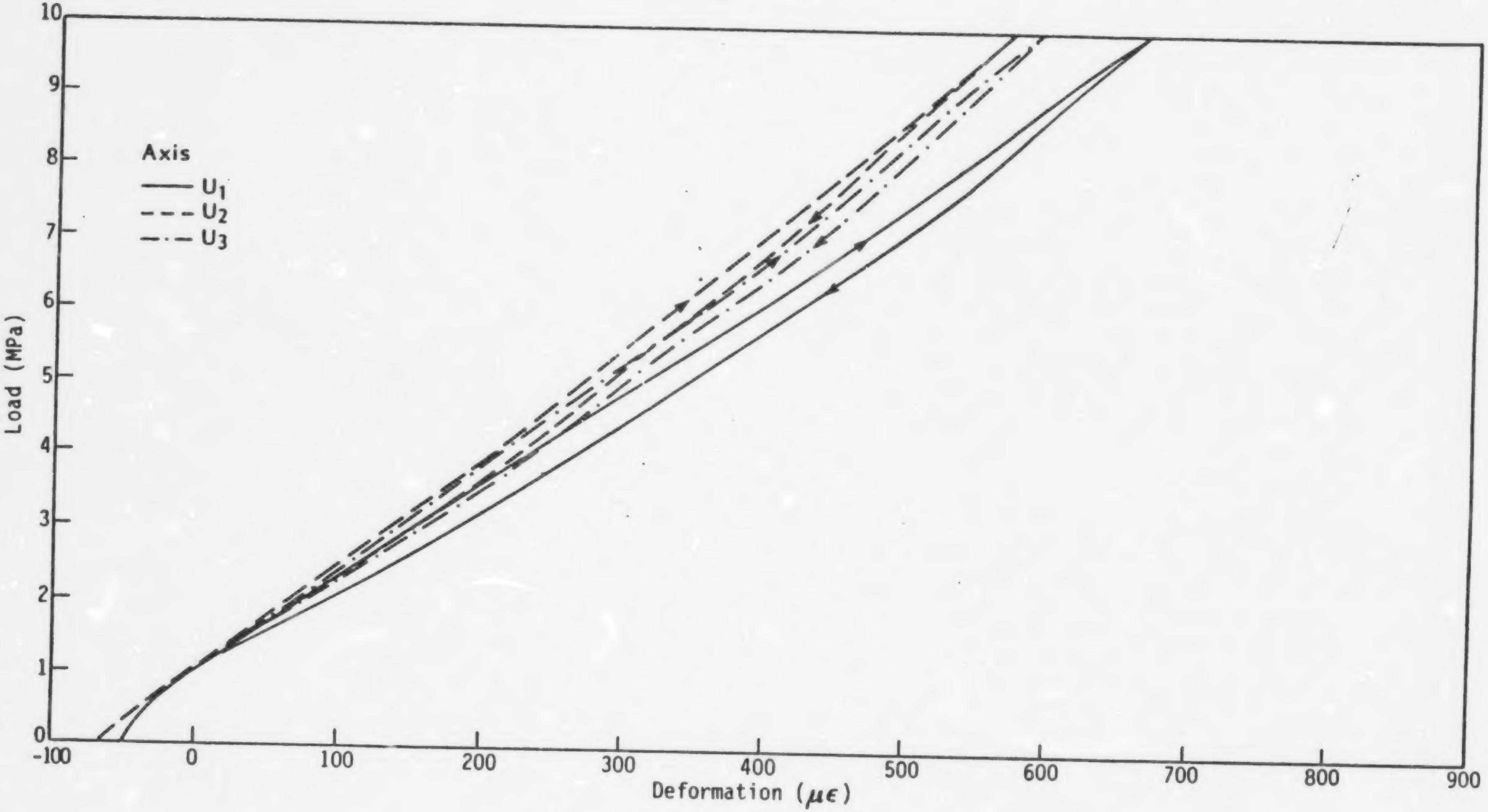

FIGURE 13
TYPICAL BIAXIAL TEST RESULTS

APPENDIX 2

DETAILED TEST RESULTS

A description of each test made during this study is given below. The tables and figures referred to are taken from the section entitled "Summary of Test Results" in the main body of the report.

Borehole 1 (BH1) - footwall main outcrop

These test results are given in Table 2 and Figure 9. The P magnitudes range from a high of 22.74 MPa (test 22) to a low of 2.71 MPa (test 8). The minor stress Q ranges from a high of 7.61 MPa (test 2) to a low of -1.47 MPa (test 7). The negative sign denotes a tensile stress. From the BH1 test results, it would appear that there is a zone of higher stress near the surface which could be related to the rock bursting observed on the main outcrop. A detailed description of these bursts is contained in the section entitled "Tremors, Rockbursts and Pop Ups". The P stress magnitude drops off to roughly half of the surface zone value in the area between the depths of 10.67m and 15.24m. Tests 7 and 8 at a depth of approximately 7.62m show lower P values as well as very low values for Q. This may be a result of the existence of the two zones of closely spaced joints at 6.40m and 9.30m. Tests 11 and 12 do not seem to be affected by the zone at 9.30m. The joints in these zones have very shallow dips (14°-20°) and the influence on the stress field may be restricted to the area very close to the joints. The low Q value in test 15 may be related to the joints at 14.32m. Tests 21 and 22 located at depths of 23.47m and 23.77m respectively are located in a zone of fairly solid rock that has not undergone a great deal of jointing and thus is not as stress relieved as other parts of the rock mass appear to be. These tests may more accurately reflect the stress levels to be expected in unjointed rock masses in this area, although the possibility of stress concentration within a competent layer in a jointed mass must be considered as well. The two deepest tests in BH1 (tests 23 and 24 give stress levels about one half of those in tests 21 and 22 but again the rock is more jointed.

Borehole 2 (BH2)

These test results are given in Table 2 and Figure 10. BH2 is located on the hanging wall of the thrust structure on the main outcrop. The epidote rich layer which is assumed to be the extension of the surface thrust feature is located at a depth of 6.90m given the top of the surface feature and the location of the epidote layer in borehole 2. The P stress varies from 0.16 MPa to 11.20 MPa and the Q stress varies from -8.21 MPa to 8.22 MPa. The direction of P changed in different sections of the borehole. Near the surface in test 28, P is aligned 075° and may be affected by the surface jointing. Test 31 and 32 are located very close to the epidote seam, which appears to correlate to the surface thrust. Tests 31 and 32 show a change in P alignments from that of test 28 to 061° and 057°. The stress magnitudes have increased greatly to nearly four times those of test 28. This may be due to a) surface stress relief affecting test 28 or b) stress concentrations near the thrust structure affecting tests 31 and 32. Test 35a, 35b, and 36 were carried out at depths of 8.93m, 10.91 and 11.31m and show P orientations of N03°W to N16°W. The P and Q stress values are of similar magnitudes to those obtained in tests 31 and 32. Test 35a was carried out at a depth 8.03m which was as close as possible to the epidote zone at 6.91m and yet be in the footwall of the surface structure. Tests 35b and 36 confirm the stress magnitudes and directions of test 35a.

Tests 39, 40 and 41 were carried out below a zone of jointed rock which extends from 13.71m to 15.23m below the surface. The P directions showed a progressive swing of the P stress with depth, ranging from 069° at 15.88m (test 39) to 085° at 16.60m (test 41). This may be the result of the decreasing effect of the jointed zone above the test locations. Test 39 showed very small stresses and for this reason tests 40 and 41 were carried out immediately below 39. It is likely that the area of test 39 is stress relieved by the joints above it, but those of tests 40 and 41 are not. The zone of stress relief around these joints would appear to be only about 0.61m below the joint zone. Tests 45 and 46 carried out at depths of 24.78m and 25.10m indicate a nearly isotropic stress field which explains why the two tests yield P orientations which are nearly orthogonal. The P stress values are of the same magnitude as tests 40,41,49 and 50. Test 49 at 29.86m shows a P direction of N64E and correlates well to test 50 at 30.17m which has a P direction of N58E. These orientations match fairly well with the other tests in the hole as stated above. The difference occurs in the Q stress magnitudes. Test 49 has a Q of -8.21 MPa and test 50 a magnitude of 1.09 MPa. The reason for this sudden change is not apparent as there does not appear to be any significant jointing in the rock mass within 1.22m of test 49. The fractures in the core which can be seen in the core photographs in Appendix 5, were caused during drilling and are not natural joints.

Borehole 3 (BH3)

These results are given in Table 4 and Figure 11. This hole was located in the centre of the epicentral block and only 4 successful tests were carried out due to rock conditions and lack of time. The possibility that the hole was located on what could be a large boulder and not solid outcrop prompted the first test in the hole (test 53) to be attempted at a depth of 7.49m to ensure finding a zone of competent rock. This was later justified when a zone of soil was encountered at a depth of 2.49m and several joints in the first few feet of the rock mass proper caused a loss of drill water. The hole was then cased to a depth of 3m to prevent caving in the hole and to minimize water loss. Test 53 gave a P orientation of N57W with a P stress of 3.11 MPa but a Q stress of essentially 0 (0.06 MPa). The next test, test

56 at a depth of 16.29m shows a P orientation of 304° but with stress magnitudes of essentially 0 for P (-0.04 MPa) and -3.41 MPa for Q. The next successful tests were tests 60 and 61 at depth of 22.85m and 23.26m respectively. These two tests were separated from test 56 by a zone of very good quality rock which contained very few natural fractures. The results indicate a shift of P to slightly east of north (009° and 004°). Both P and Q stresses are tensile for tests 60 and 61. Test 61 indicated large tensile stresses which are not the result of procedural or computational errors. A contributing factor may be the contact with a granodiorite zone starting at 27.25m or 3.96m below test 61. Above this contact are many natural, shallow-dipping joints in the diorite. The joints become much steeper dipping in the granodiorite and also exhibit weathered surfaces. The highly fractured nature of the rock made drilling extremely difficult and prevented testing at the 30m depth. The hole was extended to a depth of 30m mainly to determine the rock type and jointing that existed at that depth.

Borehole 4 (BH4)

These results are given in Table 5 and Figure 12. Of the six boreholes drilled during this project this was the only one to give a fairly consistent stress orientation required for the postulated thrust fault mechanism. All of the tests were performed in diorite. Only two of the 12 tests attempted tests 13 and 17a do not follow the nearly E-W stress trend. Test 13 at a depth of 15.74m had a crack in the overcore, which was not detected until after the overcore was recovered, and it was felt that the test results were directly affected by this crack. Test 17a indicated stress levels that are similar in magnitude as tests 14, 19 and 20. The P stress for test 17a is oriented at 006 as opposed to azimuths of 085, 086 and 088 for test 14, 19 and 20. Confirmation of test 17a's orientation is not possible because the test below 17a, test 17b, failed due to core breakage. This test may be affected by a zone of severely rock located between 23.34m and 23.54m. Tests 5,6,9 and 10 are closely grouped between 8.68 and 10.99m because although the P and Q directions do not vary greatly the magnitudes of the measured stresses do. The P stress from test 5 is 17.92 MPa while the P stress from tests 6,9, and 10 drop from 5.57 MPa to 2.18 MPa to 1.96 MPa. The Q stress changes from 5.85 MPa for test 5 to a more or less constant tensile stress that ranges from -2.49 MPa to -2.39 MPa to -2.19 MPa for tests 6,9, and 10. The reasons for this dramatic change are not readily apparent. Test 5 is close to a granitic intrusion and below a well jointed zone while tests 6,9, and 10 are above a second well jointed zone. The effect of these zones on the test results is not known at present. Temperature did not influence the results as all tests were made using a drill water with a temperature of 6° to 8°C which is very close to the assumed ambient rock temperature of 10°C and should not induce a great affect on the measured stresses (Hooker and Duval, 1971). Tests 19 and 20 were carried out at depths of 29.31m and 29.69m and duplicated the approximate P orientations of most of the other tests in the hole, although the P stress magnitudes are slightly higher.

Borehole 5 (BH5)

These results are given in Table 6 and Figure 13. Boreholes 5 and 6 were the only borings that were all in granite. Borehole 5 was located on the side of a hill with an approximately 15° slope. There appears to be joint stress relief influence on test 25 at 3.56m and possibly on test 26 at 3.92m because of the lower stress magnitudes measured. The tests below test 26 in the hole starting with test 29 at 8.16m seem to have approximately the same P and Q stress magnitudes. These stresses are roughly 2 to 3 times the stresses determined in tests 25 and 26. Test 29 had a P stress of 20.62 MPa although the Q stress was only 6.45 MPa. The Q stresses for the tests located below test 29 ranged from 8.06 MPa to 14.85 MPa.

Borehole 5 had very few natural fractures in it although depths of 3.04m and 3.96m, drillwater was lost and the hole had to be grouted. This was a difficult zone of rock to test as the water was lost ahead of the drill bit through open joints in the rock and made drilling extremely awkward. This problem was not encountered again below this depth in the granite. A characteristic of the granite in this hole was that the rock was highly anisotropic. From the normal visual logging of the core, there does not appear to be any relation of this behaviour to mineral grain alignment, grain size, grain distribution or weathering along joints. The direction of the highest value of Young's modulus varies throughout the hole. The stresses measured in borehole 5 are, with the exception of tests 25 and 26, markedly higher than those measured in other five boreholes. The only three exceptions to this are test 21, borehole 1 (P = 16.41 MPa, Q = 6.89), test 22, borehole 1 (P = 17.92 MPa, Q = 5.85, and test 5, borehole 4 (P = 17.92, Q = 5.85).

Borehole 6 (BH6)

These results are given in Table 7 and Figure 14. There was seven successful tests in this hole. The only failure occurred with test 62 when the overcore broke due to intersecting a 5cm wide fault at a depth of 30.52m. Test 62, although incomplete, did indicate greater strain relief in the U and U directions than test 63 with tensile behaviour in the U direction. This strain relief behaviour is consistent with other tests in the hole and may indicate higher compressive stress in the northeast direction than test 63. This would indicate a build up of compressive stress as this small fault is approached. However, drill vibration in the core increased as the bit neared the fault and this could have caused an error in the readings due to movement of the gauge.

In general the P and Q stress magnitudes are much lower than those measured in hole 5 although hole 6 is located on the opposite side of a shallow valley to hole 5 and may be affected by near field geologic structures other than those encountered in the borehole itself. Two faults were encountered in borehole 6. The largest fault was situated between depths 17.07m and 17.62m. The material in this zone was very coarse grained and weathered and had the appearance of a very coarse beach sand. The orientation of the fault plane and the exact width of it are unknown due to the poor quality of the core and the low core recovery in this zone. Natural joints above and below the fault zone have shallow dips varying from 10° to 20° and may be parallel to the fault. Tests 54 and 55 are located above the fault at 15.17m and 15.44 while tests 58 and 59 are below the fault at 22.82m and 23.18. Both sets of tests indicate an increase in tensile stresses as the fault is approached. The second smaller fault at 30.52m may exhibit the same characteristics, but because test 62 was incomplete, it is not possible to definitely state this about the small fault. The possibility of increased core vibration prior to breaking generating an increased tensile response on the U3 axis must be considered as well when interpreting the significance of test 62.

APPENDIX 3

GEOLOGICAL BOREHOLE LOGS

ABBREVIATIONS USED:

Medium-grained, dark grey diorite	dr
Coarse-grained, light grey granodiorite	gd
Coarse-grained, light pink biotite granite	gt

BH-1

0 - 9"	gd
9" - 7'7"	dr
7'7" - 9'3"	gd
9'3" - 12'11"	dr
12'11" - 24'7"	gd
24'7" - 27'7"	dr
27'7" - 29'11"	gd
29'11" - 35'7"	dr
35'7" - 35'9"	gd
35'9" - 53'0"	dr
53'0" - 57'9"	gd
57'9" - 62'10"	dr
62'10" - 63'8"	gd
63'8" - 75'7"	dr
75'7" - 76'5"	gd
76'5" - 89'11"	dr
89'11" - 91'7"	gd
91'7" - 95'10"	dr
95'10" - 97'0"	gd
97'0" - 102'3"	dr

Horizontal fractures which are common throughout the entire length of the core generally have a spacing between 1" to 1'.

The granodiorite injects the diorite and probably represents veins of the main body of granite that have assimilated some diorite resulting in a more mafic composition for the veins.

BH-2

0 - 2'0"	dr
2'0" - 5'5"	gt
5'5" - 7'0"	dr
7'0" - 7'3"	gt
7"3" - 14'3"	dr
14'3" - 14'6"	gt
14'6" - 100'0"	dr

Epidote vein at 60° to horizontal at 23'3"

BH-3

(Note: This is BH-6, the logs were interchanged)

0 - 89'	gt

Fractures are conspicuously weathered to 30'
Well-developed horizontal fractures are present at 51'
Hole incomplete at time of logging

BH-4

0 - 13'4"	gt
13'4" - 26'10"	dr
26'10" - 28'0"	gt
28'0" - 43'10"	dr
43'10" - 44'8"	gt
44'8" - 45'5"	dr
45'5" - 46'0"	gt
46'0" - 82'2"	dr
82'2" - 85'3"	gt containing diorite xenolith
85'3" - 100'10"	dr

Narrow granite veins at 15'4", 17'8", 19'8", 22'2", 24'2", 55'3", 57'6", 58'1", 59'5", 61'8", 63'9", 67'1", 69'0", 74'4"

Subvertical flow-layering in diorite from 64' to 71'.
Weathered horizontal fractures from 26'10" to 28'0".
Well developed horizontal fractures at 55'3", 57'6" to 58'2", 74'4", 76'6", 78'2", 79'0".
Weathered fracture at 60° to horizontal at 50'4".

BH-5

0 - 102'5"	gt

Fractures are weathered to 25'.
Diorite xenoliths at 29'0", 39'8", 66'0".
Fracture at 80° to horizontal at 24'8"
Quartz vein in fracture at 80° to horizontal at 67'10" belongs to regional 120° joint set.

BH-6

(Note: This is BH-3, the logs were interchanged)

0 - 3'6"	dr
3'6" - 6'2"	gt
6'2" - 9'8"	dr
9'8" - 10'8"	gt
10'8" - 12'2"	dr
12'2" - 12'7"	gt
12'7" - 13'7"	dr
13'7" - 15'7"	gt
15'7" - 19'6"	dr
19'6" - 19'10"	gt
19'10" - 24'4"	dr
24'4" - 32'9"	dr with some gt veins
32'9" - 37'10"	gt with some dr xenoliths
37'10" - 40'0"	dr with some gt veins
40'0" - 43'	dr

Hole incomplete at time of logging

APPENDIX 4

ENGINEERING BOREHOLE LOGS

Key
Geology

□ Medium Grained, Dary Grey Diorite

░ Coarse Grained Light Grey Granodiorite

■ Coarse Grained, Light Pink Biotite Granite

Fractures

— Material Joint or Fracture in Rock Core

▩ Heavily Fractured Zone

▓ No Core Recovered

Overcore
Tests

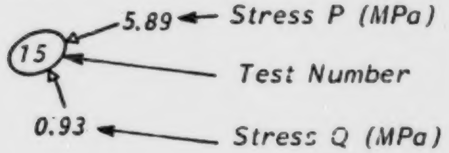
5.89
Stress P (MPa)
15
Test Number
0.93
Stress Q (MPa)

← Compressive Stress

→ Tensile Stress

16 No Test - Test Attempted at this Location but was Unsuccessful

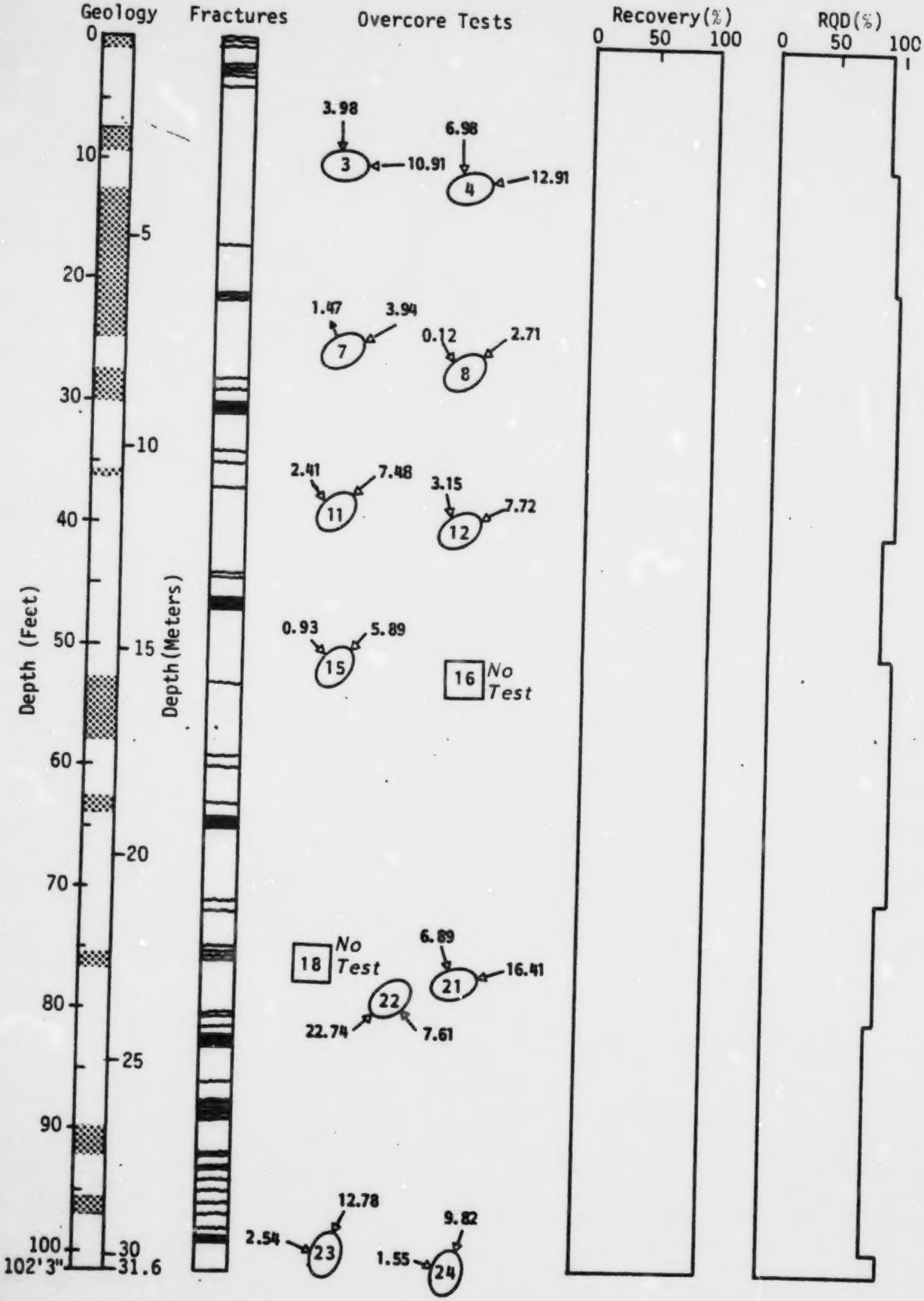

BOREHOLE 1 (BH1)

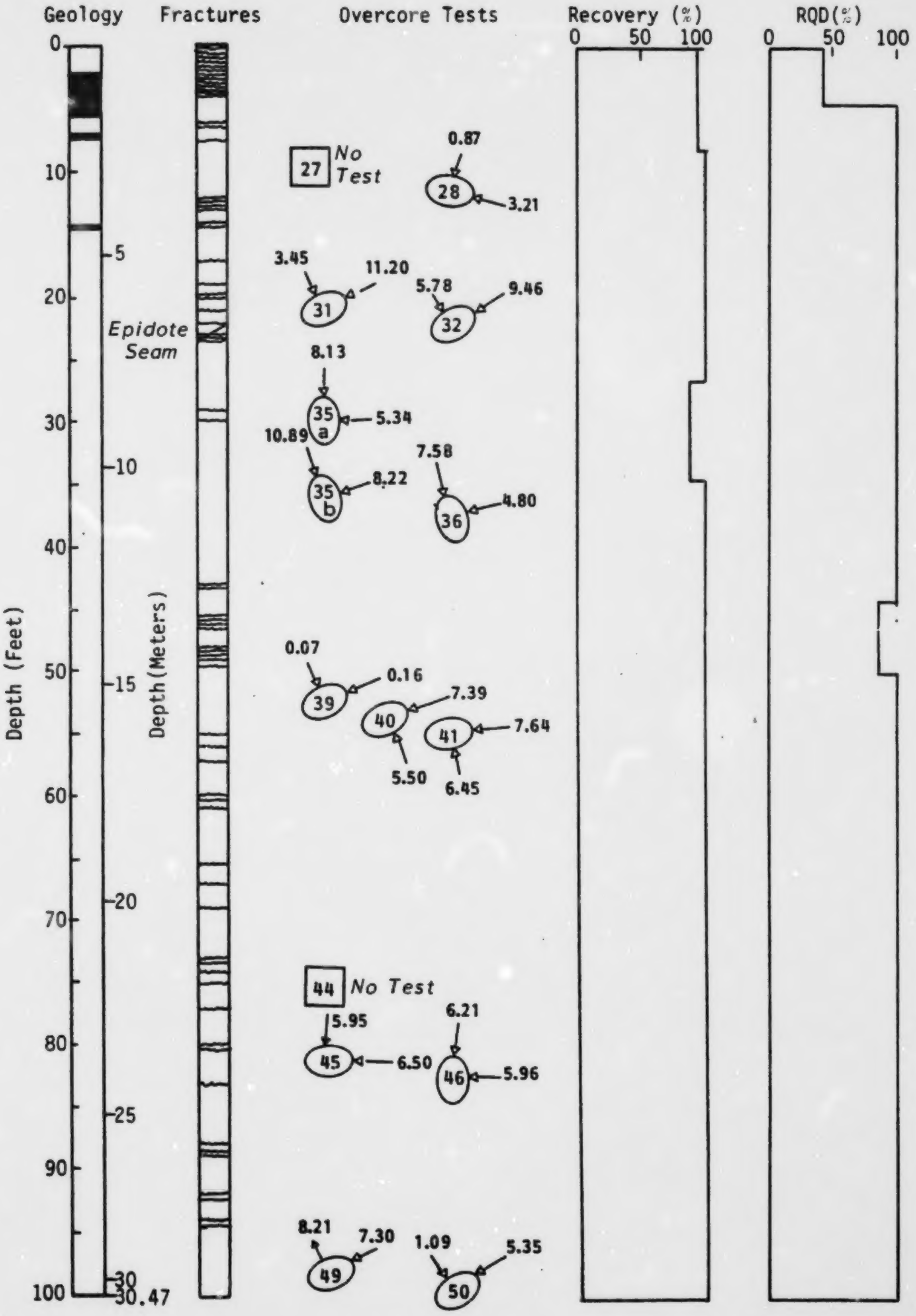

BOREHOLE 2 (BH2)

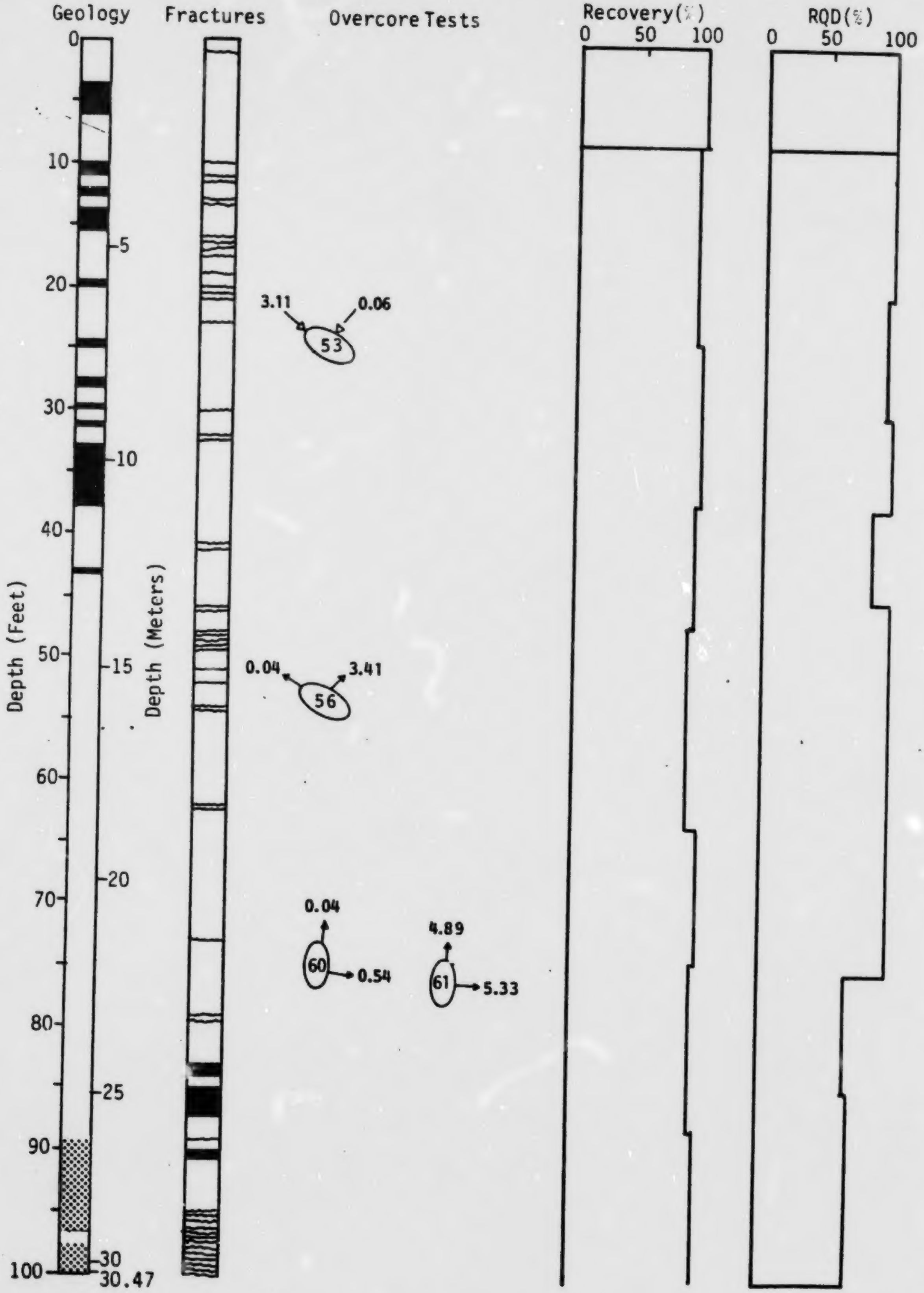

BOREHOLE 3 (BH3)

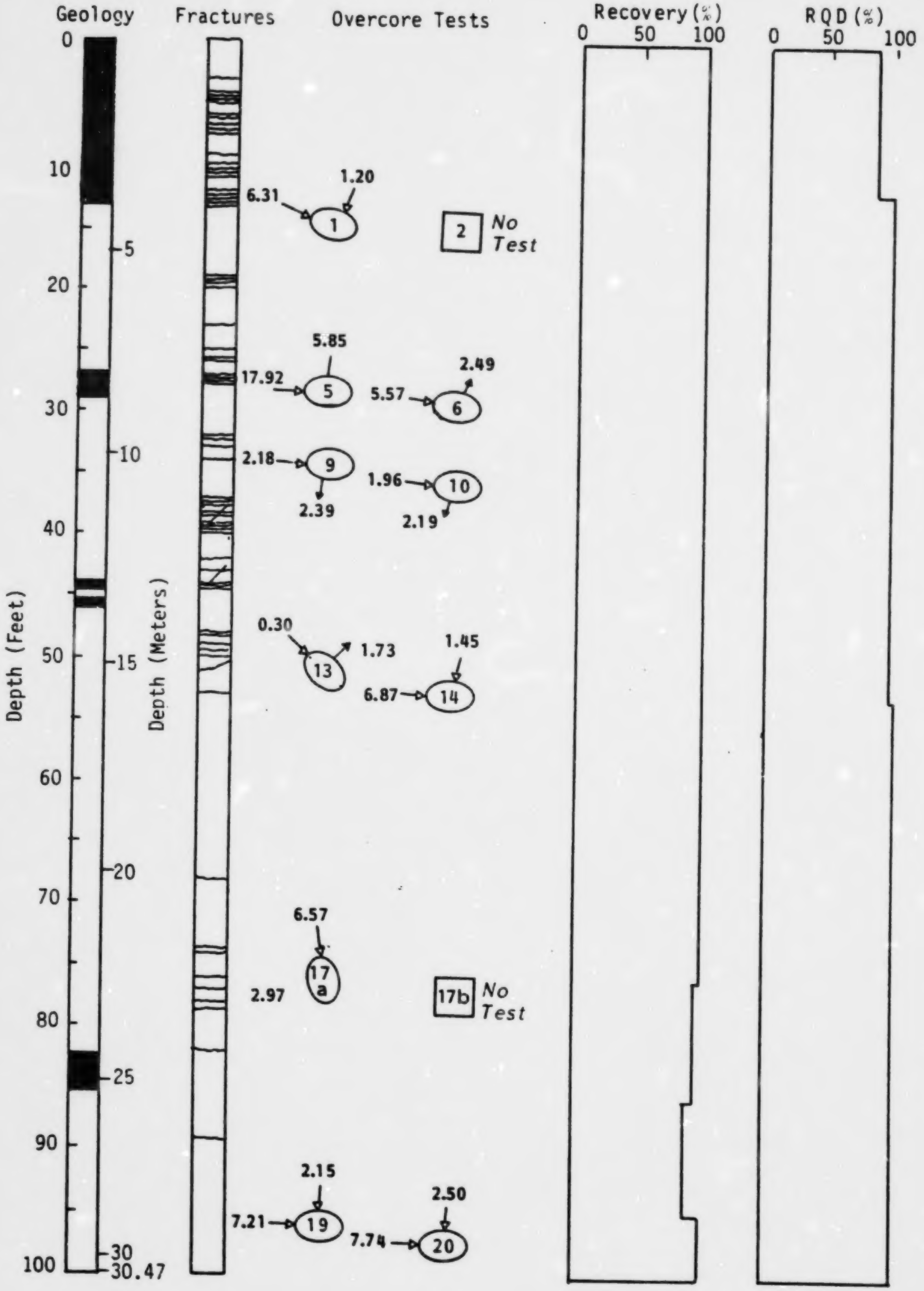

BOREHOLE 4 (BH4)

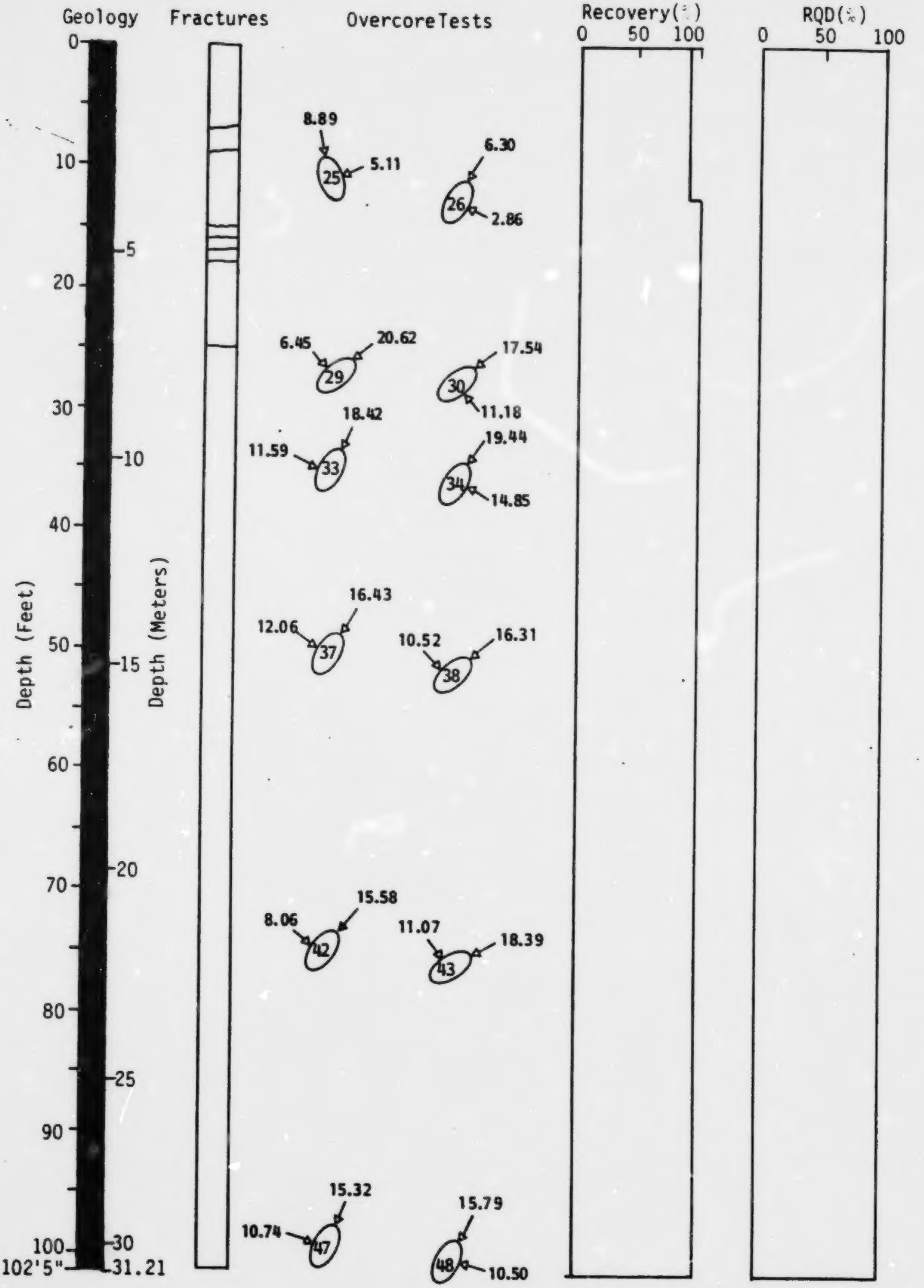

BOREHOLE 5 (BH5)

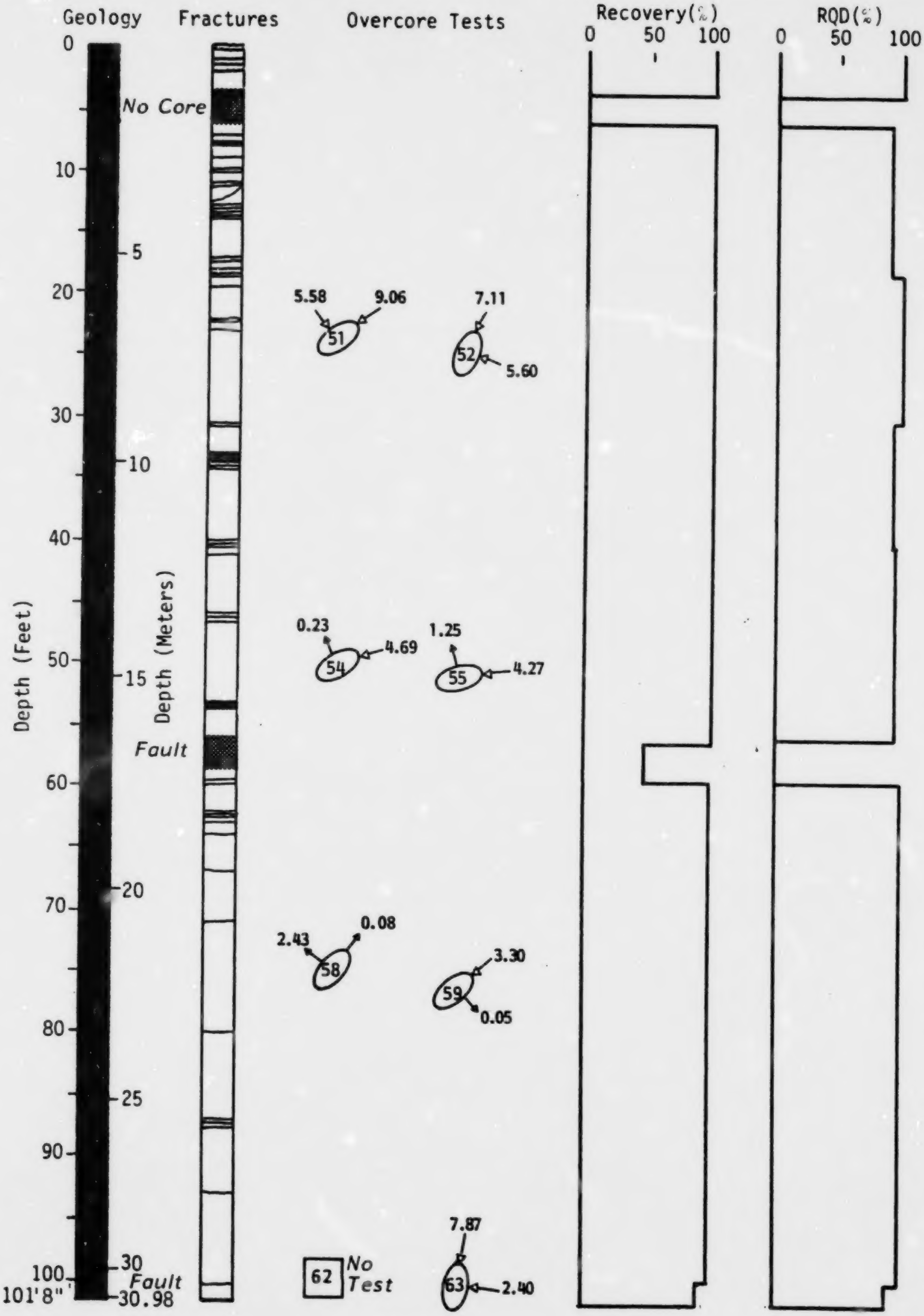

BOREHOLE 6 (BH6)

APPENDIX 5

PHOTOGRAPHIC RECORD OF CORE FROM TEST HOLES

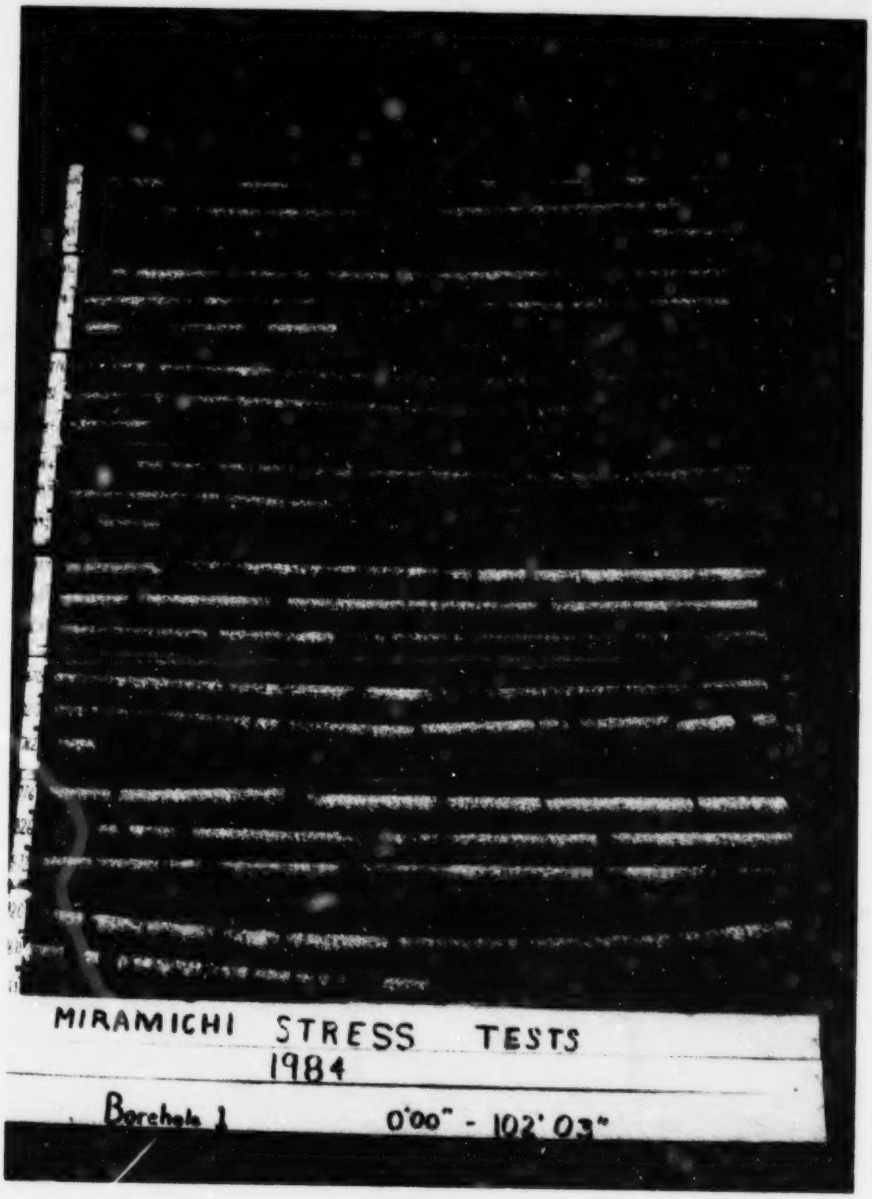
MIRAMICHI STRESS TESTS
1984
Borehole 1
0'00" - 102'03"

ROCK CORE FROM BOREHOLE 1

Note:
Small Diameter Core Indicate the Location of Overcoring Tests

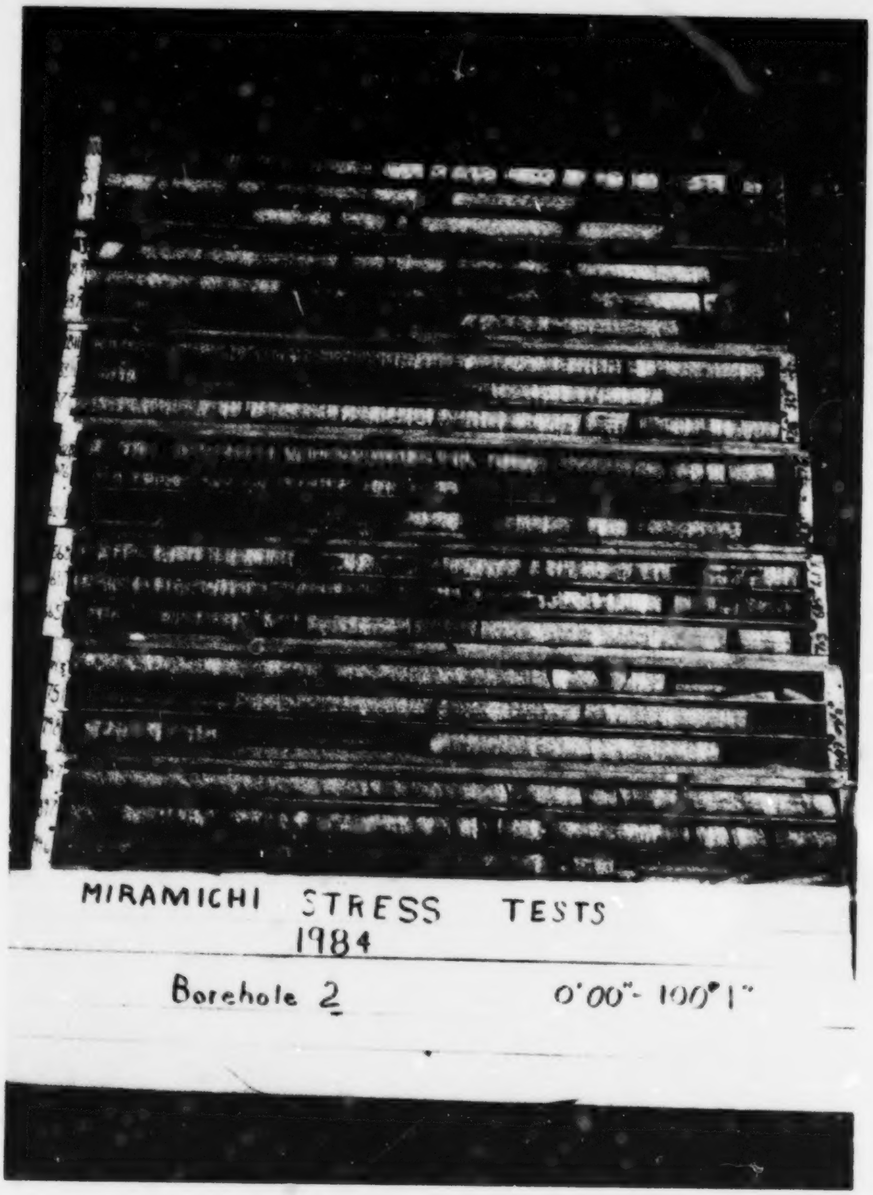
MIRAMICHI STRESS TESTS
1984
Borehole 2
0'00"- 100'1"

ROCK CORE FROM BOREHOLE 2

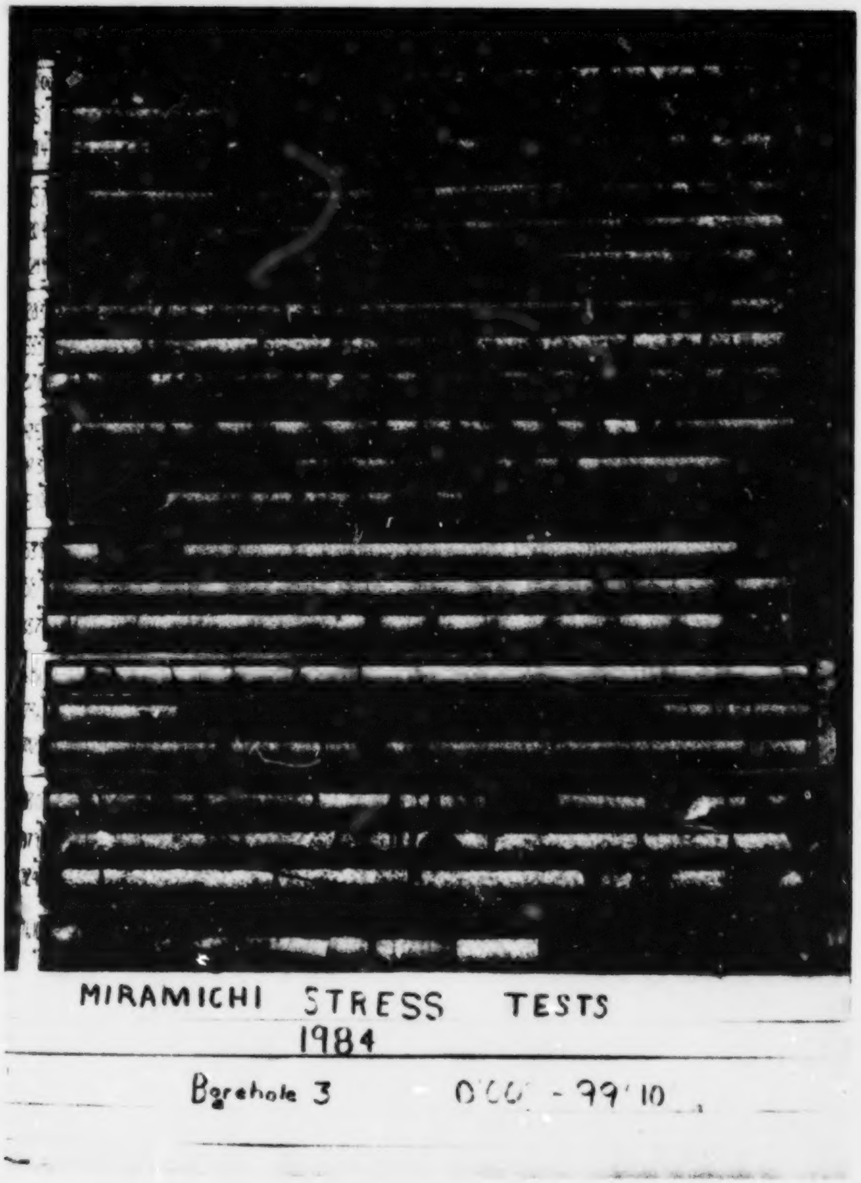
MIRAMICHI STRESS TESTS
1984
Borehole 3 0'00 - 79'10

ROCK CORE FROM BOREHOLE 3

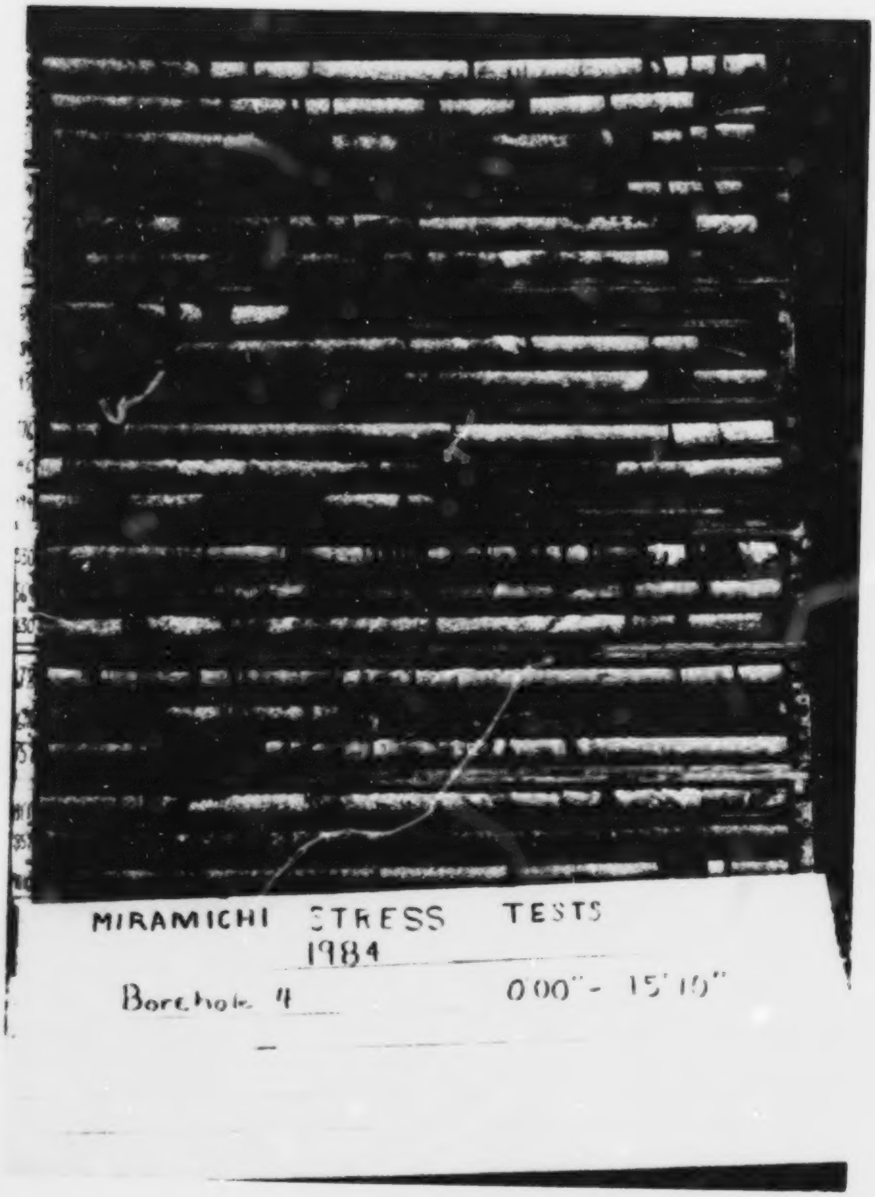
MIRAMICHI STRESS TESTS
1984
Borehole 4
0'00" - 15'10"

ROCK CORE FROM BOREHOLE 4

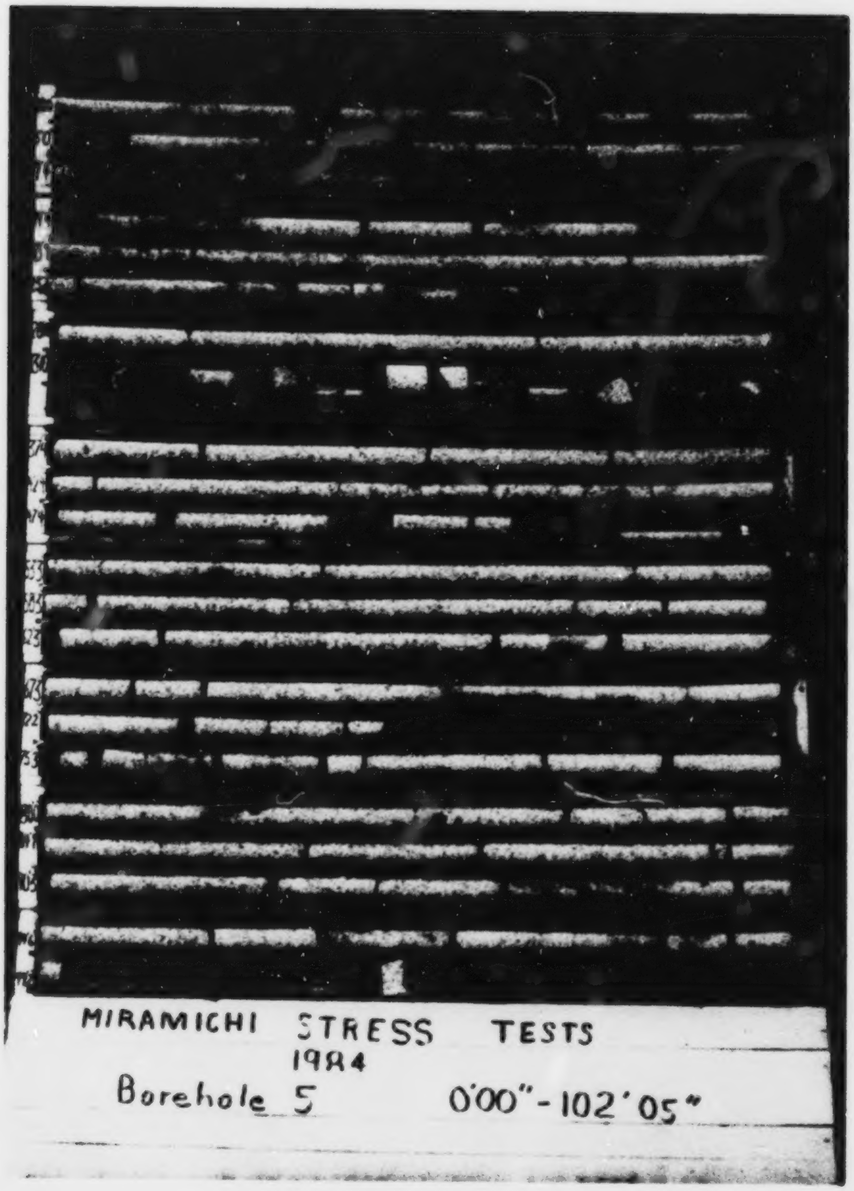
MIRAMICHI STRESS TESTS
1984
Borehole 5 0'00"-102'05"

ROCK CORE FROM BOREHOLE 5

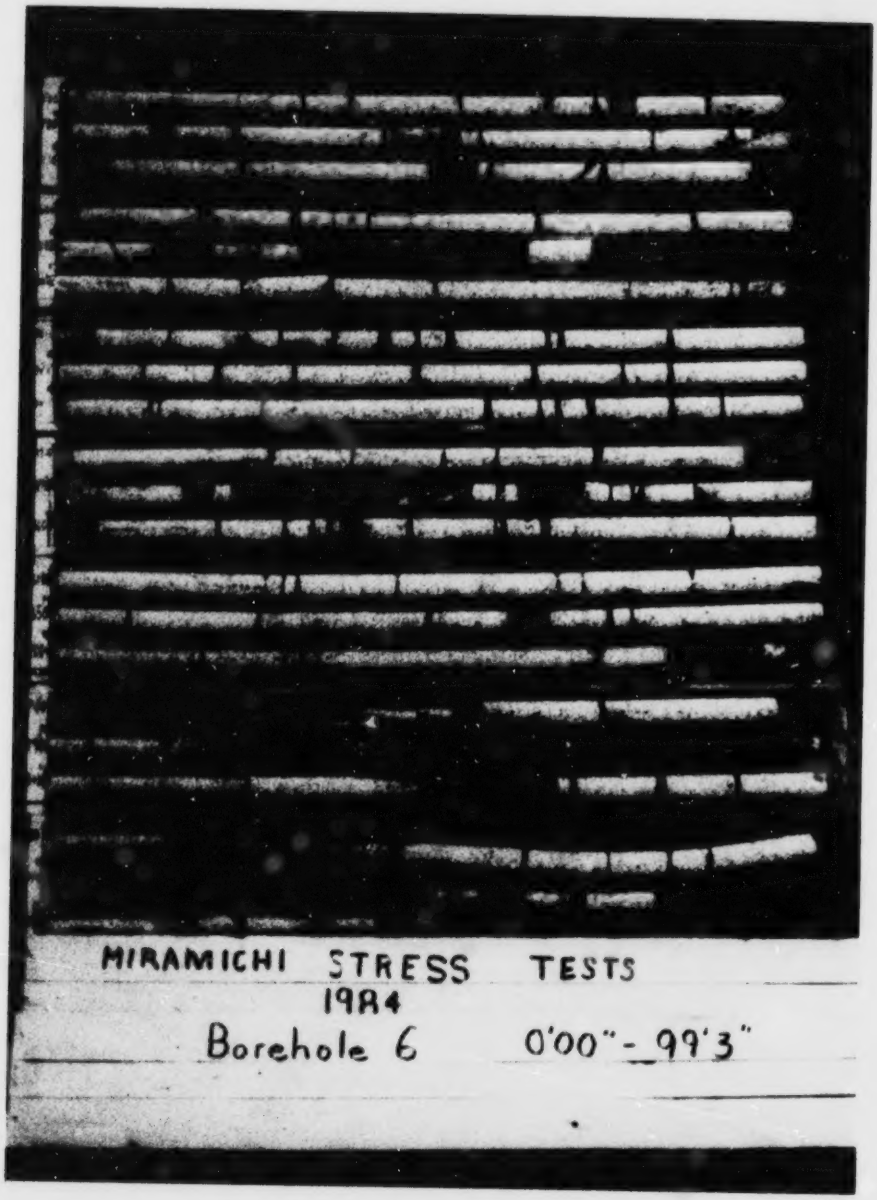

MIRAMICHI STRESS TESTS
1984
Borehole 6 0'00"-99'3"

ROCK CORE FROM BOREHOLE 6

Note:

Fault Zones were Detected at Depths of 56'00" to 57'10" and 100'02" to 100'04"

APPENDIX 6

FIELD TEST CURVES

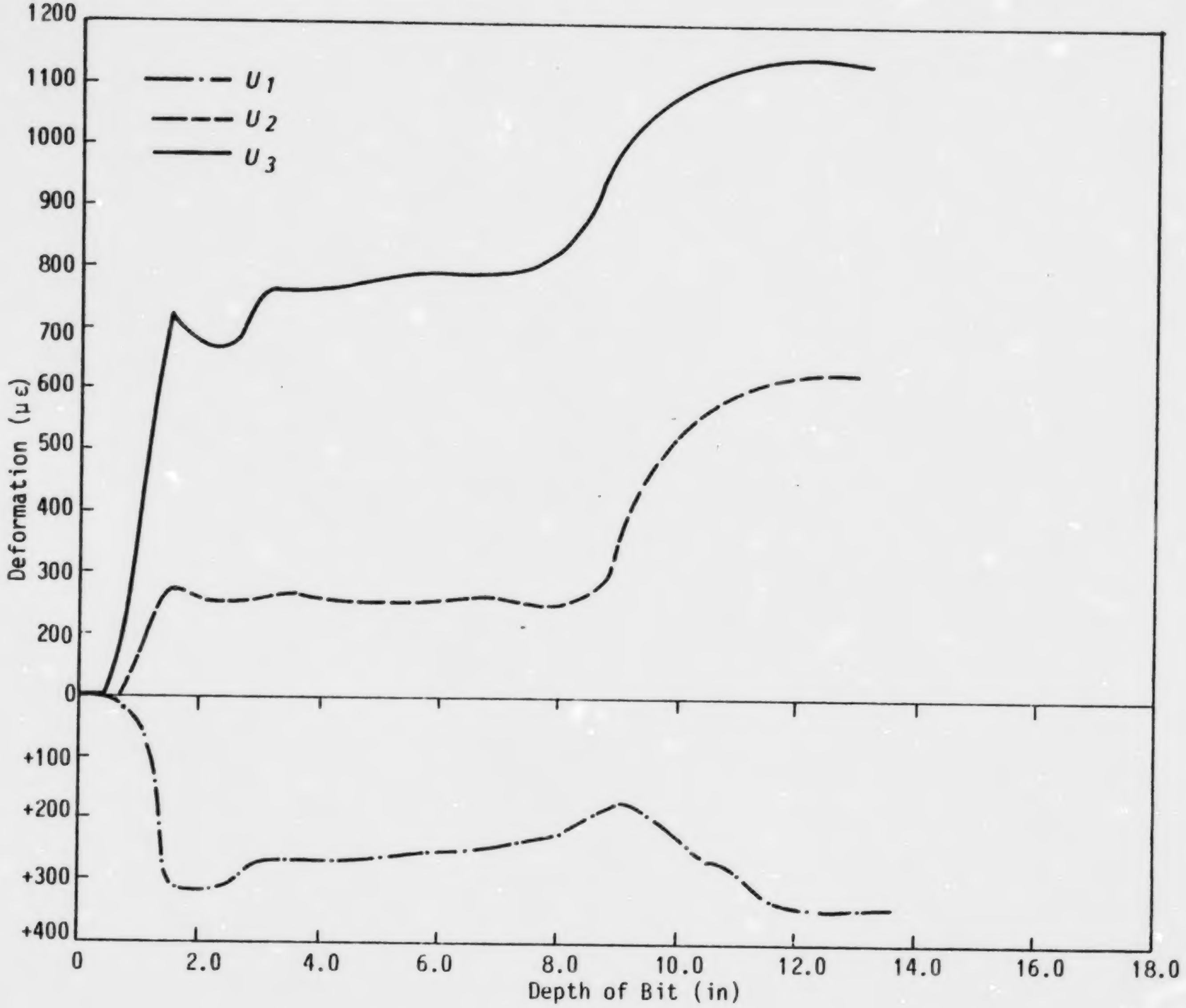

MIRAMICHI - BH4 - TEST 1 - GAUGE DEPTH 4.58m

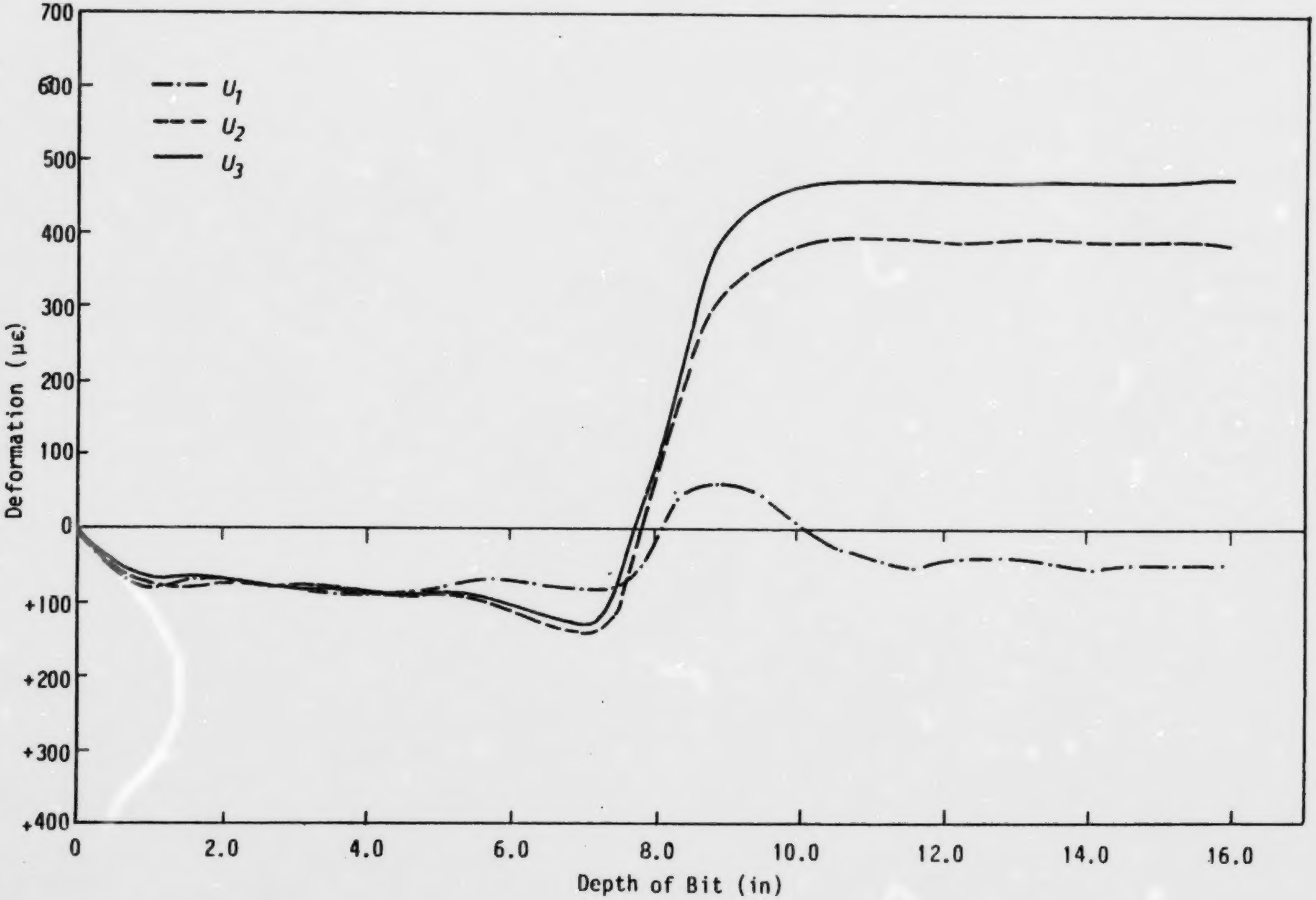

MIRAMICHI - BH 1 - TEST 3 - GAUGE DEPTH 3.0m

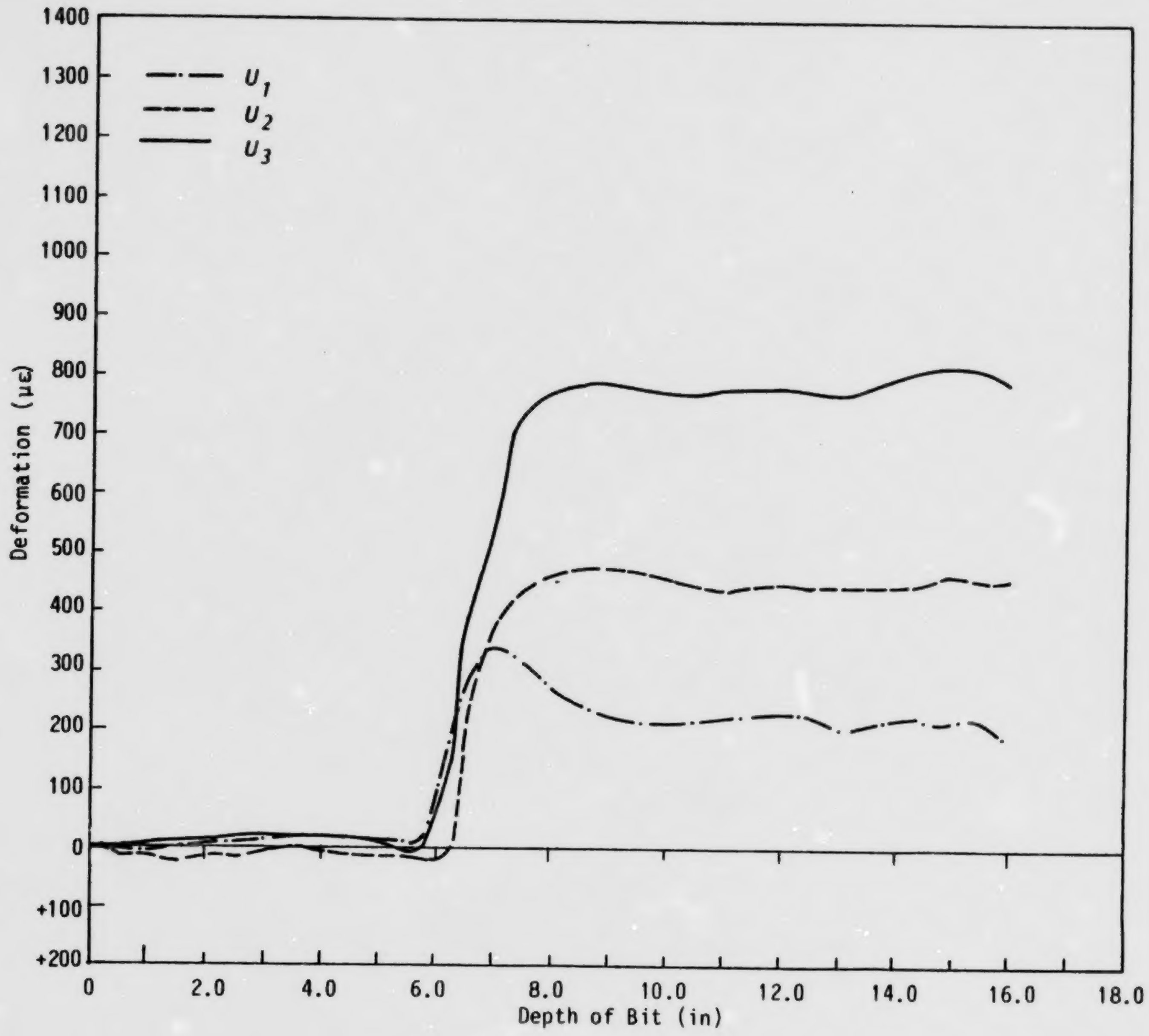

MIRAMICHI - BH 1 - TEST 4 - GAUGE DEPTH 3.47m

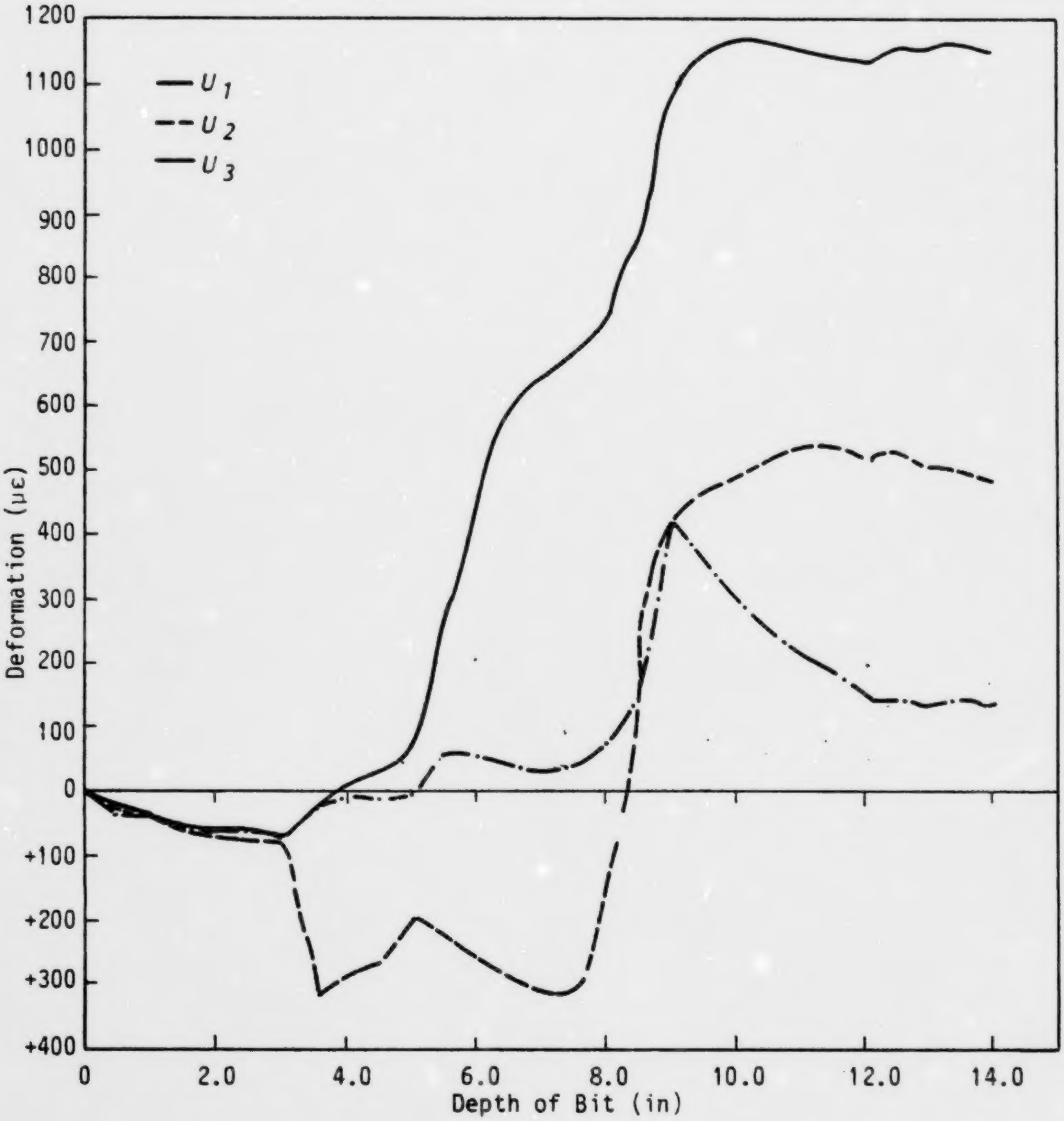

MIRAMICHI - BH1 - TEST 5 - GAUGE DEPTH 8.68m

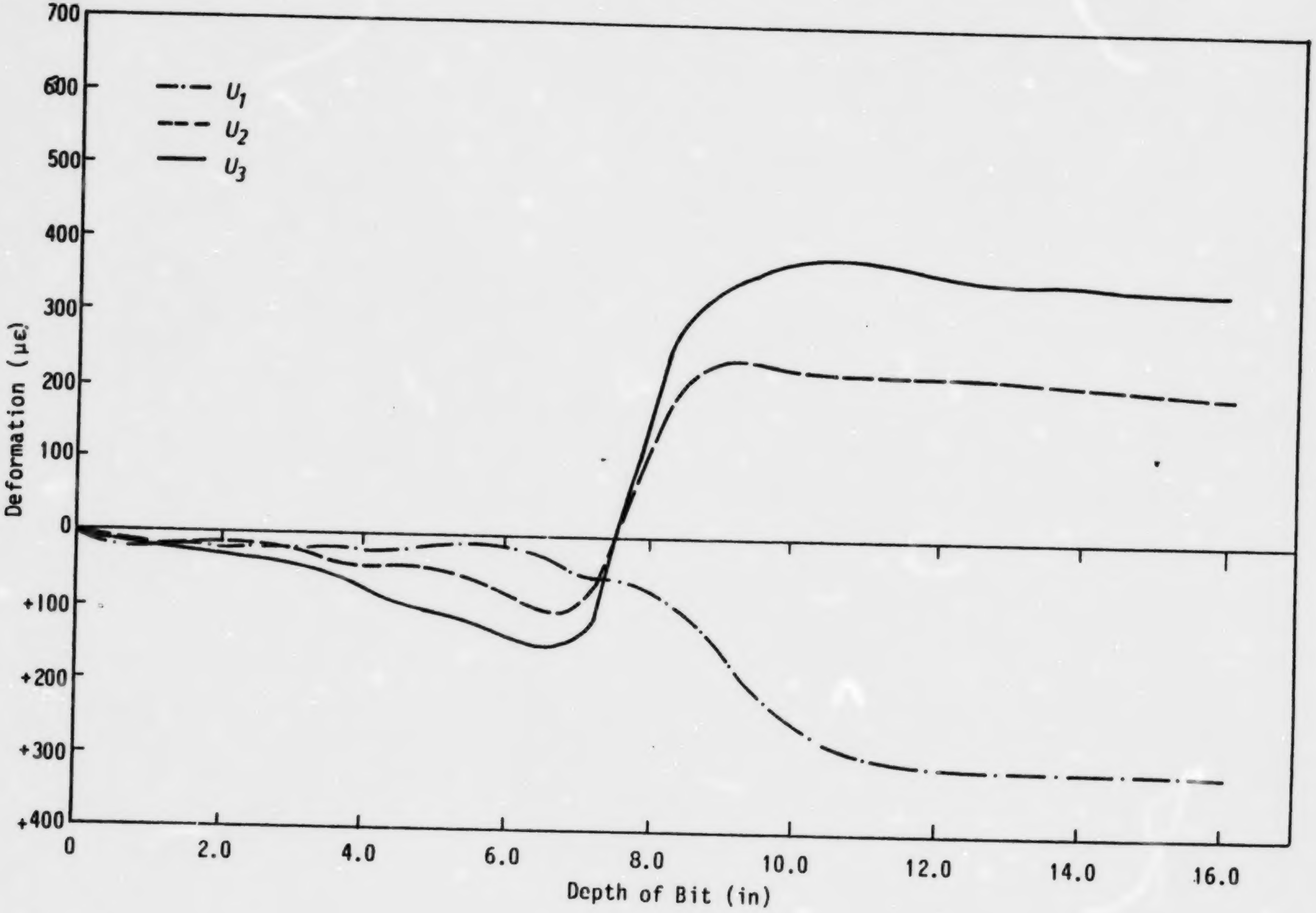

MIRAMICHI - BH 4 - TEST 6 - GAUGE DEPTH 9.03m

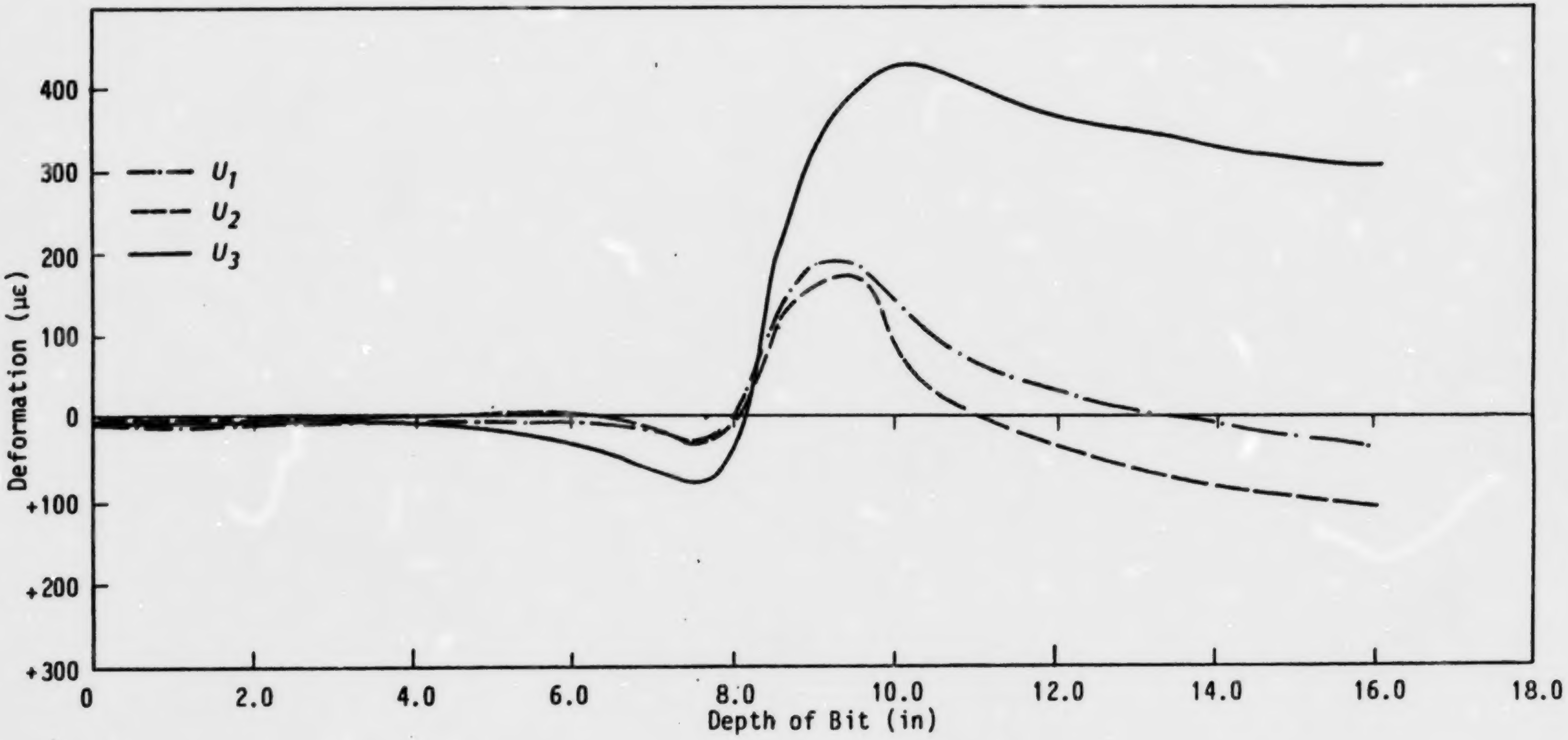

MIRAMICHI - BH 1 - TEST 7 - GAUGE DEPTH 7.63m

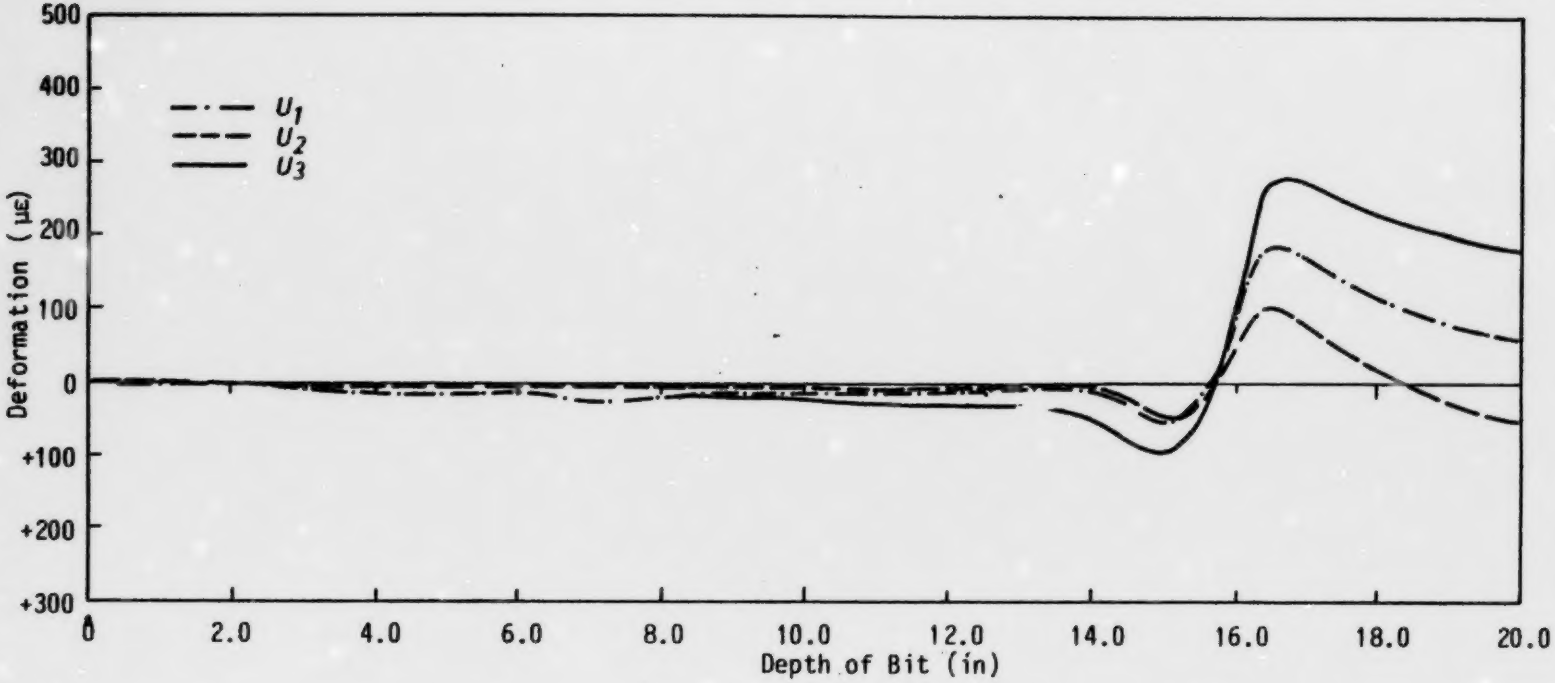

MIRAMICHI - BH1 - TEST 8 - GAUGE DEPTH 8.08m

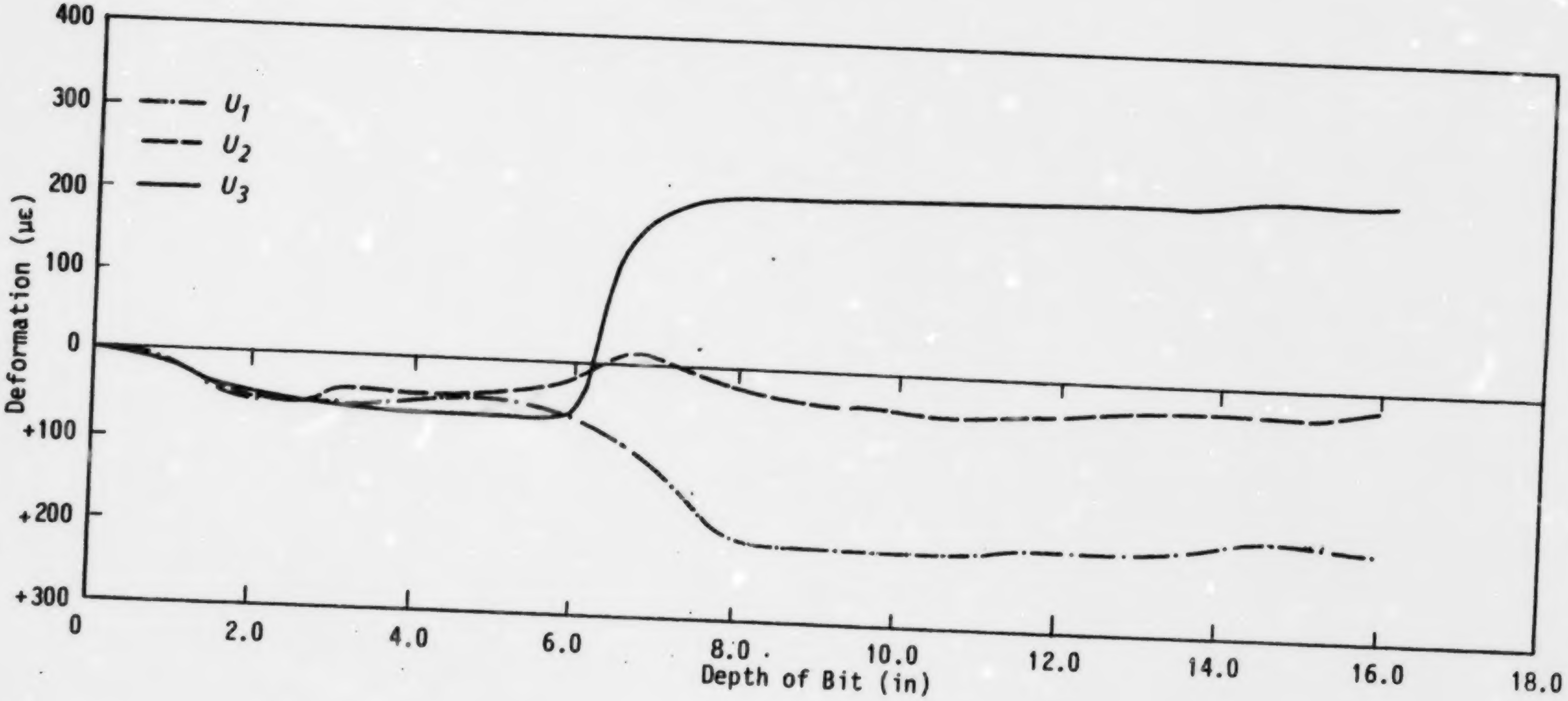

MIRAMICHI - BH 4 - TEST 9 - GAUGE DEPTH 10.59m

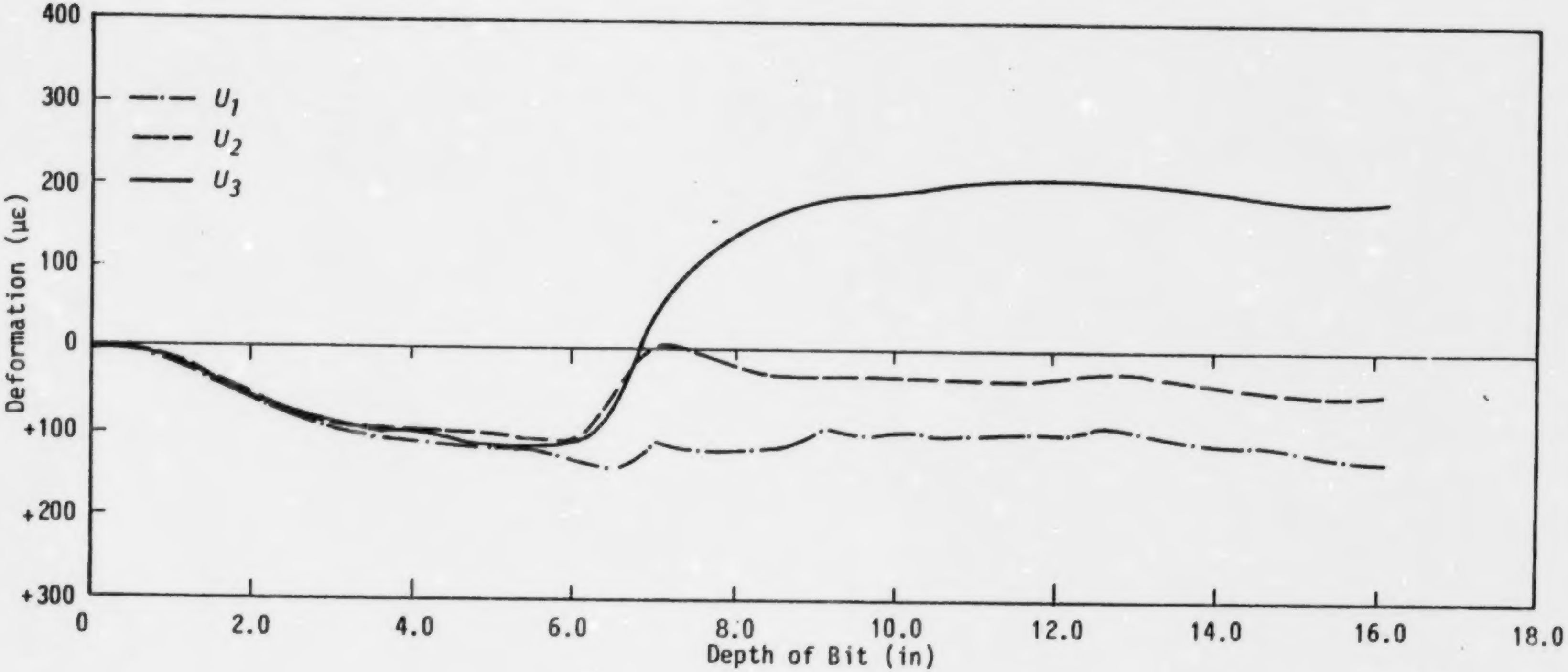

MIRAMICHI - BH4 - TEST 10- GAUGE DEPTH 10.99m

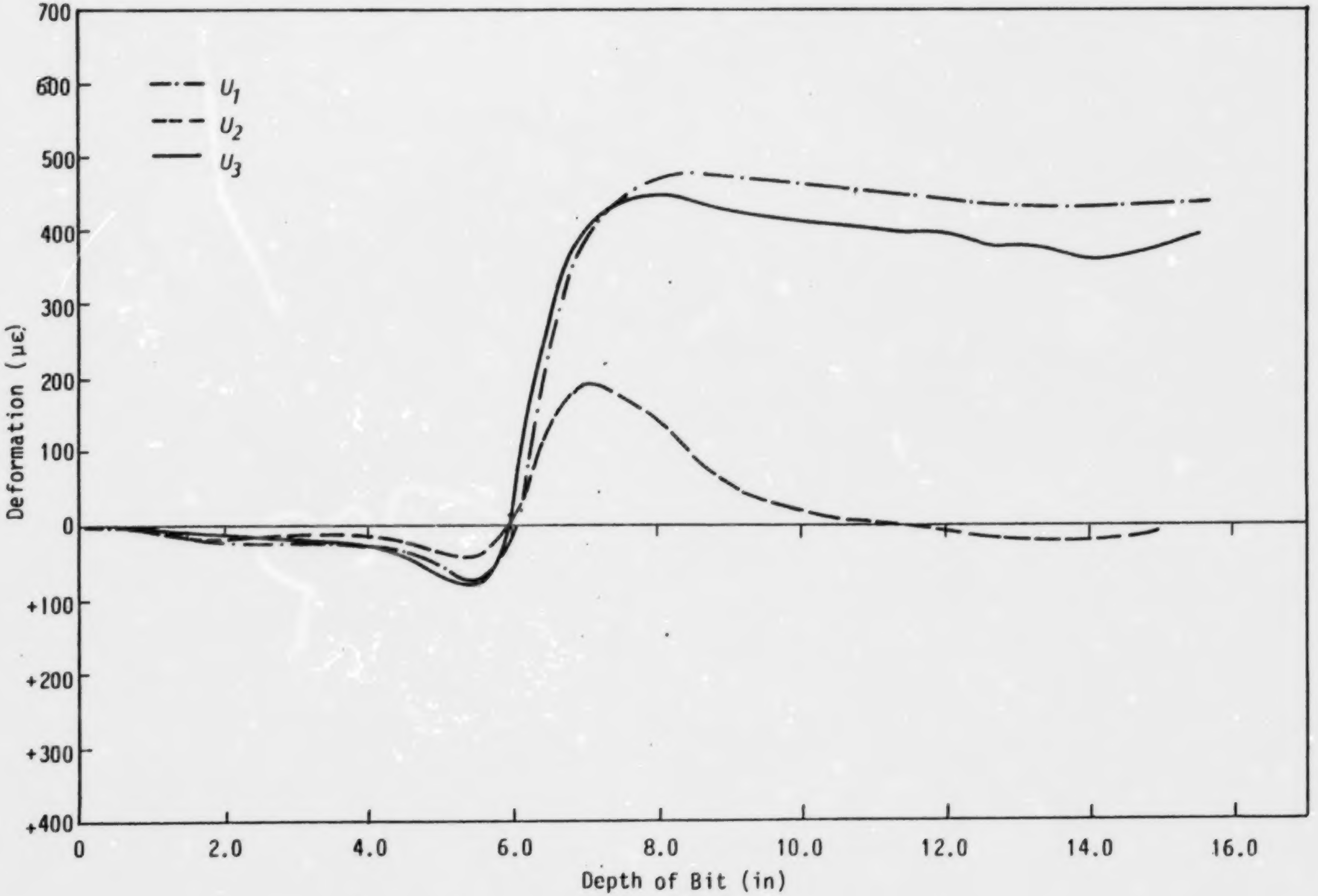

MIRAMICHI - BH 1 - TEST 11- GAUGE DEPTH 11.67m

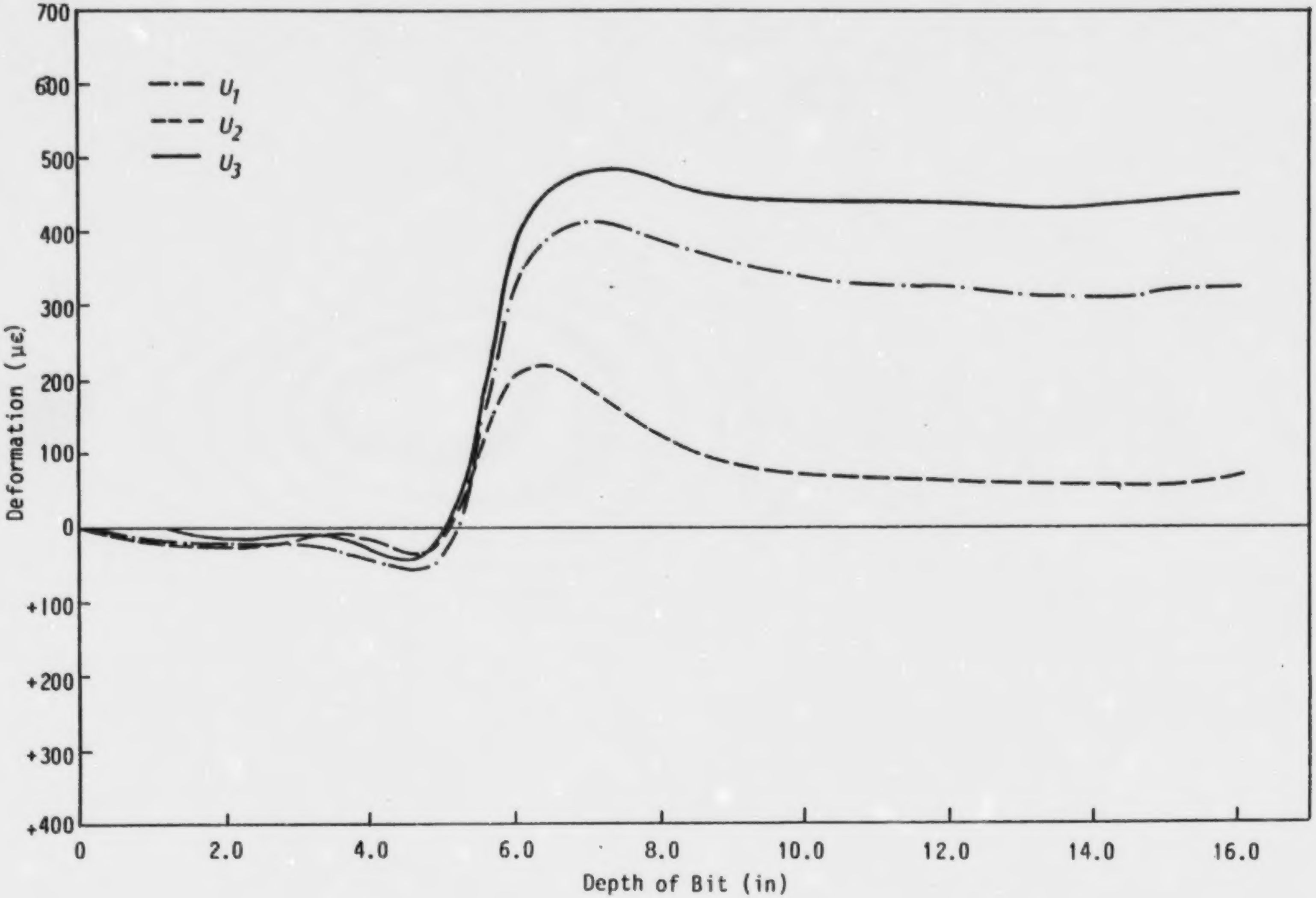

MIRAMICHI - BH 1 - TEST 12-GAUGE DEPTH 12.07m

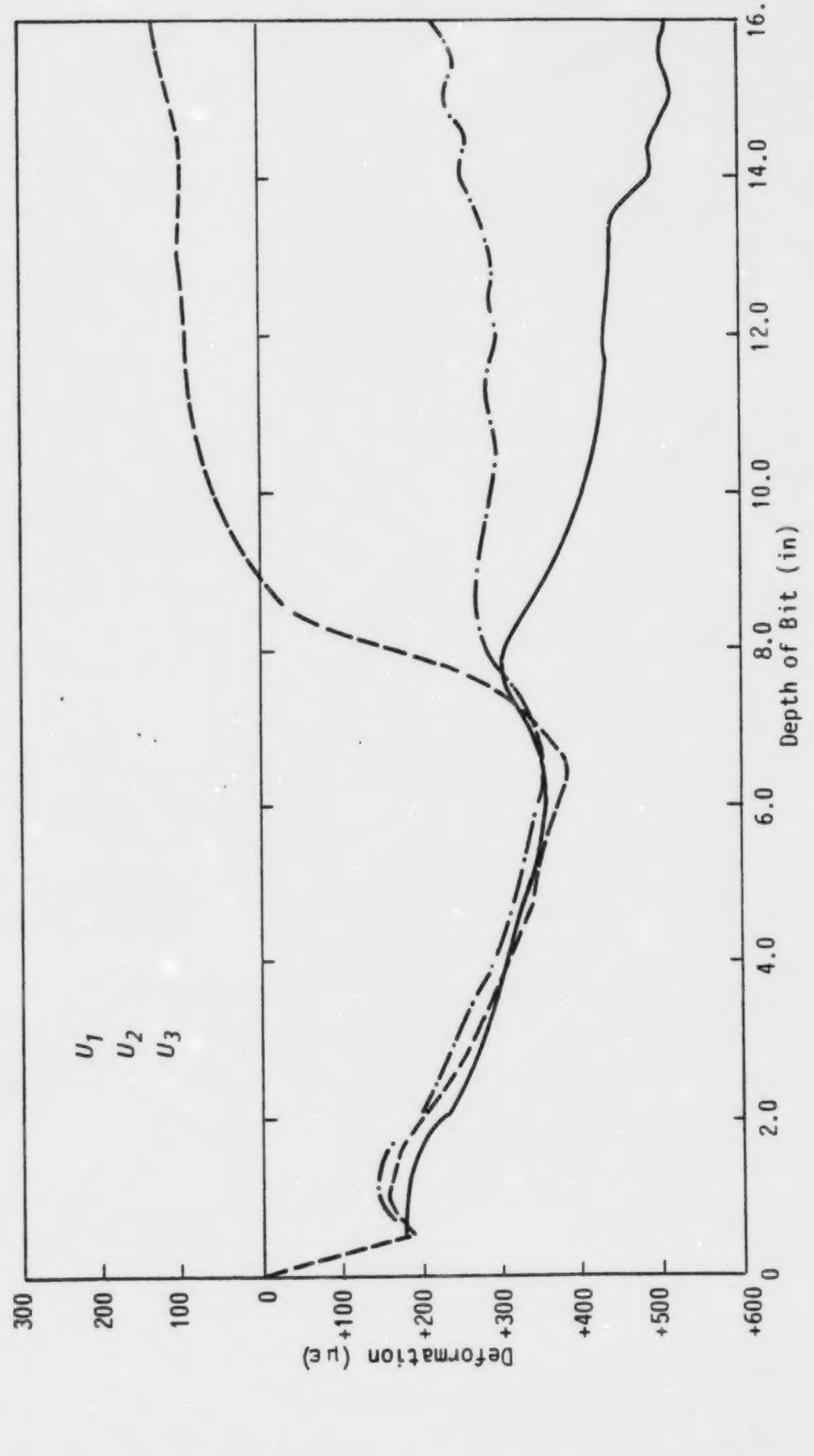

MIRAMICHI - BH 4 - TEST 13 - GAUGE DEPTH 15.78m

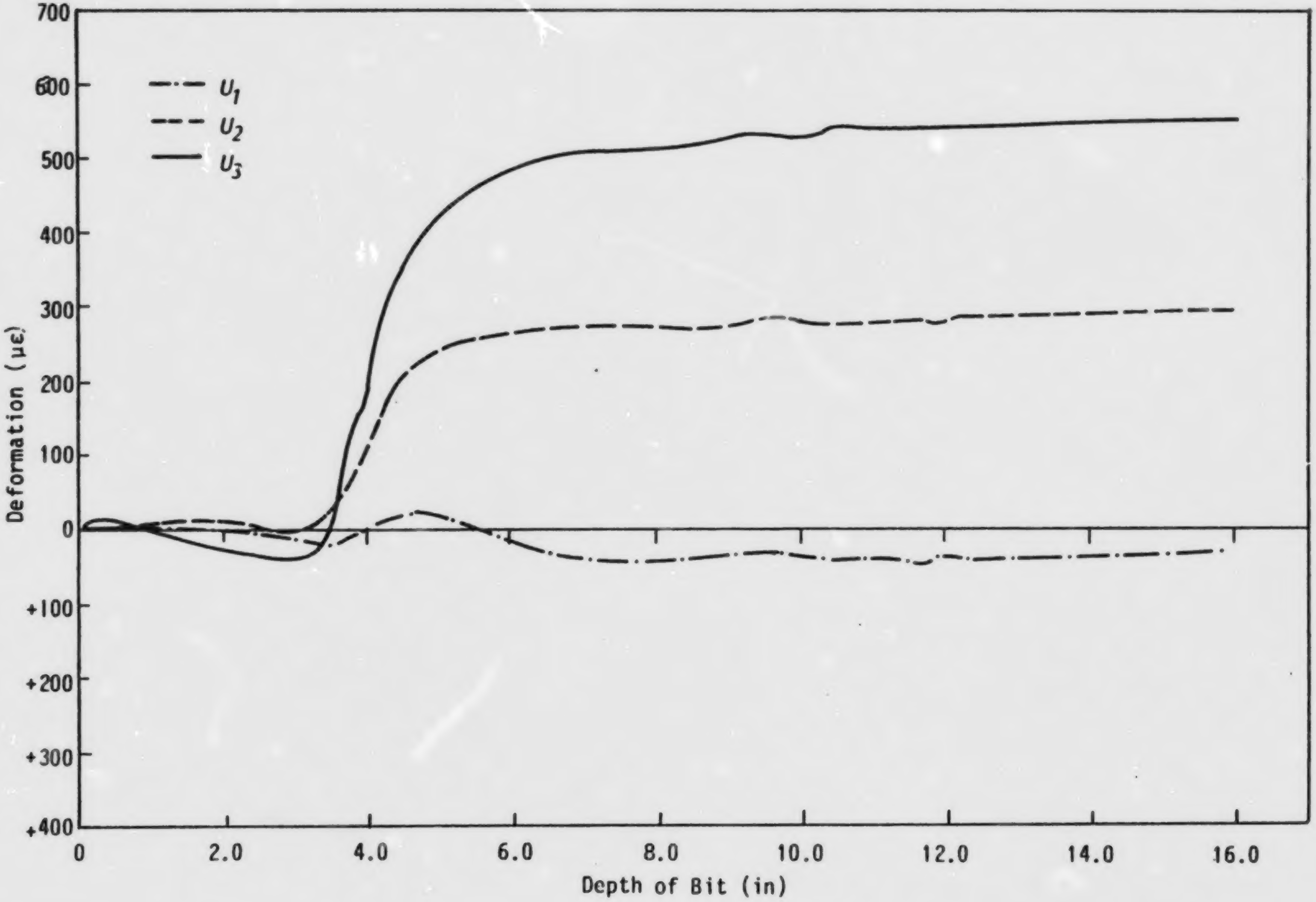

MIRAMICHI - BH 4 - TEST 14 - GAUGE DEPTH 16.14m

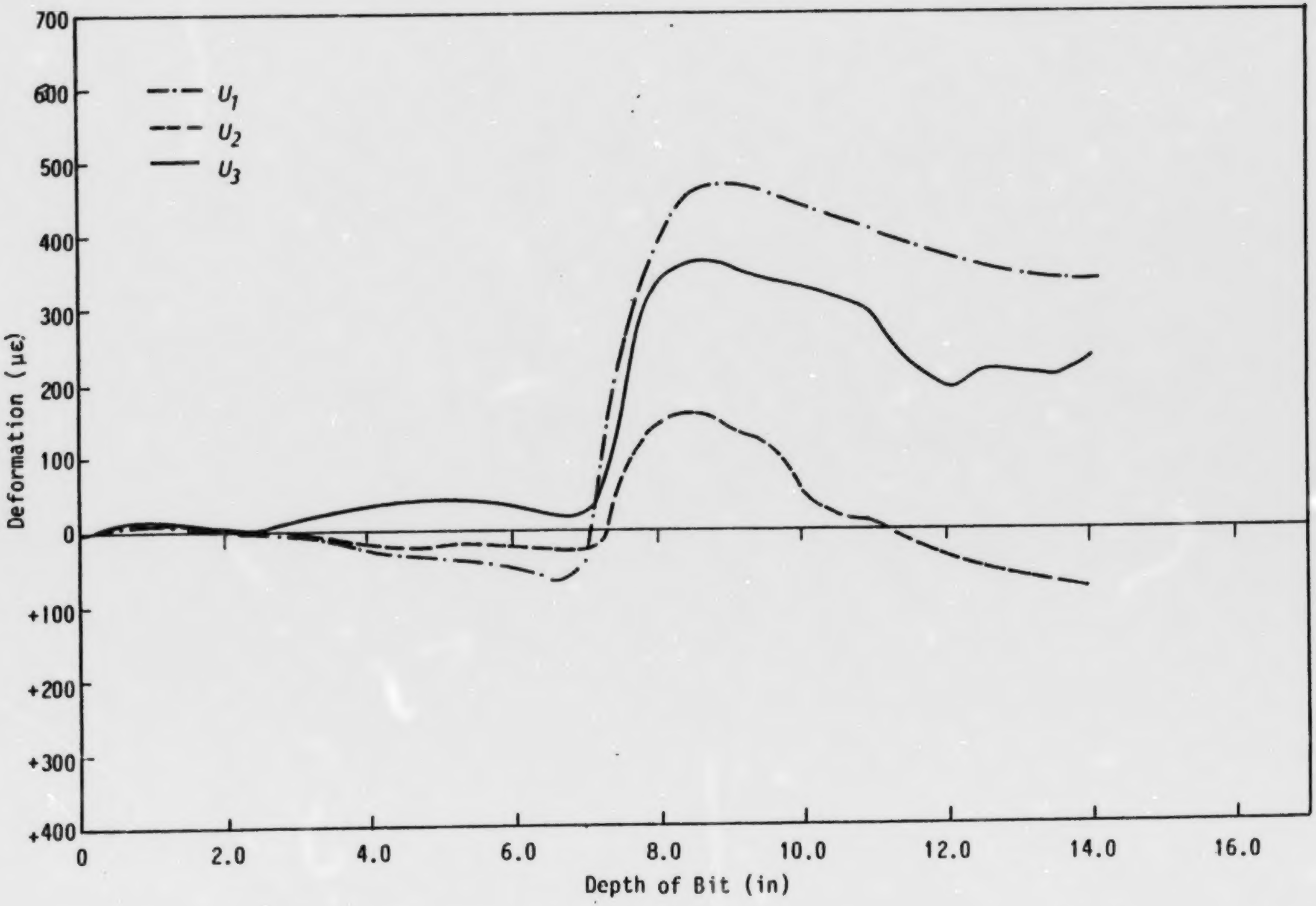

MIRAMICHI - BH 1 - TEST 15-GAUGE DEPTH 15.60m

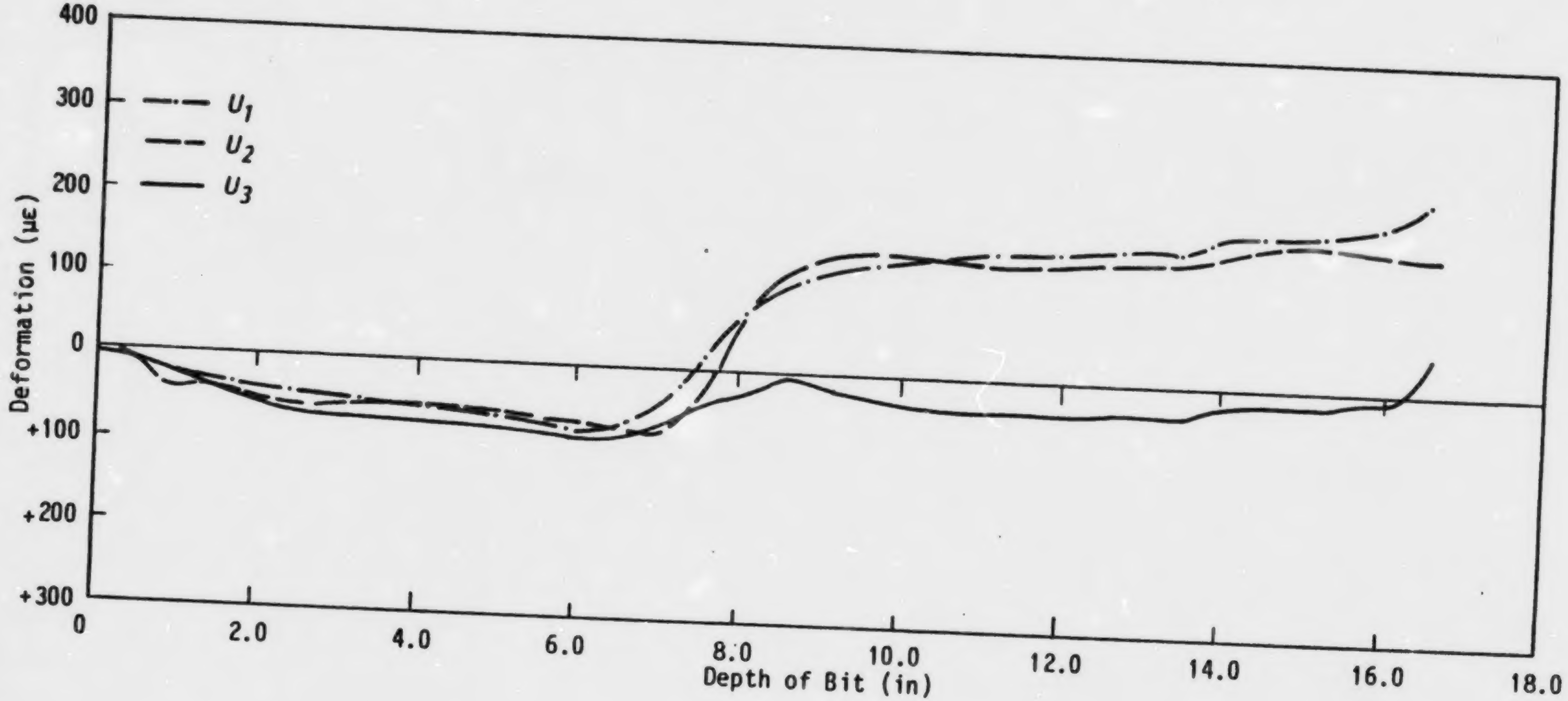

MIRAMICHI - BH 4 - TEST 17 - GAUGE DEPTH 23.17m

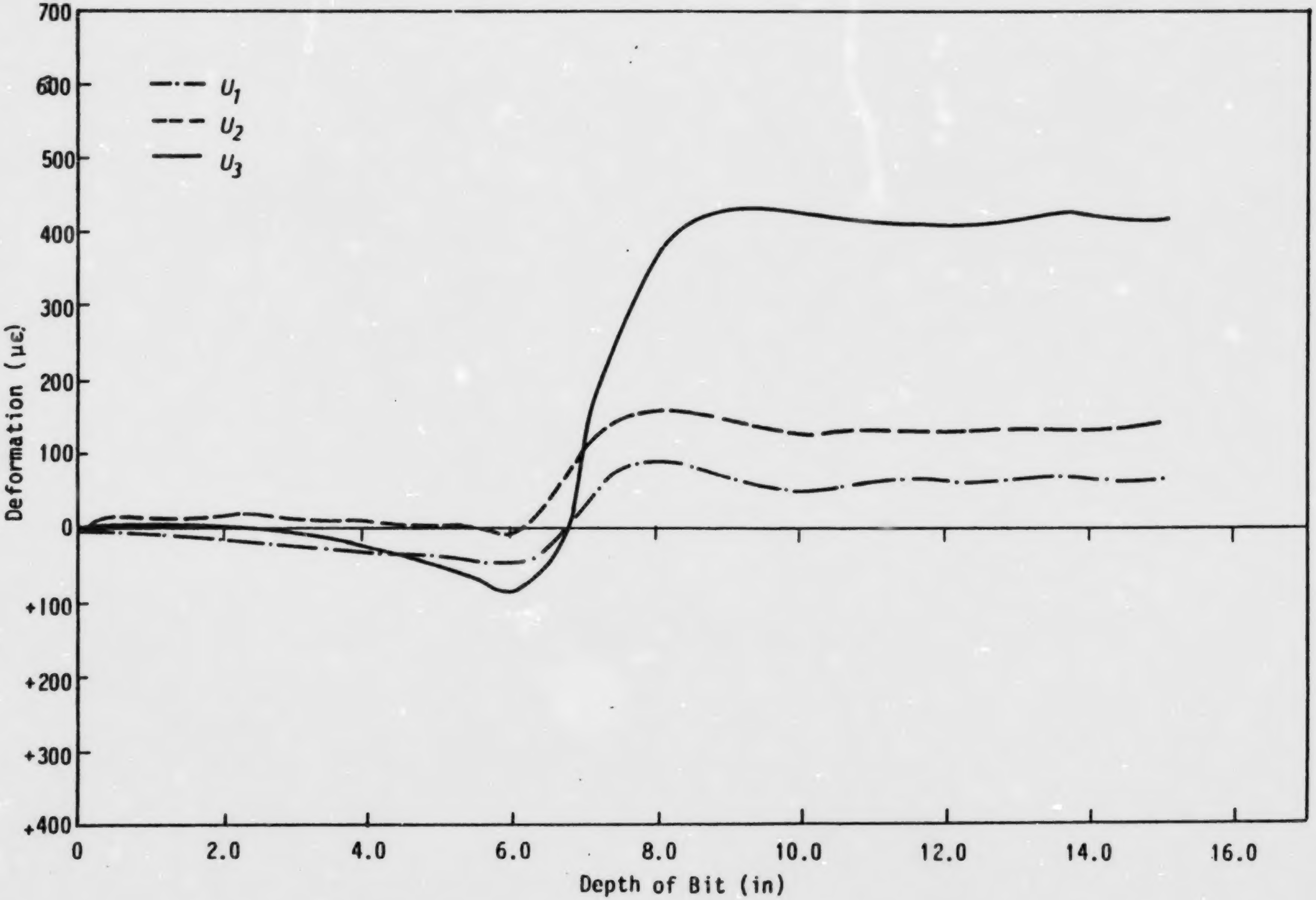

MIRAMICHI - BH 4 - TEST 19 - GAUGE DEPTH 29.31m

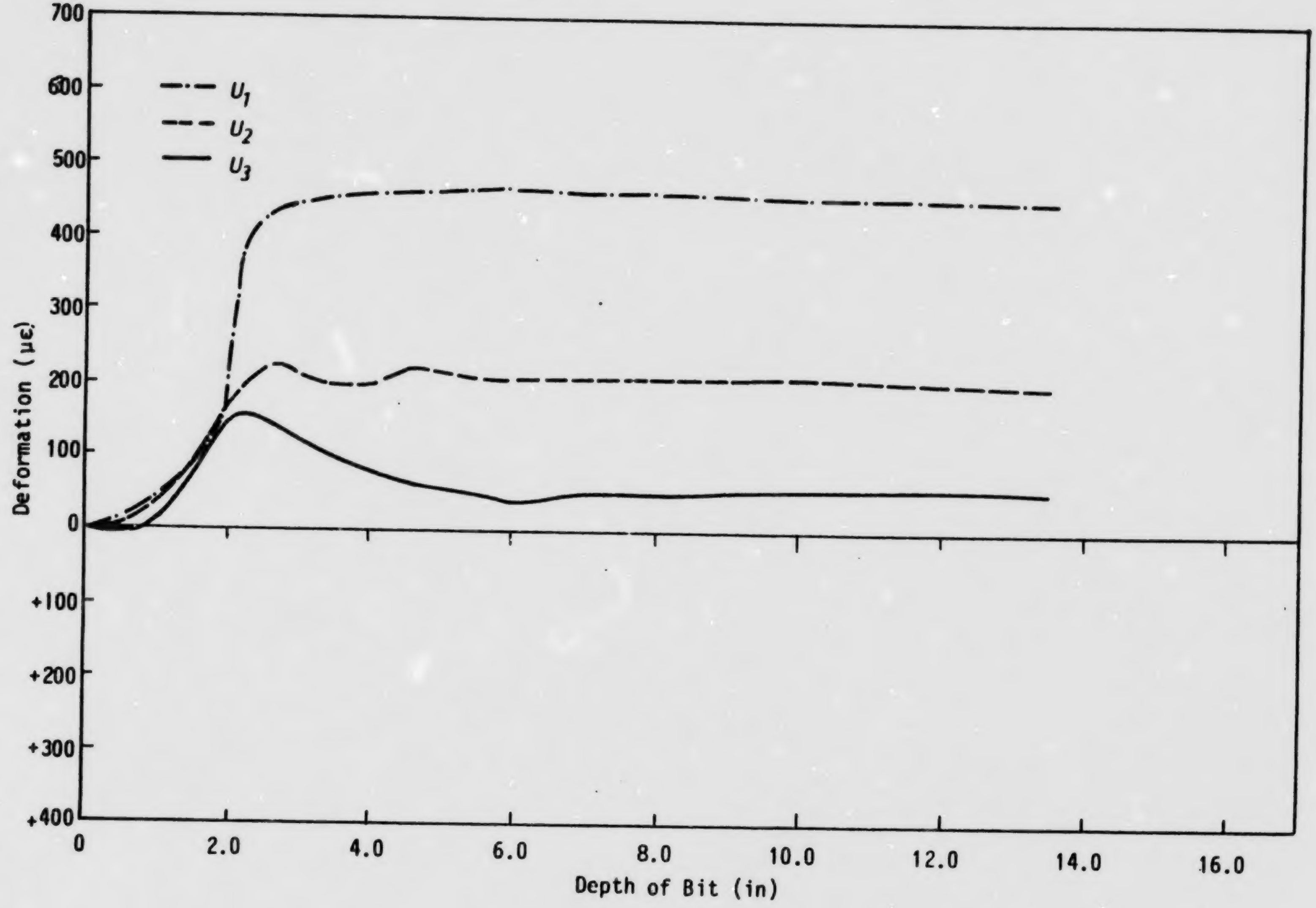

MIRAMICHI - BH 1- TEST 20 - GAUGE DEPTH 23.69m

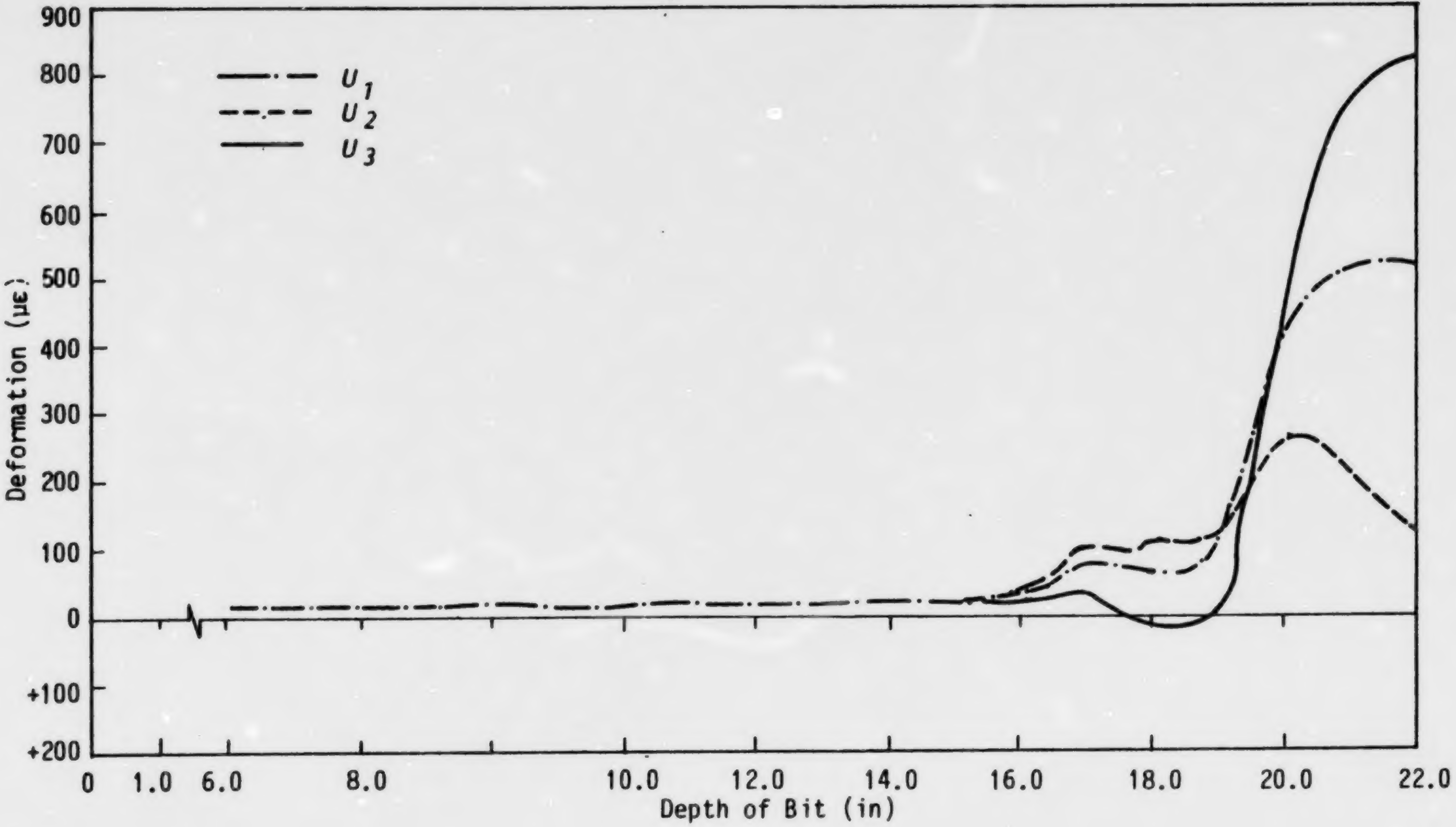

MIRAMICHI - BH 1 - TEST 21 - GAUGE DEPTH 23.48m

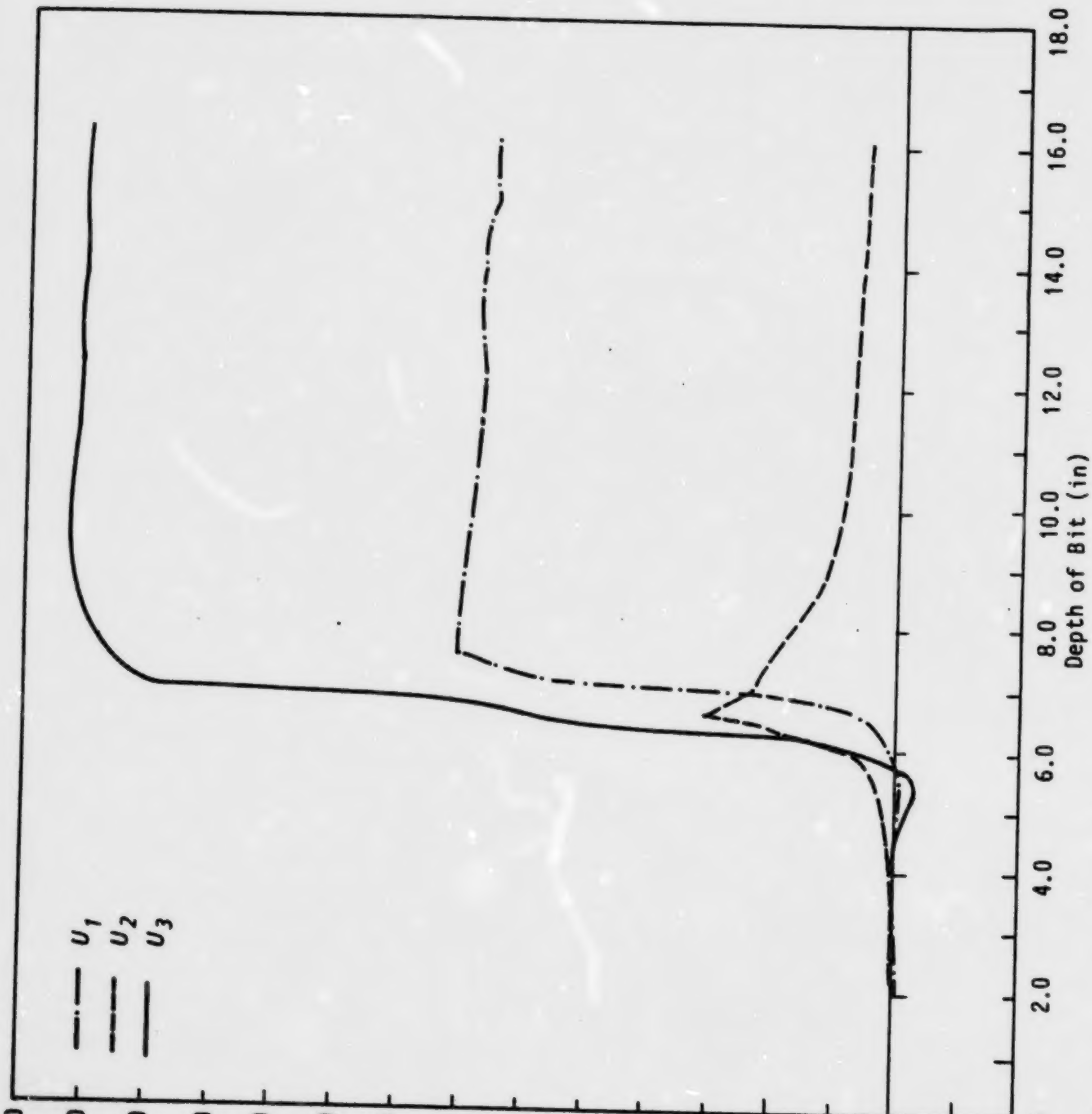

MIRAMICHI - BH 1 - TEST 22 - GAUGE DEPTH 23.65m

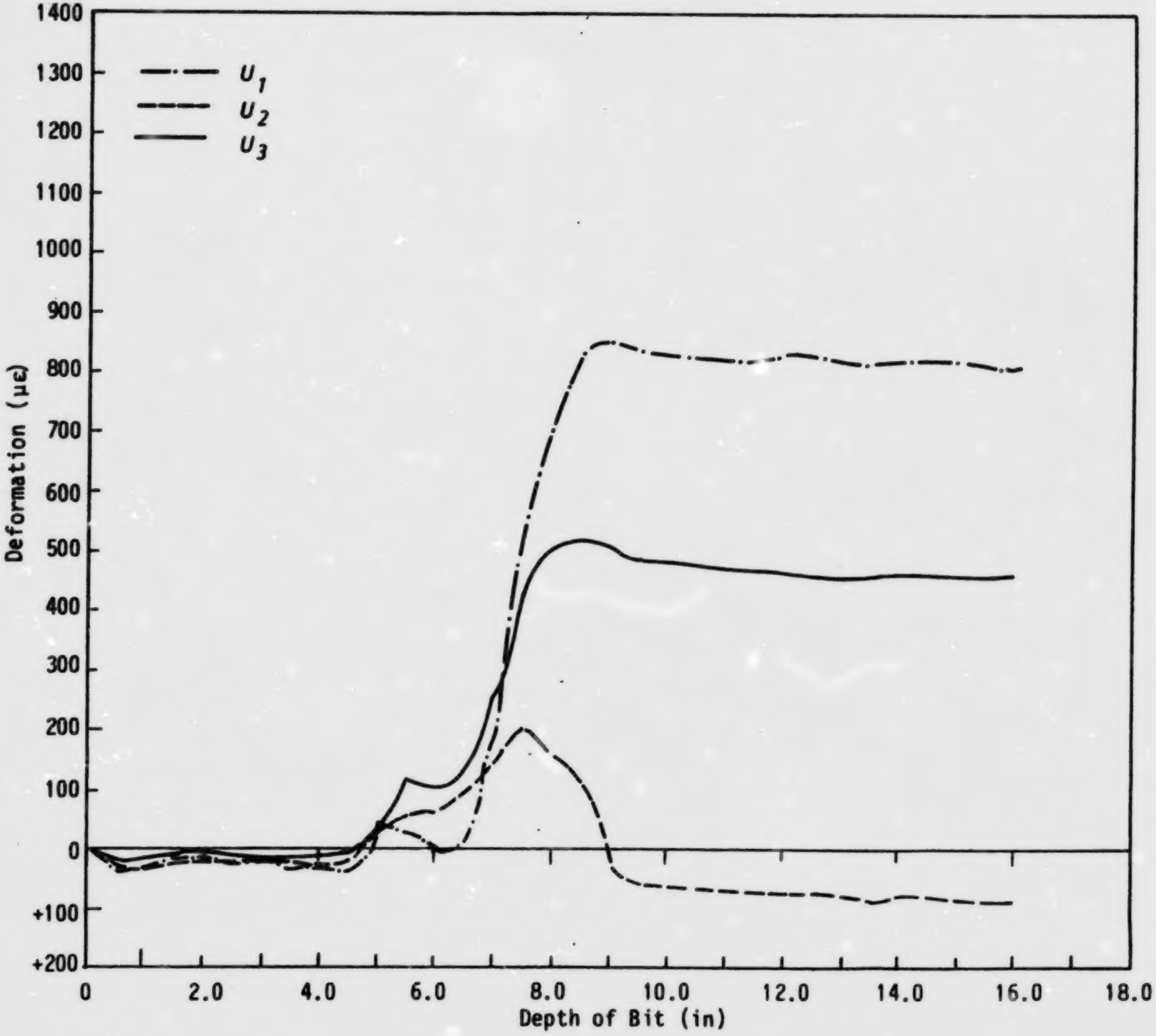

MIRAMICHI - BH 1 - TEST 23 - GAUGE DEPTH 30.46m

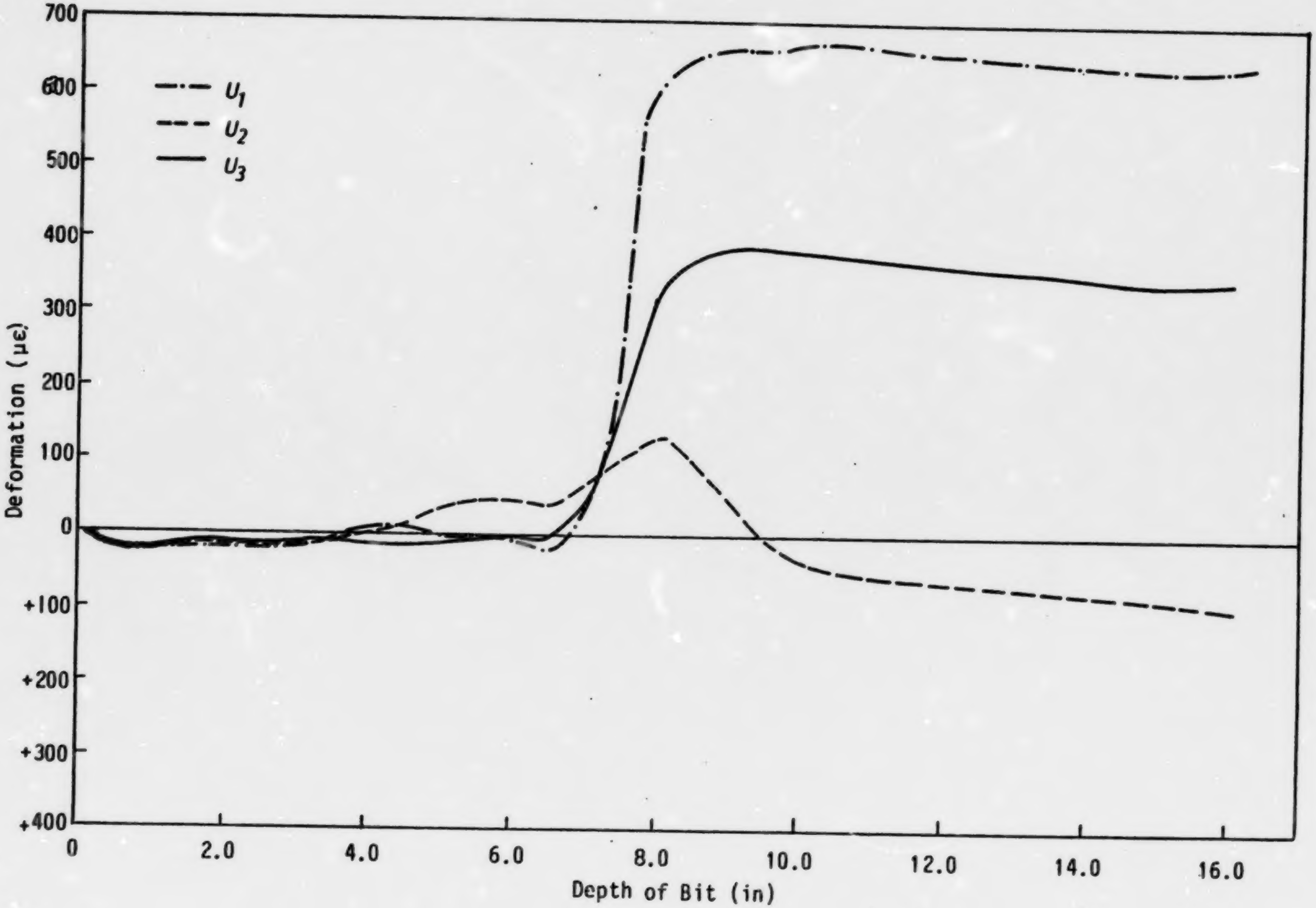

MIRAMICHI - BH 1 - TEST 24 - GAUGE DEPTH 30.86m

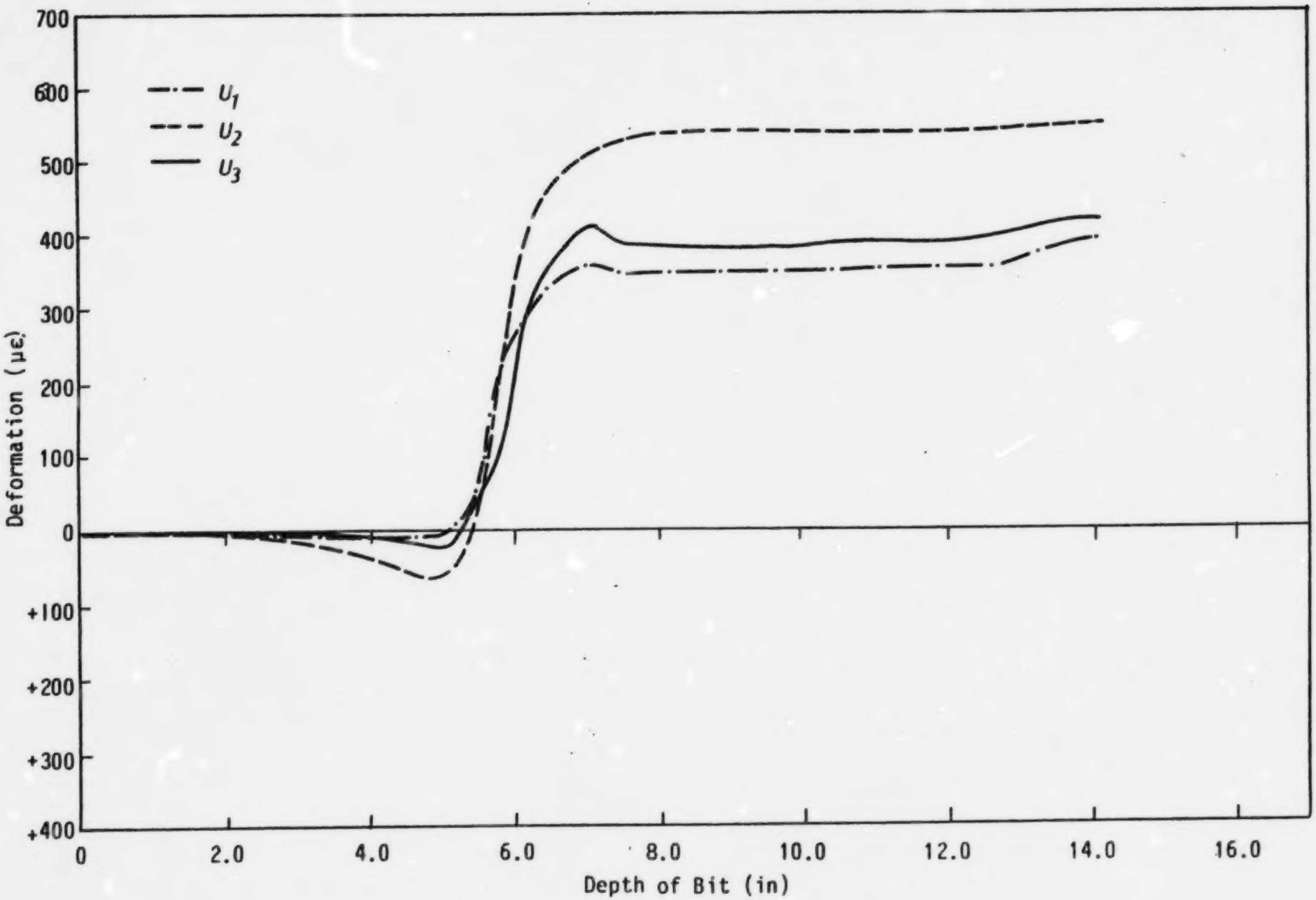

MIRAMICHI - BH 5 - TEST 25-GAUGE DEPTH 3.56m

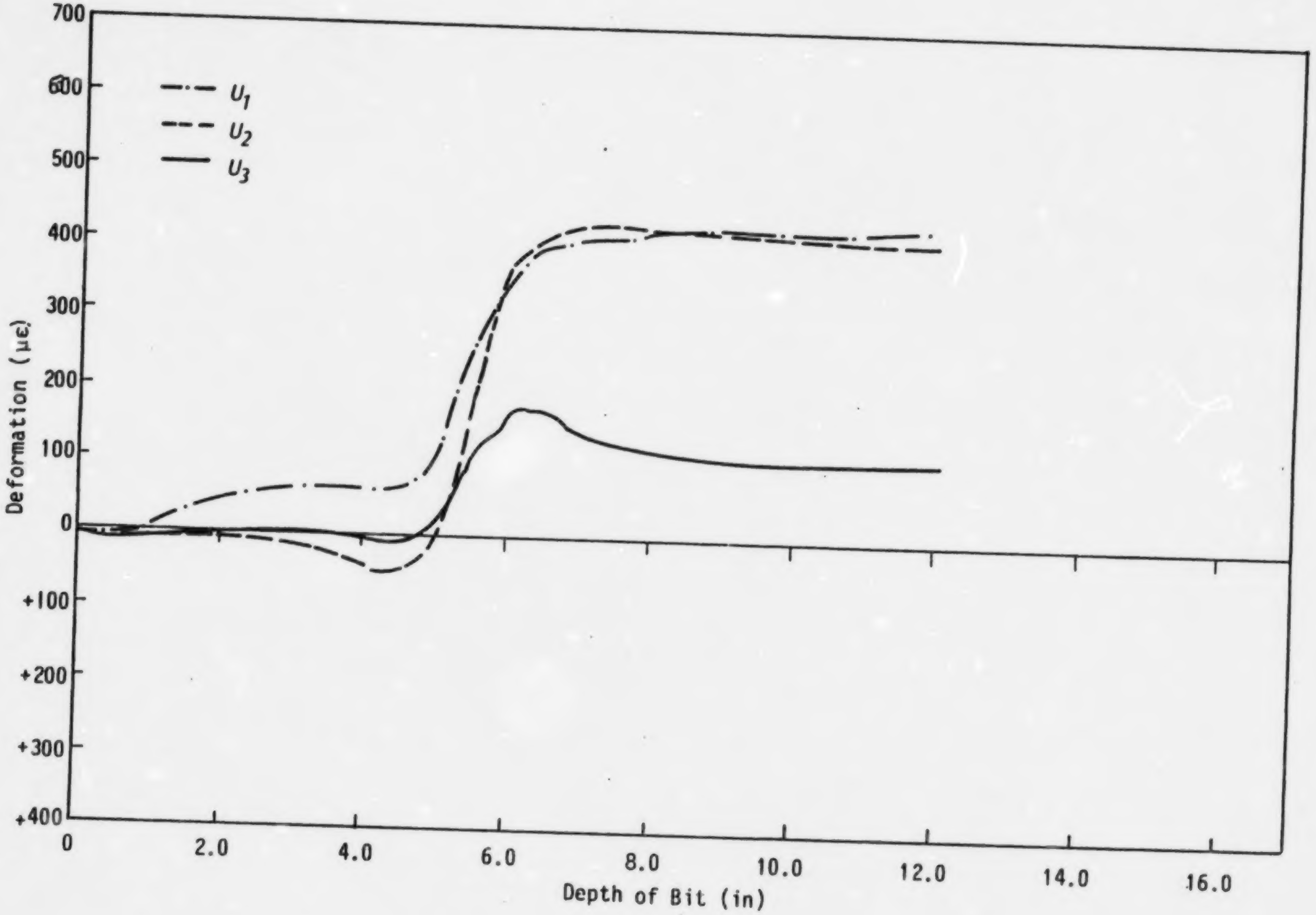

MIRAMICHI - BH 5- TEST 26-GAUGE DEPTH 3.92m

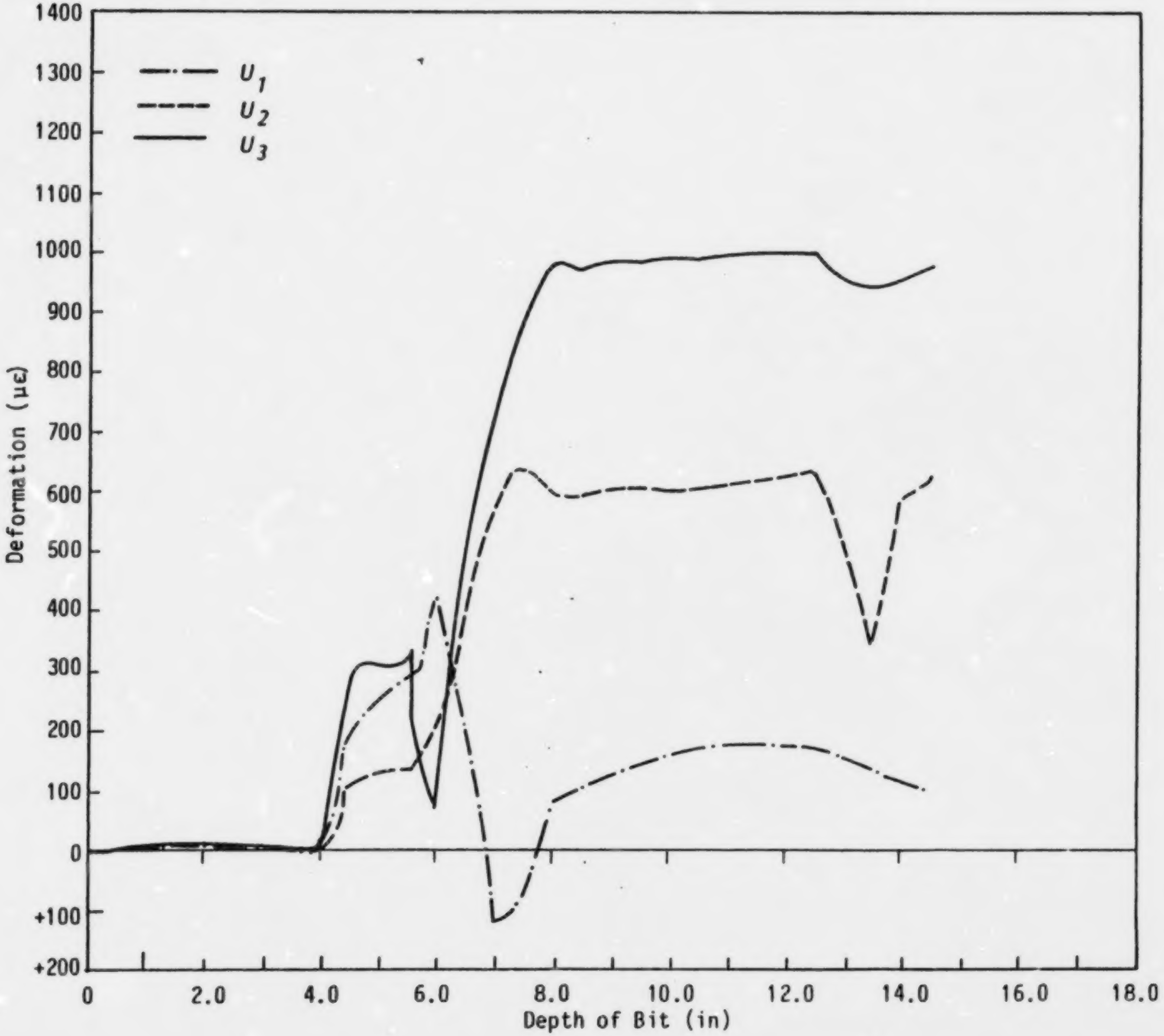

MIRAMICHI - BH 2 - TEST 27 - GAUGE DEPTH 3.02m

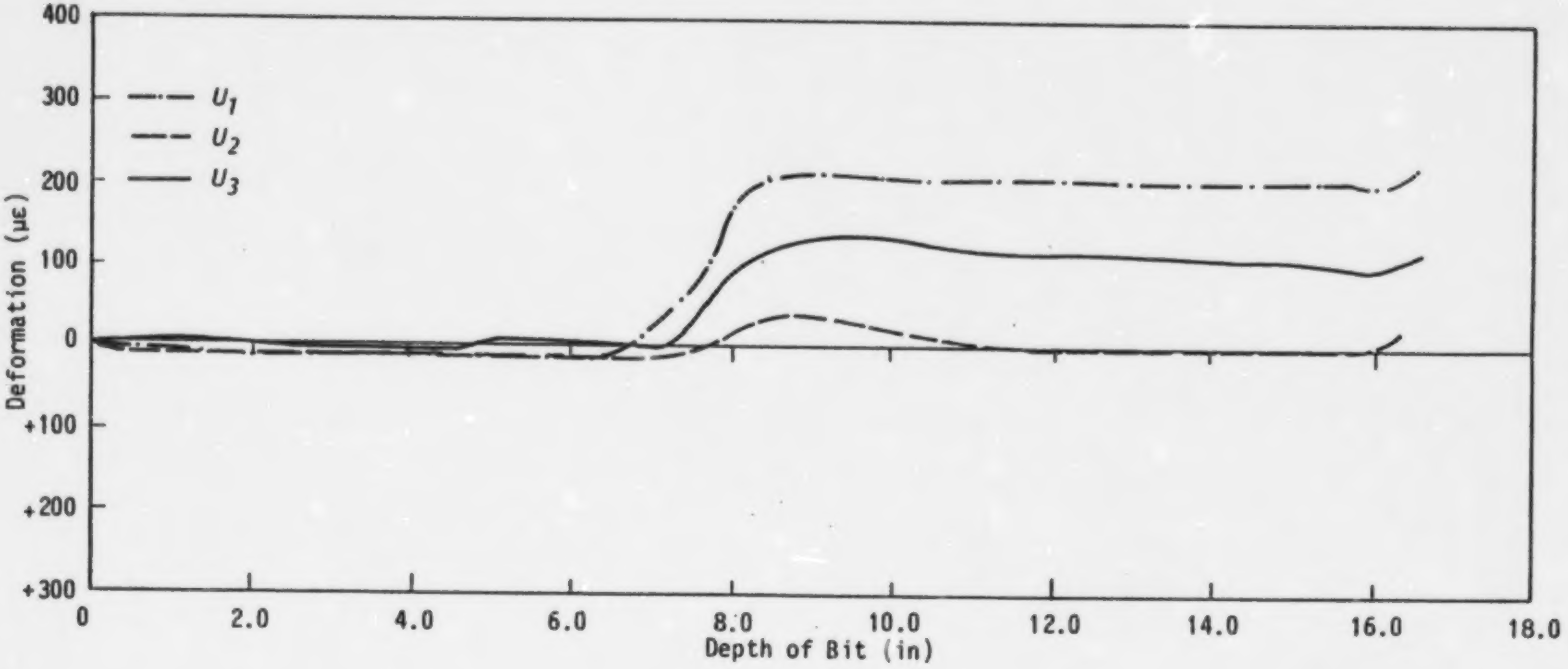

MIRAMICHI - BH 2 - TEST 28 - GAUGE DEPTH 3.38m

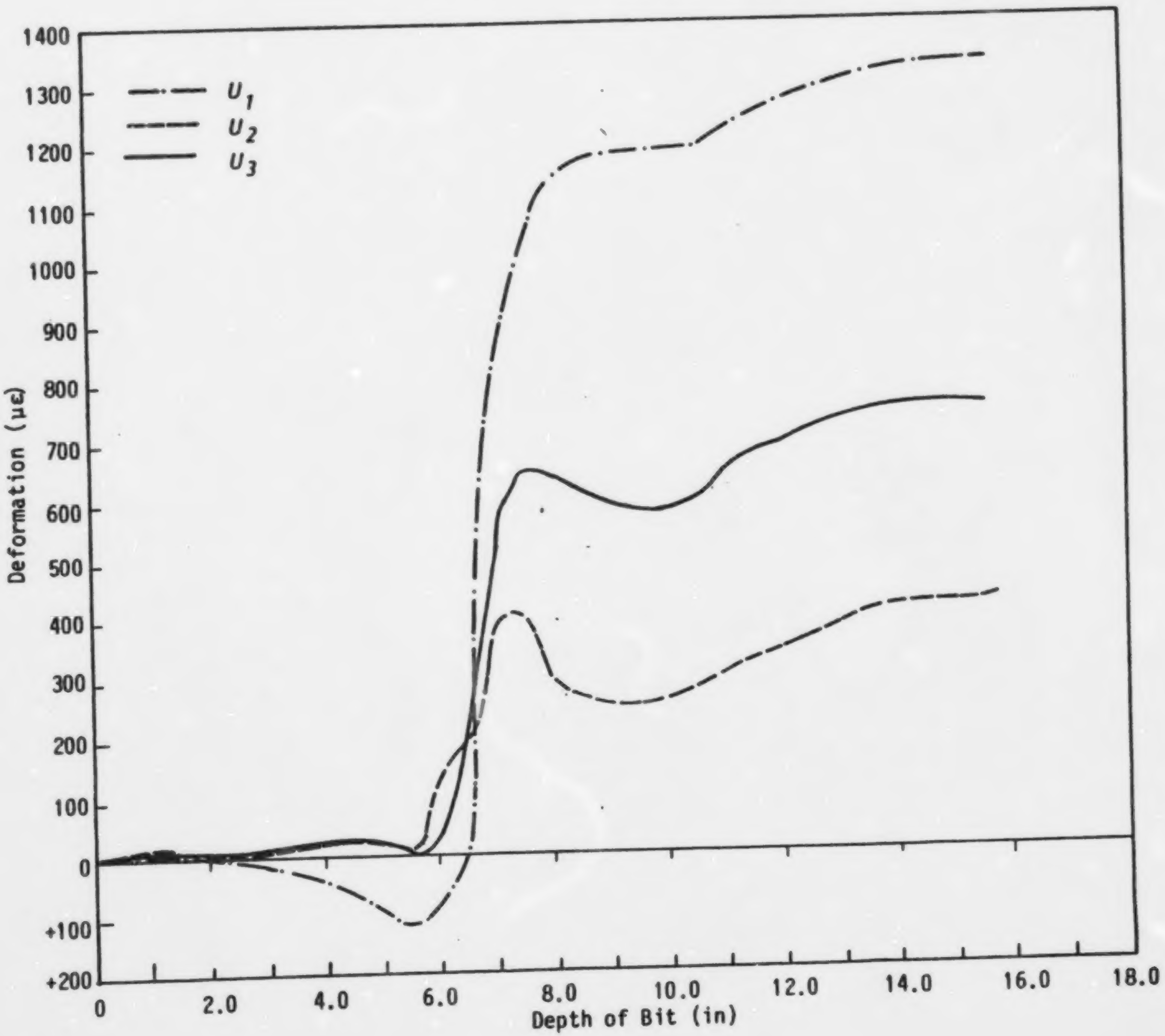

MIRAMICHI - BH 5 - TEST 29 - GAUGE DEPTH 8.16 m

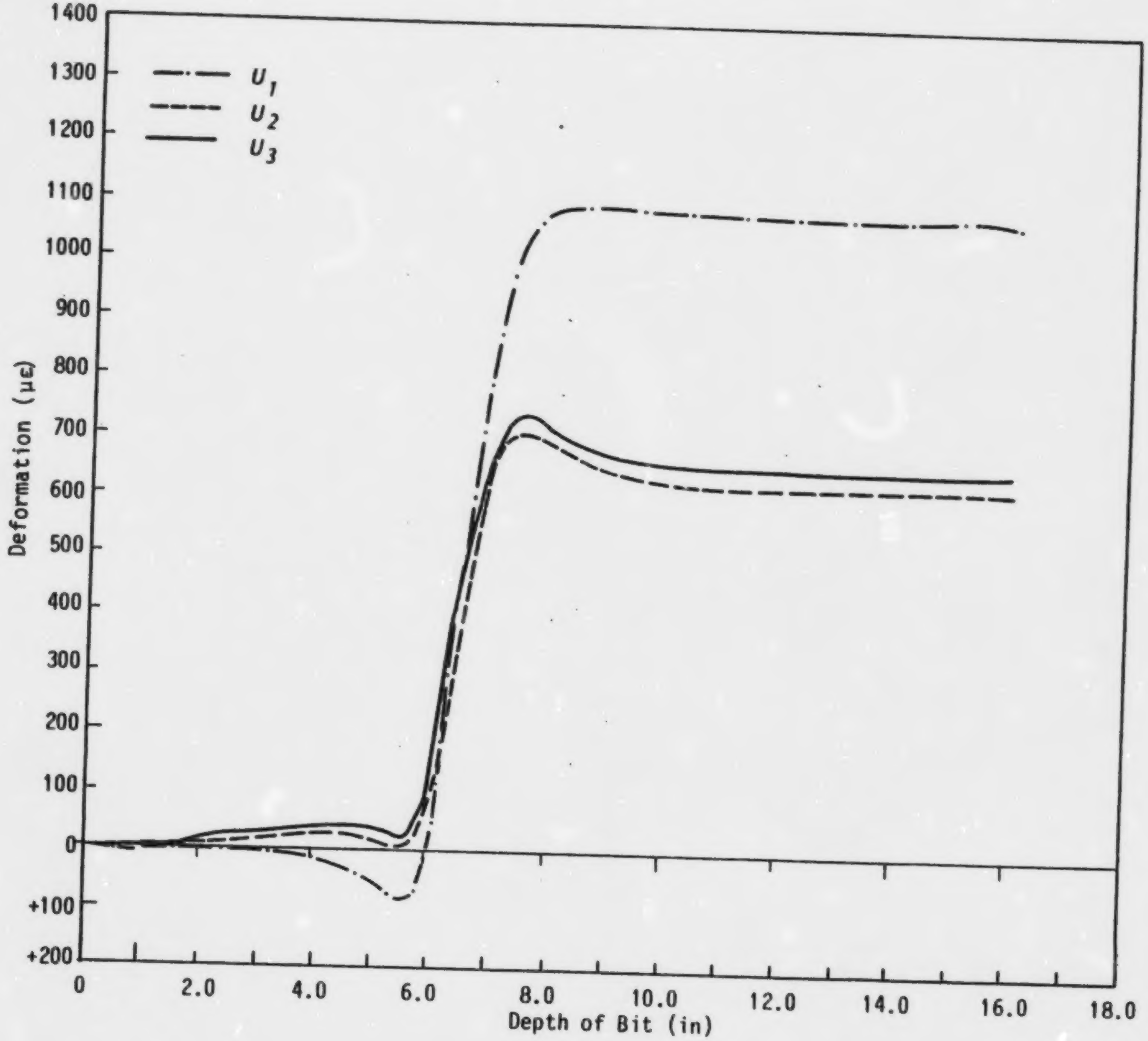

MIRAMICHI - BH 5 - TEST 30 - GAUGE DEPTH 8.60m

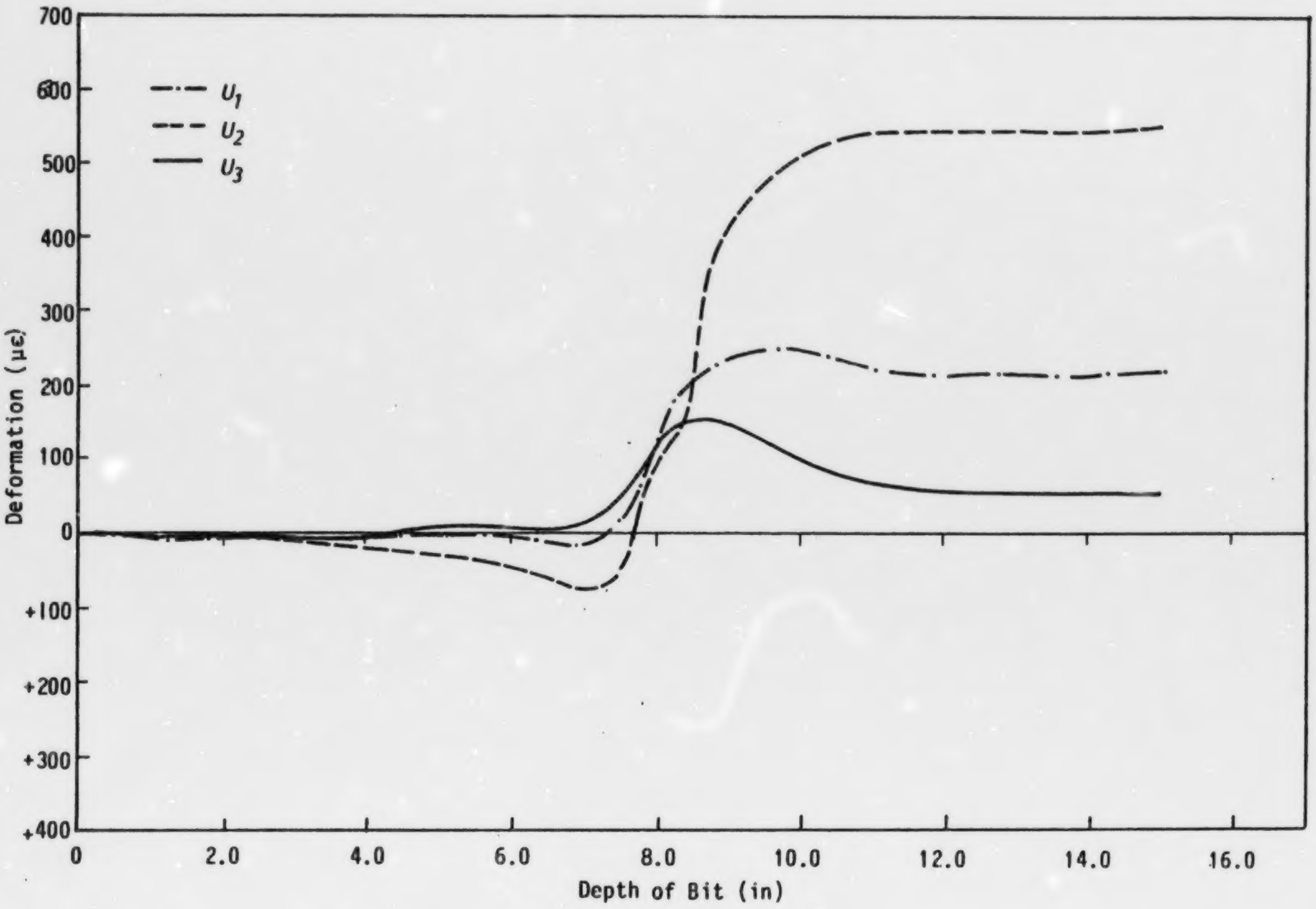

MIRAMICHI - BH 2 - TEST 31 - GAUGE DEPTH 6.30m

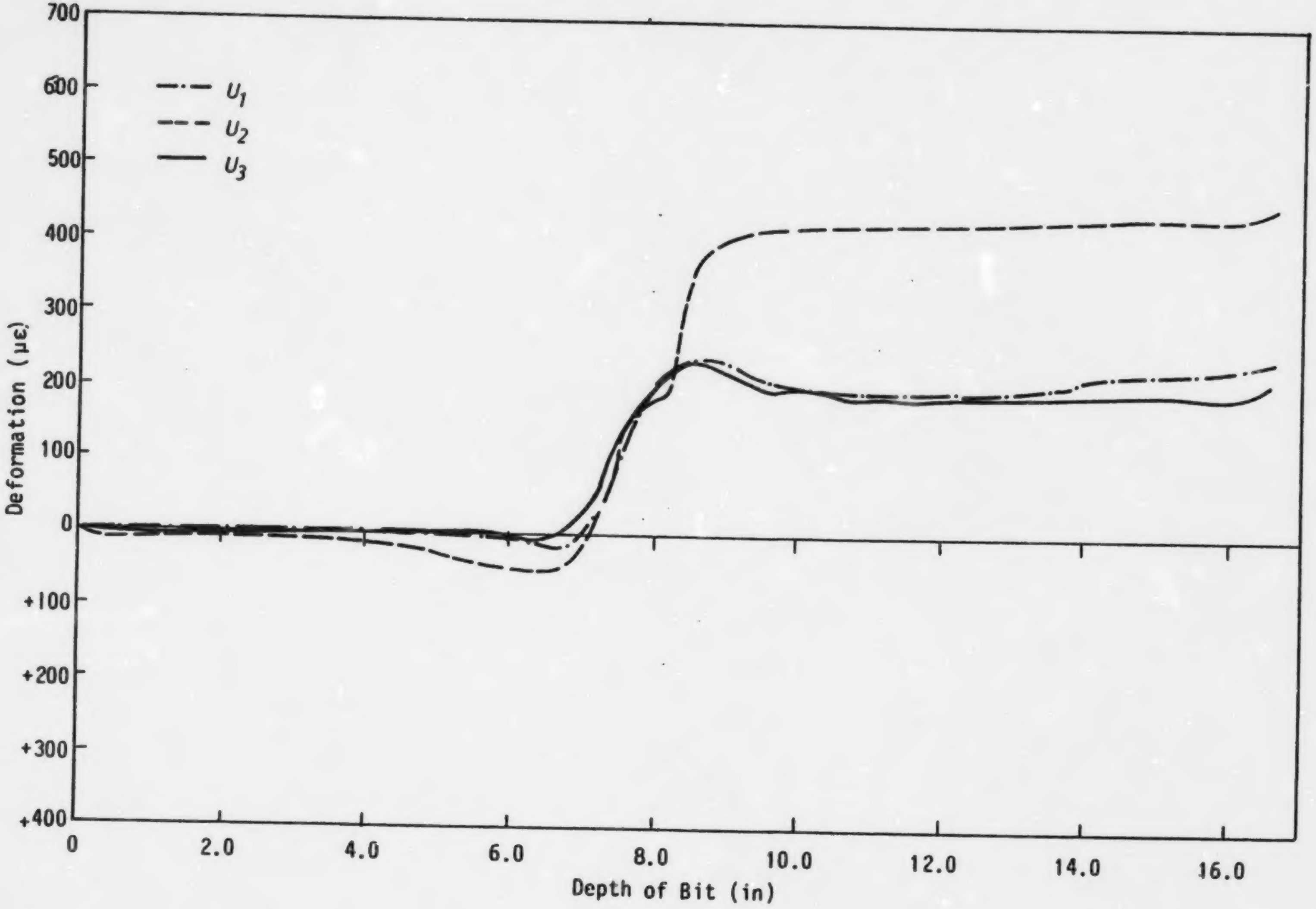

MIRAMICHI - BH 2- TEST 32-GAUGE DEPTH 6.75m

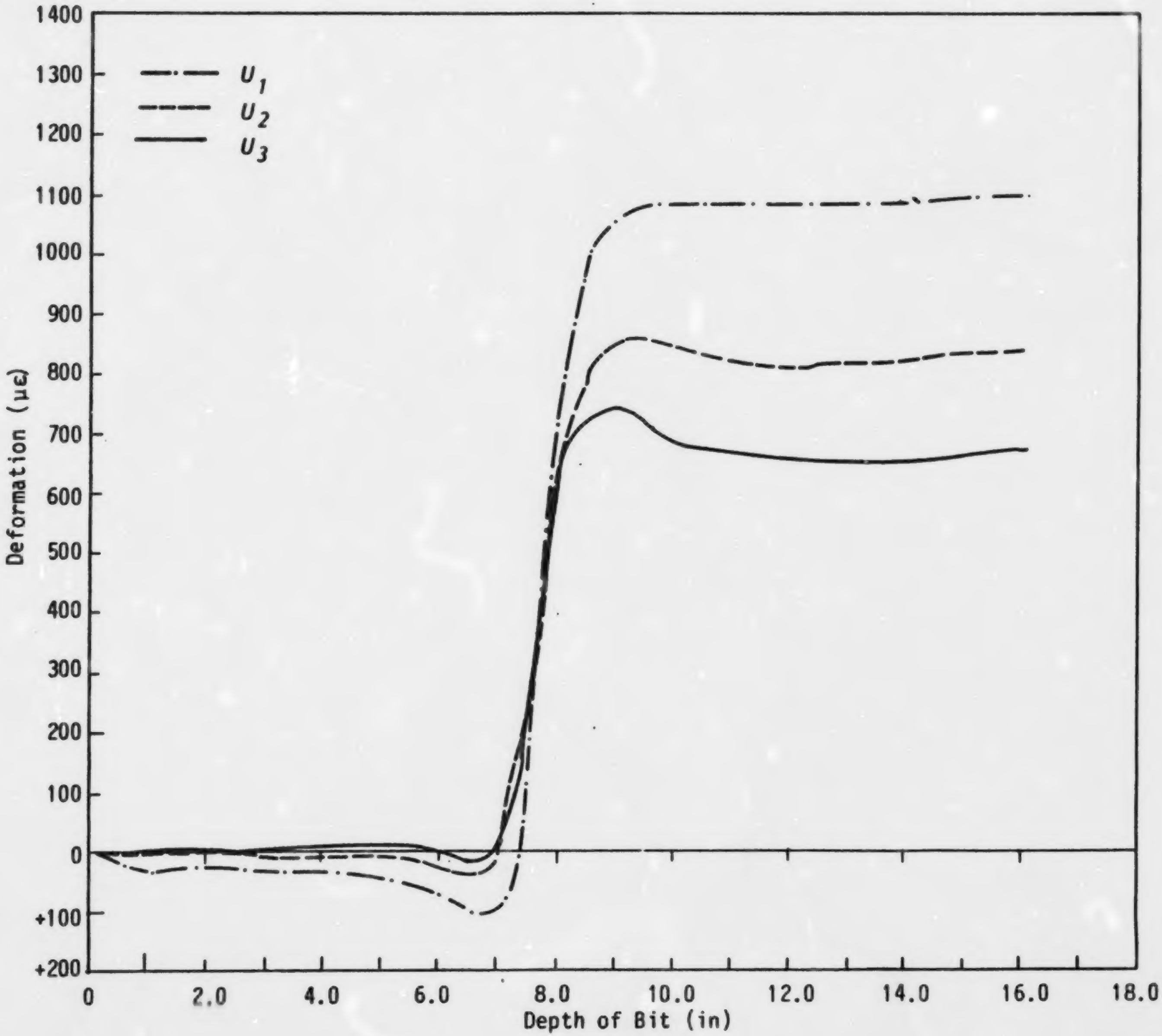

MIRAMICHI - BH 5 - TEST 33 - GAUGE DEPTH 10.65m

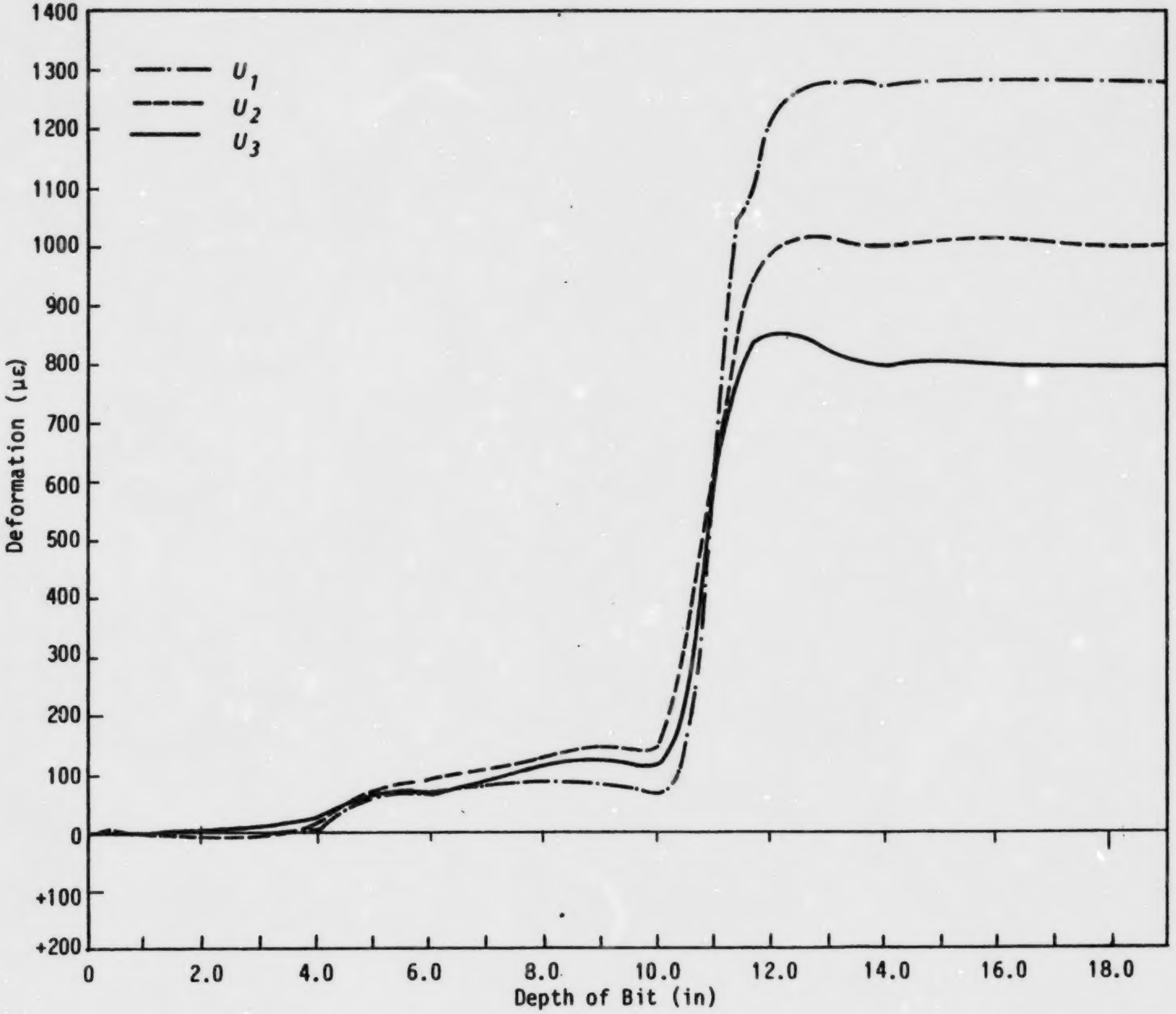

MIRAMICHI - BH5 - TEST 34 - GAUGE DEPTH 11.13m

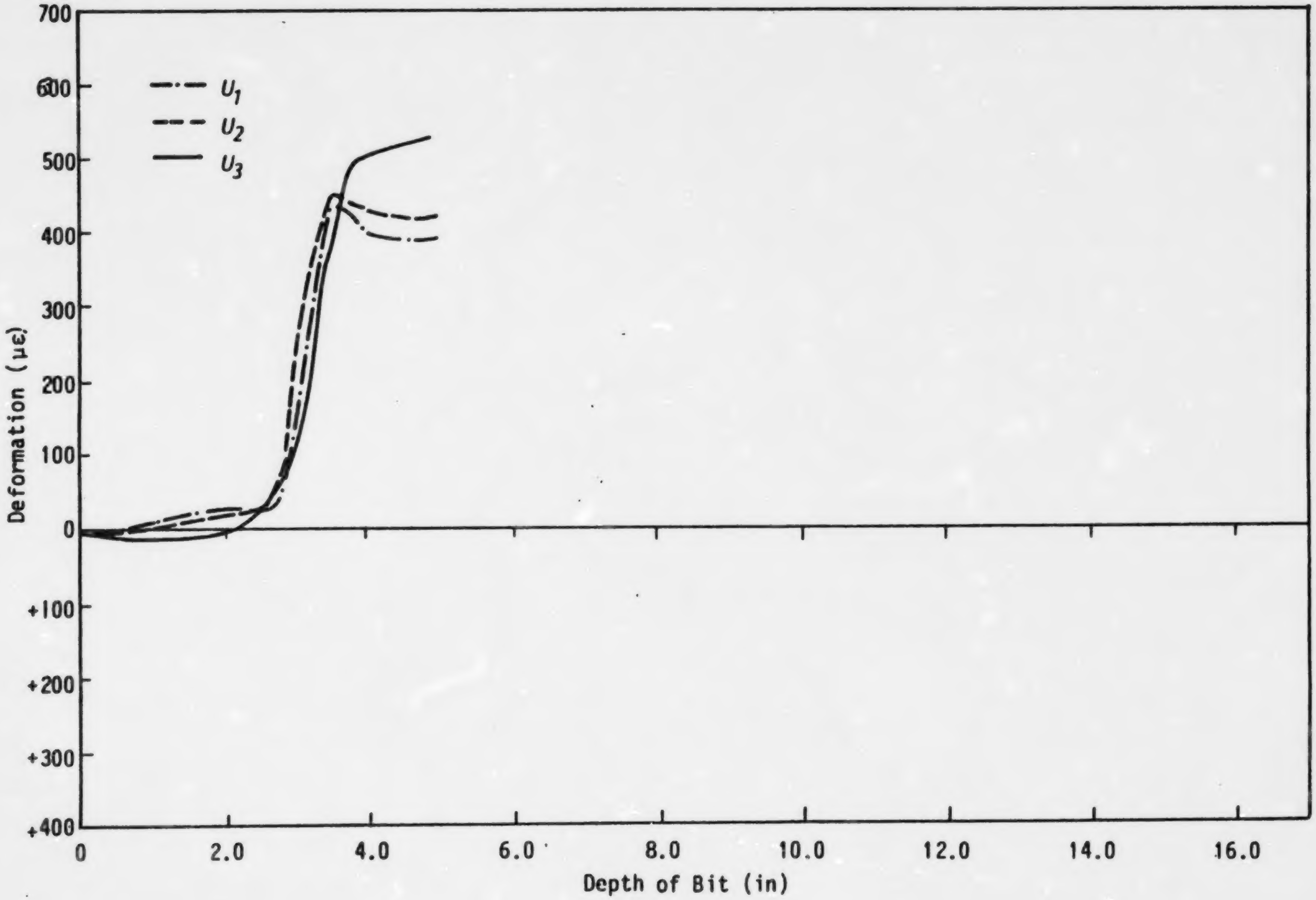

MIRAMICHI - BH 2 - TEST 35a - GAUGE DEPTH 10.63m

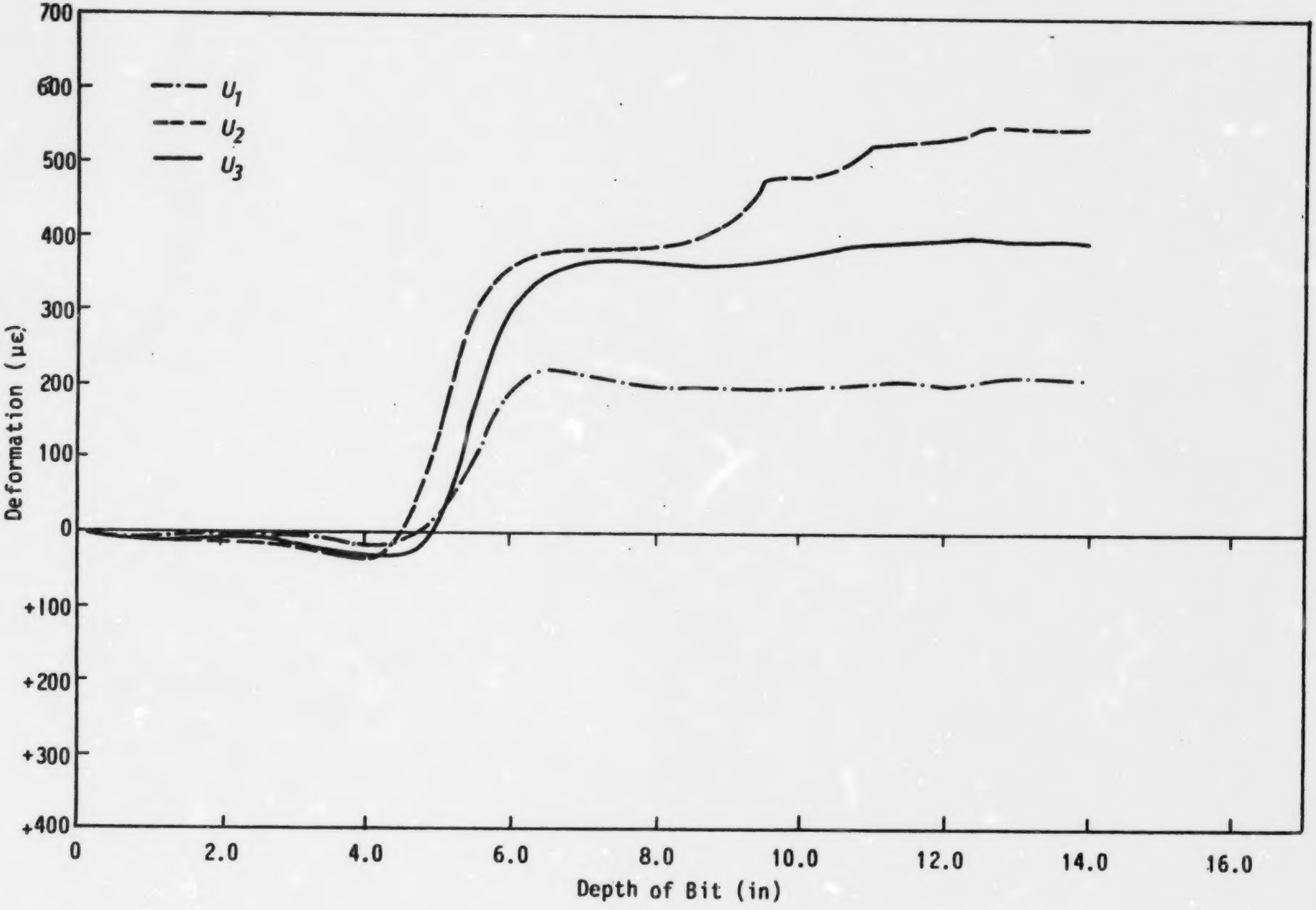

MIRAMICHI - BH 2 - TEST 35b - GAUGE DEPTH 10.91m

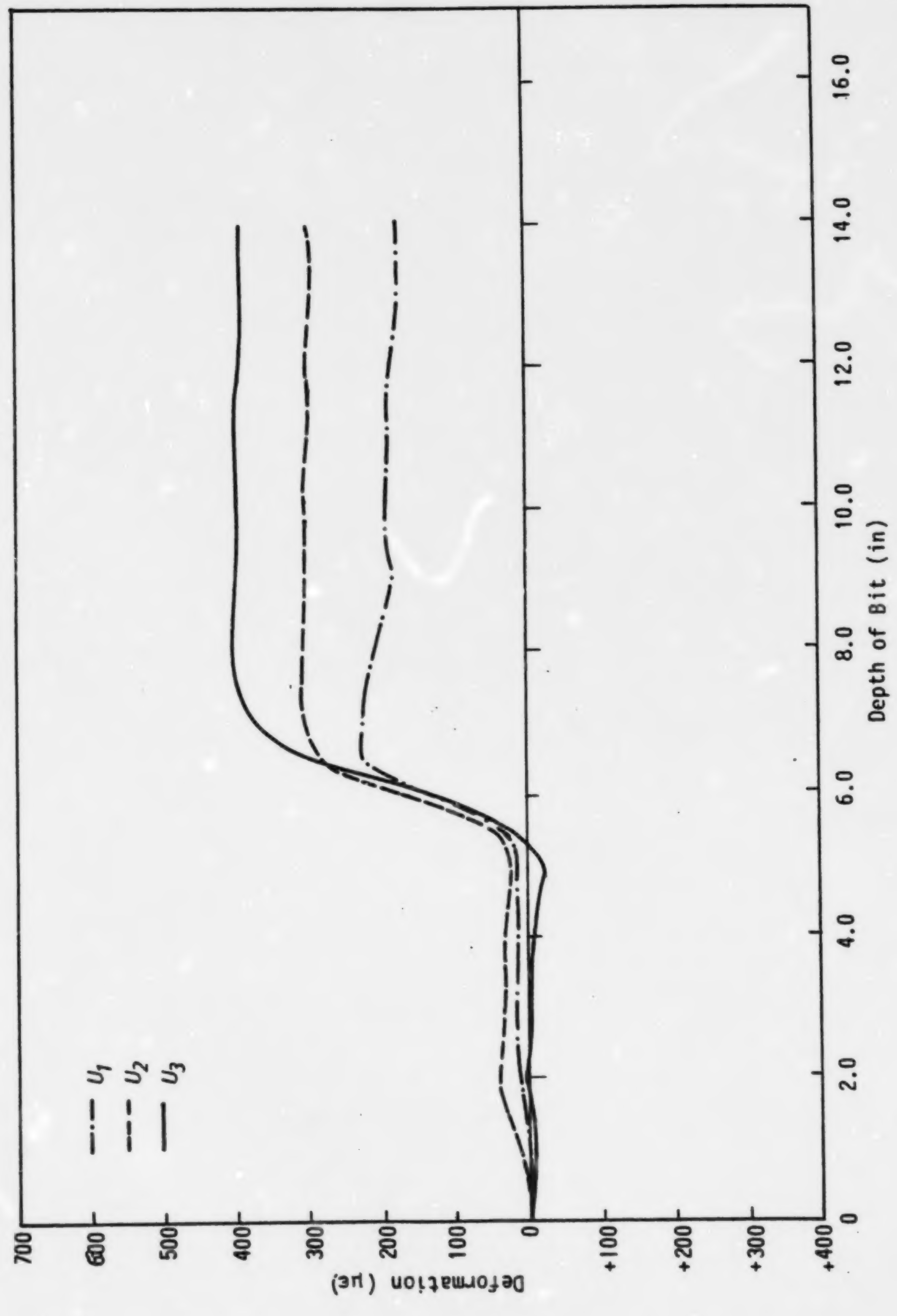

MIRAMICHI - BH 2 - TEST 36 - GAUGE DEPTH 11.31m

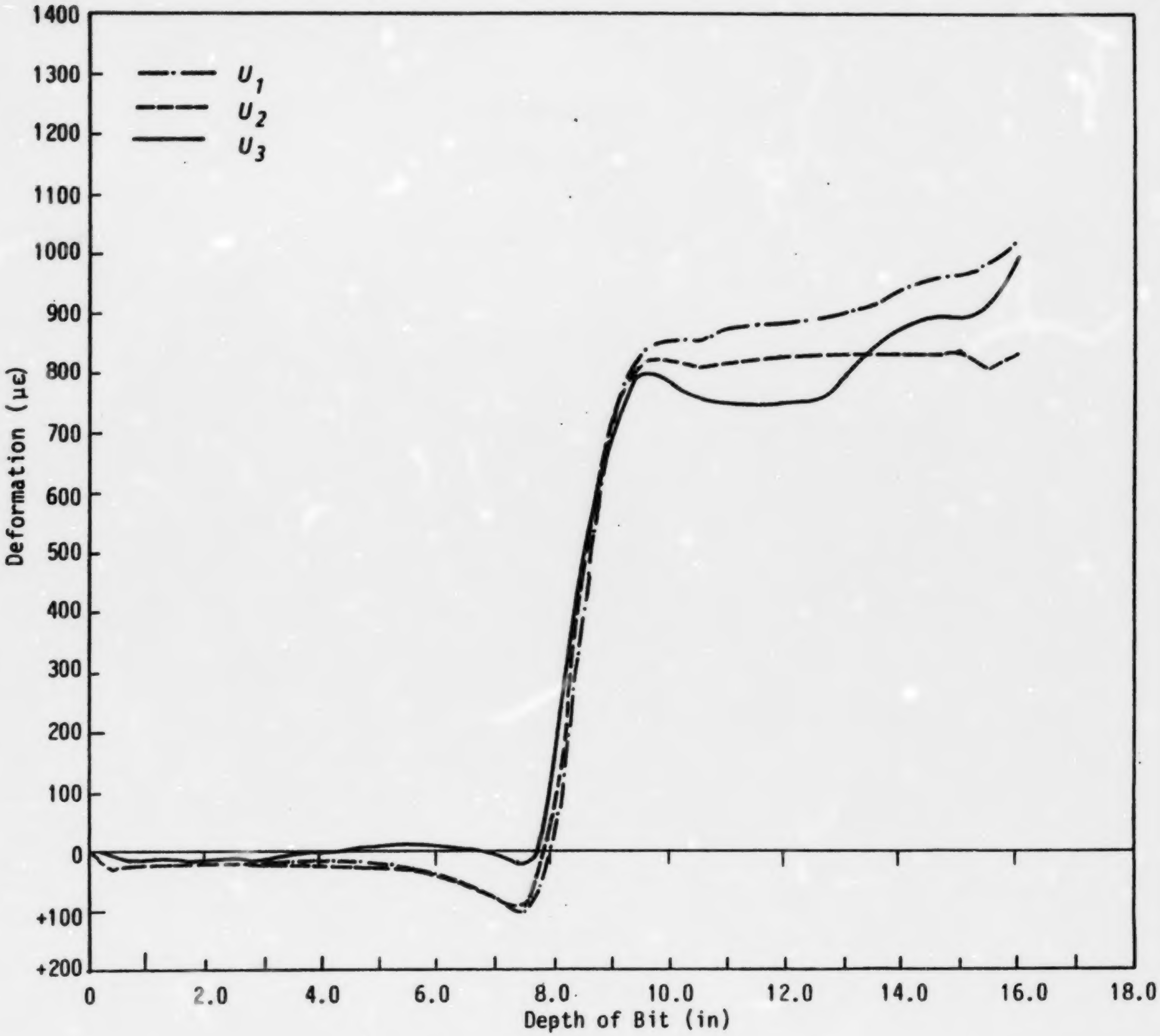

MIRAMICHI - BH 5 - TEST 37 - GAUGE DEPTH 15.45m

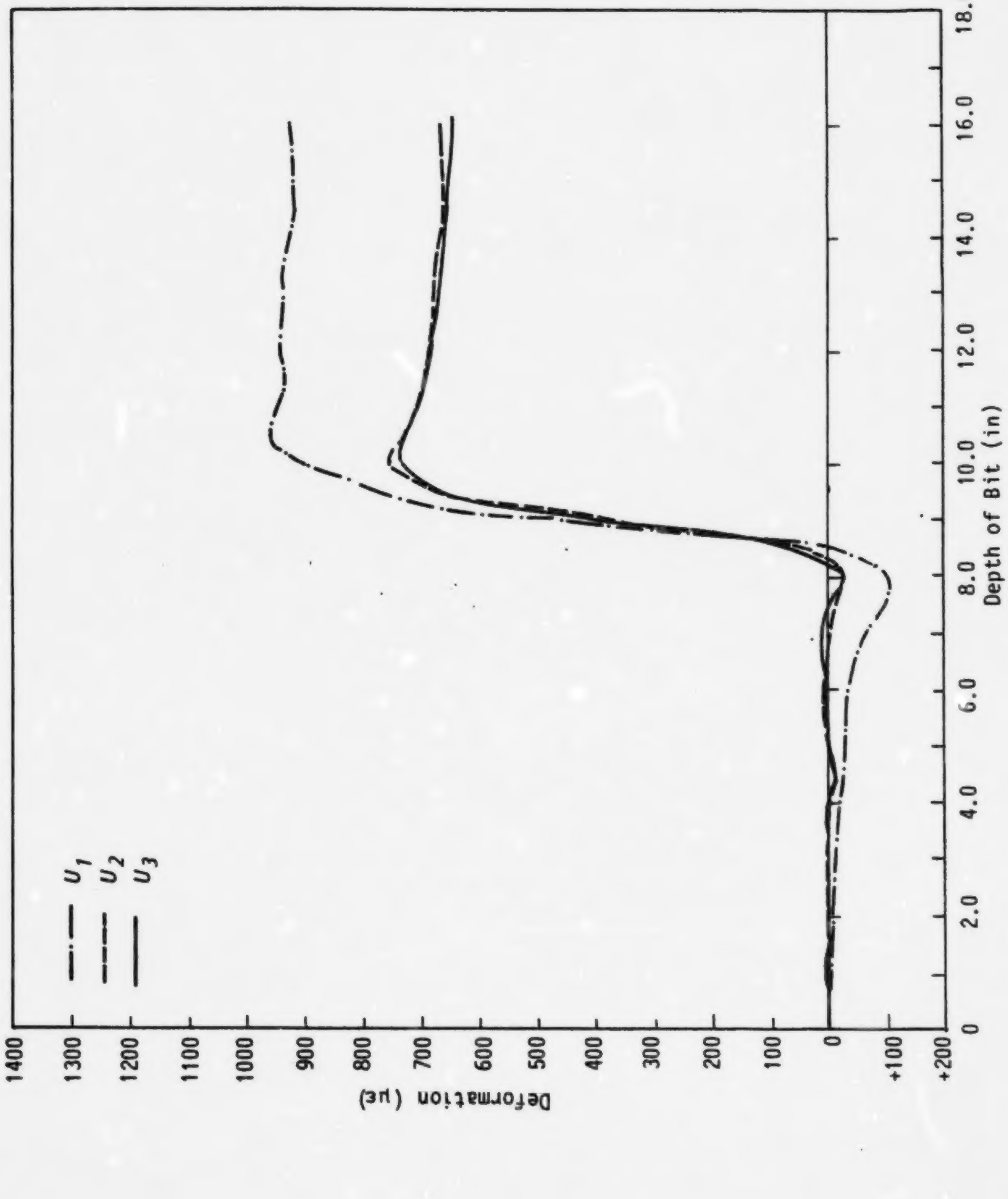

MIRAMICHI - BH 5 - TEST 38- GAUGE DEPTH 15.85m

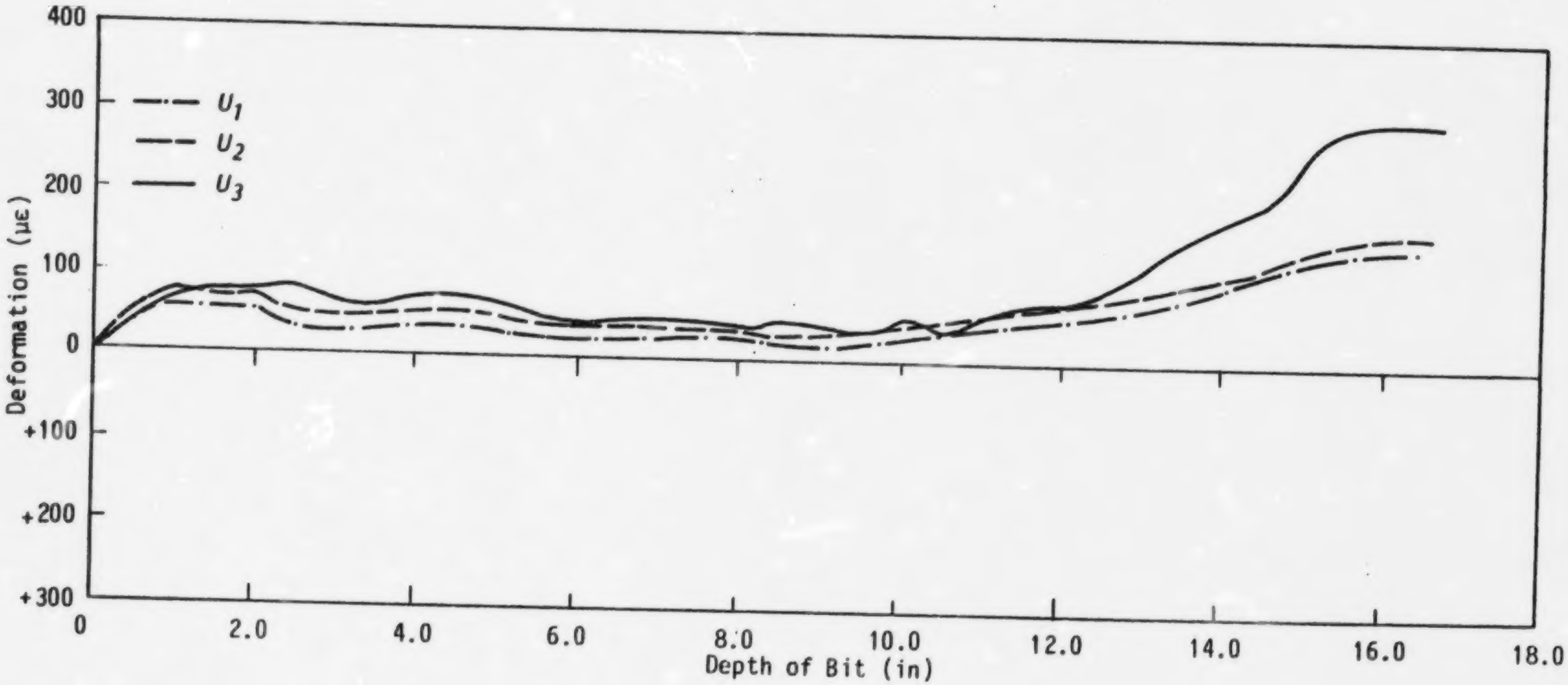

MIRAMICHI - BH 2 - TEST 39 - GAUGE DEPTH 15.88m

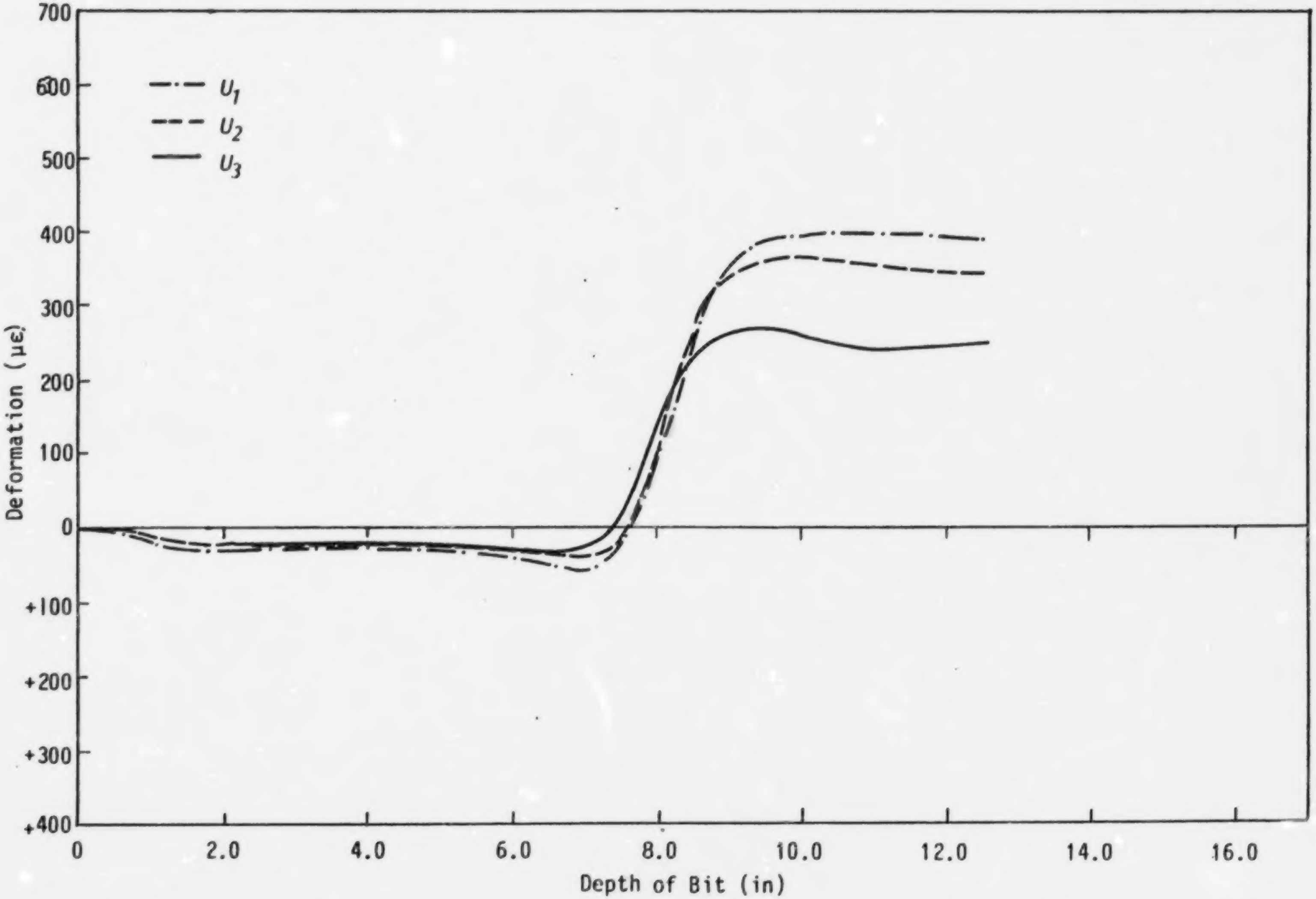

MIRAMICHI - BH 2 - TEST 40 - GAUGE DEPTH 16.32m

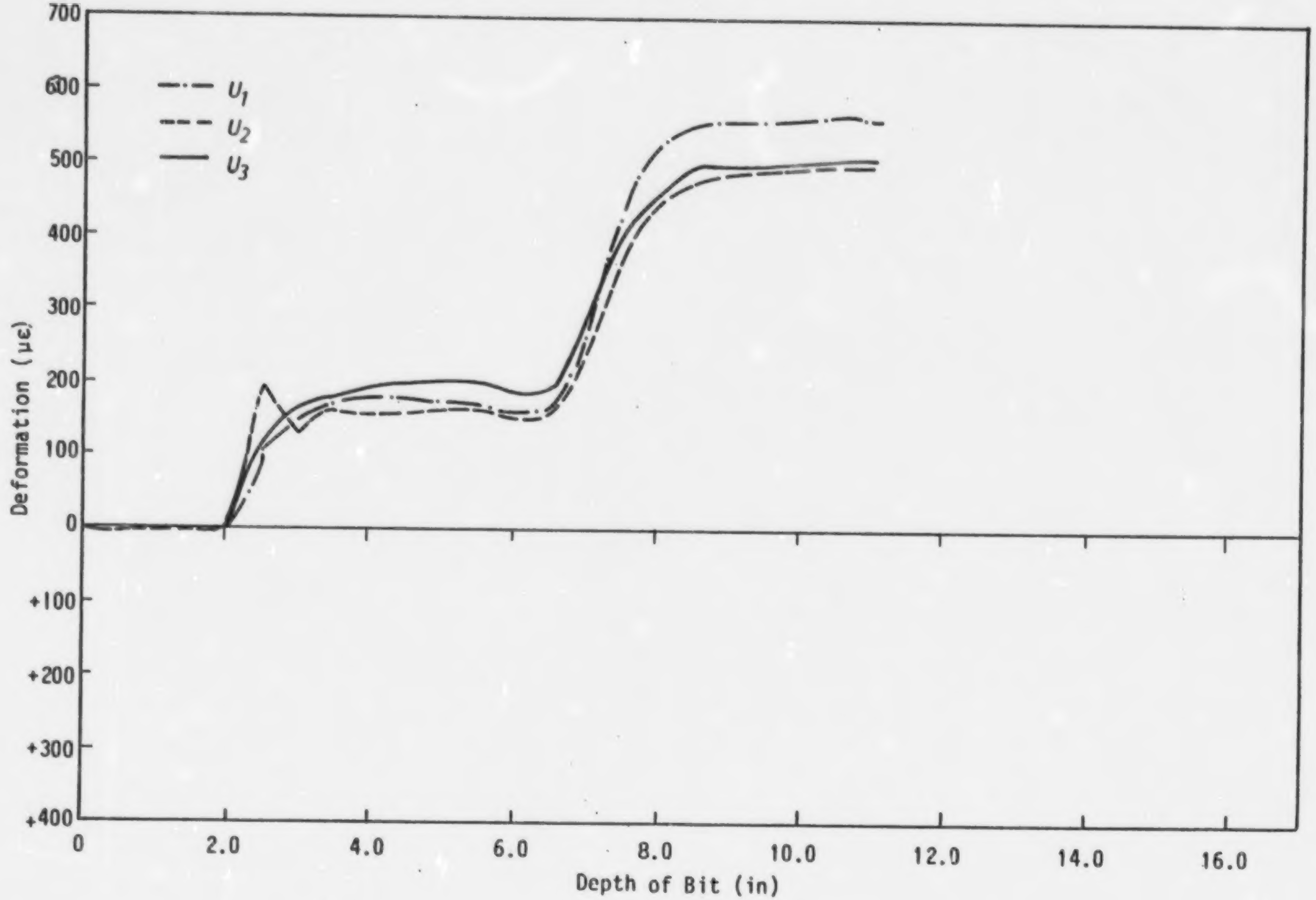

MIRAMICHI - BH 2 - TEST 41- GAUGE DEPTH 16.60m

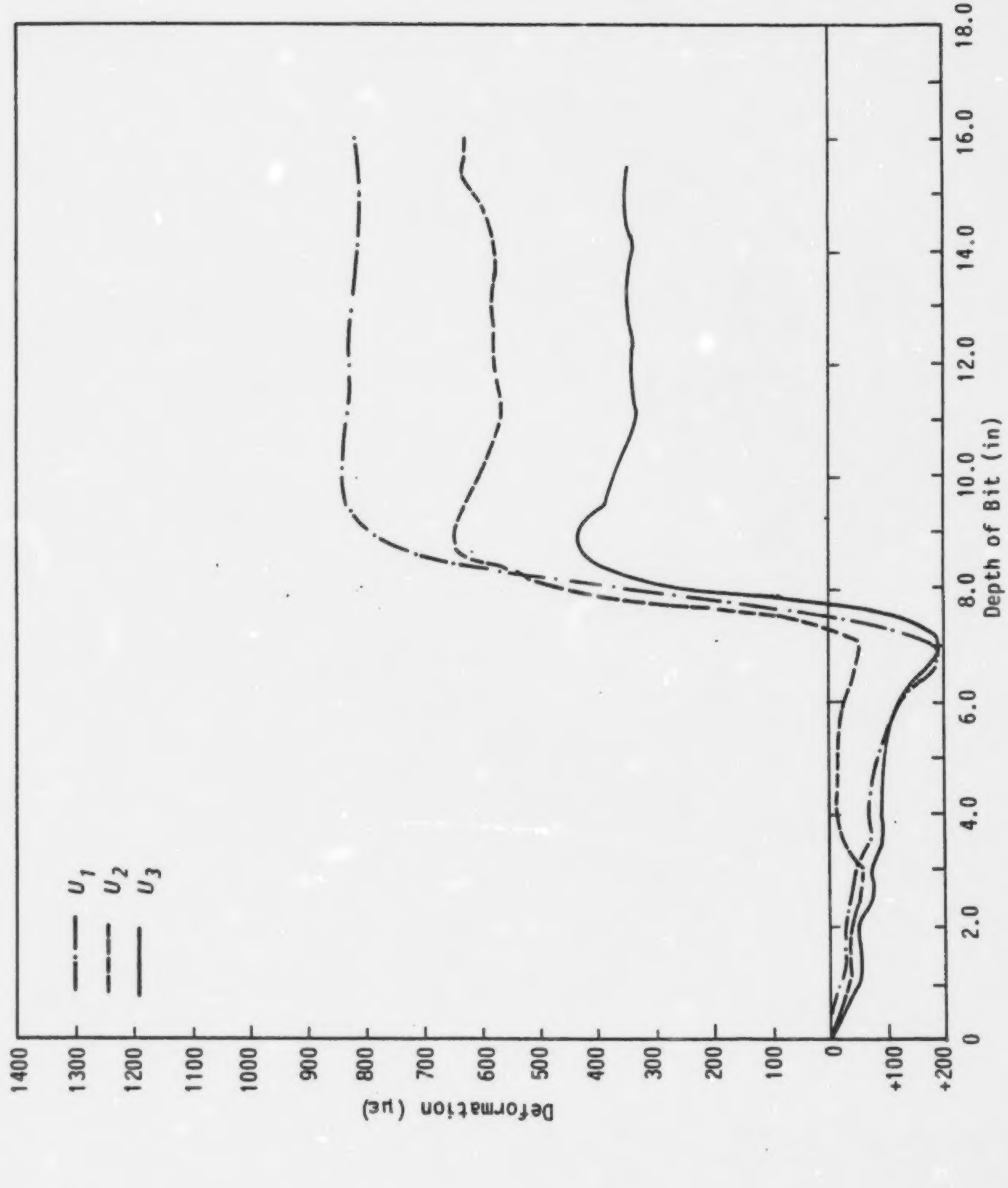

MIRAMICHI - BH 5 - TEST 42- GAUGE DEPTH 22.83m

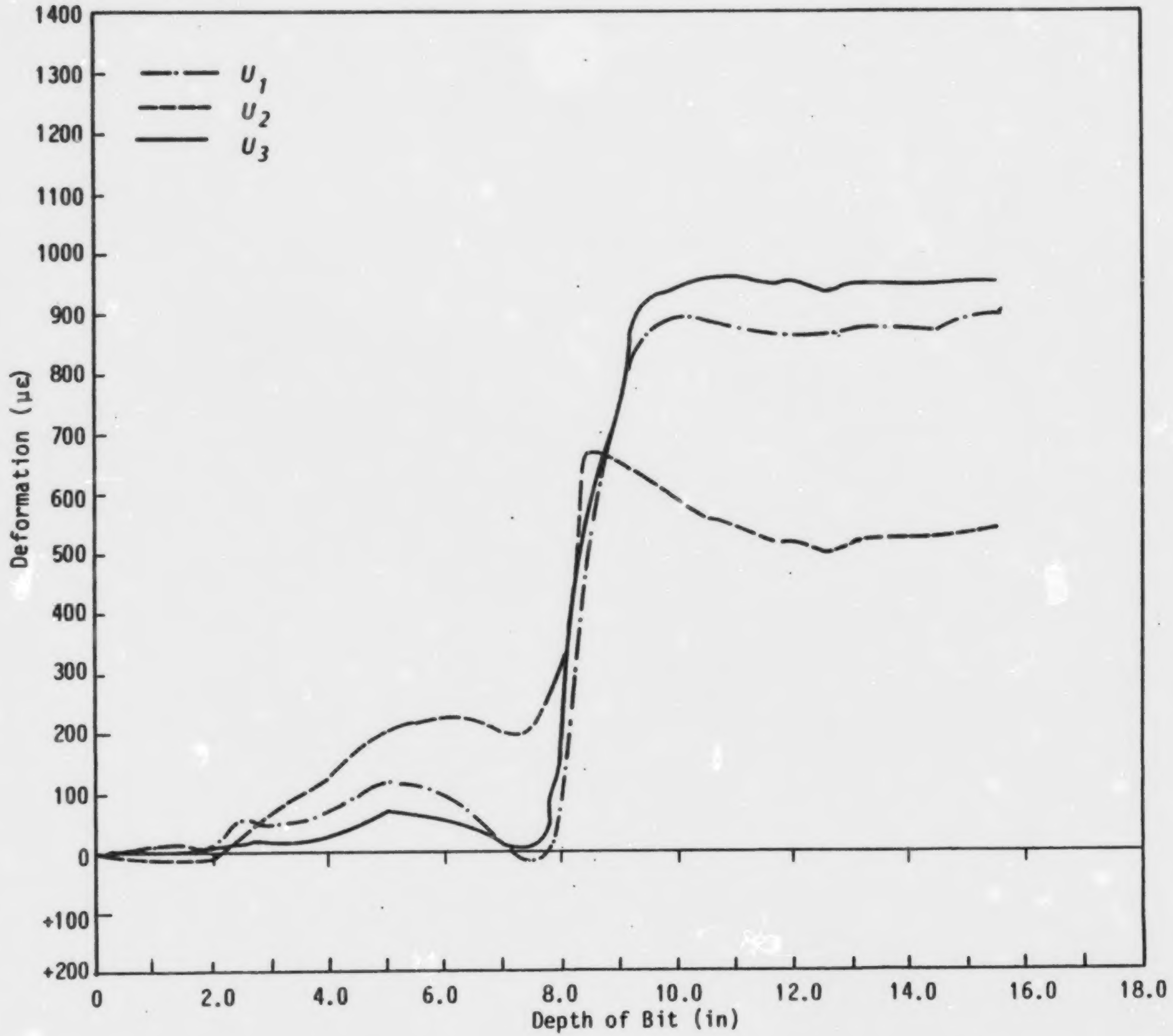

MIRAMICHI - BH 5 - TEST 43 - GAUGE DEPTH 23.23m

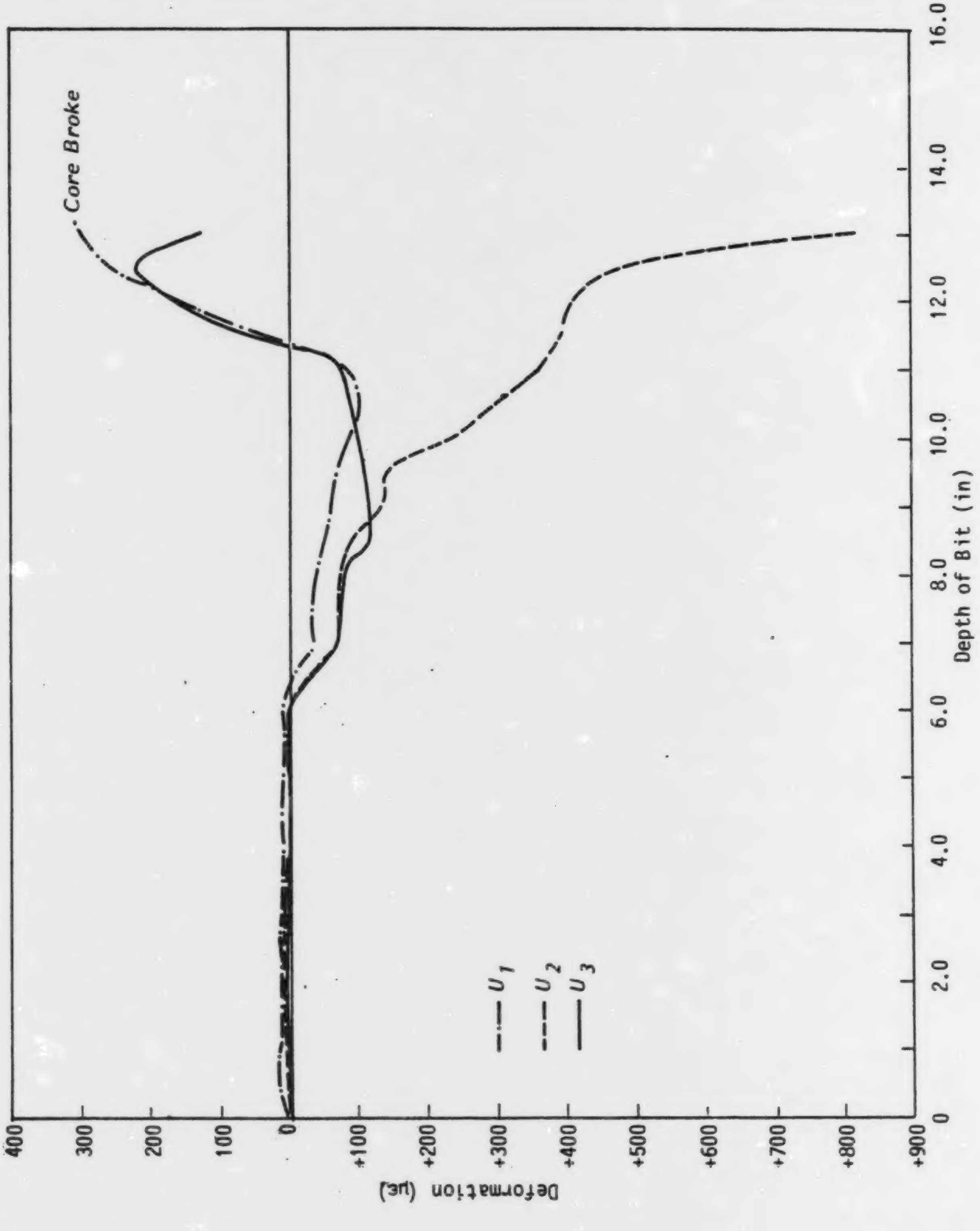

MIRAMICHI - BH2 - TEST 44 - GAUGE DEPTH 22.98m

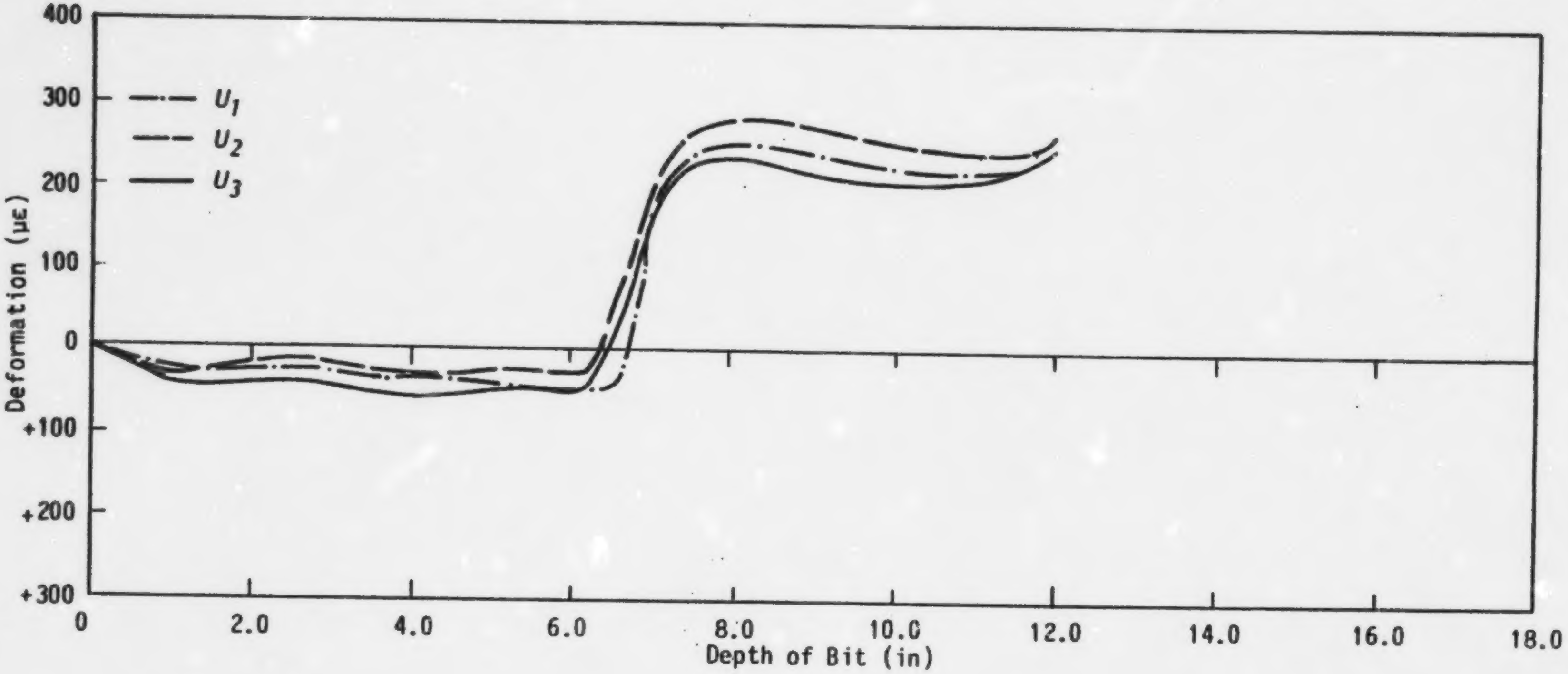

MIRAMICHI - BH 2 - TEST 45 - GAUGE DEPTH 24.78m

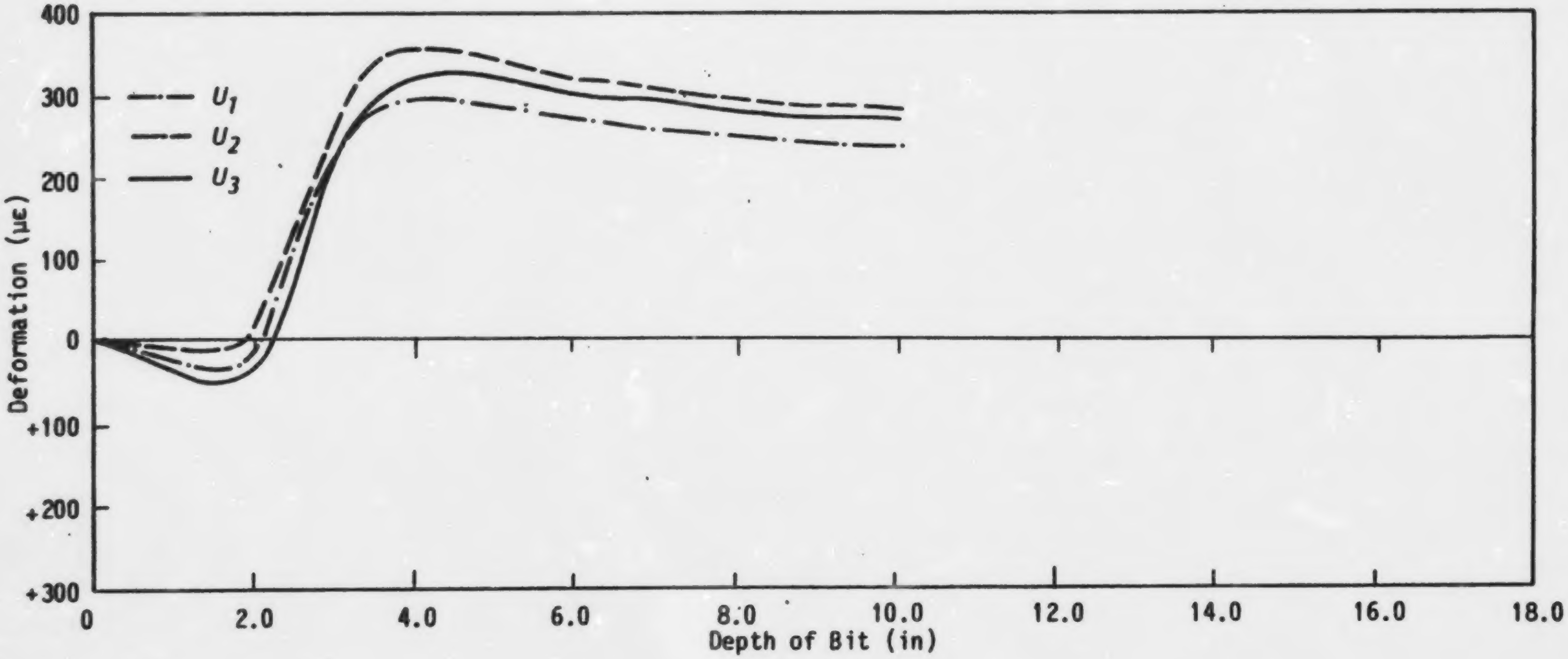

MIRAMICHI - BH 2 - TEST 46 - GAUGE DEPTH 25.10m

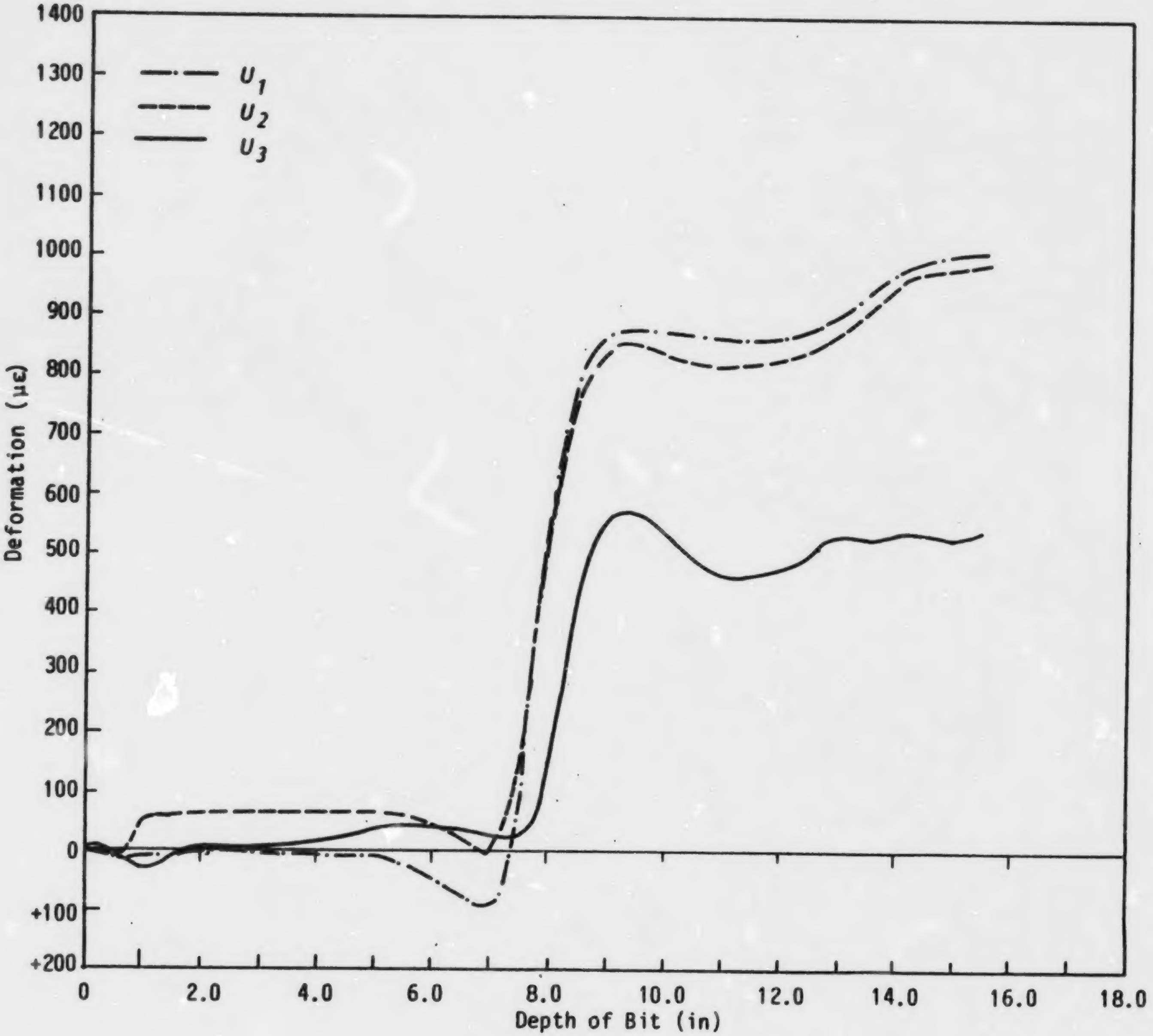

MIRAMICHI - BH 5 - TEST 47 - GAUGE DEPTH 30.58m

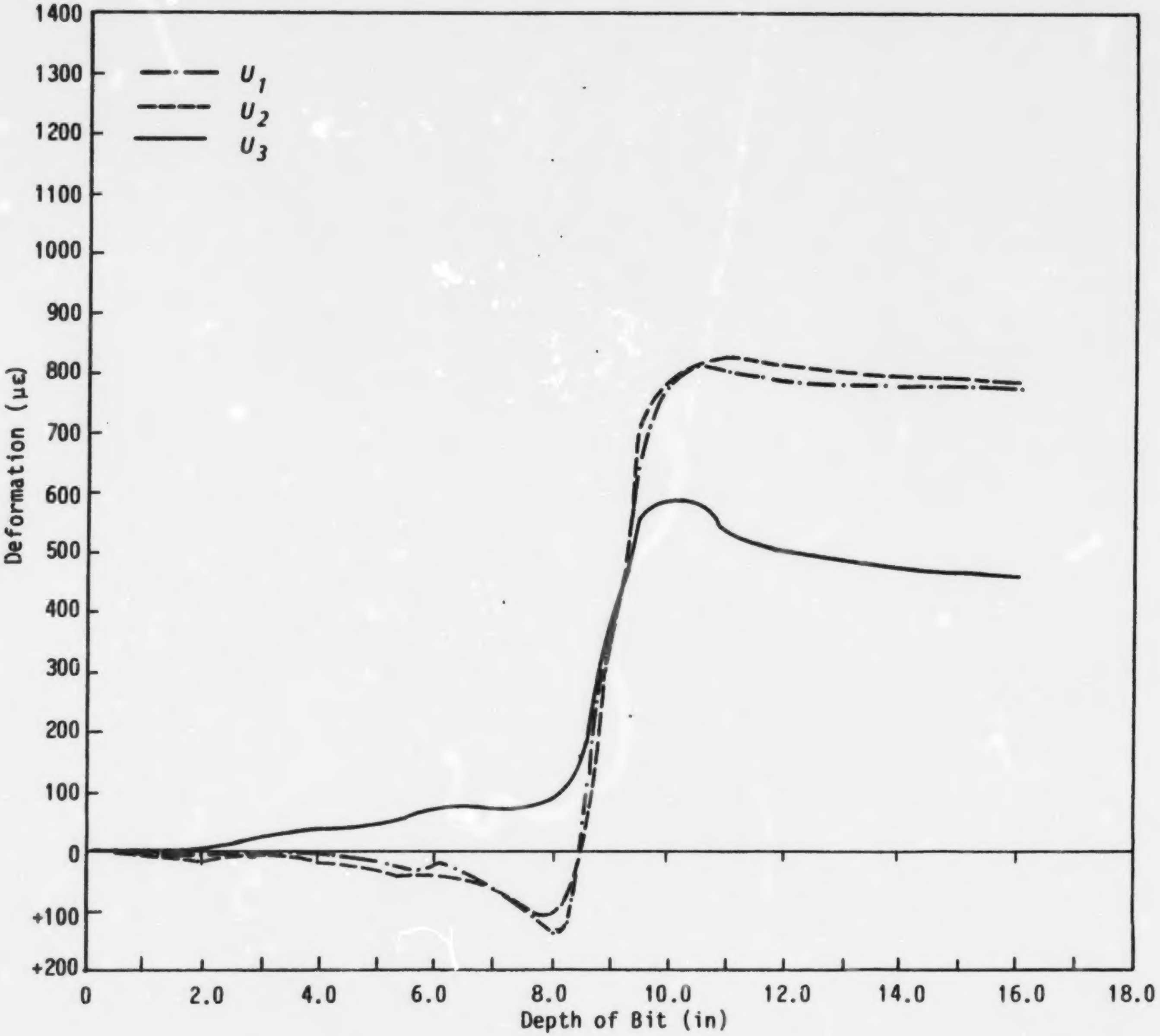

MIRAMICHI - BH 5 - TEST 48 - GAUGE DEPTH 31.00m

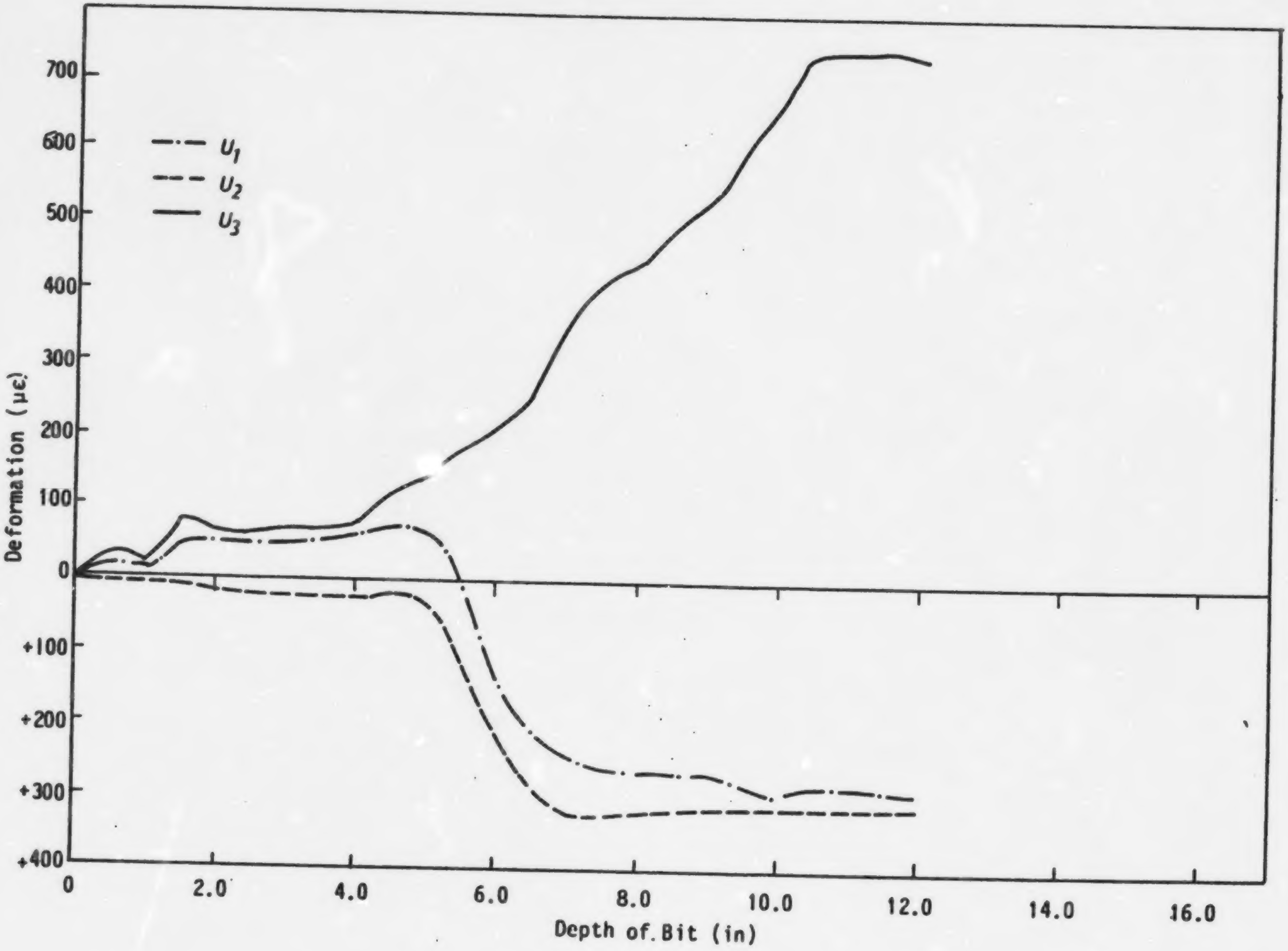

MIRAMICHI - BH 2 - TEST 49-GAUGE DEPTH 29.86m

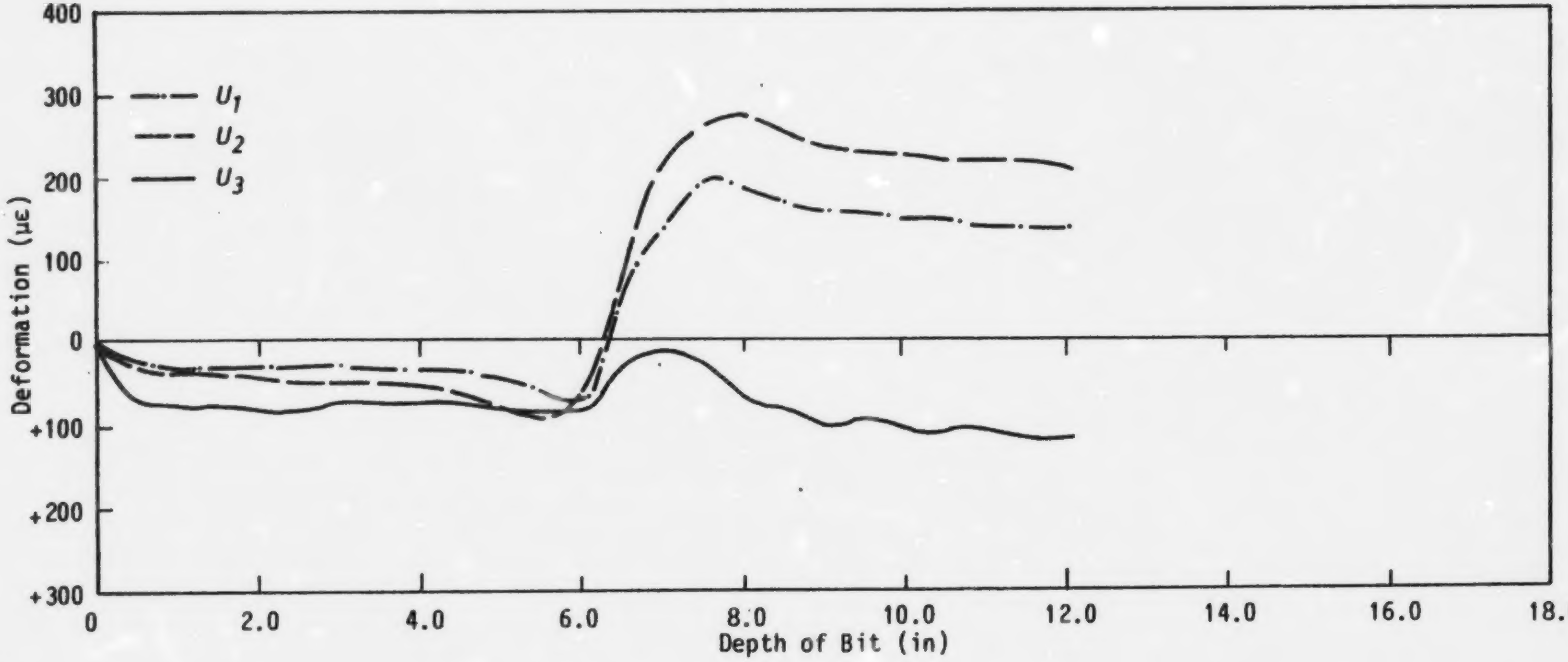

MIRAMICHI - BH 2 - TEST 50 - GAUGE DEPTH 30.17m

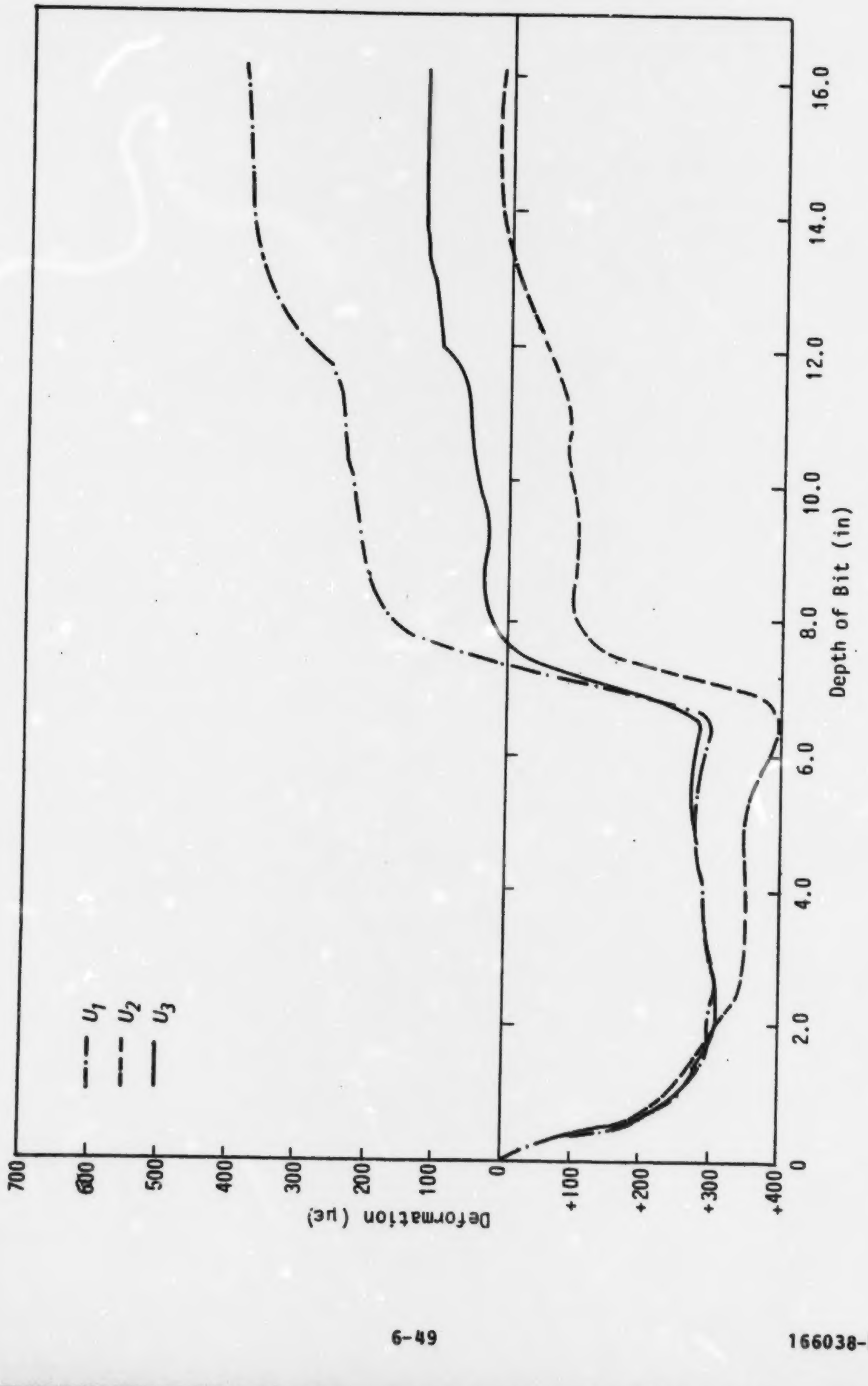

MIRAMICHI - BH 6 - TEST 51 - GAUGE DEPTH 7.18m

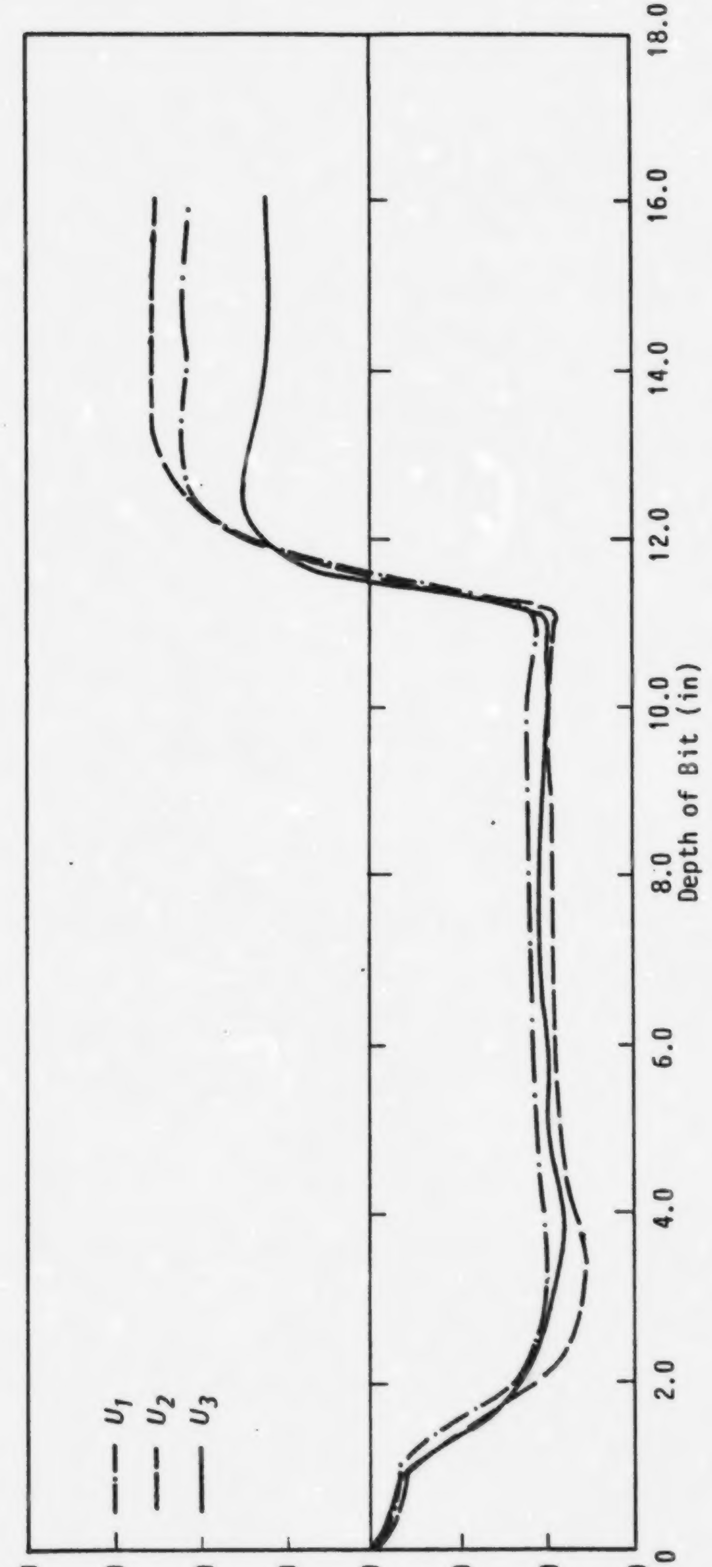

MIRAMICHI - BH 6 - TEST 52 - GAUGE DEPTH 7.58m

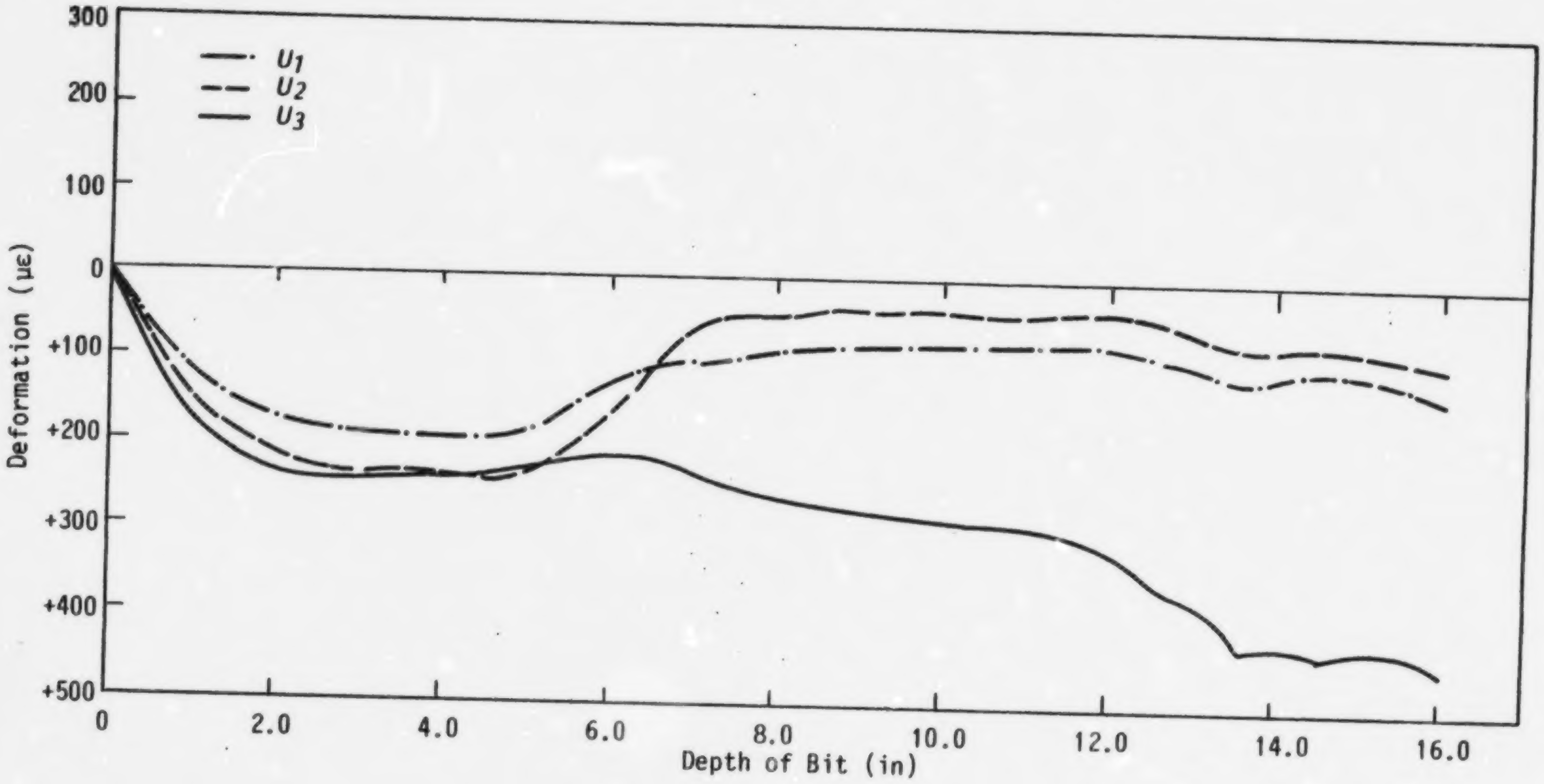

MIRAMICHI - BH3 - TEST 53 - GAUGE DEPTH 7.49m

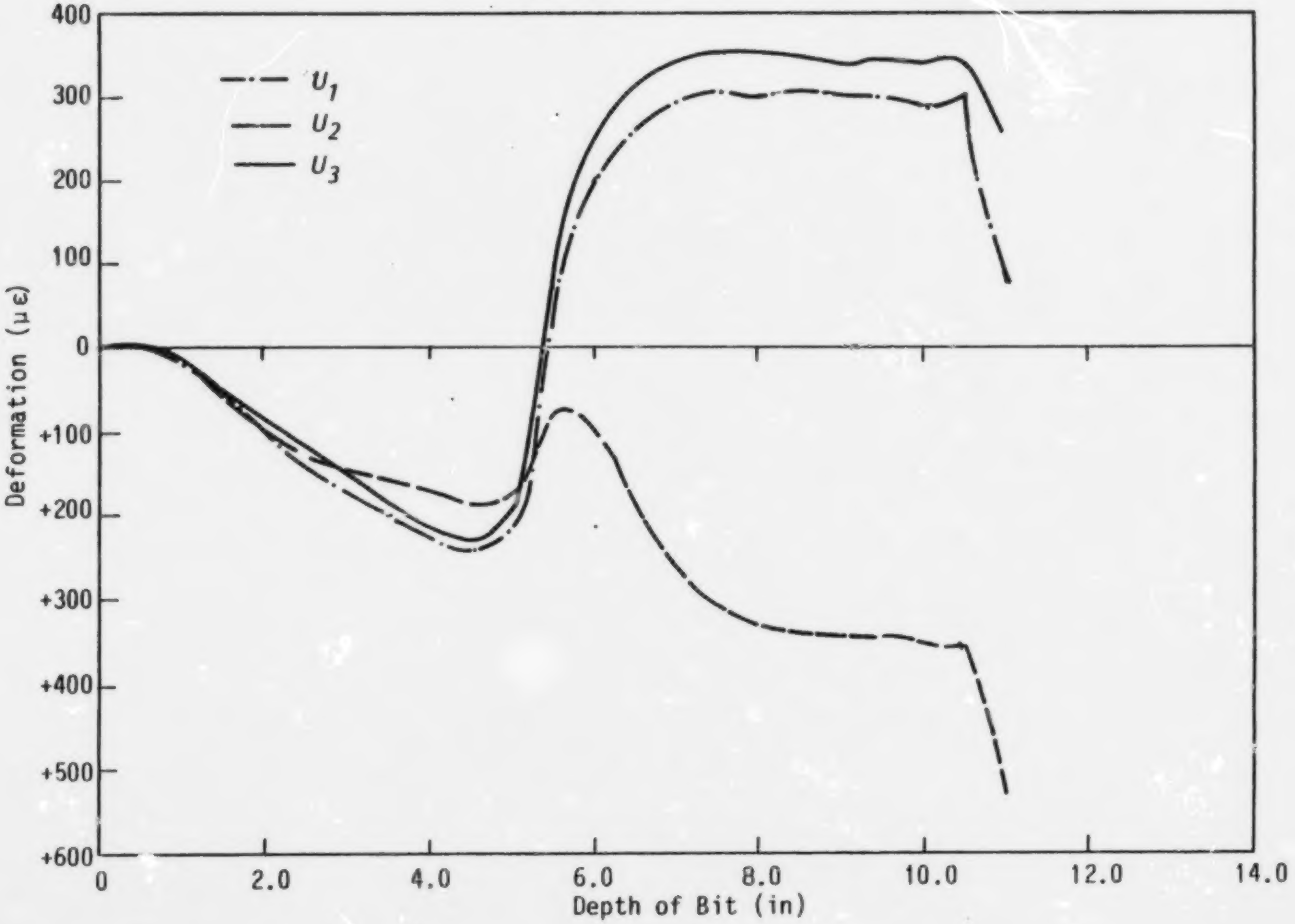

MIRAMICHI - BH6 - TEST 55 - GAUGE DEPTH 15.44m

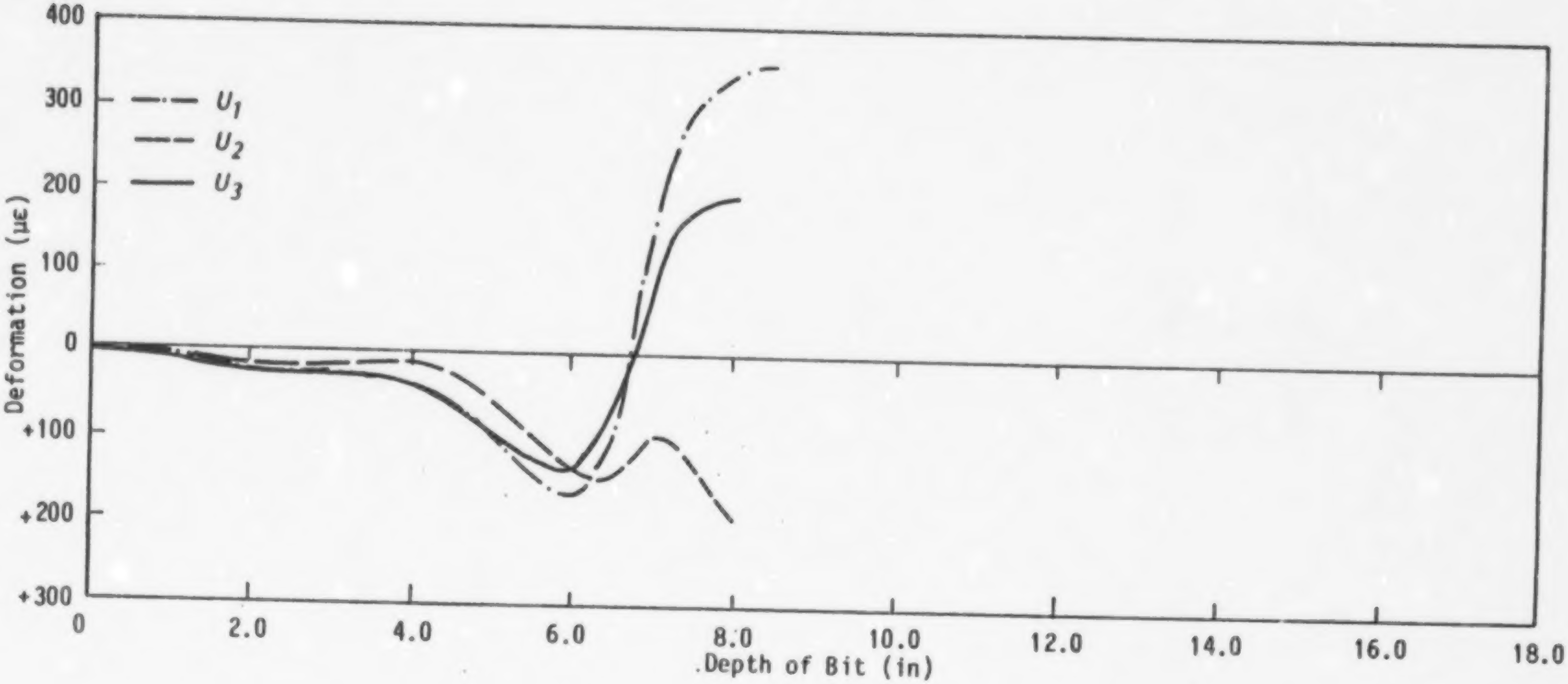

MIRAMICHI - BH 6 - TEST 56 - GAUGE DEPTH 15.17m

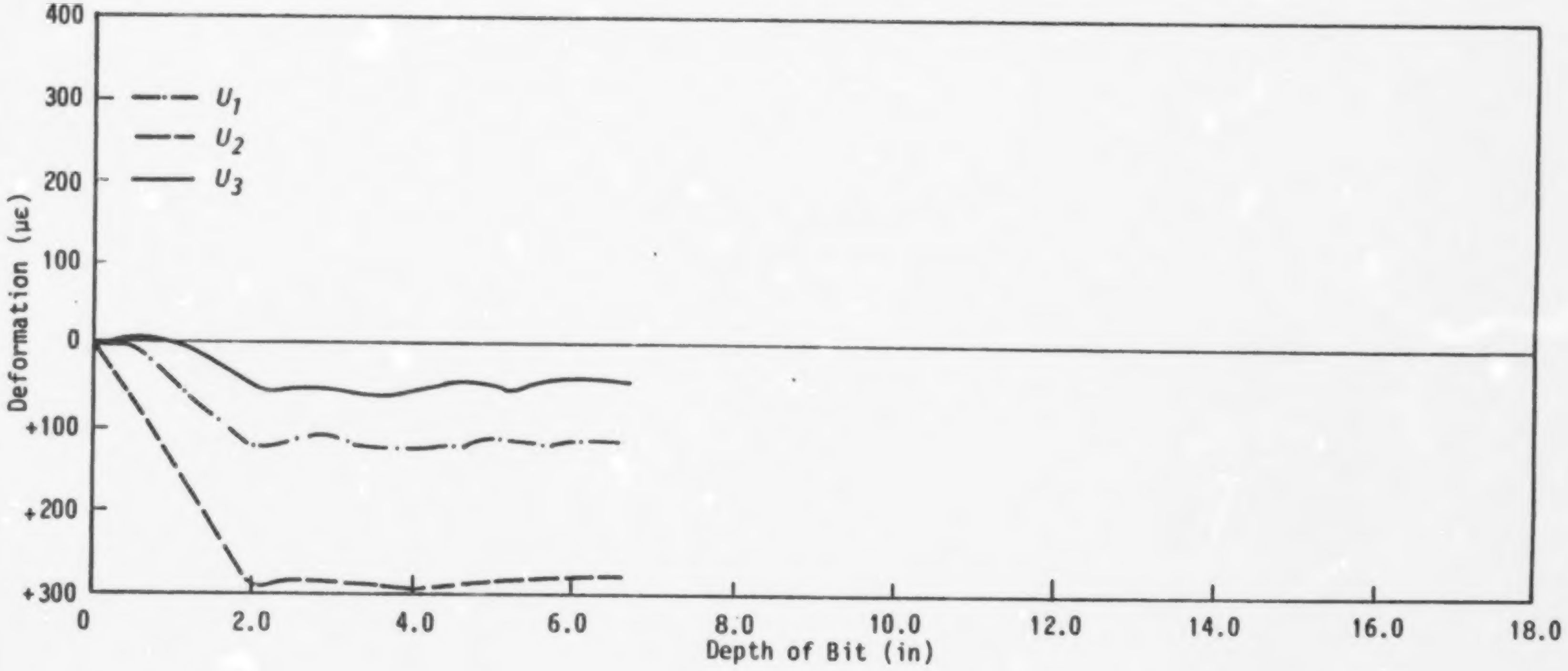

MIRAMICHI - BH 3 - TEST 57 - GAUGE DEPTH 16.47m

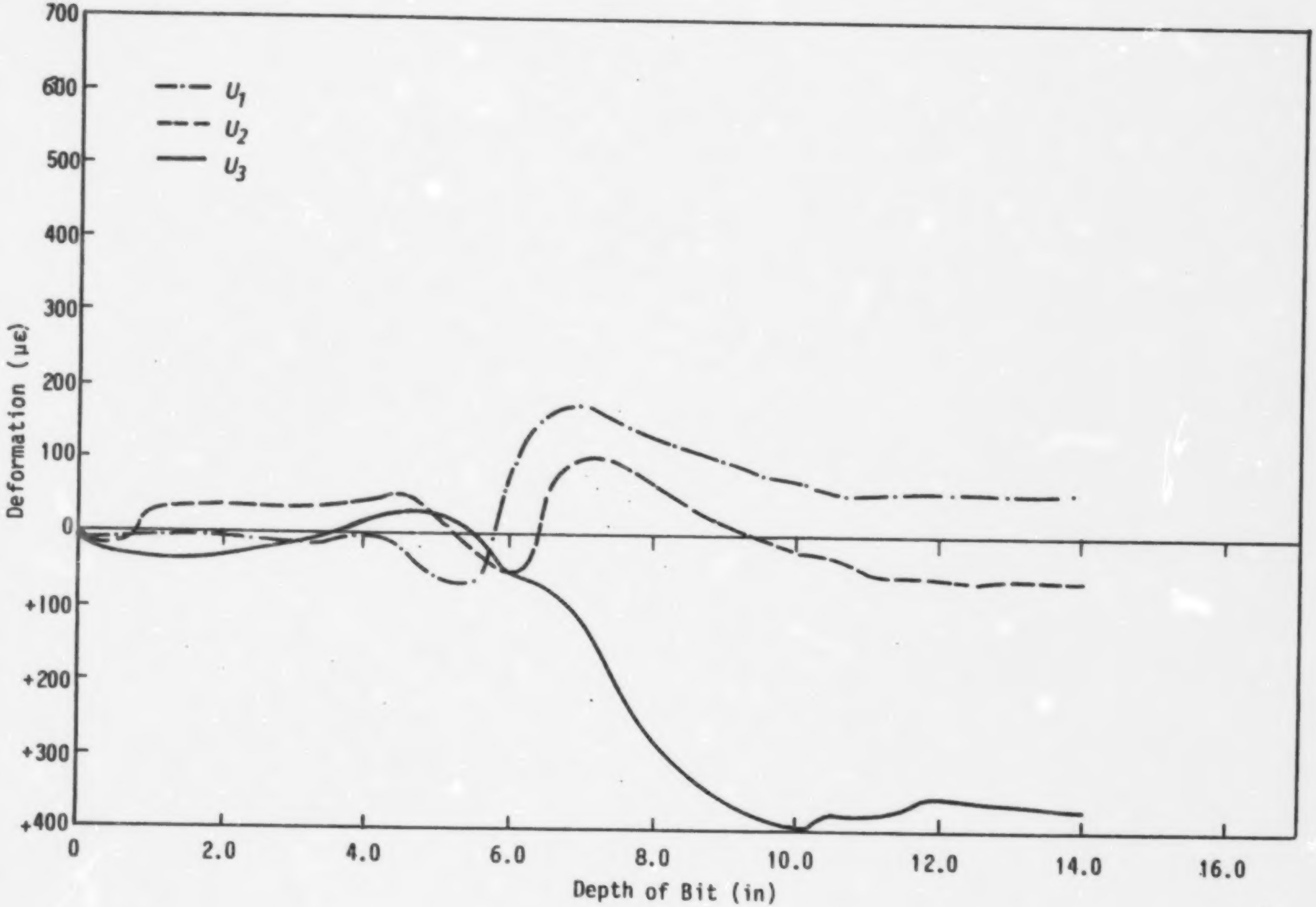

MIRAMICHI - BH 6 - TEST 58 - GAUGE DEPTH 22.82m

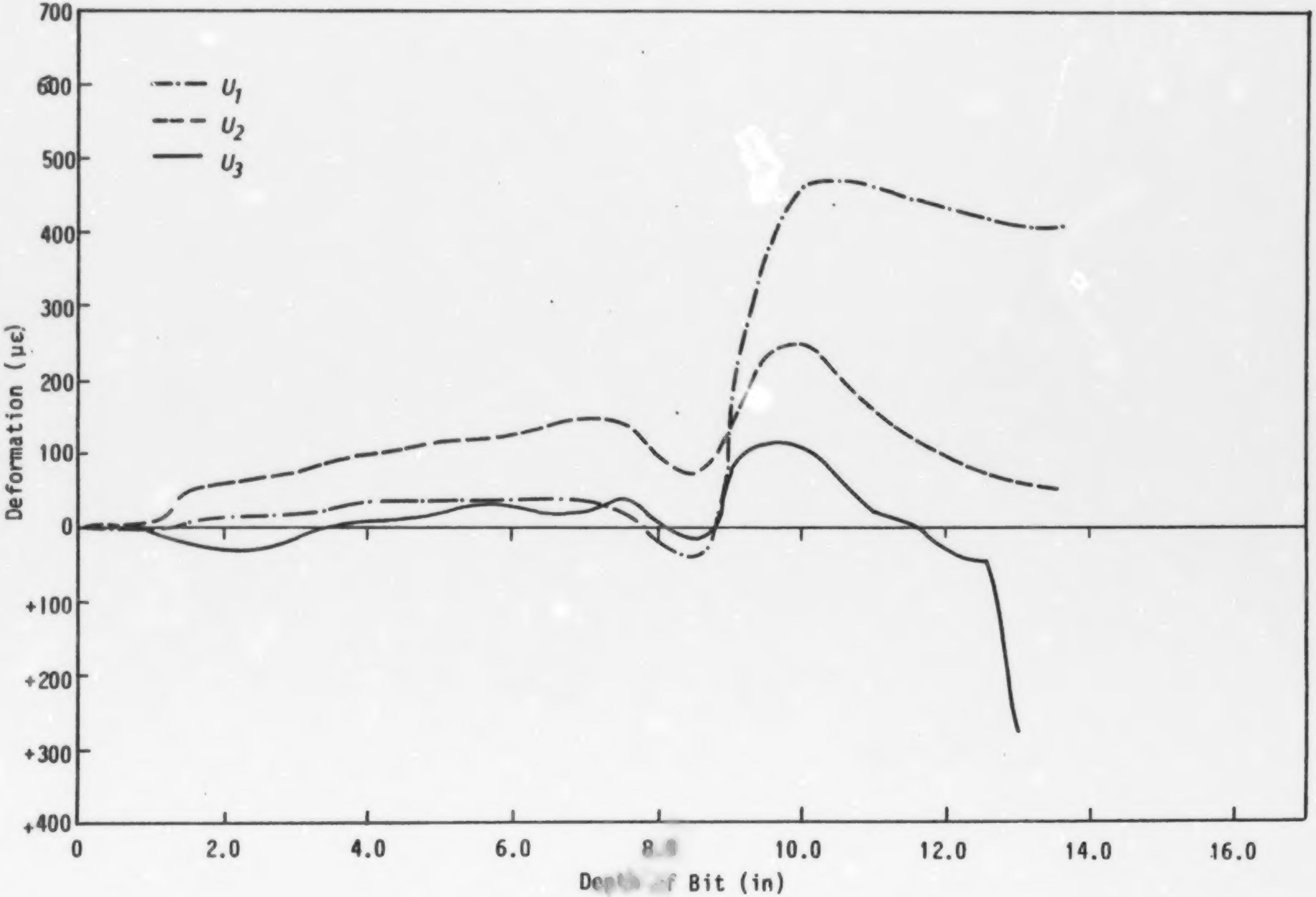

MIRAMICHI - BH 6 - TEST 59- GAUGE DEPTH 23.18m

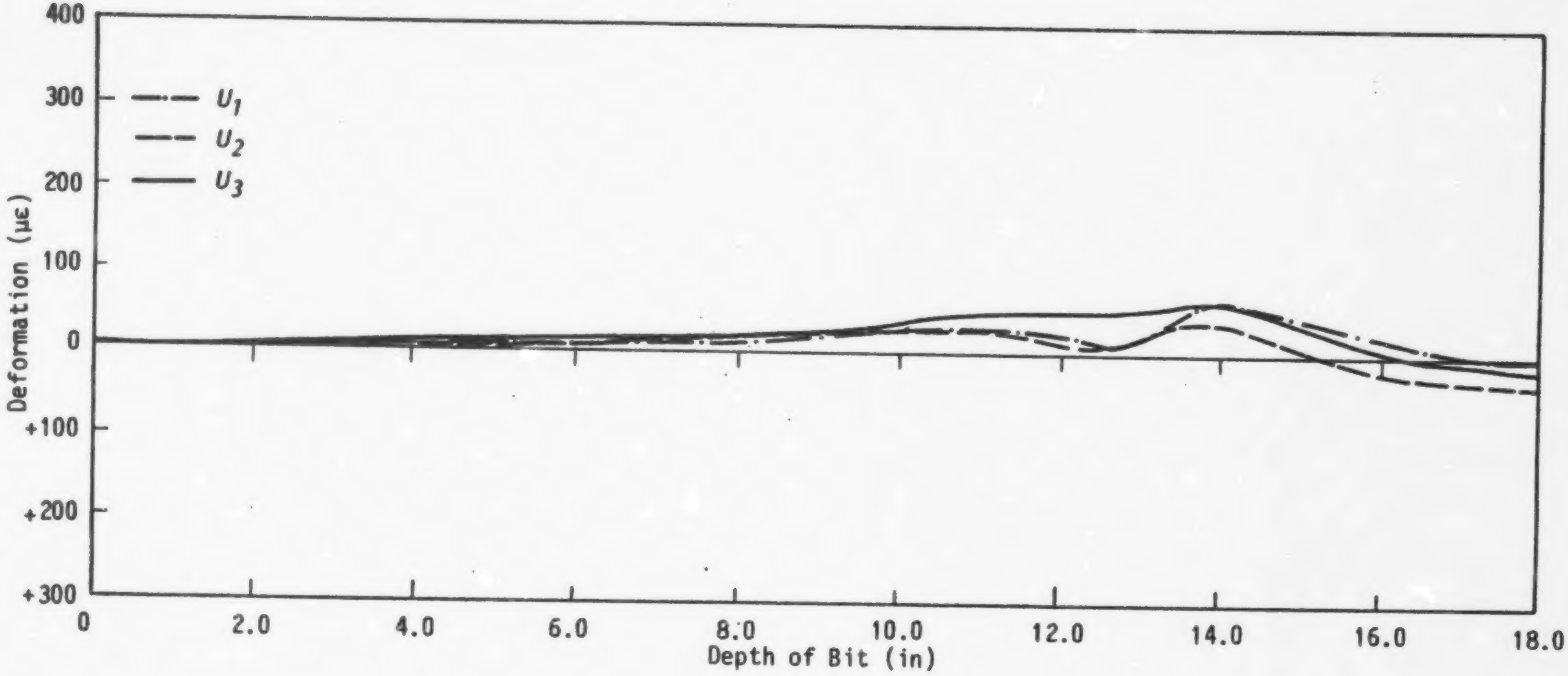

MIRAMICHI - BH 3 - TEST 60 - GAUGE DEPTH 22.85m

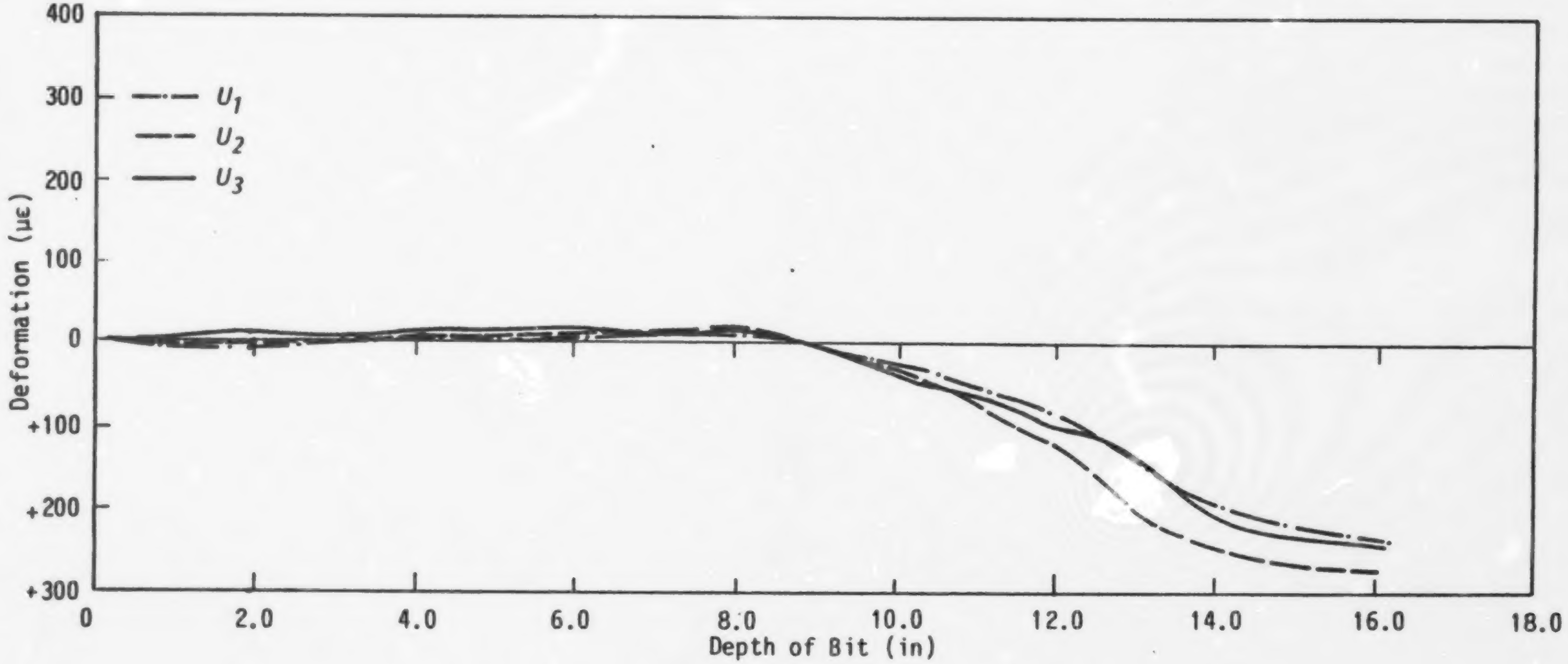

MIRAMICHI - BH 3 - TEST 61 - GAUGE DEPTH 23.26m

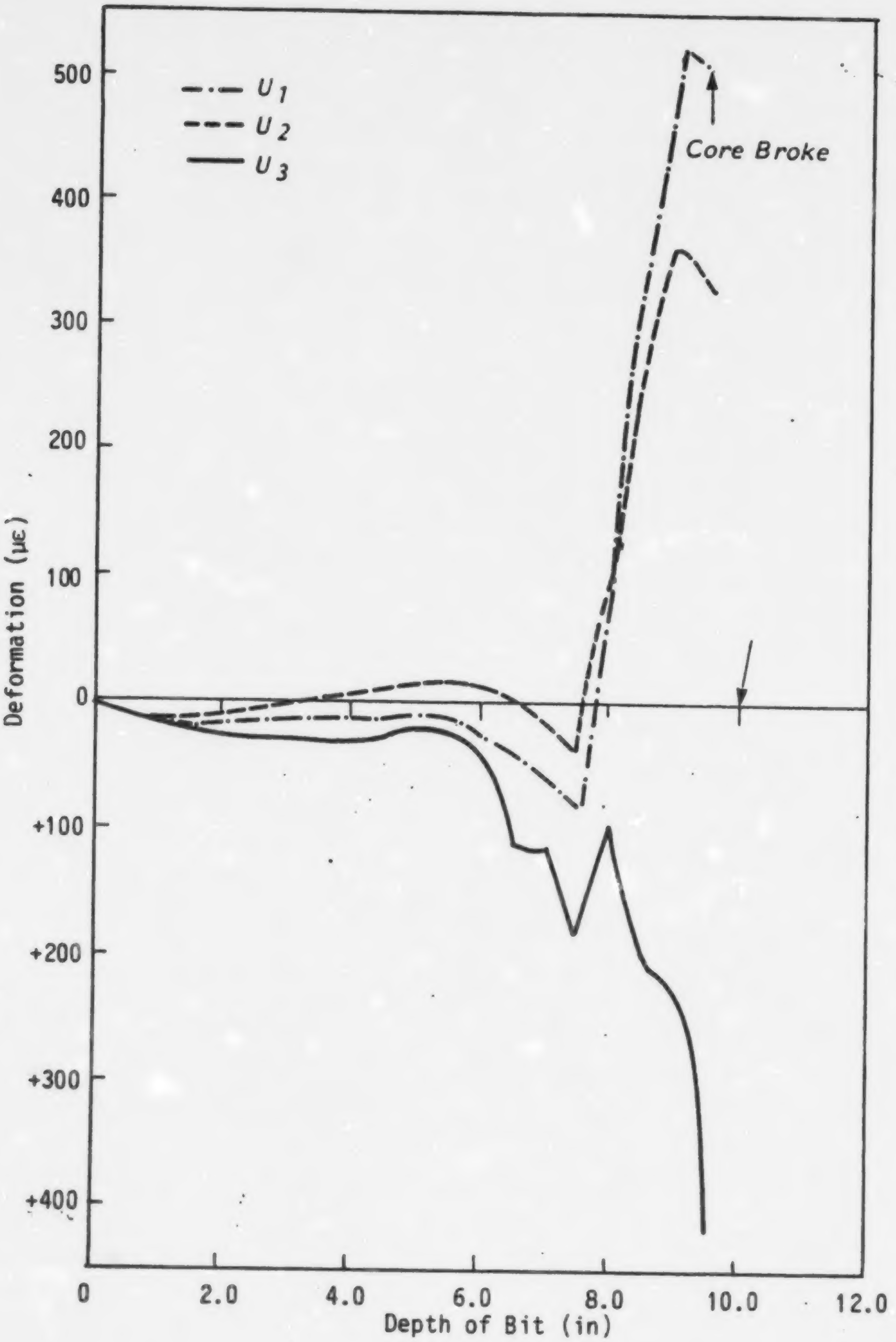

MIRACHI - BH 6 - TEST 62 GAUGE DEPTH 30.44m

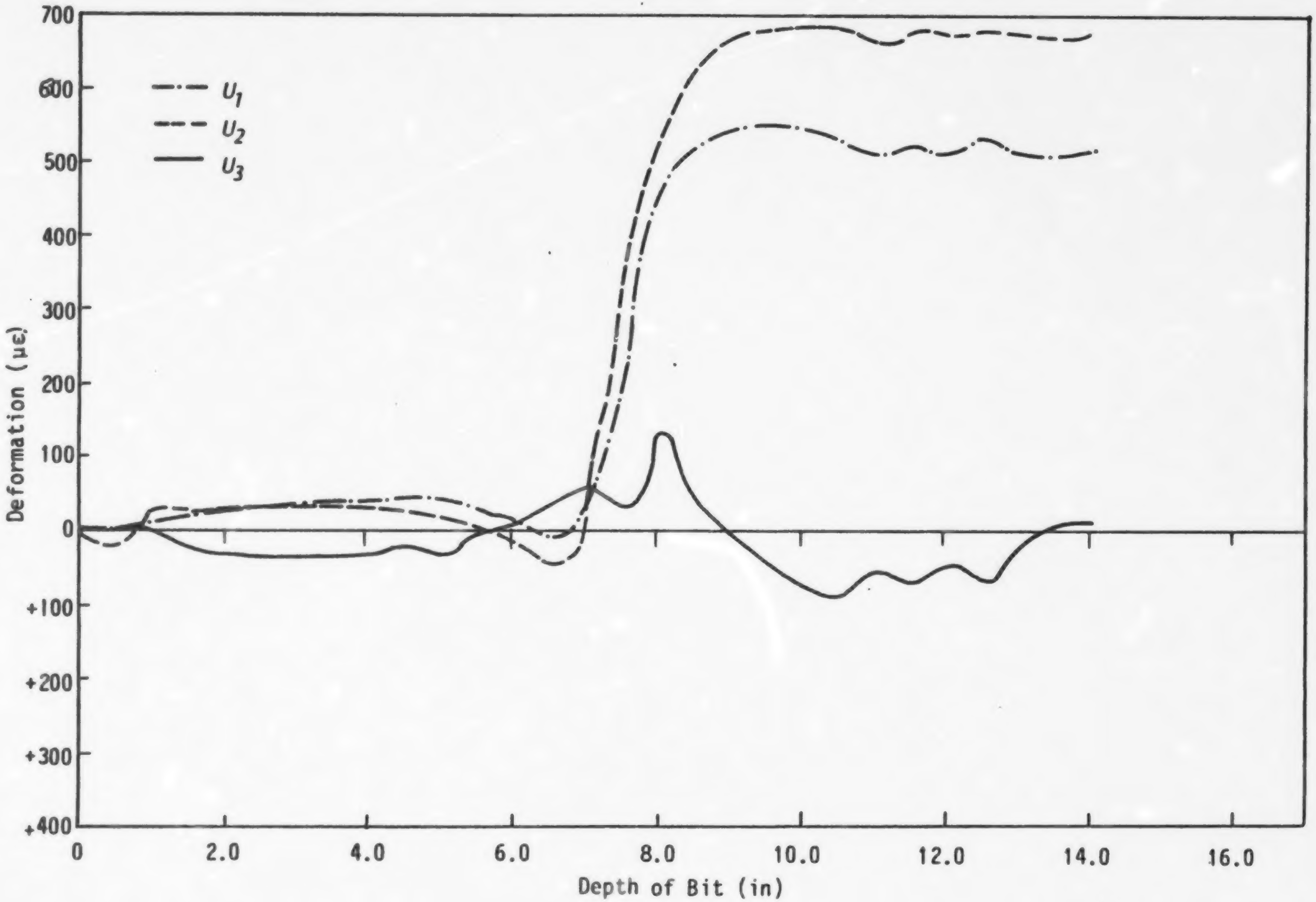

MIRAMICHI - BH 6 - TEST 63 - GAUGE DEPTH 30.83m

APPENDIX 7

BIAXIAL TEST CURVES

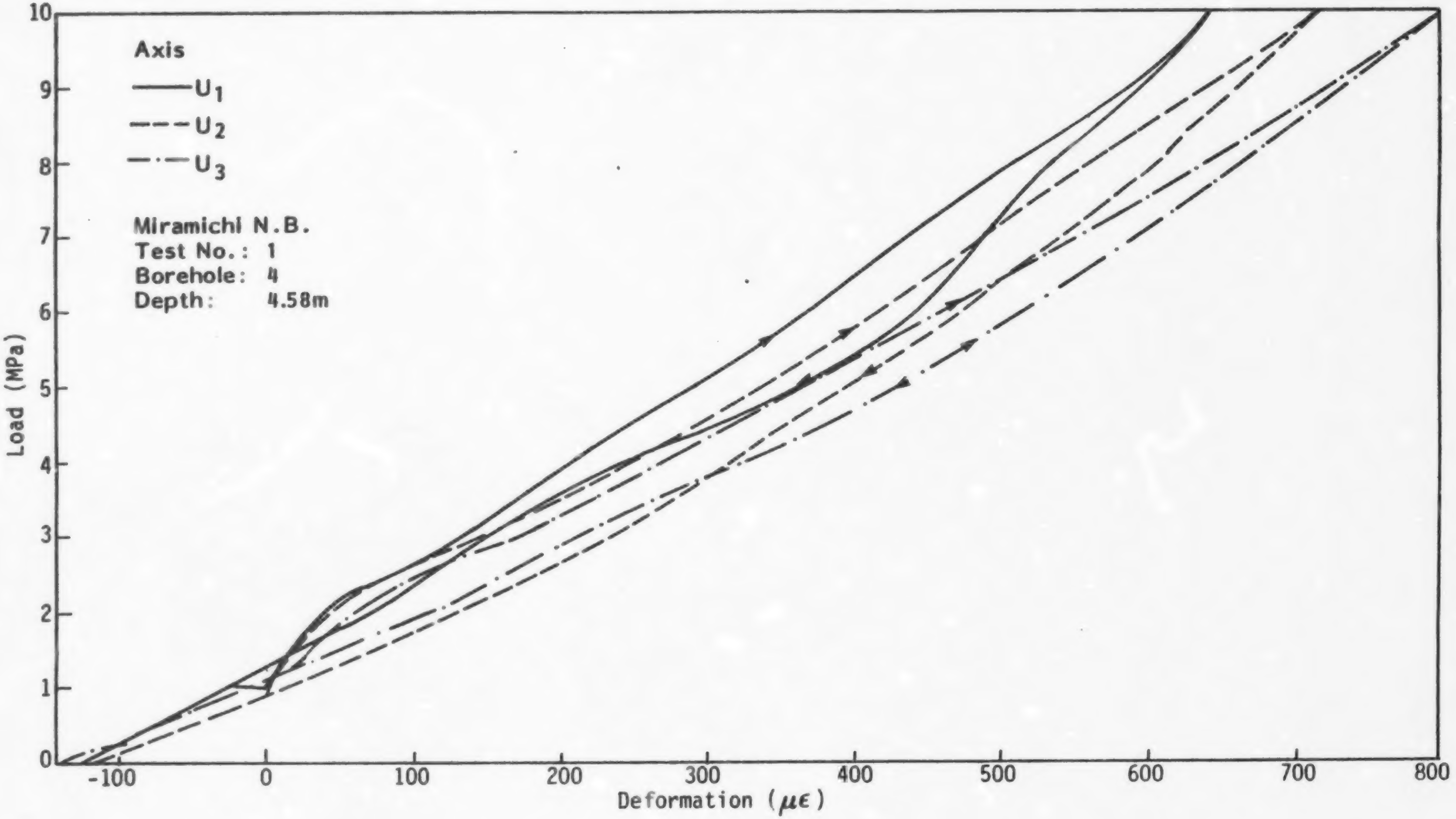
Axis
U$_1$
U$_2$
U$_3$
Miramichi N.B.
Test No.: 1
Borehole: 4
Depth: 4.58m
Load (MPa)
0
1
2
3
4
5
6
7
8
9
10
Deformation ($\mu\epsilon$)
-100
0
100
200
300
400
500
600
700
800

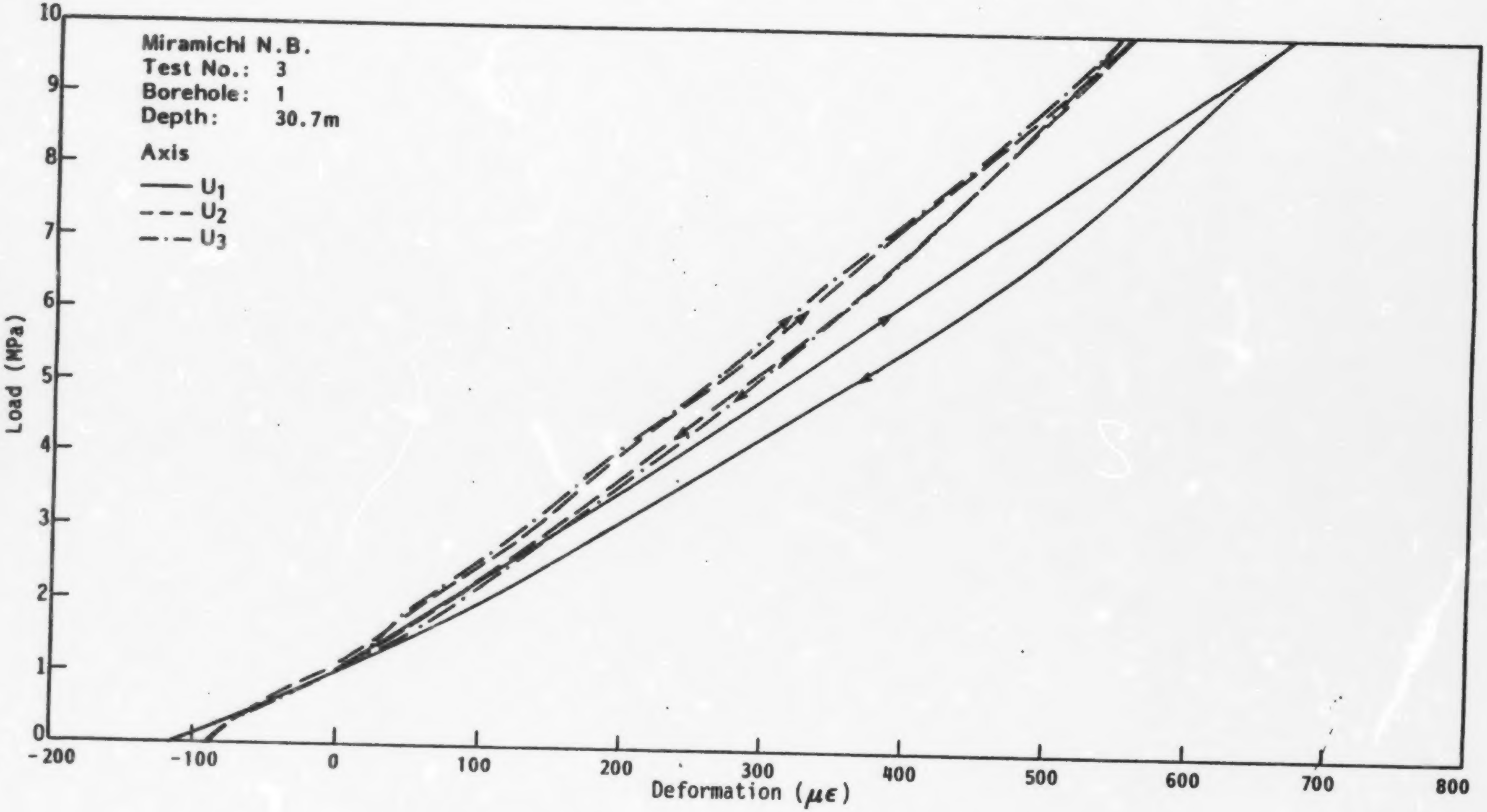
Miramichi N.B.
Test No.: 3
Borehole: 1
Depth: 30.7m
Axis
—— U_1
– – – U_2
–·–· U_3
Load (MPa)
0
1
2
3
4
5
6
7
8
9
10
-200
-100
0
100
200
300
400
500
600
700
800
Deformation ($\mu\epsilon$)

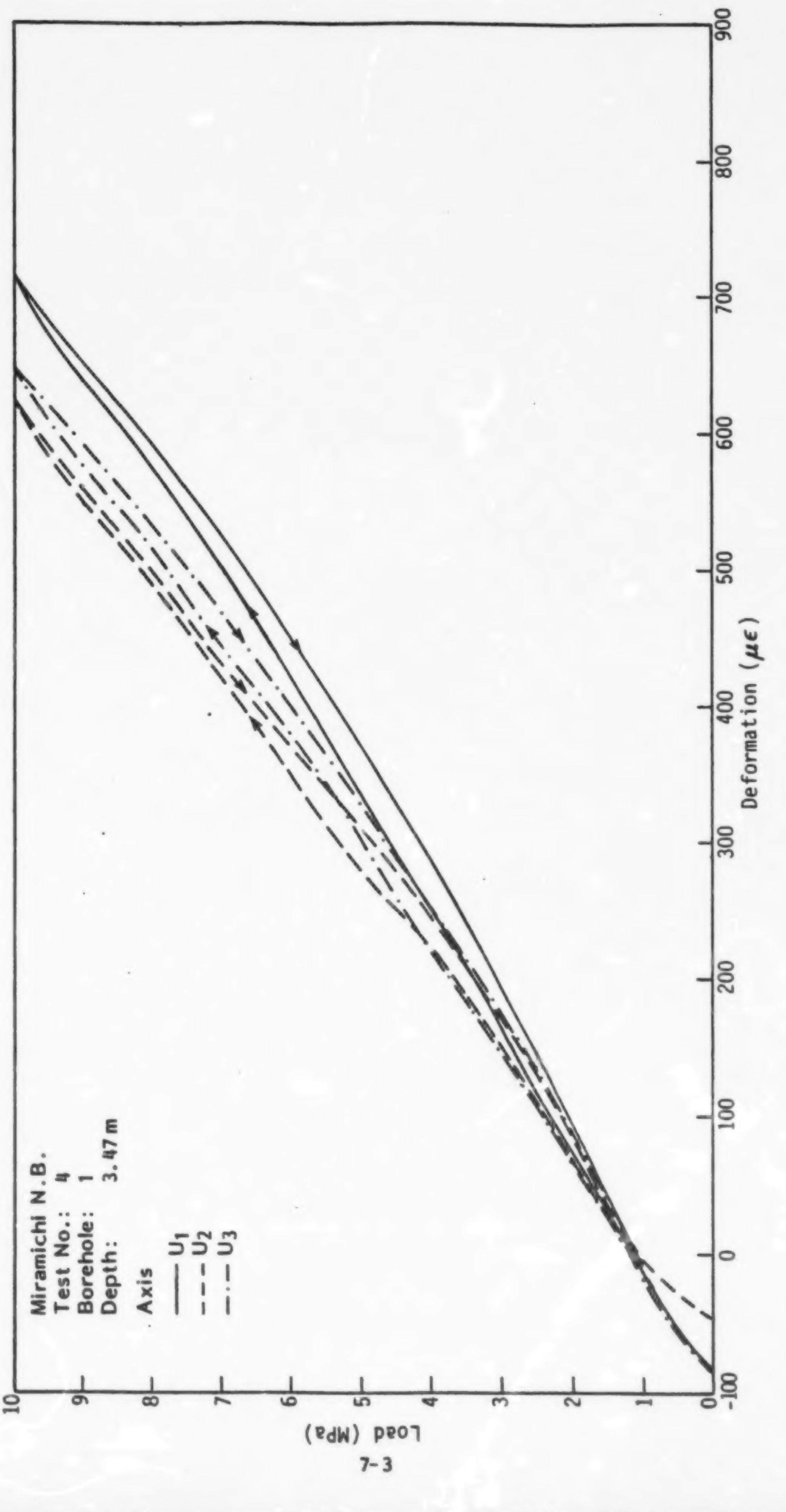
Miramichi N.B.
Test No.: 4
Borehole: 1
Depth: 3.47 m
Axis
—— U1
- - - U2
-·-·- U3
Load (MPa)
0
1
2
3
4
5
6
7
8
9
10
Deformation (με)
-100
0
100
200
300
400
500
600
700
800
900

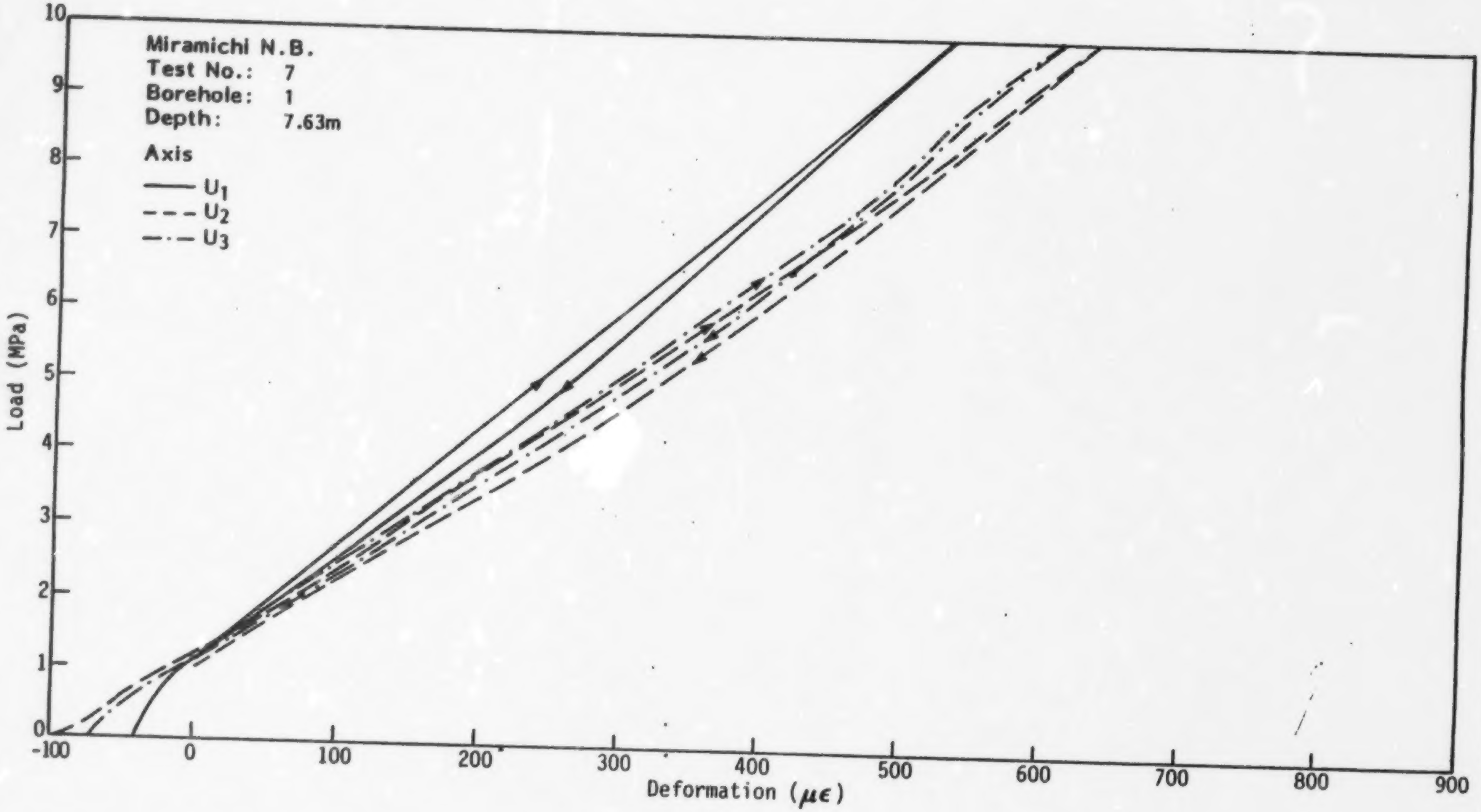
Miramichi N.B.
Test No.: 7
Borehole: 1
Depth: 7.63m
Axis
—— U_1
- - - U_2
—·— U_3
Load (MPa)
0
1
2
3
4
5
6
7
8
9
10
-100
0
100
200
300
400
500
600
700
800
900
Deformation ($\mu\epsilon$)

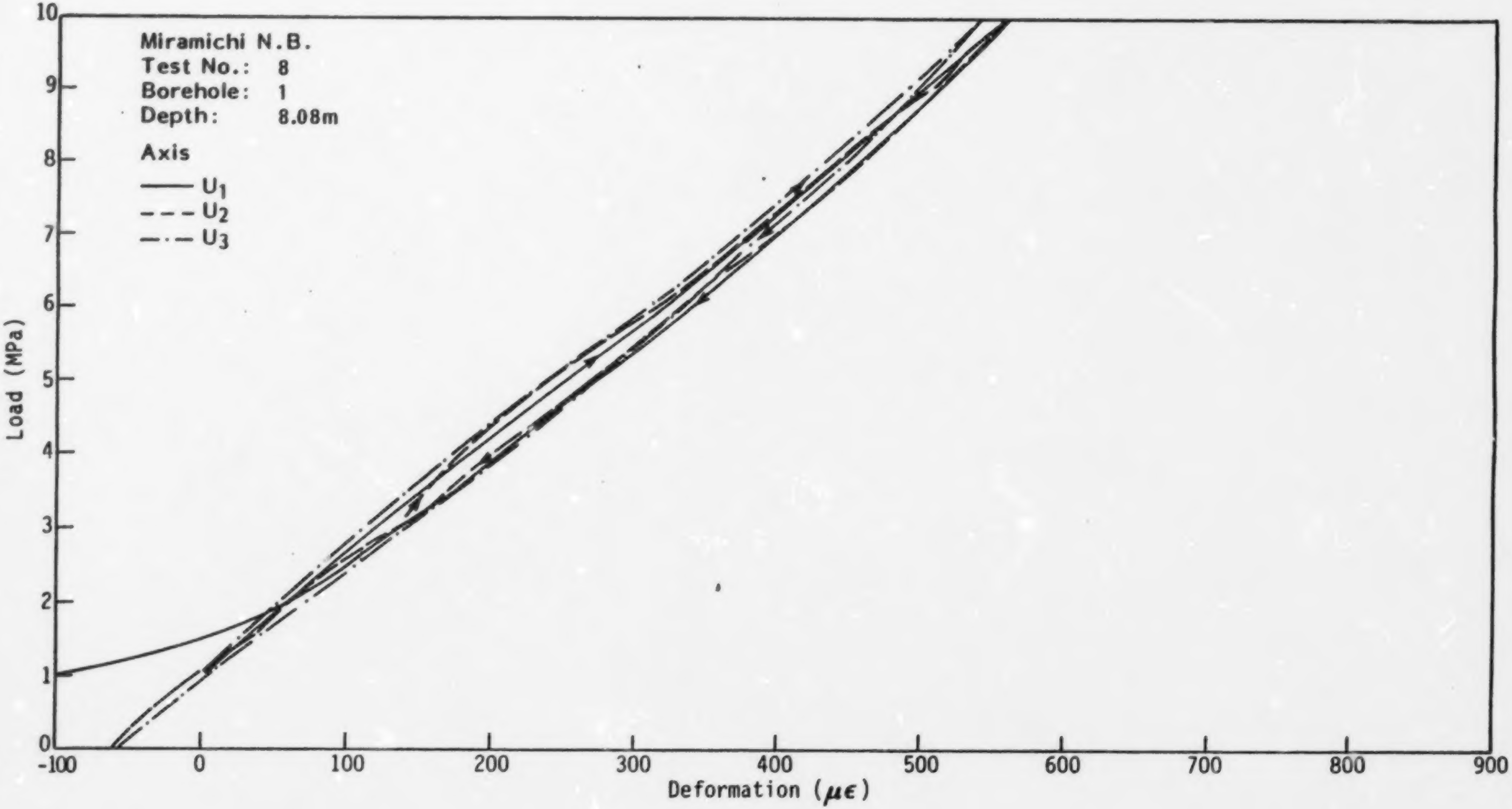
Miramichi N.B.
Test No.: 8
Borehole: 1
Depth: 8.08m
Axis
—— U_1
- - - U_2
—·— U_3
Load (MPa)
0
1
2
3
4
5
6
7
8
9
10
-100
0
100
200
300
400
500
600
700
800
900
Deformation ($\mu\epsilon$)

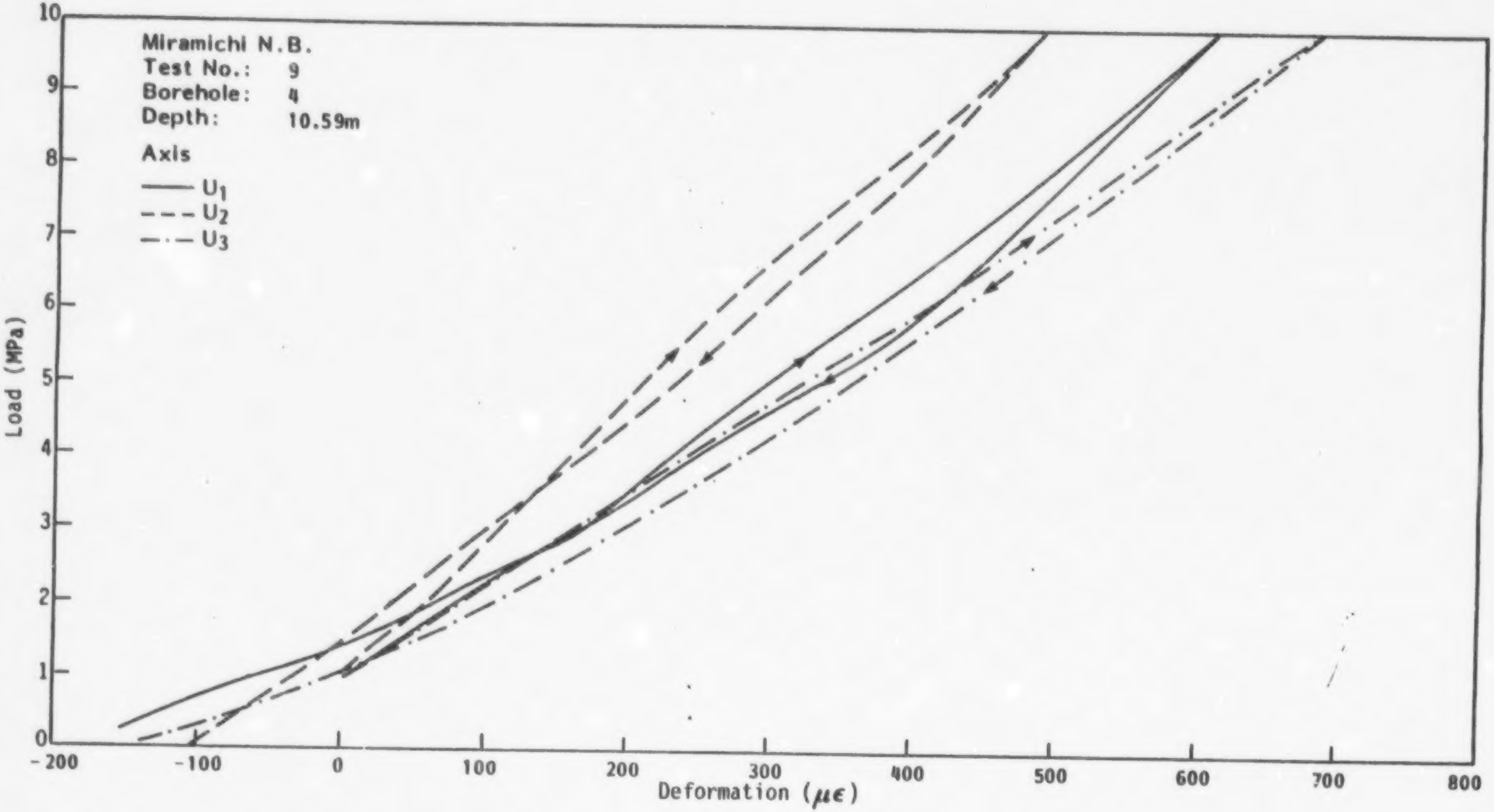
Miramichi N.B.
Test No.: 9
Borehole: 4
Depth: 10.59m
Axis
U1
U2
U3
Load (MPa)
0
1
2
3
4
5
6
7
8
9
10
Deformation (με)
-200
-100
0
100
200
300
400
500
600
700
800

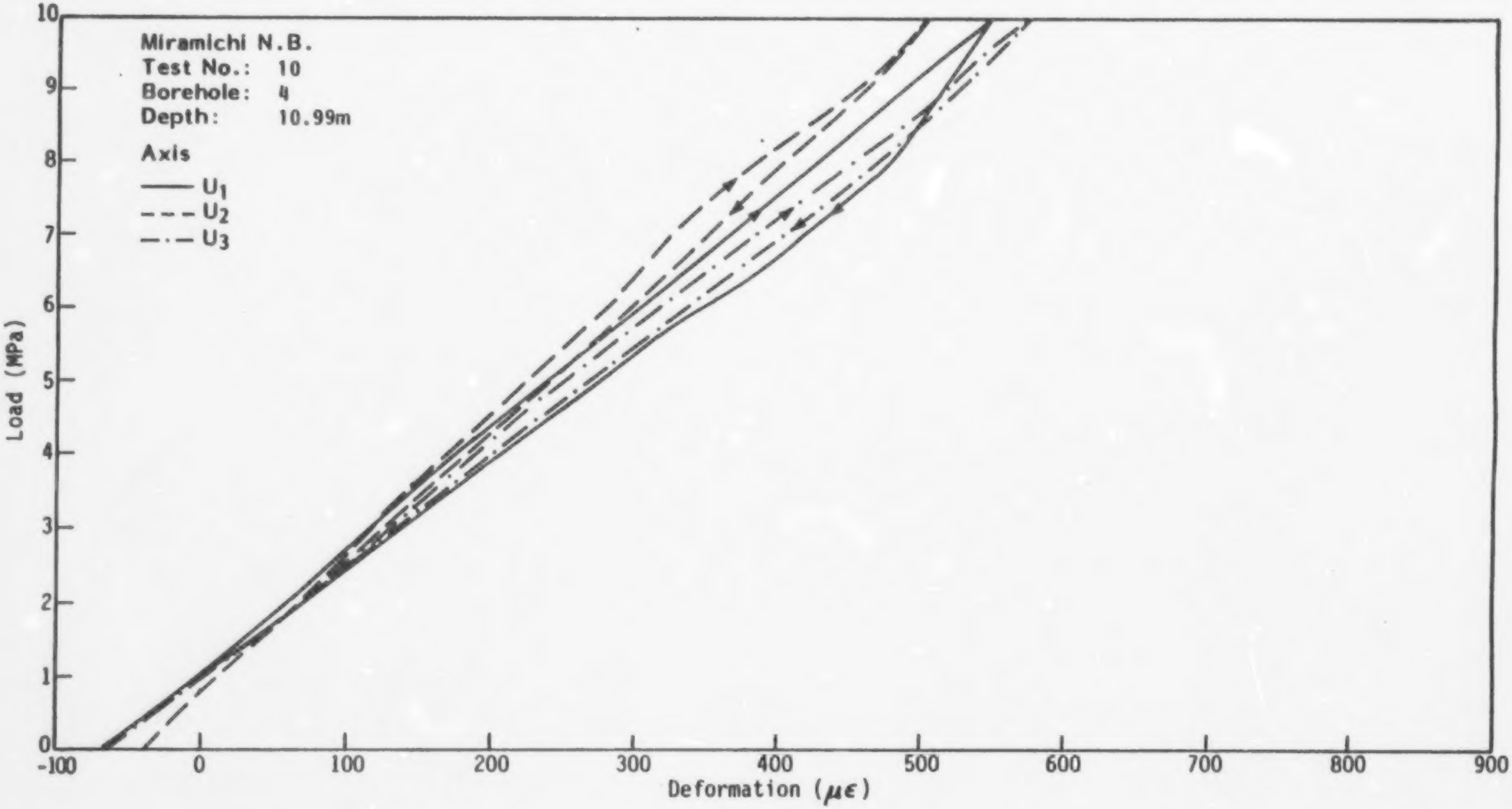
Miramichi N.B.
Test No.: 10
Borehole: 4
Depth: 10.99m
Axis
U1
U2
U3
Load (MPa)
0
1
2
3
4
5
6
7
8
9
10
-100
0
100
200
300
400
500
600
700
800
900
Deformation (με)

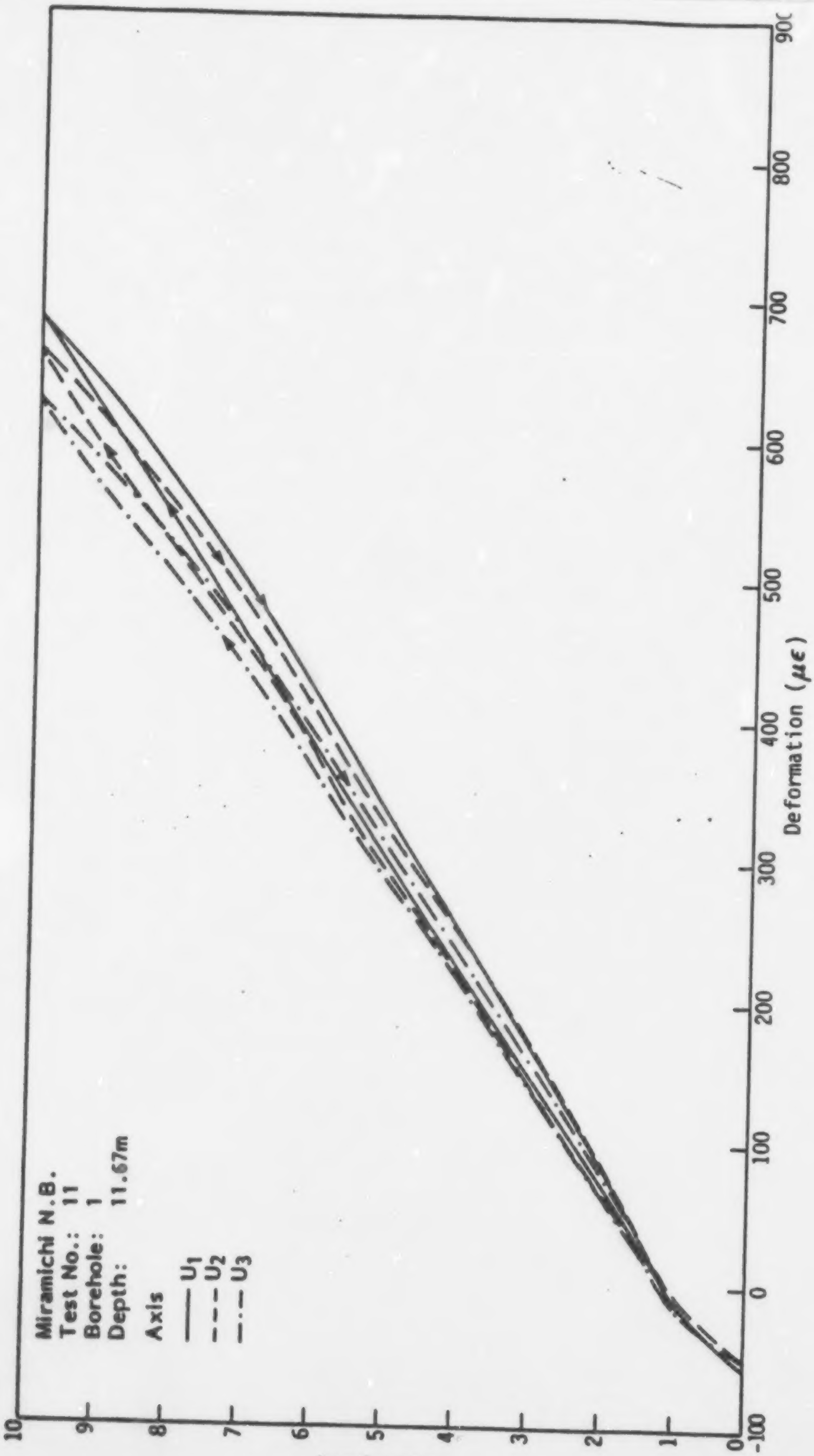
Miramichi N.B.
Test No.: 11
Borehole: 1
Depth: 11.67m
Axis
—— U1
- - - U2
-·-·- U3
Load (MPa)
0
1
2
3
4
5
6
7
8
9
10
Deformation (με)
-100
0
100
200
300
400
500
600
700
800
900

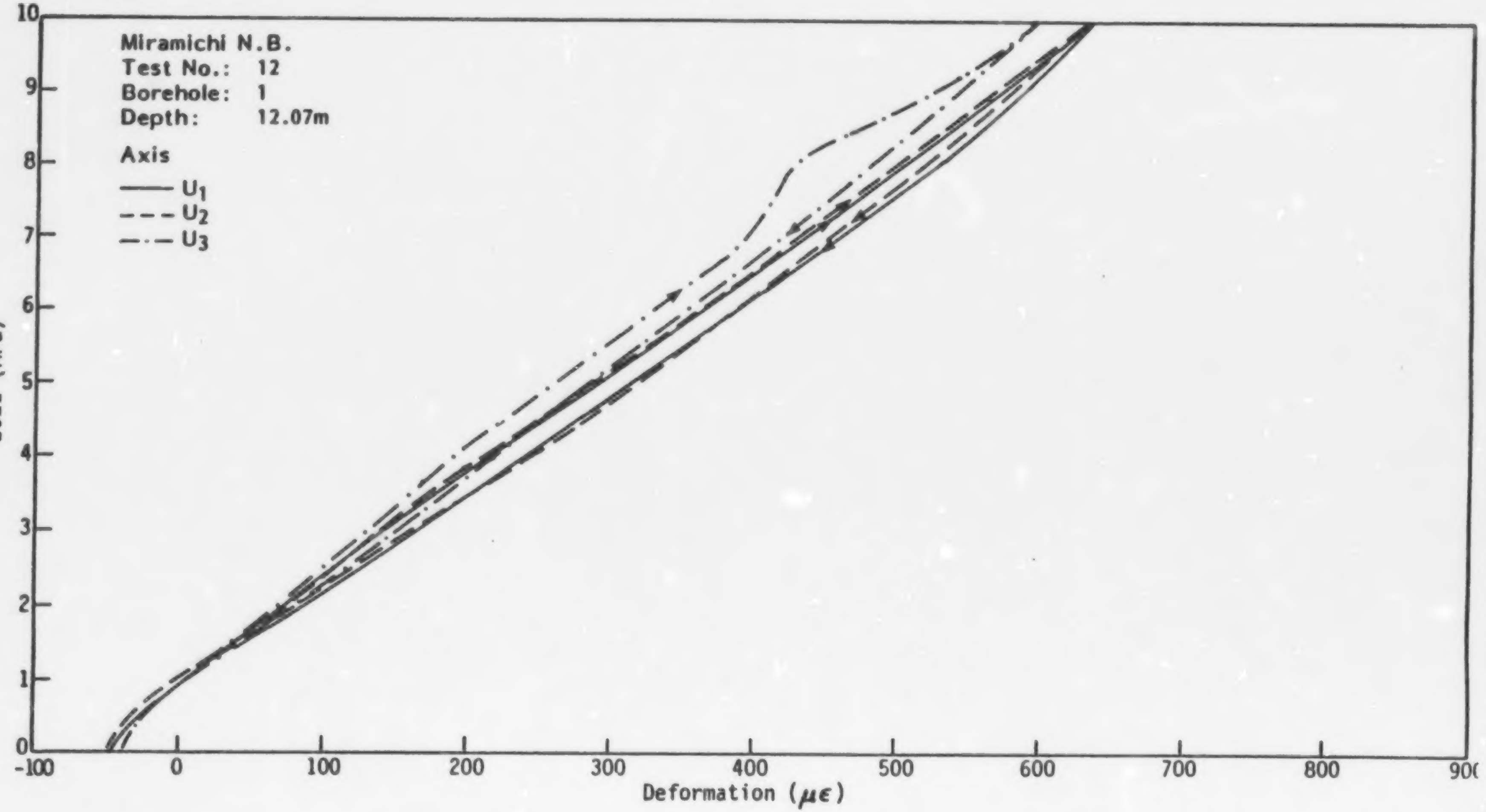
Miramichi N.B.
Test No.: 12
Borehole: 1
Depth: 12.07m
Axis
—— U_1
- - - U_2
-·-· U_3
Load (MPa)
0
1
2
3
4
5
6
7
8
9
10
-100
0
100
200
300
400
500
600
700
800
900
Deformation ($\mu\epsilon$)

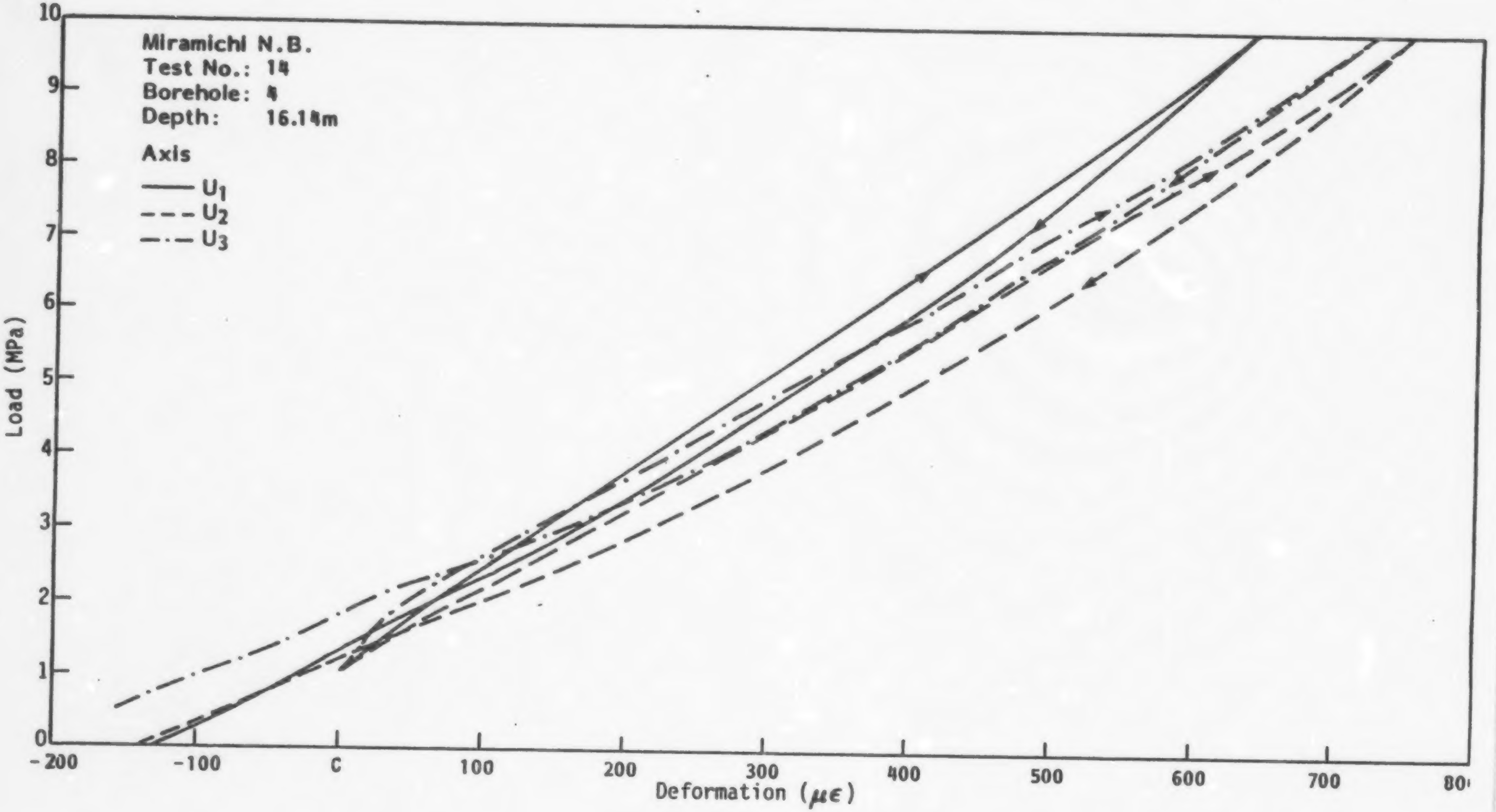
Miramichi N.B.
Test No.: 14
Borehole: 4
Depth: 16.14m
Axis
U_1
U_2
U_3
Load (MPa)
0
1
2
3
4
5
6
7
8
9
10
-200
-100
C
100
200
300
400
500
600
700
80
Deformation ($\mu\epsilon$)

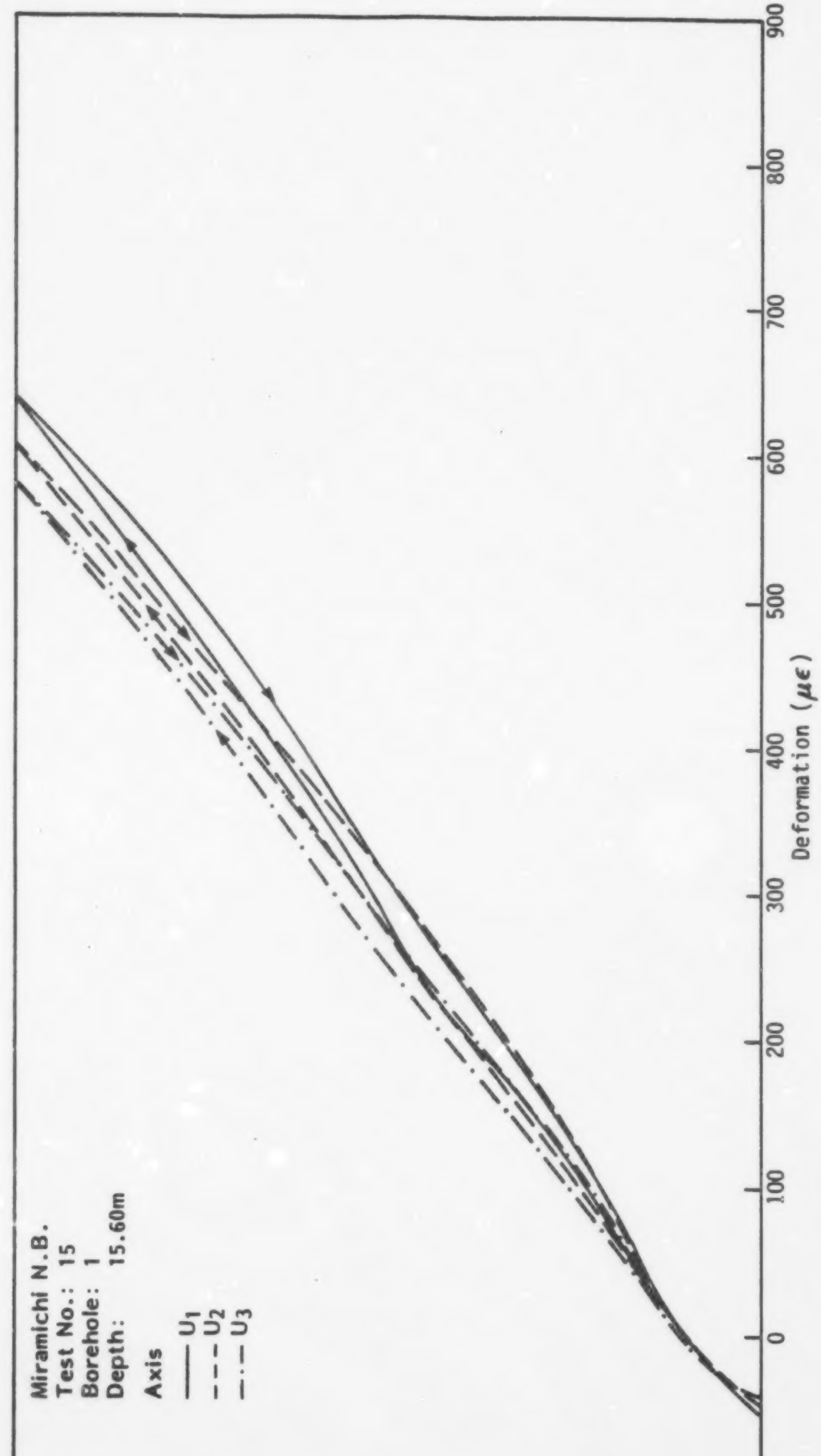
Miramichi N.B.
Test No.: 15
Borehole: 1
Depth: 15.60m
Axis
—— U_1
- - - U_2
-·-· U_3
Load (MPa)
0
1
2
3
4
5
6
7
8
9
10
Deformation ($\mu\epsilon$)
-100
0
100
200
300
400
500
600
700
800
900

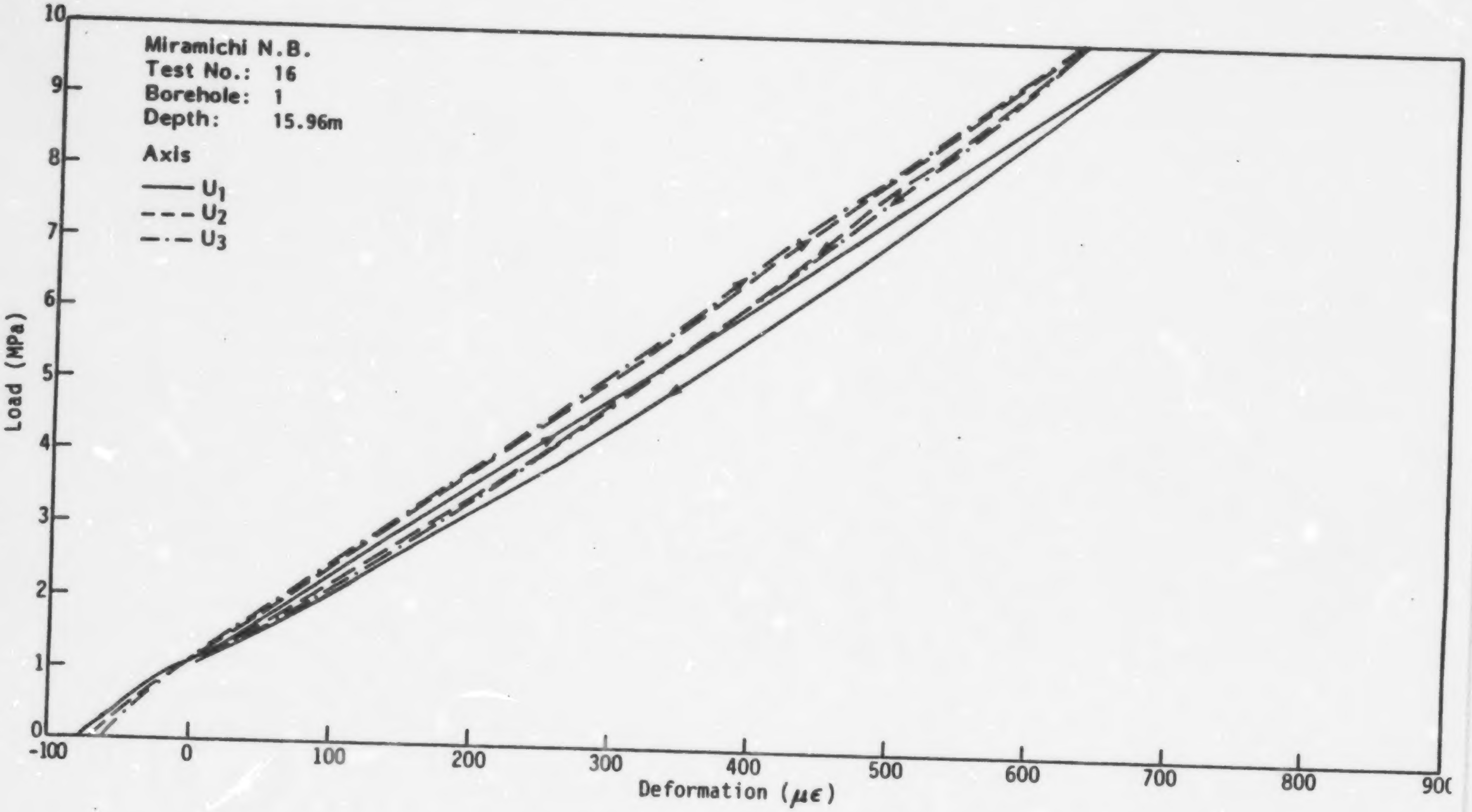
Miramichi N.B.
Test No.: 16
Borehole: 1
Depth: 15.96m
Axis
U1
U2
U3
Load (MPa)
0
1
2
3
4
5
6
7
8
9
10
-100
0
100
200
300
400
500
600
700
800
90
Deformation (με)

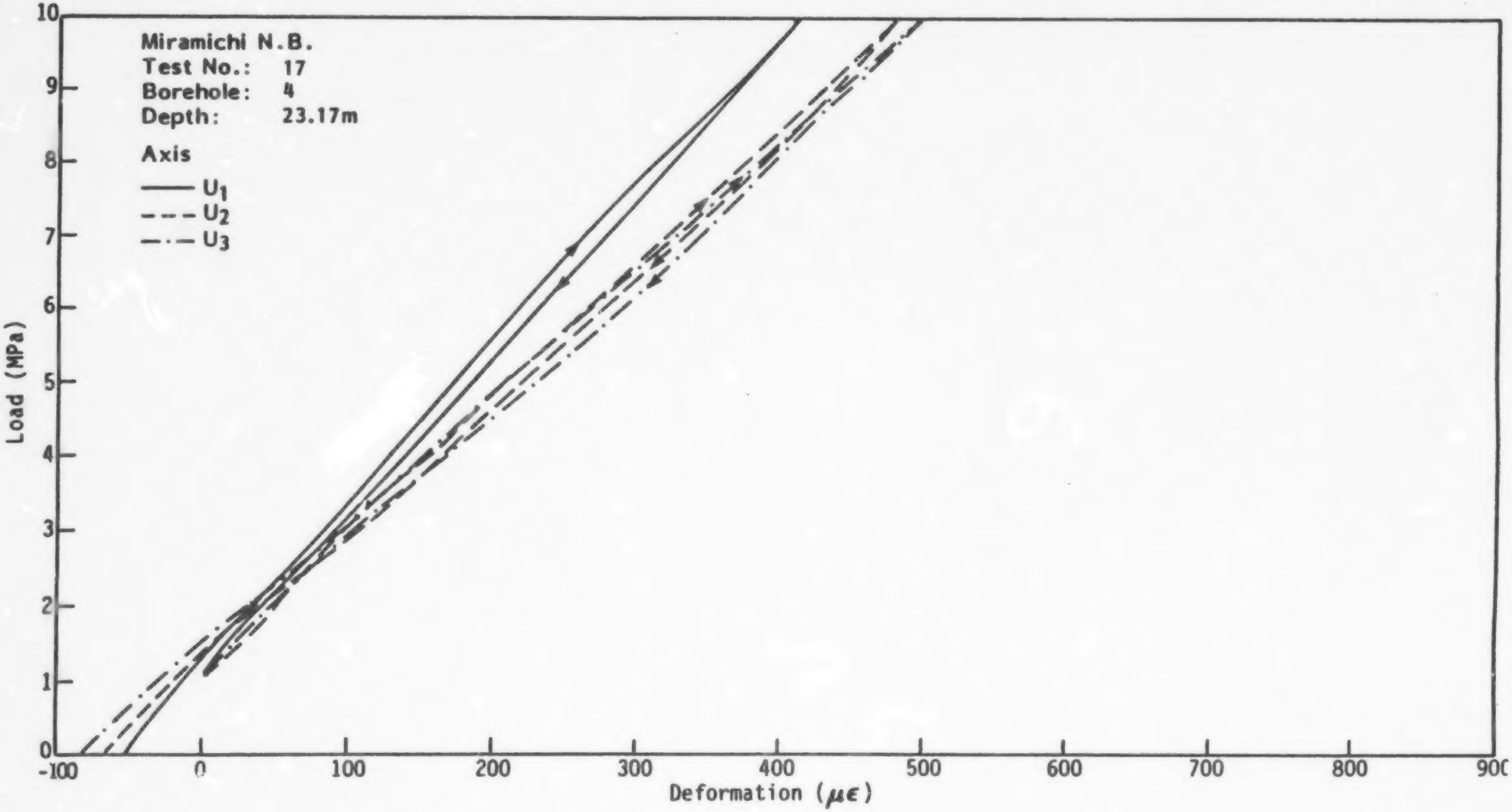
Miramichi N.B.
Test No.: 17
Borehole: 4
Depth: 23.17m
Axis
U1
U2
U3
Load (MPa)
0
1
2
3
4
5
6
7
8
9
10
-100
0
100
200
300
400
500
600
700
800
900
Deformation (με)

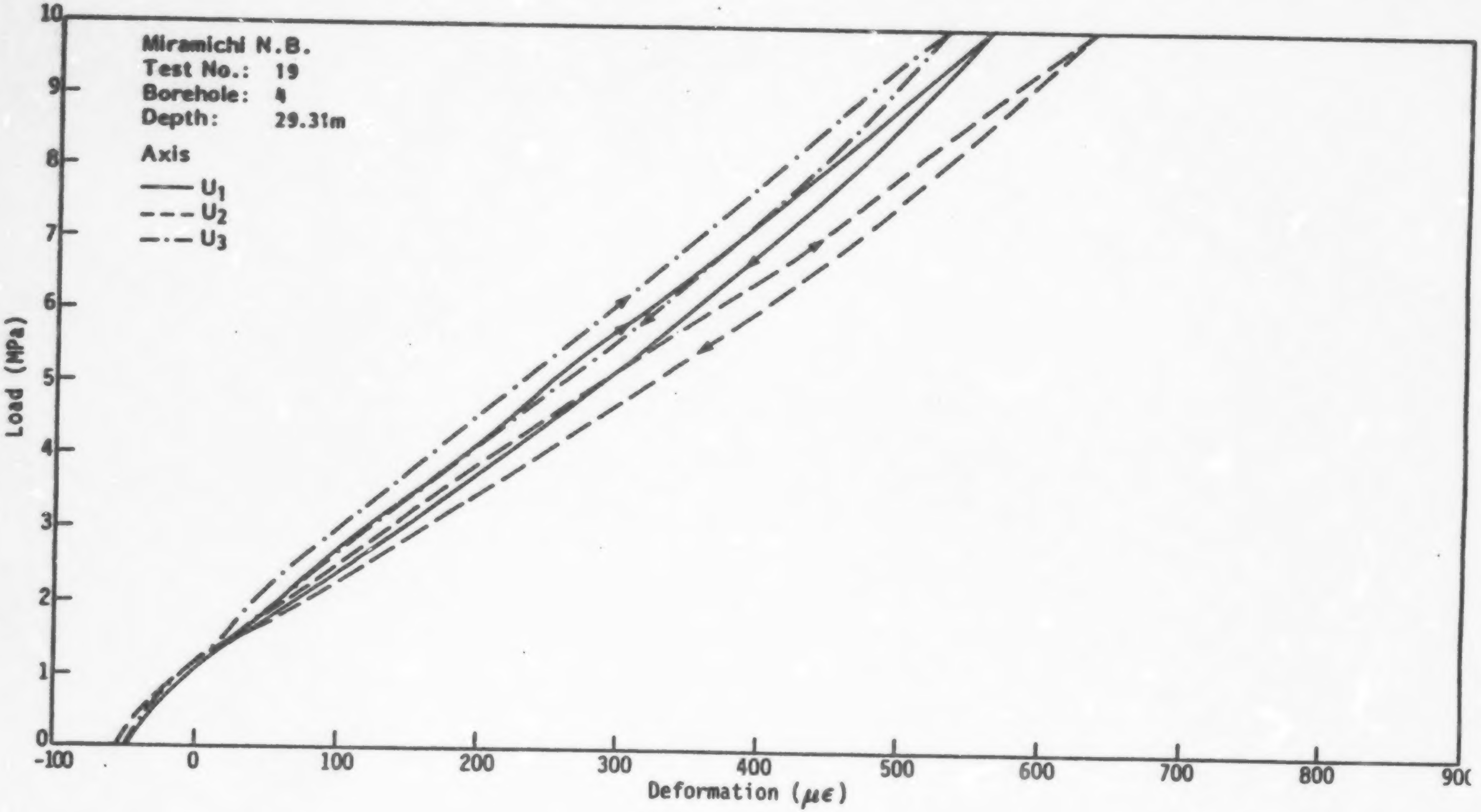
Miramichi N.B.
Test No.: 19
Borehole: 4
Depth: 29.31m
Axis
U1
U2
U3
Load (MPa)
0
1
2
3
4
5
6
7
8
9
10
-100
0
100
200
300
400
500
600
700
800
90
Deformation (µε)

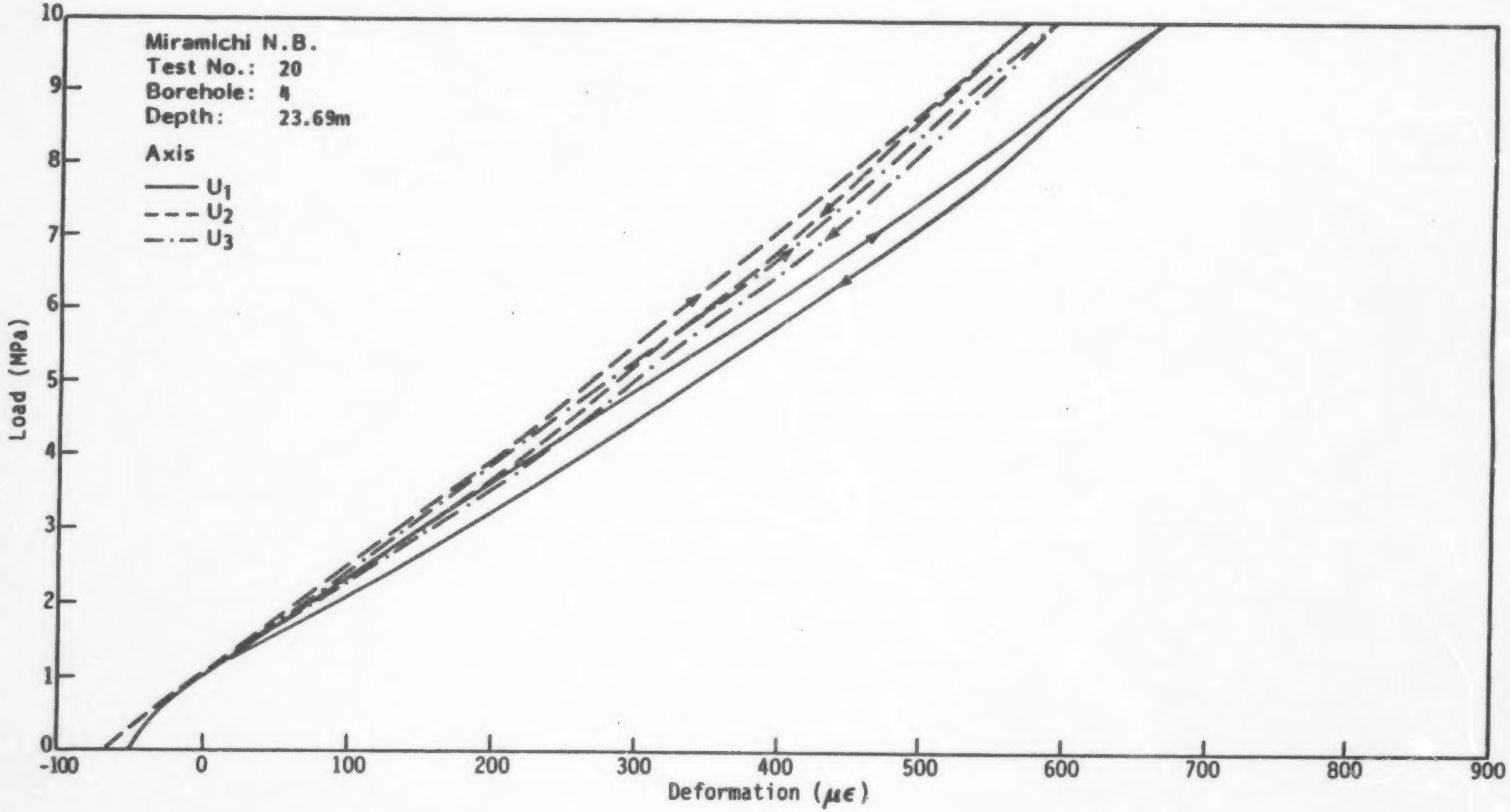
Miramichi N.B.
Test No.: 20
Borehole: 4
Depth: 23.69m
Axis
U1
U2
U3
Load (MPa)
0
1
2
3
4
5
6
7
8
9
10
-100
0
100
200
300
400
500
600
700
800
900
Deformation (με)

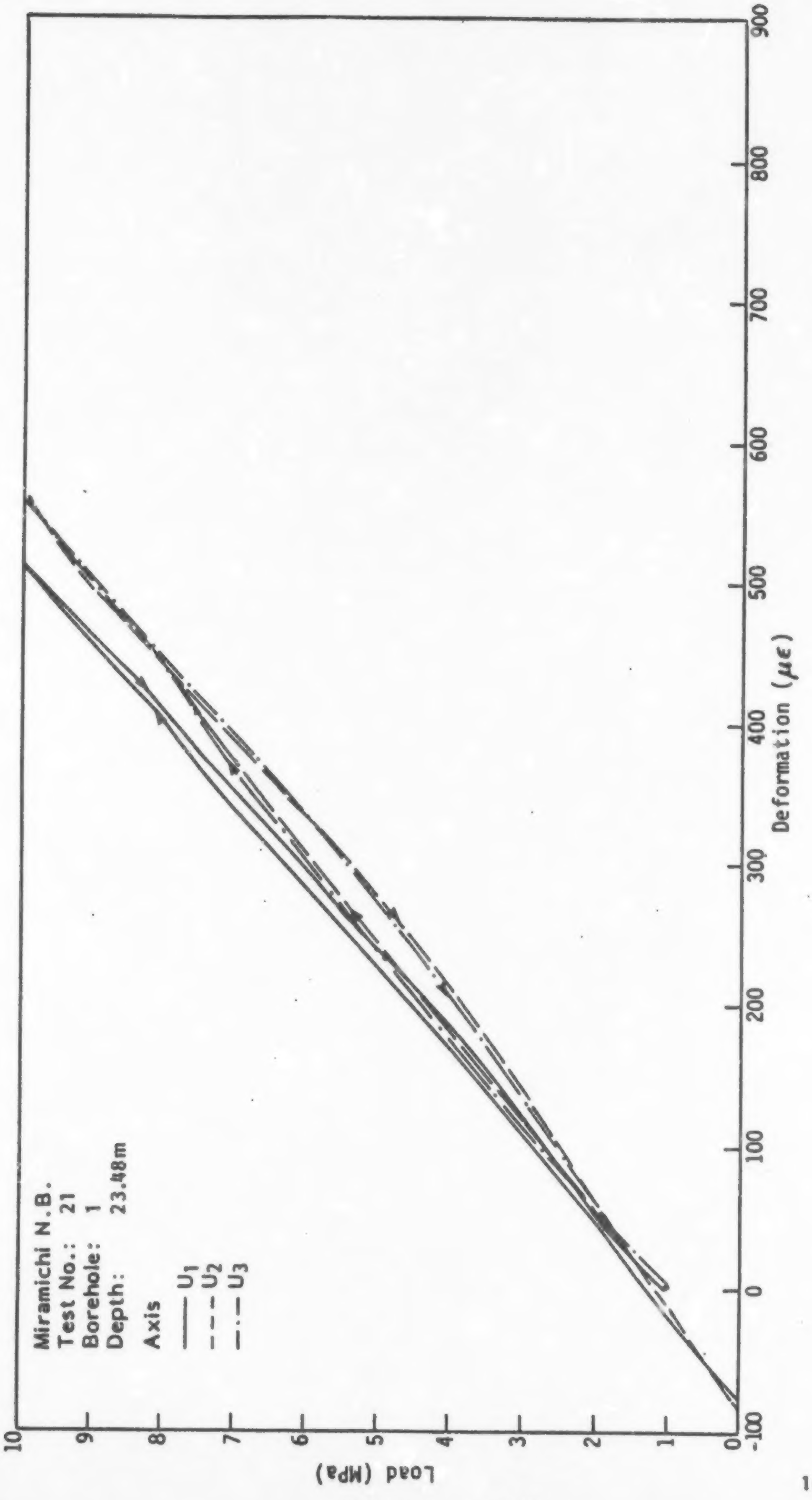
Miramichi N.B.
Test No.: 21
Borehole: 1
Depth: 23.48m
Axis
U1
U2
U3
Load (MPa)
0
1
2
3
4
5
6
7
8
9
10
Deformation (με)
-100
0
100
200
300
400
500
600
700
800
900

167047 RD

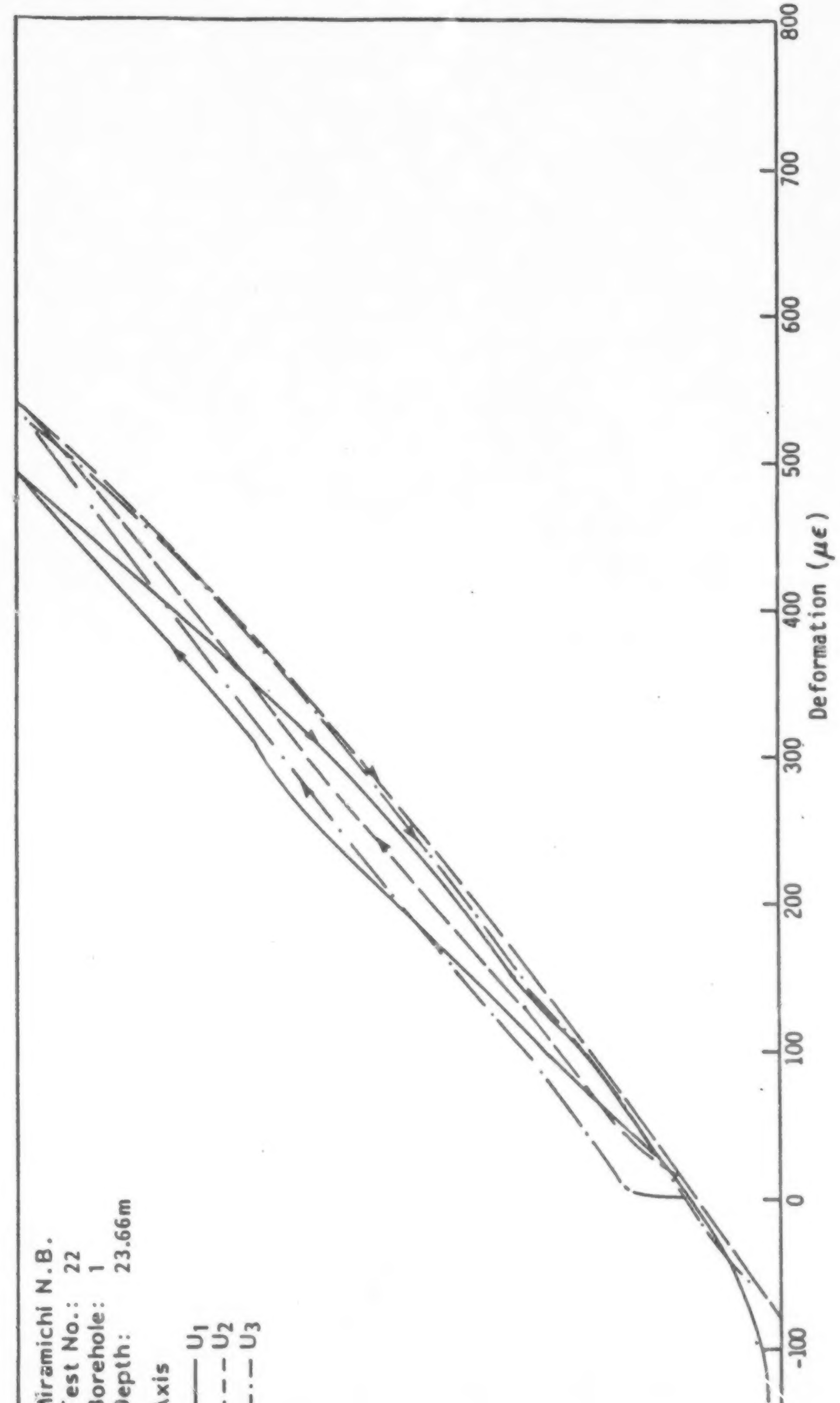
Miramichi N.B.
Test No.: 22
Borehole: 1
Depth: 23.66m
Axis
U1
U2
U3
Load (MPa)
0
1
2
3
4
5
6
7
8
9
10
Deformation (με)
-100
0
100
200
300
400
500
600
700
800

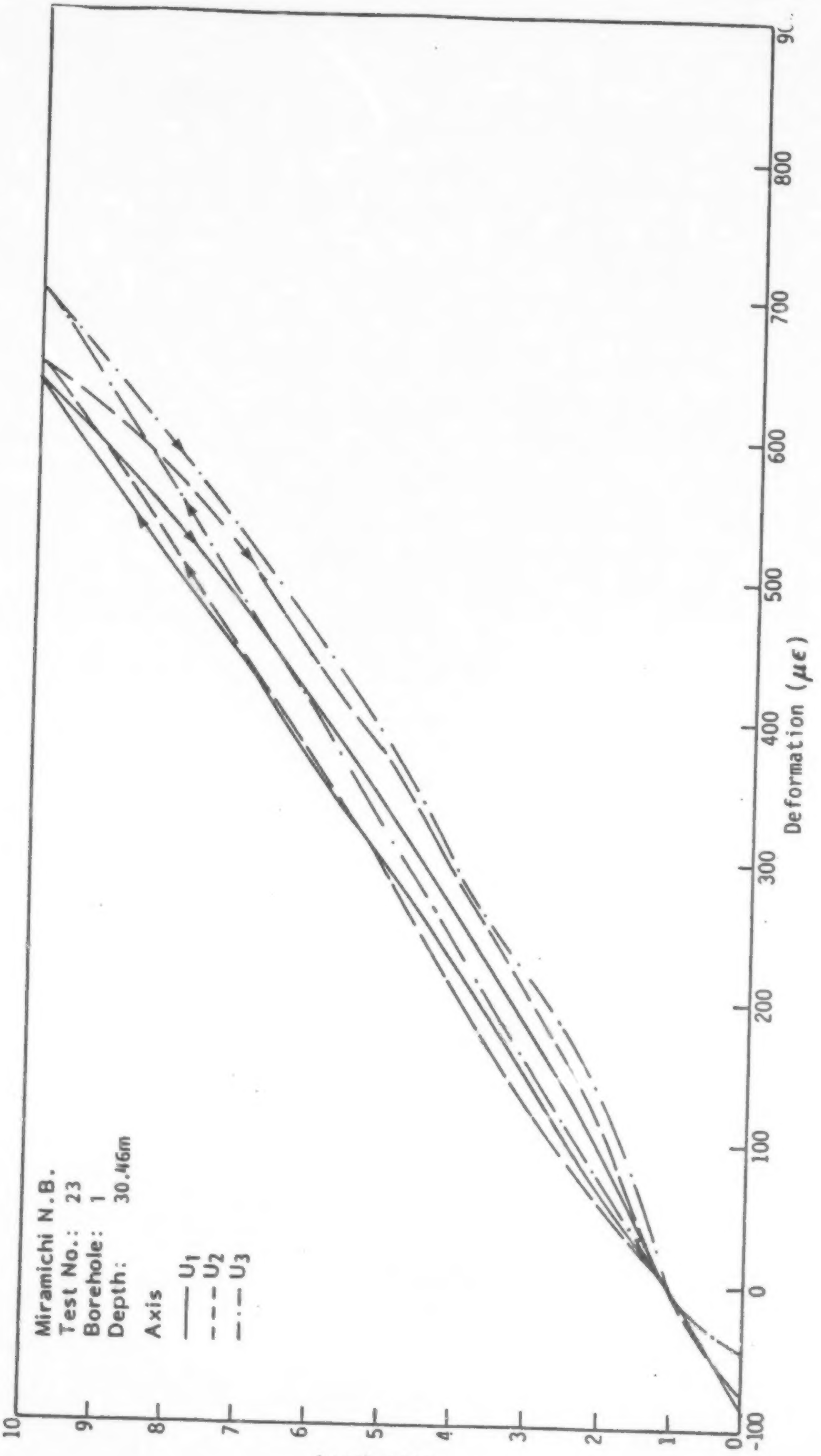
Miramichi N.B.
Test No.: 23
Borehole: 1
Depth: 30.46m
Axis
U1
U2
U3
Load (MPa)
0
1
2
3
4
5
6
7
8
9
10
Deformation (με)
-100
0
100
200
300
400
500
600
700
800

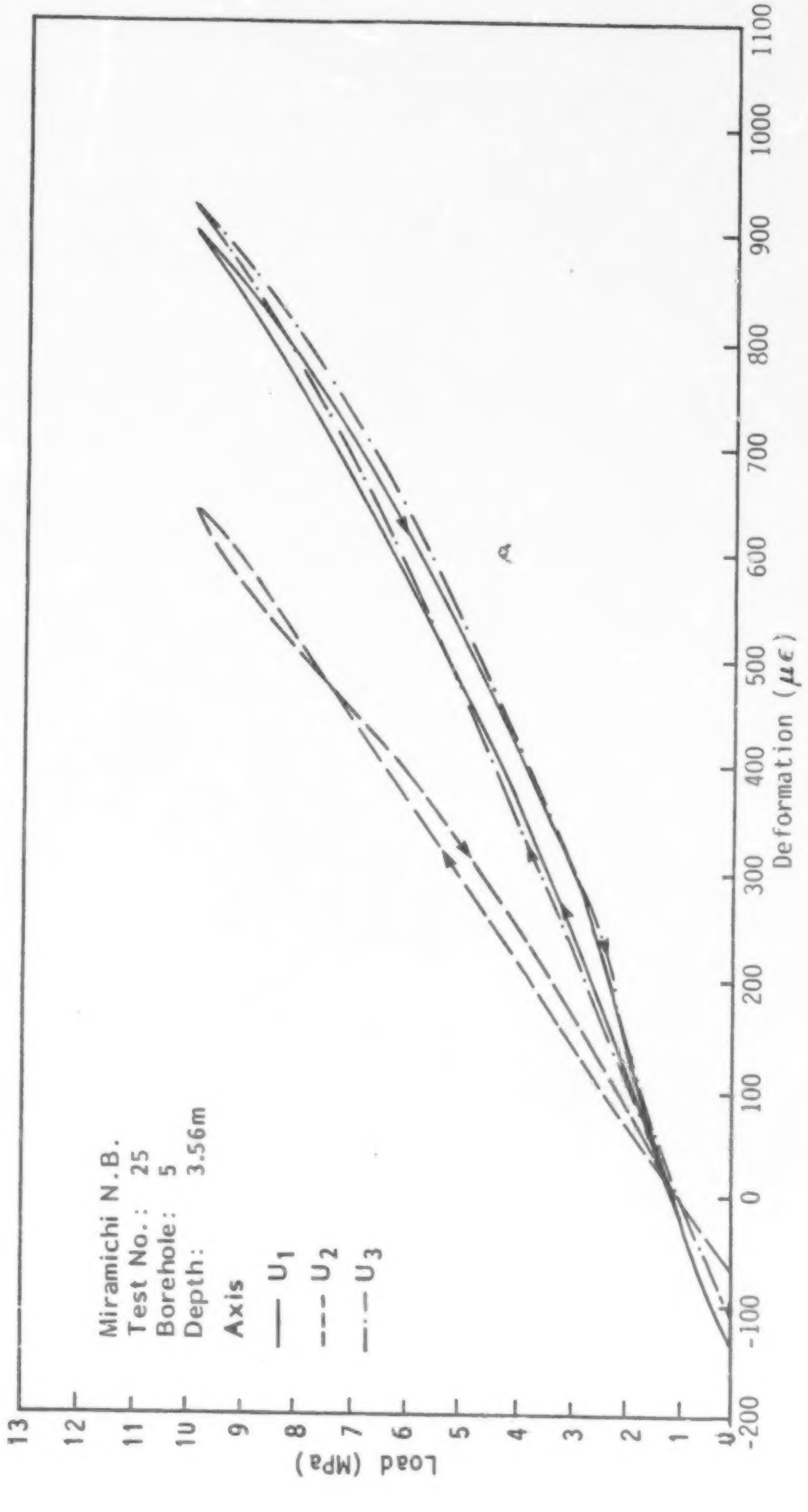
Miramichi N.B.
Test No.: 25
Borehole: 5
Depth: 3.56m
Axis
U1
U2
U3
Load (MPa)
0
1
2
3
4
5
6
7
8
9
10
11
12
13
Deformation (με)
-200
-100
0
100
200
300
400
500
600
700
800
900
1000
1100

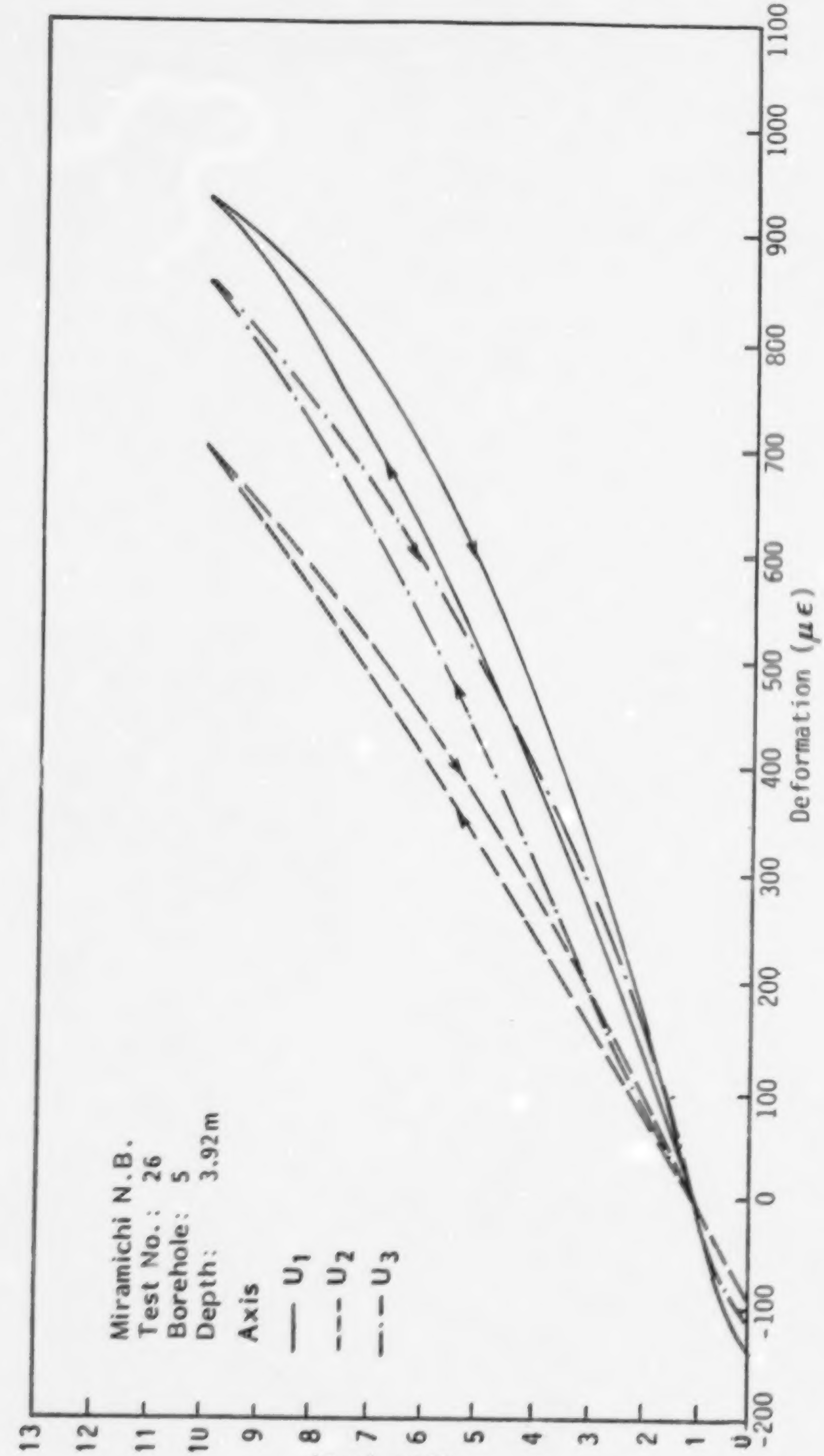
Miramichi N.B.
Test No.: 26
Borehole: 5
Depth: 3.92m
Axis
— U1
--- U2
-·- U3
Load (MPa)
0
1
2
3
4
5
6
7
8
9
10
11
12
13
Deformation ($\mu\epsilon$)
-200
-100
0
100
200
300
400
500
600
700
800
900
1000
1100

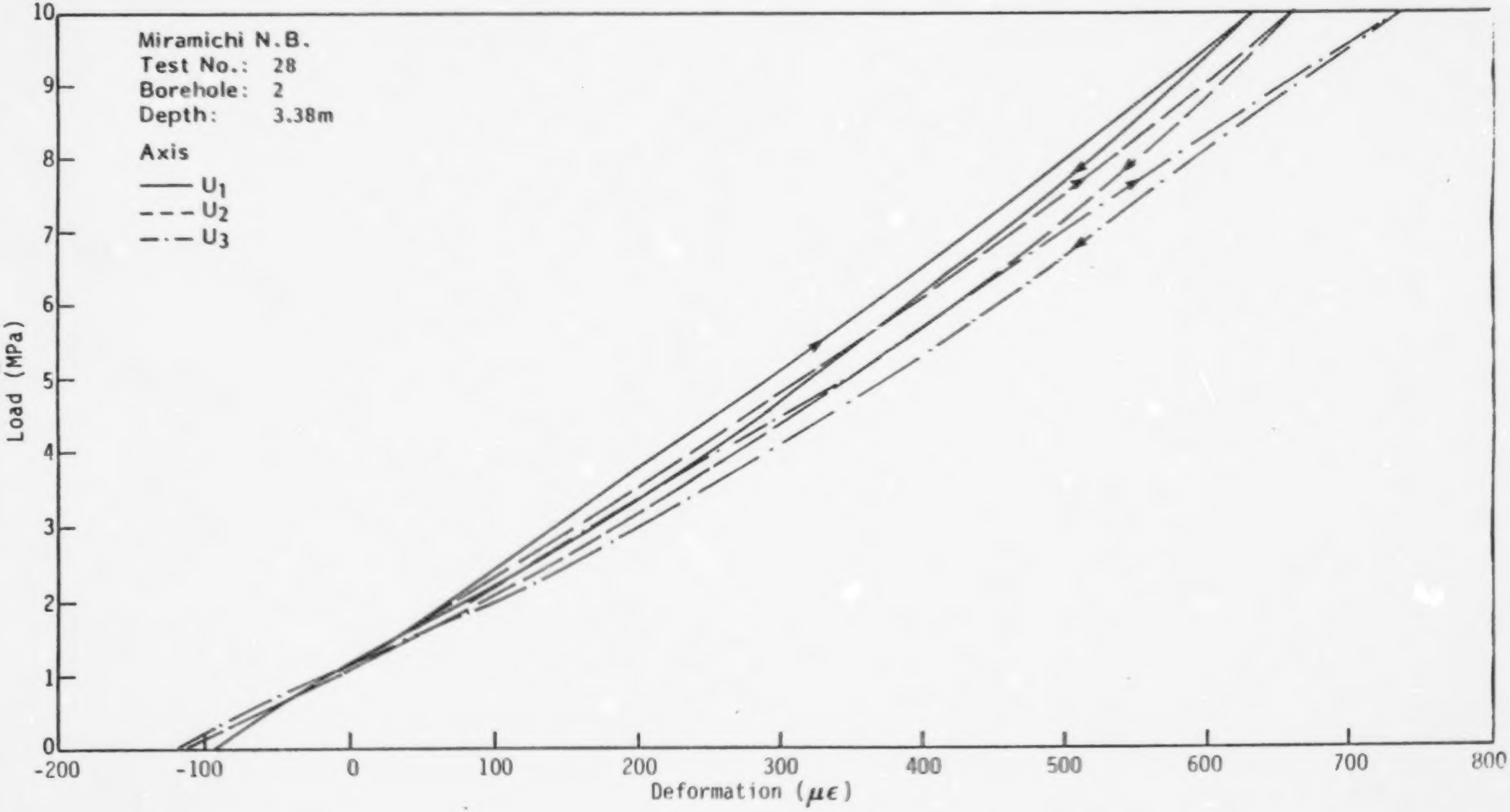
Miramichi N.B.
Test No.: 28
Borehole: 2
Depth: 3.38m
Axis
U1
U2
U3
Load (MPa)
10
9
8
7
6
5
4
3
2
1
0
-200
-100
0
100
200
300
400
500
600
700
800
Deformation (με)

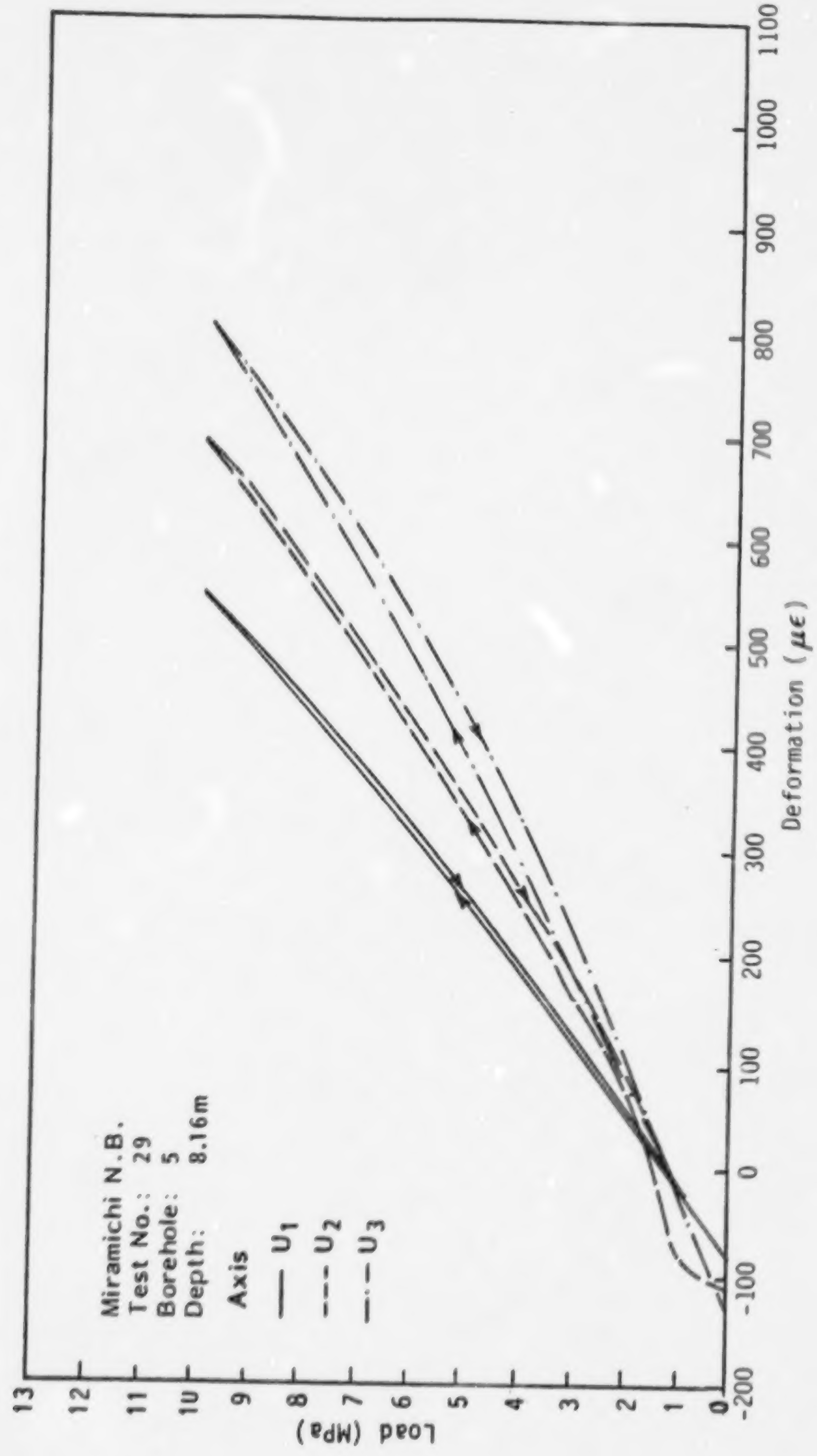
Miramichi N.B.
Test No.: 29
Borehole: 5
Depth: 8.16m
Axis
U$_1$
U$_2$
U$_3$
Load (MPa)
0
1
2
3
4
5
6
7
8
9
10
11
12
13
Deformation ($\mu\epsilon$)
-200
-100
0
100
200
300
400
500
600
700
800
900
1000
1100

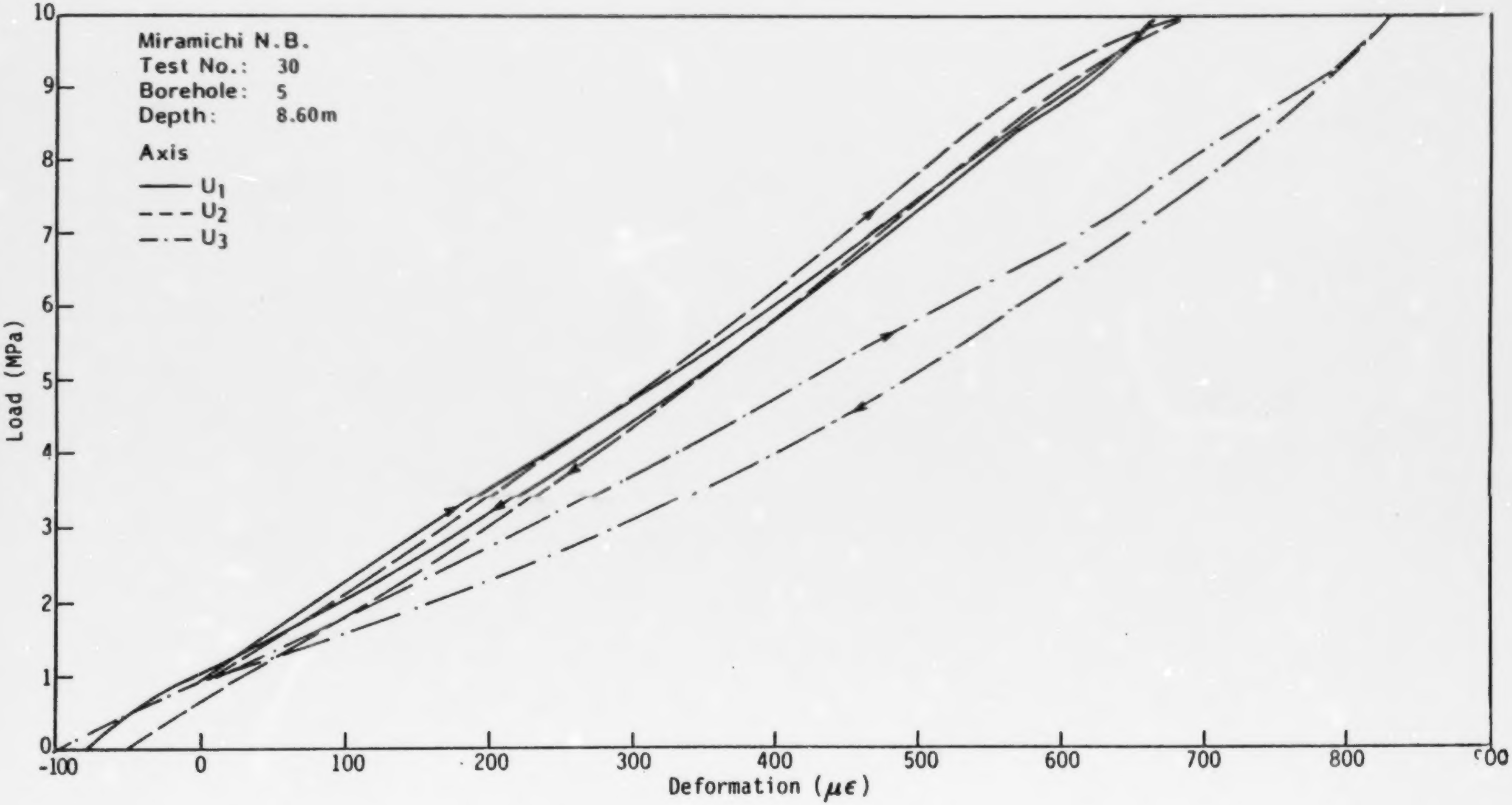
Miramichi N.B.
Test No.: 30
Borehole: 5
Depth: 8.60m
Axis
U1
U2
U3
Load (MPa)
0
1
2
3
4
5
6
7
8
9
10
Deformation (με)
-100
0
100
200
300
400
500
600
700
800
900

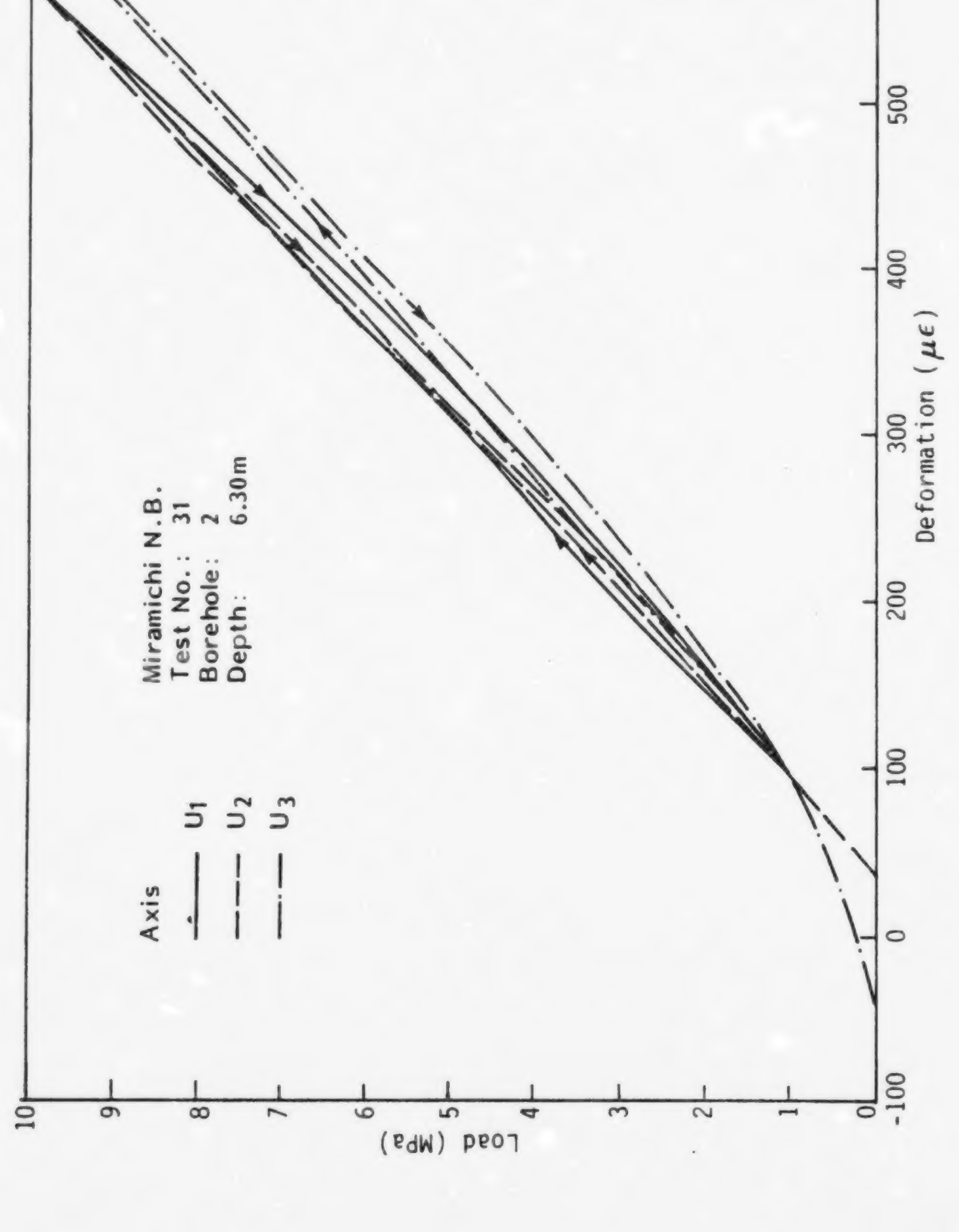
Axis
U_1
U_2
U_3
Miramichi N.B.
Test No.: 31
Borehole: 2
Depth: 6.30m
Load (MPa)
0
1
2
3
4
5
6
7
8
9
10
Deformation ($\mu\epsilon$)
-100
0
100
200
300
400
500
600
700

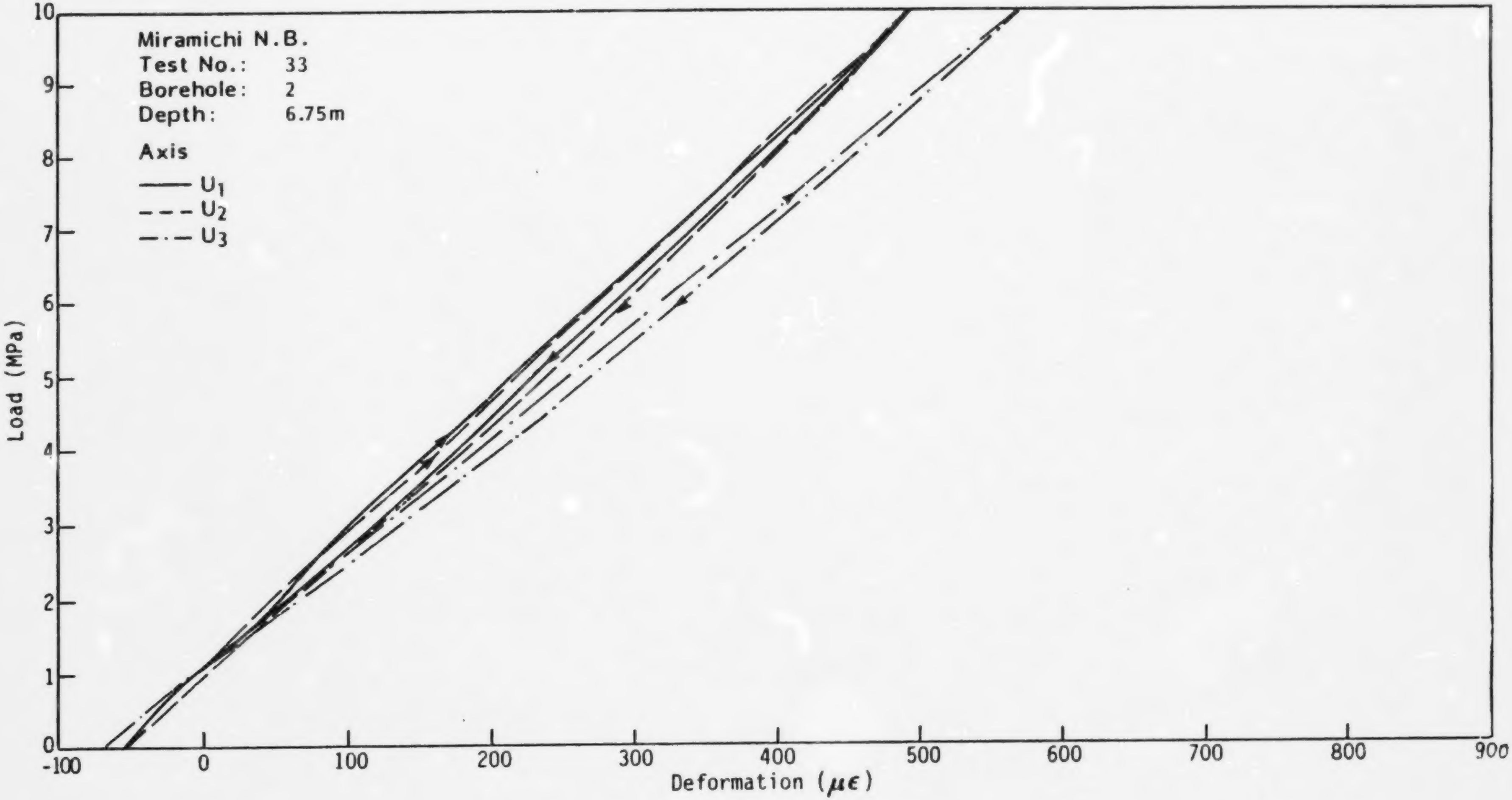
Miramichi N.B.
Test No.: 33
Borehole: 2
Depth: 6.75m
Axis
—— U_1
- - - U_2
—·— U_3
Load (MPa)
0
1
2
3
4
5
6
7
8
9
10
-100
0
100
200
300
400
500
600
700
800
900
Deformation ($\mu\epsilon$)

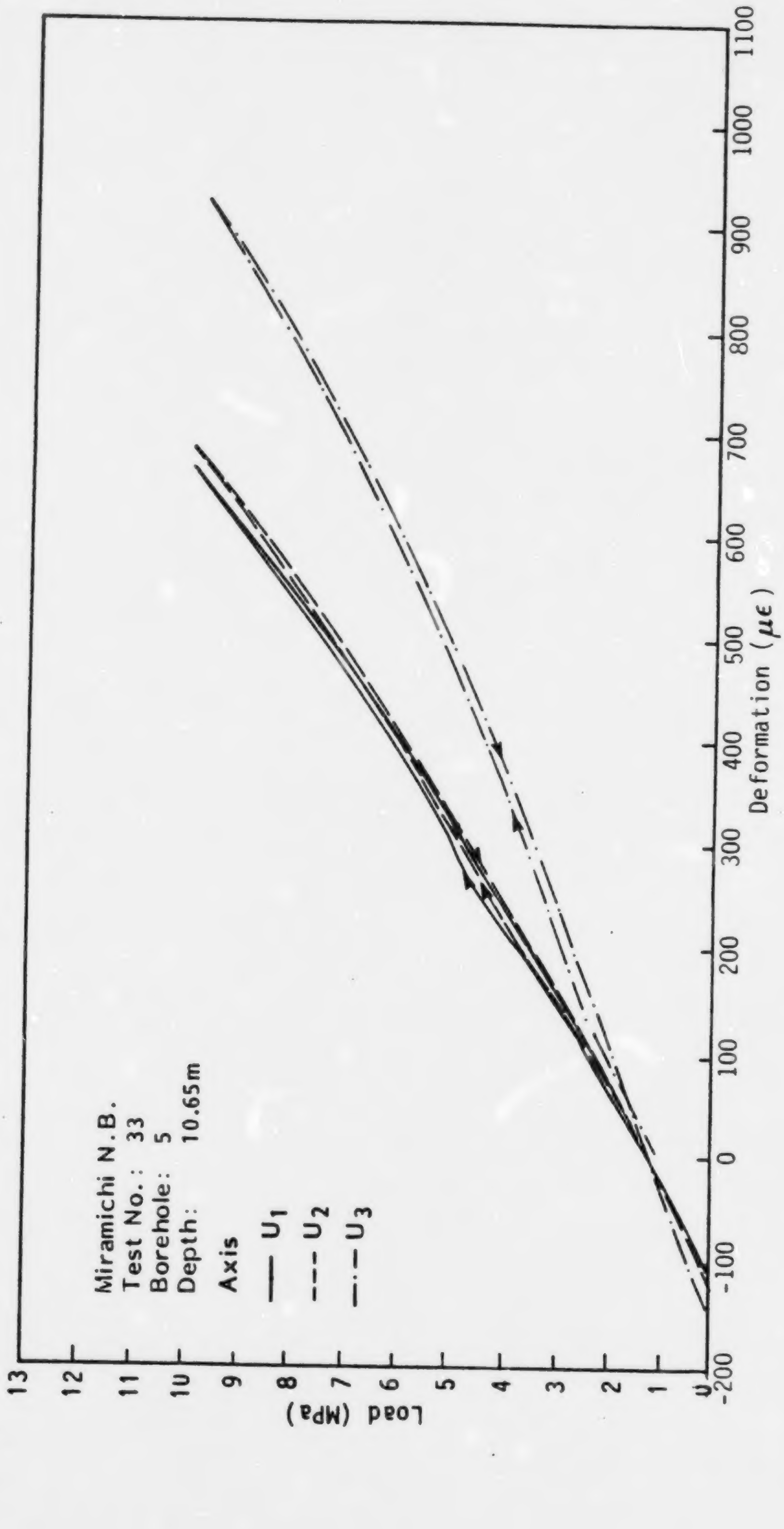
Miramichi N.B.
Test No.: 33
Borehole: 5
Depth: 10.65m
Axis
—— U_1
--- U_2
-·-- U_3
Load (MPa)
0
1
2
3
4
5
6
7
8
9
10
11
12
13
-200
-100
0
100
200
300
400
500
600
700
800
900
1000
1100
Deformation (με)

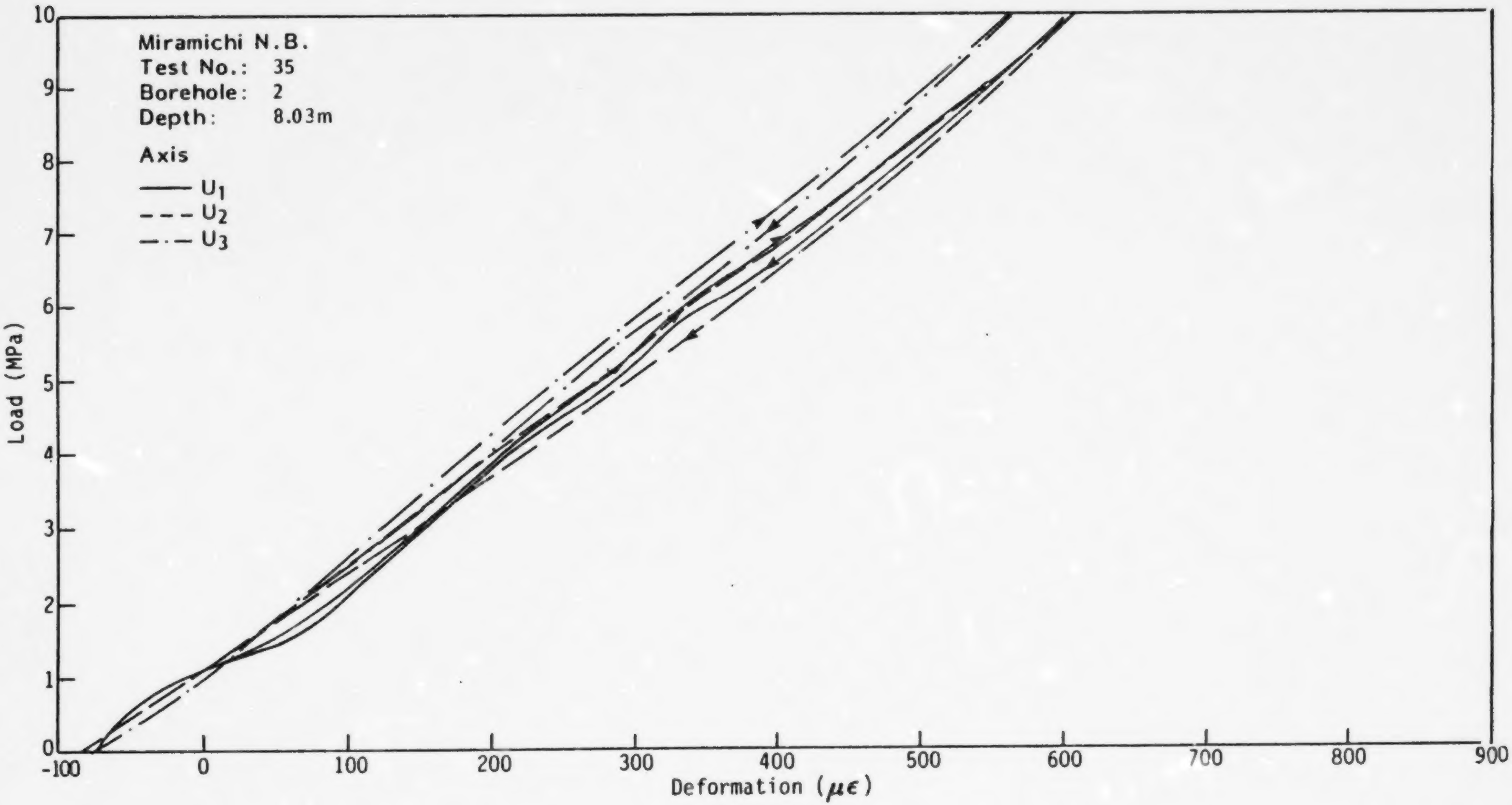
Miramichi N.B.
Test No.: 35
Borehole: 2
Depth: 8.03m
Axis
—— U_1
- - - U_2
—·— U_3
Load (MPa)
0
1
2
3
4
5
6
7
8
9
10
-100
0
100
200
300
400
500
600
700
800
900
Deformation ($\mu\epsilon$)

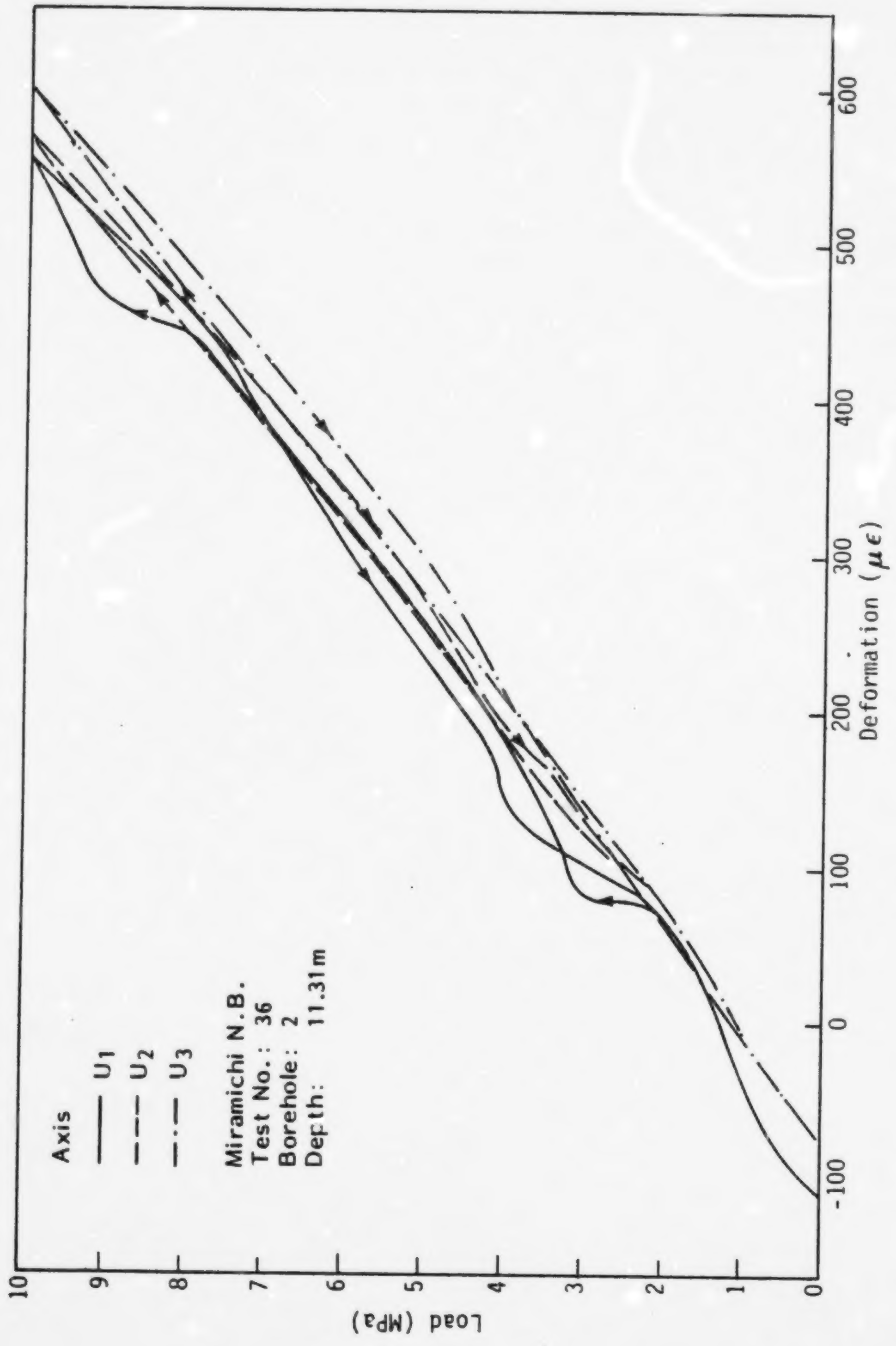
Axis
U$_1$
U$_2$
U$_3$
Miramichi N.B.
Test No.: 36
Borehole: 2
Depth: 11.31m
Load (MPa)
0
1
2
3
4
5
6
7
8
9
10
Deformation ($\mu\epsilon$)
-100
0
100
200
300
400
500
600

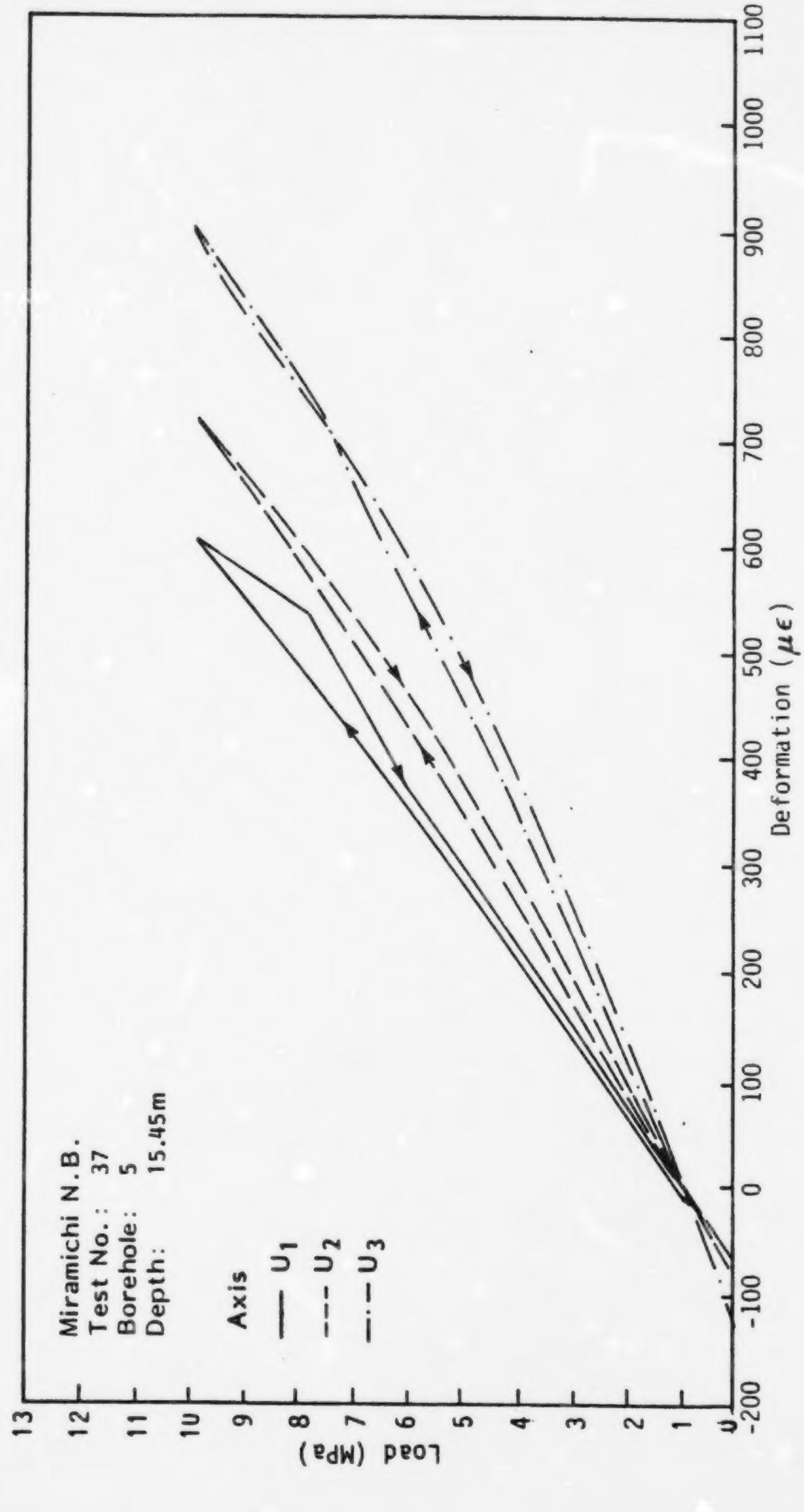
Miramichi N.B.
Test No.: 37
Borehole: 5
Depth: 15.45m
Axis
U1
U2
U3
Load (MPa)
0
1
2
3
4
5
6
7
8
9
10
11
12
13
Deformation (με)
-200
-100
0
100
200
300
400
500
600
700
800
900
1000
1100

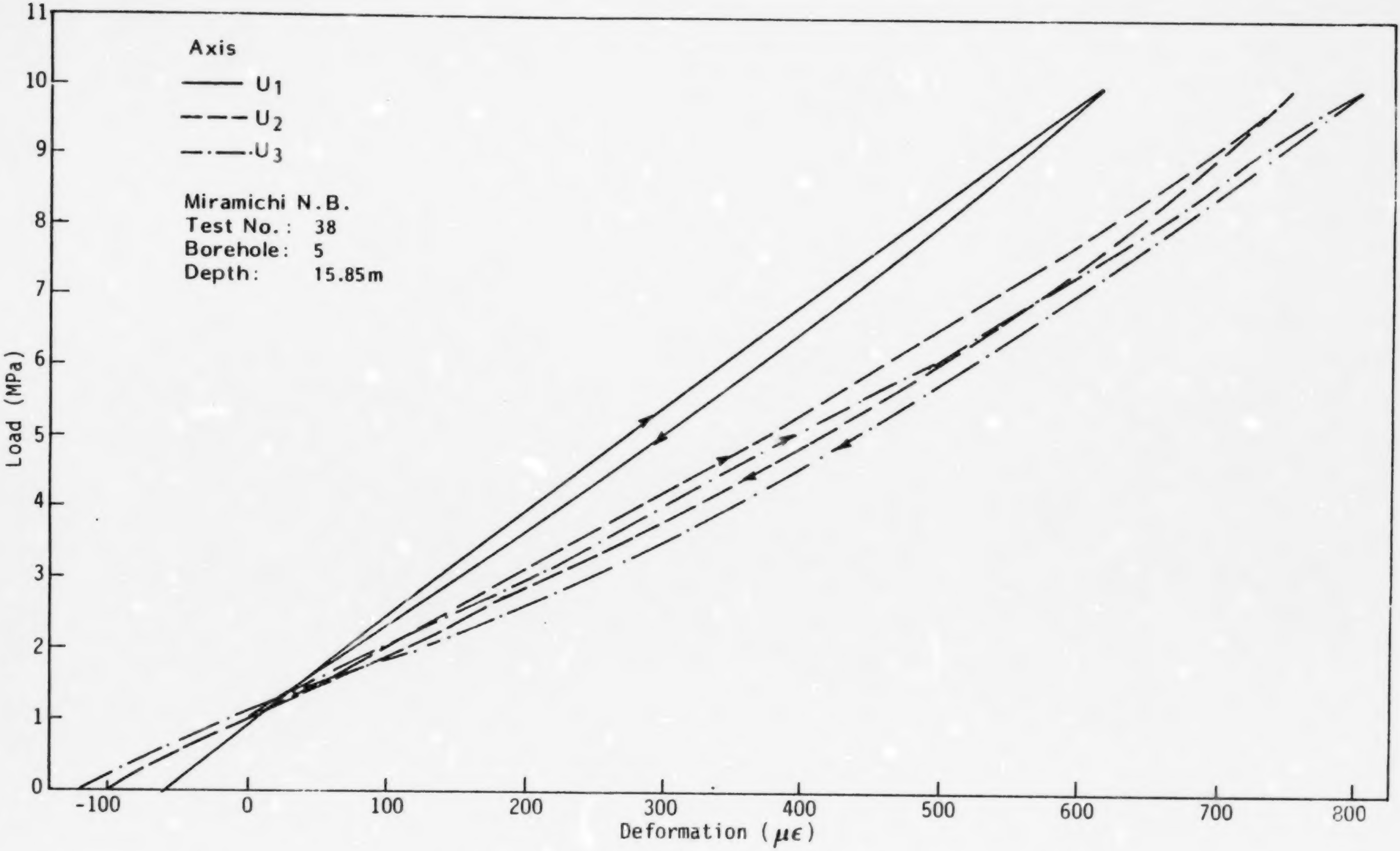
Axis
U1
U2
U3
Miramichi N.B.
Test No.: 38
Borehole: 5
Depth: 15.85m
Load (MPa)
0
1
2
3
4
5
6
7
8
9
10
11
Deformation (με)
-100
0
100
200
300
400
500
600
700
800

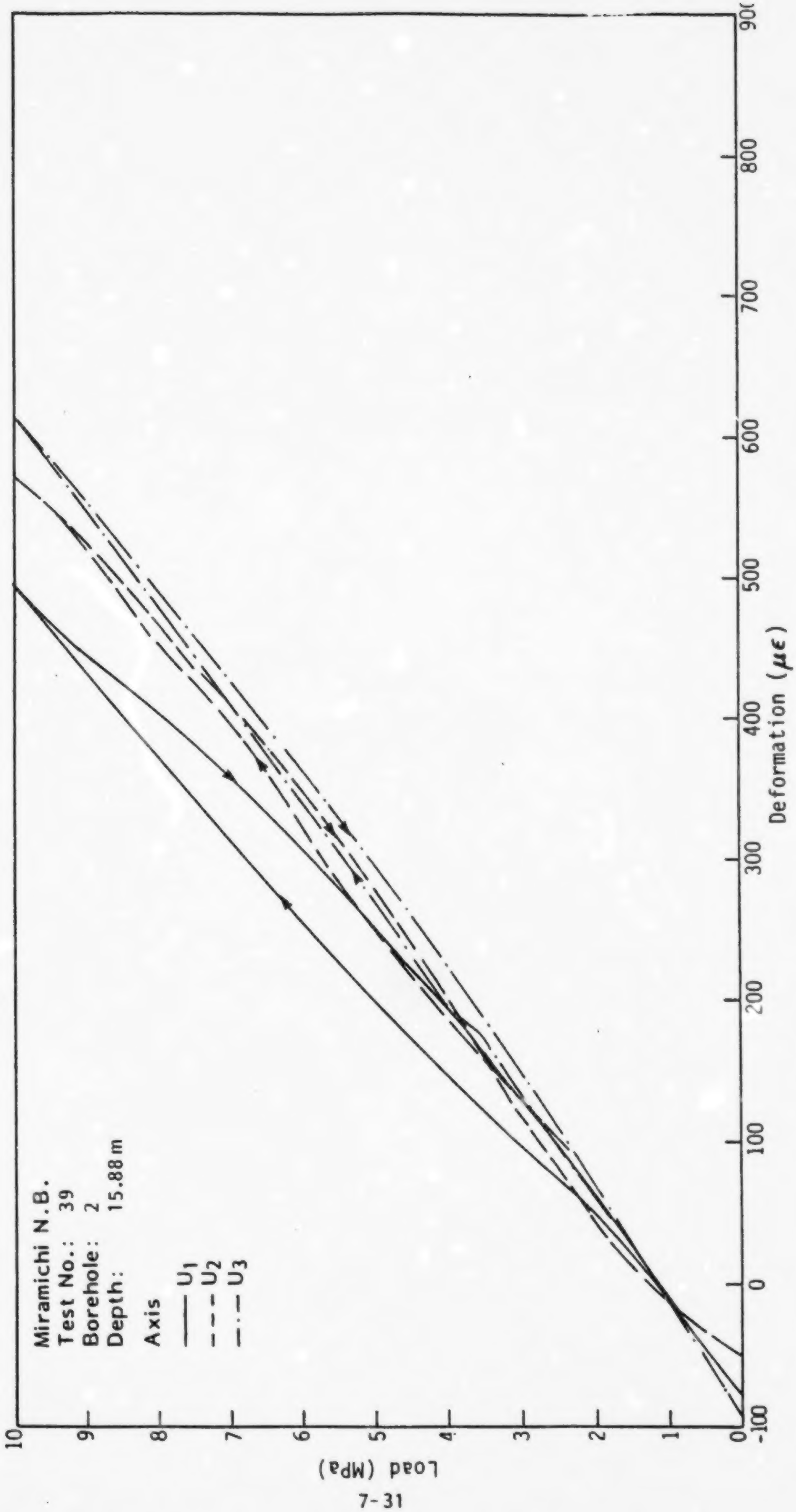
Miramichi N.B.
Test No.: 39
Borehole: 2
Depth: 15.88 m
Axis
—— U_1
- - - U_2
-·-· U_3
Load (MPa)
0
1
2
3
4
5
6
7
8
9
10
Deformation ($\mu\epsilon$)
-100
0
100
200
300
400
500
600
700
800
90(

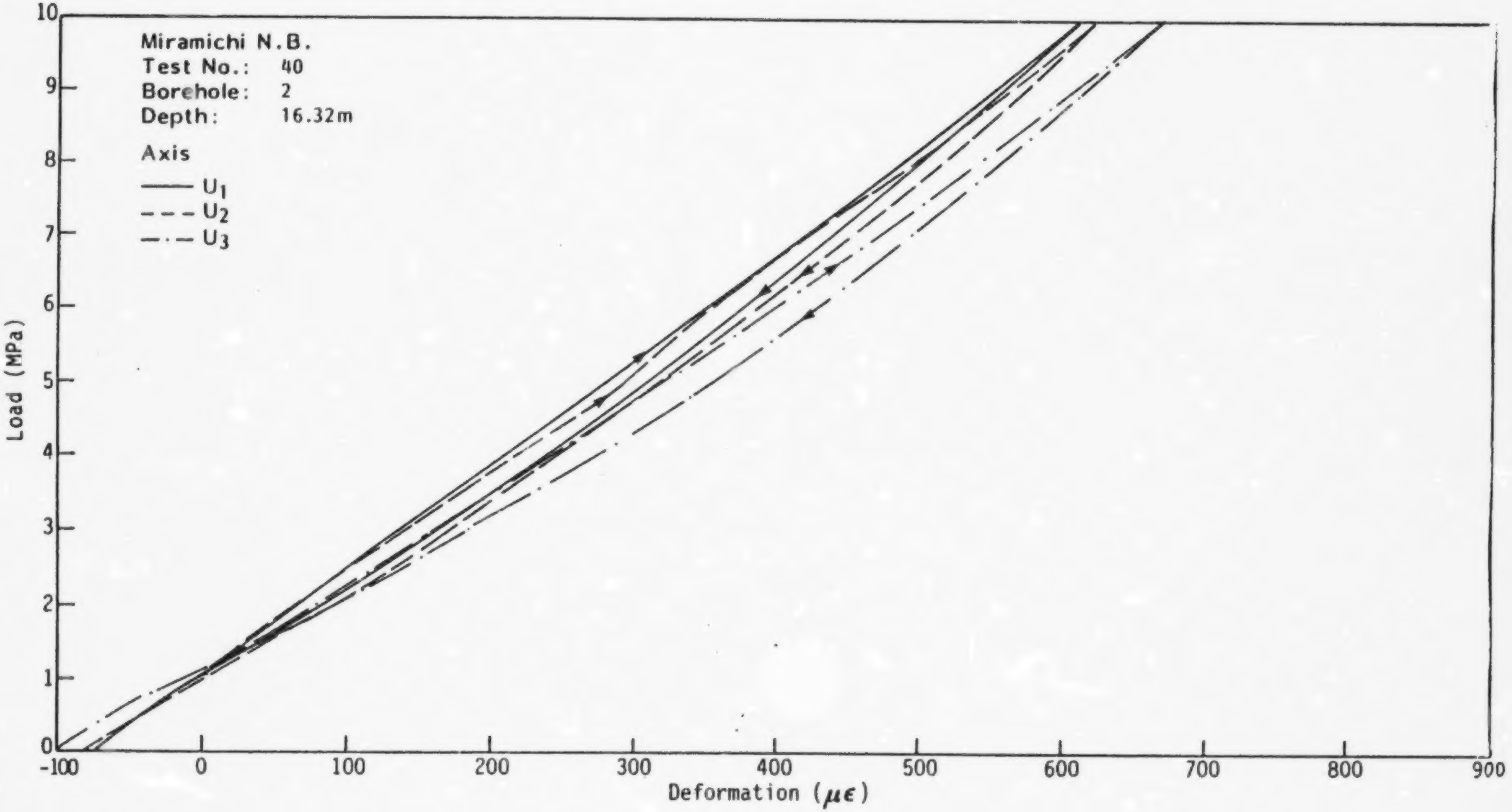

Miramichi N.B.
Test No.: 40
Borehole: 2
Depth: 16.32m
Axis
U1
U2
U3
Load (MPa)
0
1
2
3
4
5
6
7
8
9
10
-100
0
100
200
300
400
500
600
700
800
900
Deformation (με)

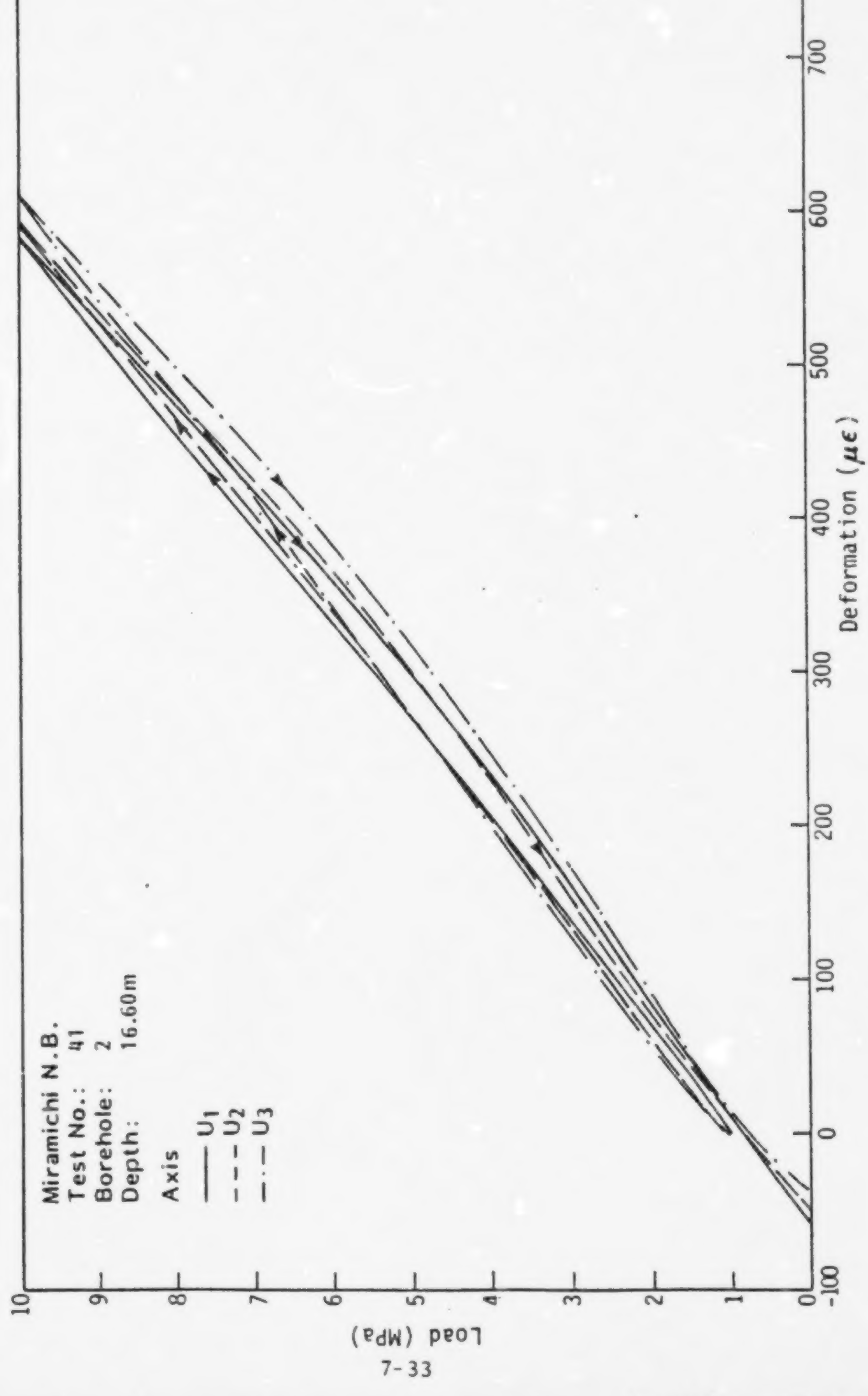
Miramichi N.B.
Test No.: 41
Borehole: 2
Depth: 16.60m
Axis
—— U_1
– – – U_2
–·–·– U_3
Load (MPa)
0
1
2
3
4
5
6
7
8
9
10
Deformation ($\mu\epsilon$)
-100
0
100
200
300
400
500
600
700
800
9

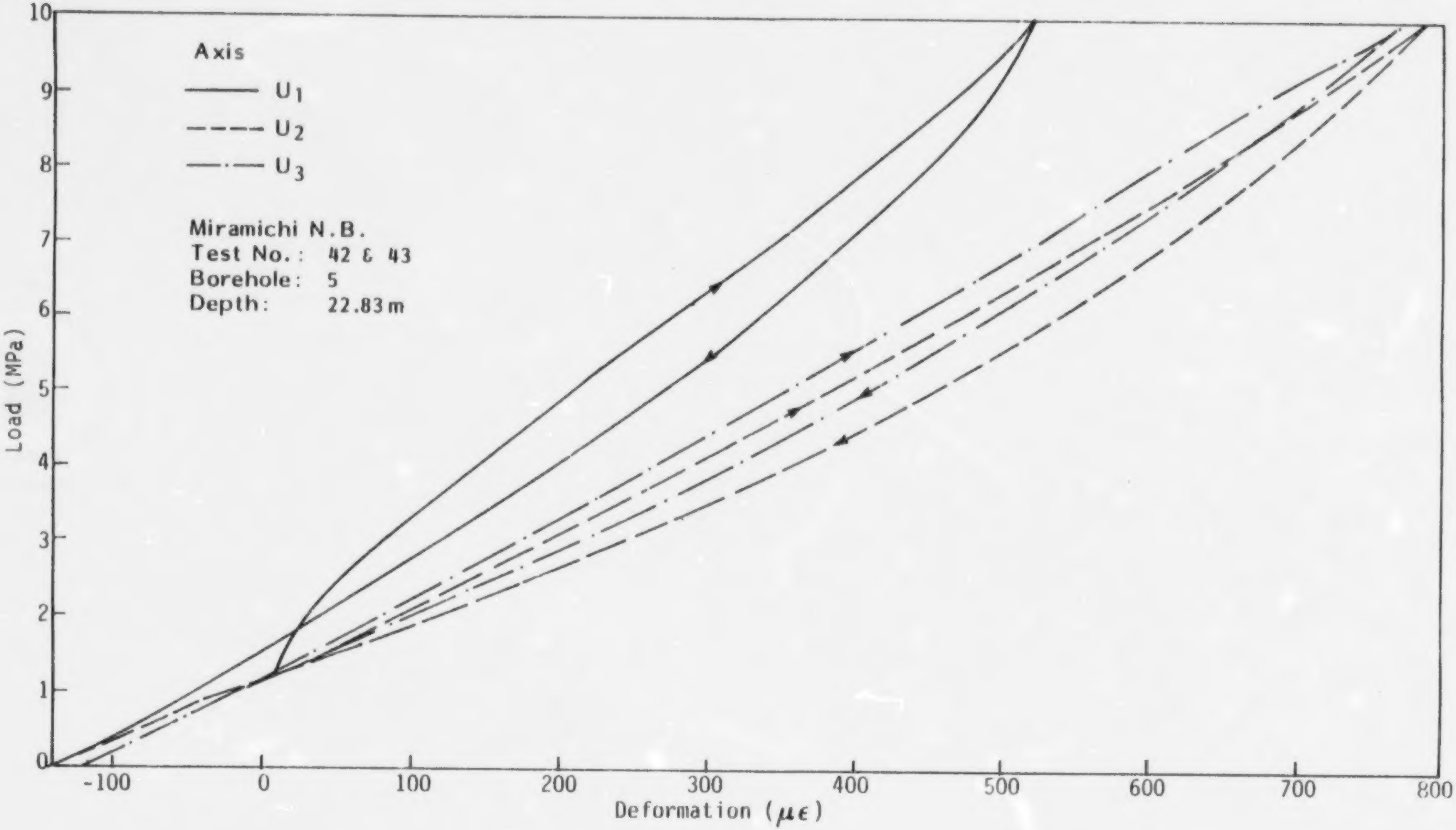
Axis
U$_1$
U$_2$
U$_3$
Miramichi N.B.
Test No.: 42 & 43
Borehole: 5
Depth: 22.83 m
Load (MPa)
0
1
2
3
4
5
6
7
8
9
10
Deformation ($\mu\epsilon$)
-100
0
100
200
300
400
500
600
700
800

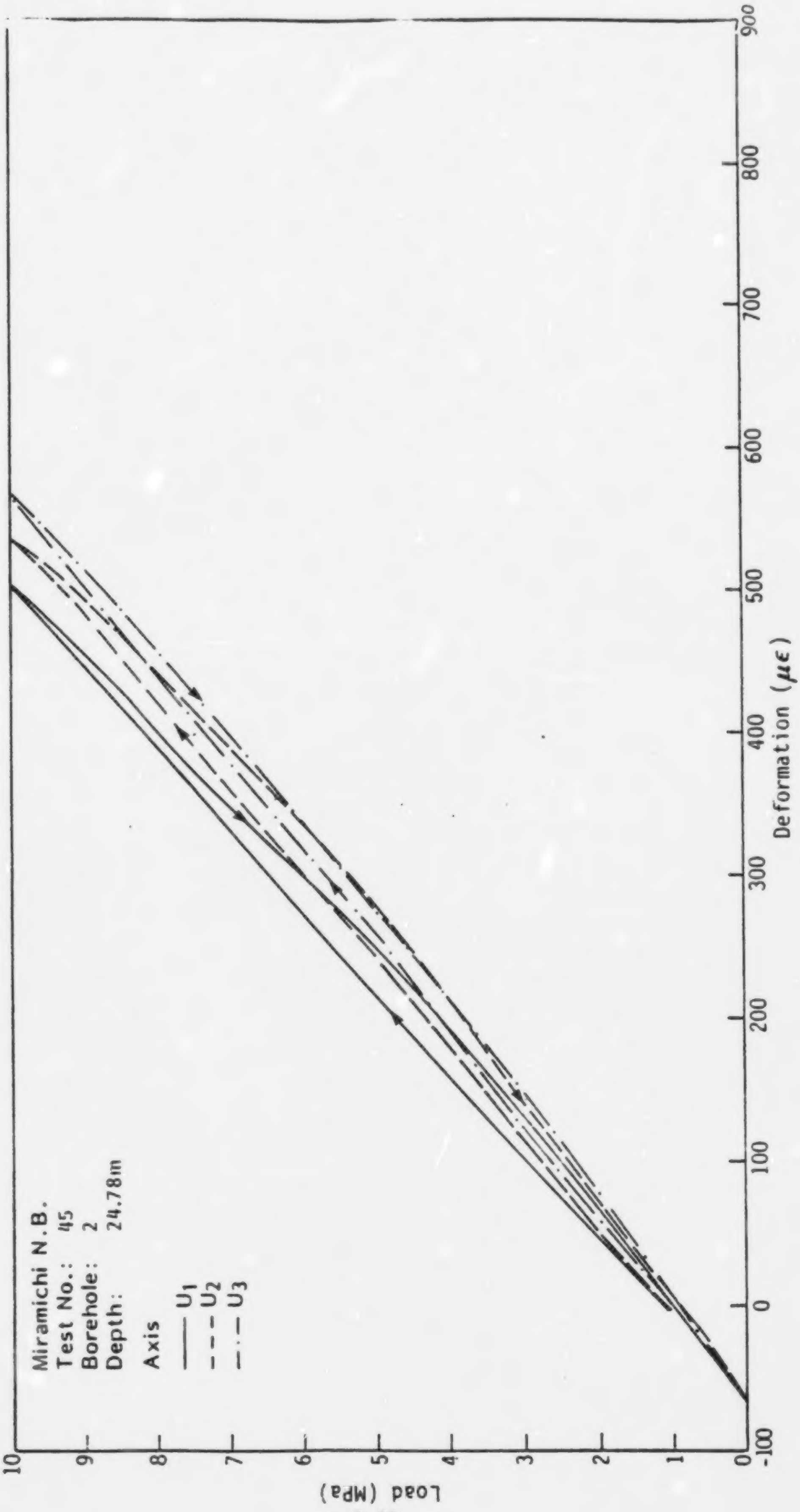
Miramichi N.B.
Test No.: 45
Borehole: 2
Depth: 24.78m
Axis
—— U1
- - - U2
-·- U3
Load (MPa)
0
1
2
3
4
5
6
7
8
9
10
Deformation (με)
-100
0
100
200
300
400
500
600
700
800
900

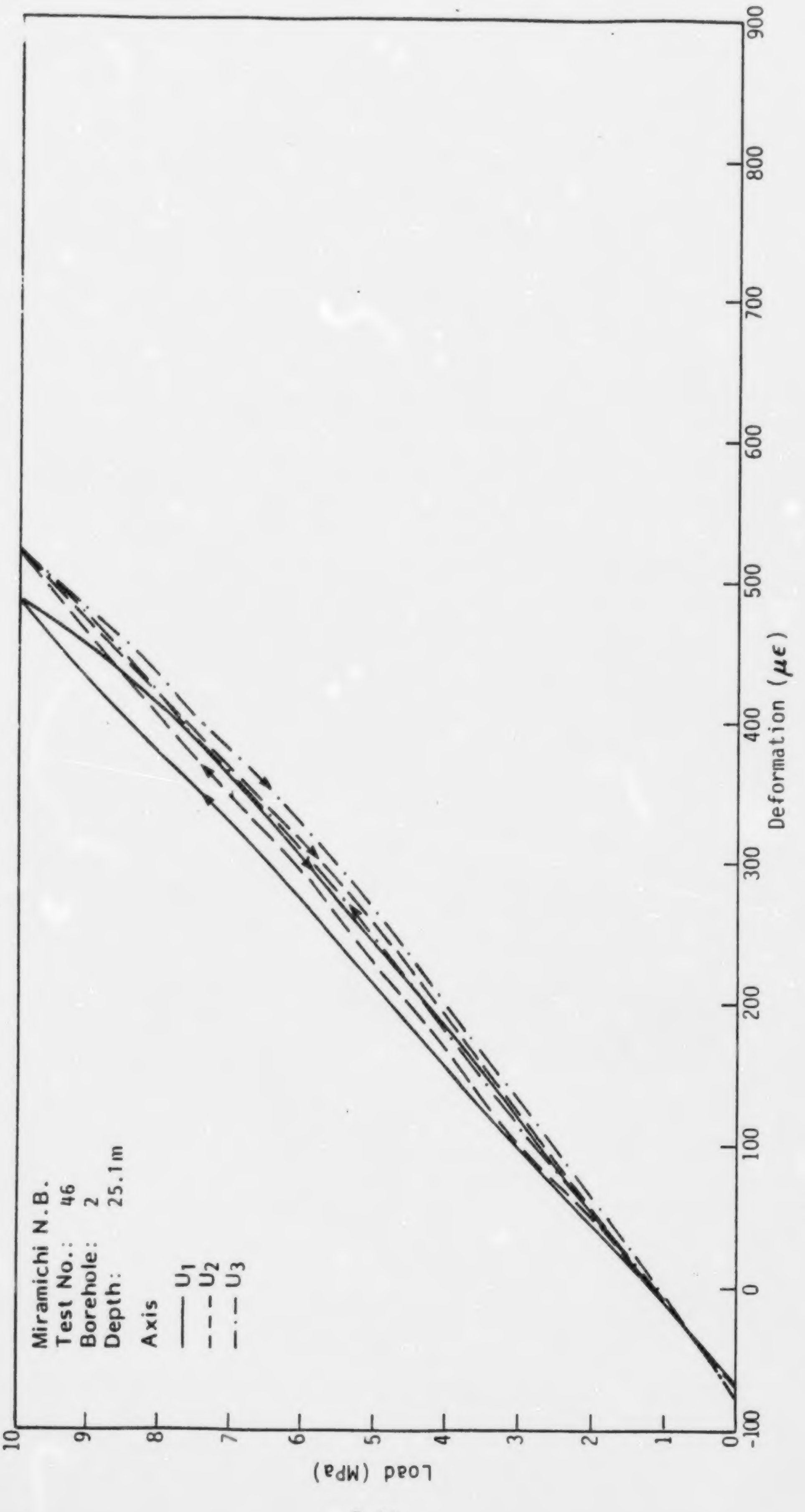
Miramichi N.B.
Test No.: 46
Borehole: 2
Depth: 25.1m
Axis
U$_1$
U$_2$
U$_3$
Load (MPa)
0
1
2
3
4
5
6
7
8
9
10
Deformation ($\mu\epsilon$)
-100
0
100
200
300
400
500
600
700
800
900

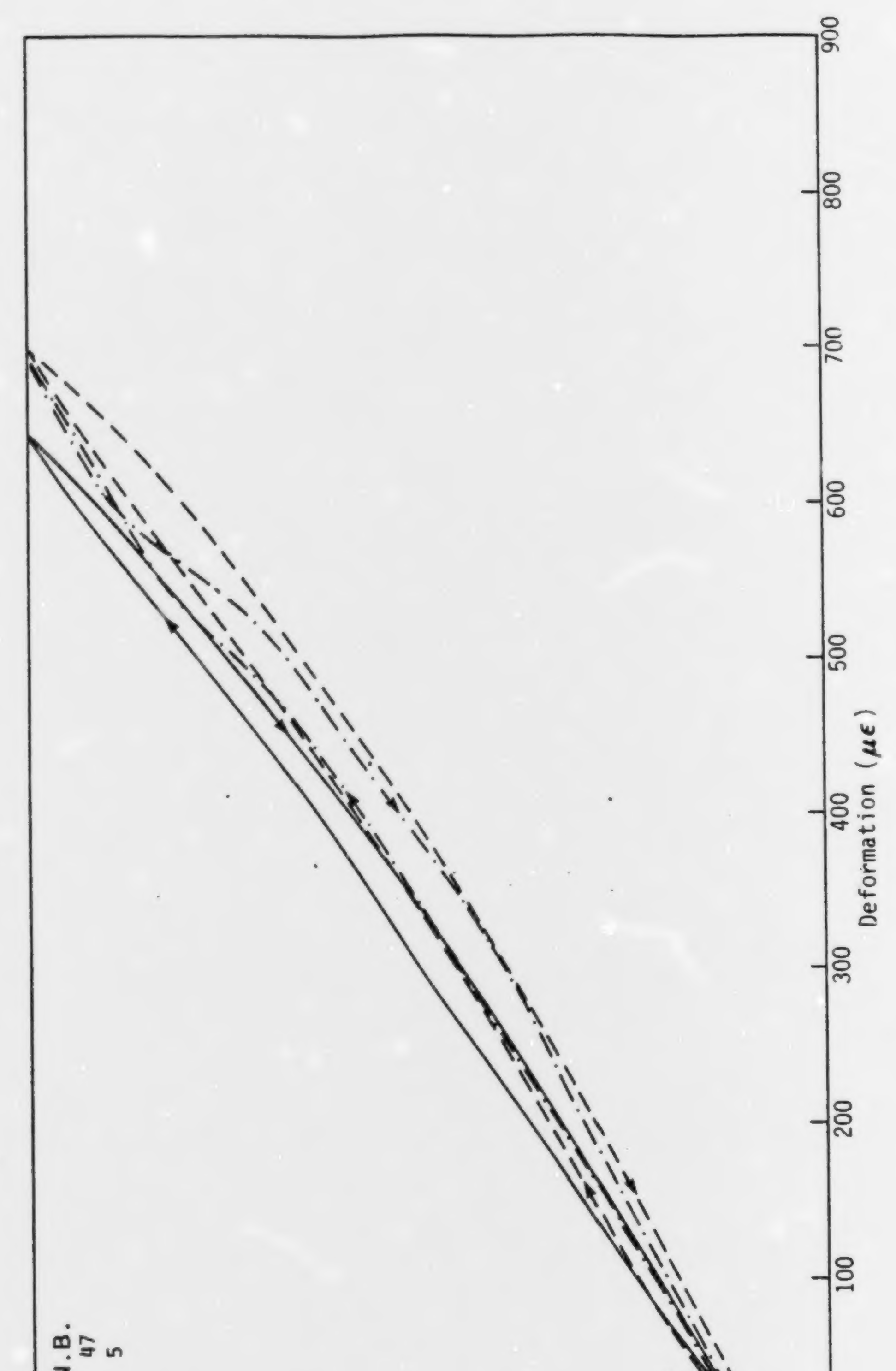
Miramichi N.B.
Test No.: 47
Borehole: 5
Depth:
Axis
—— U_1
– – – U_2
–·–·– U_3
Load (MPa)
0
1
2
3
4
5
6
7
8
9
10
Deformation (με)
-100
0
100
200
300
400
500
600
700
800
900

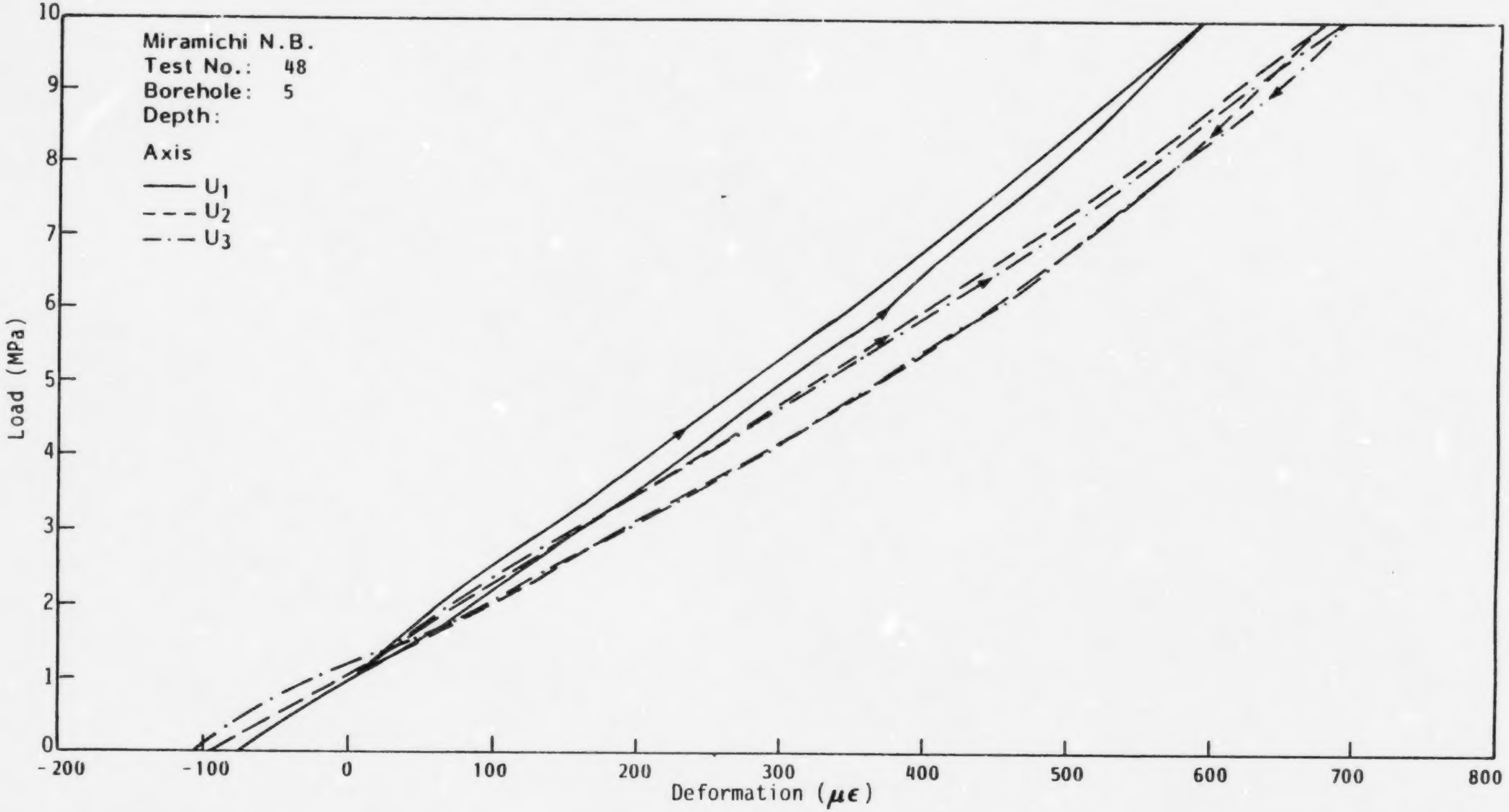
Miramichi N.B.
Test No.: 48
Borehole: 5
Depth:
Axis
U1
U2
U3
Load (MPa)
0
1
2
3
4
5
6
7
8
9
10
-200
-100
0
100
200
300
400
500
600
700
800
Deformation (με)

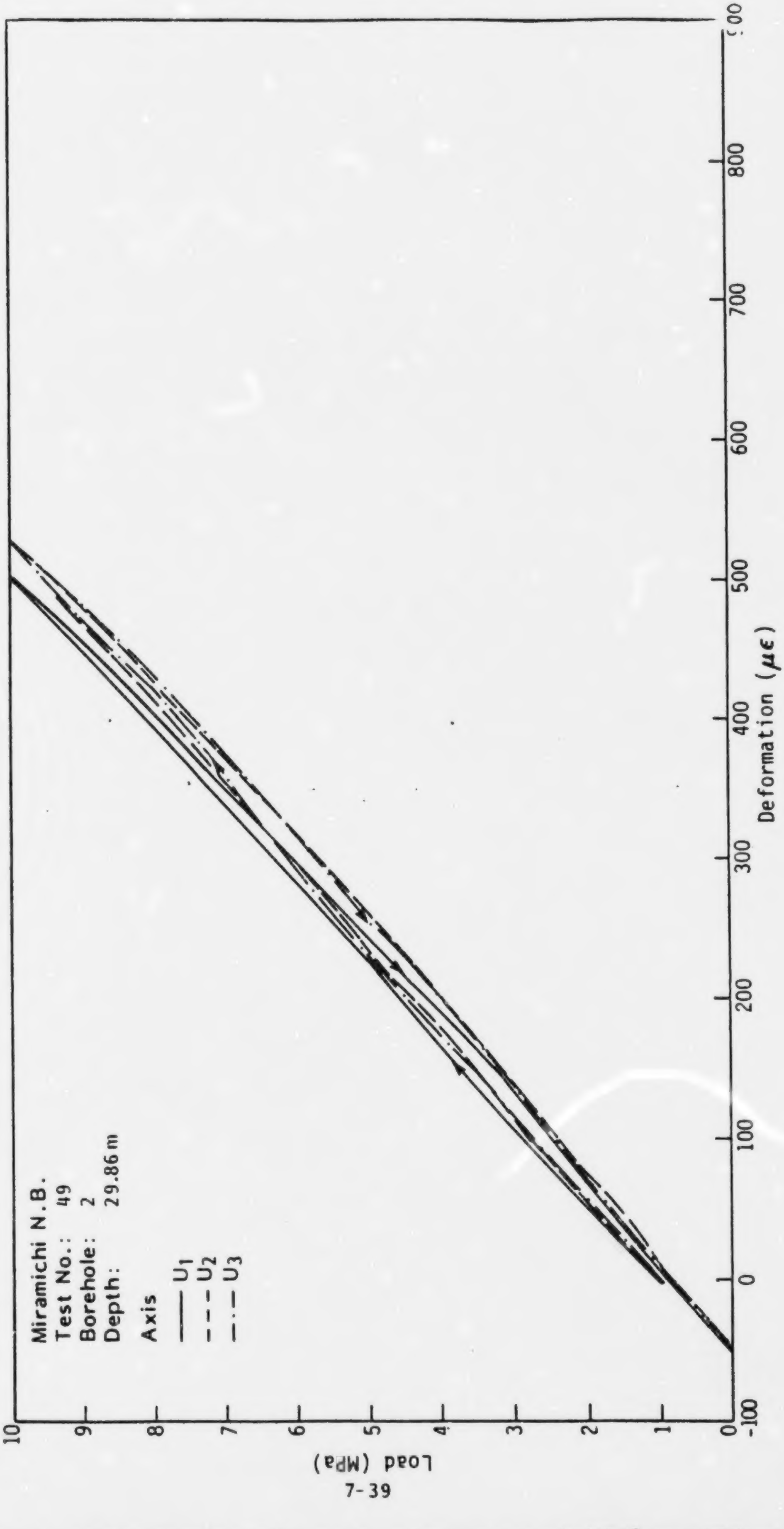
Miramichi N.B.
Test No.: 49
Borehole: 2
Depth: 29.86 m
Axis
—— U1
– – – U2
–·–·– U3
Load (MPa)
0
1
2
3
4
5
6
7
8
9
10
Deformation (με)
-100
0
100
200
300
400
500
600
700
800
900

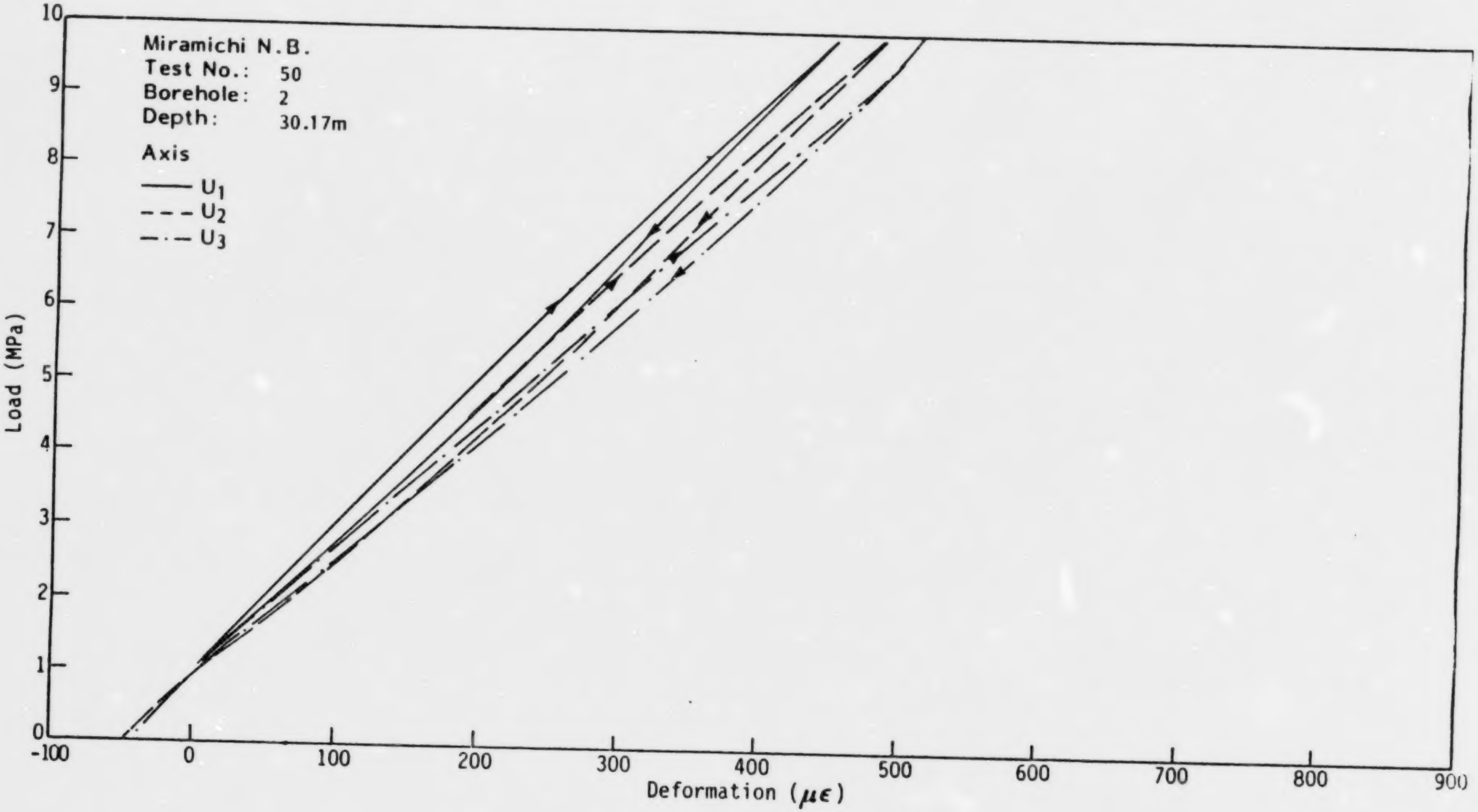
Miramichi N.B.
Test No.: 50
Borehole: 2
Depth: 30.17m
Axis
—— U1
- - - U2
—·— U3
Load (MPa)
10
9
8
7
6
5
4
3
2
1
0
-100
0
100
200
300
400
500
600
700
800
900
Deformation (με)

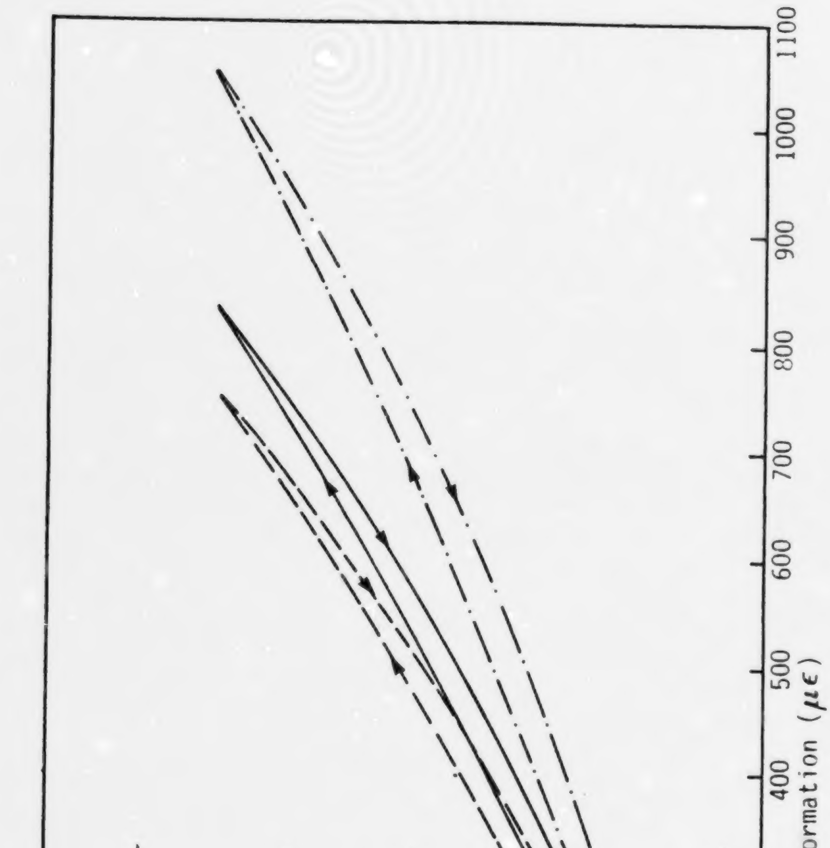
Miramichi N.B.
Test No.: 51
Borehole: 6
Depth: 7.18m
Axis
U1
U2
U3
Load (MPa)
0
1
2
3
4
5
6
7
8
9
10
11
12
13
Deformation (με)
-200
-100
0
100
200
300
400
500
600
700
800
900
1000
1100

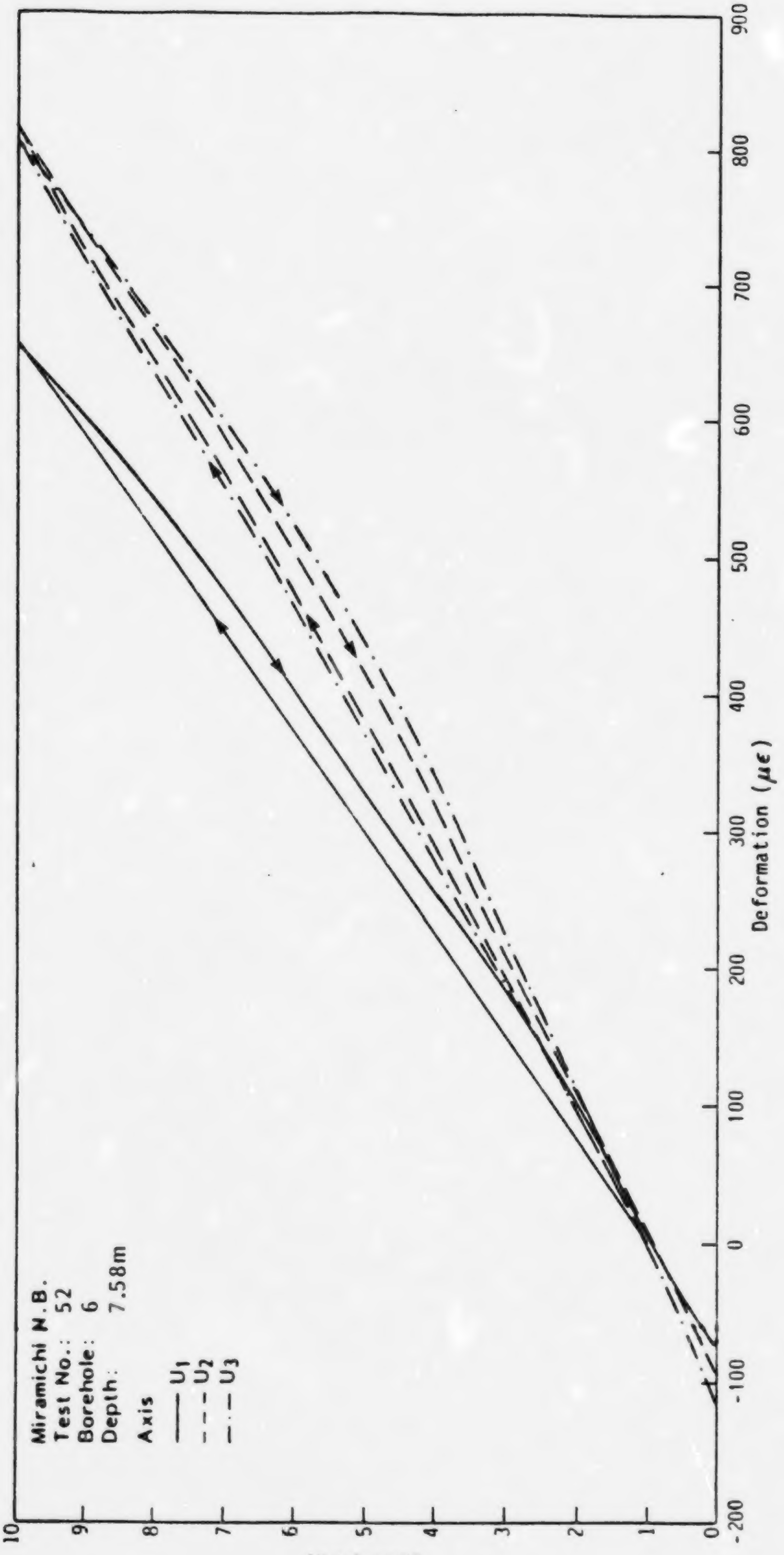
Miramichi N.B.
Test No.: 52
Borehole: 6
Depth: 7.58m
Axis
U$_1$
U$_2$
U$_3$
Load (MPa)
0
1
2
3
4
5
6
7
8
9
10
Deformation ($\mu\epsilon$)
-200
-100
0
100
200
300
400
500
600
700
800
900

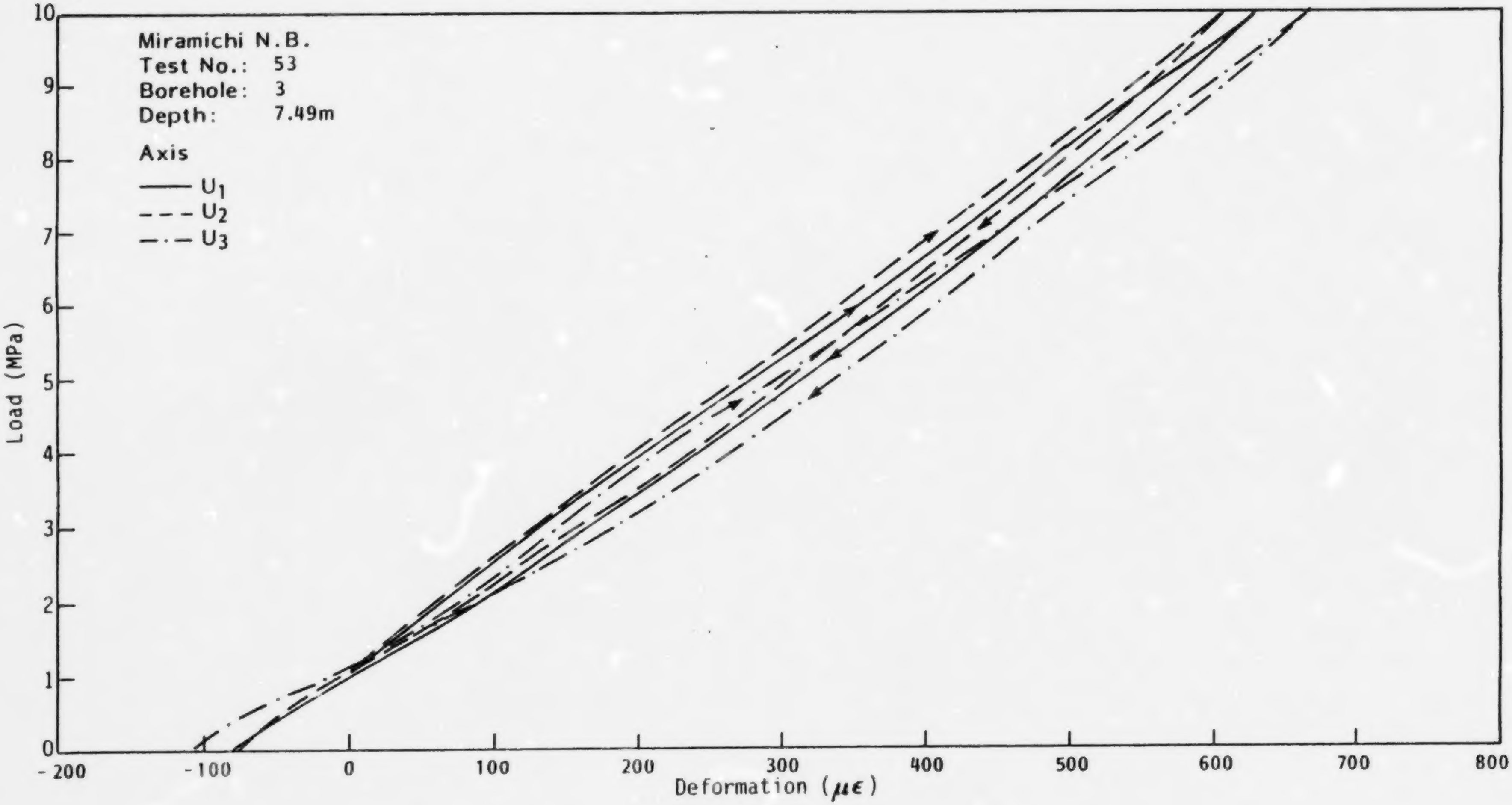
Miramichi N.B.
Test No.: 53
Borehole: 3
Depth: 7.49m
Axis
—— U_1
- - - U_2
—·— U_3
Load (MPa)
0
1
2
3
4
5
6
7
8
9
10
-200
-100
0
100
200
300
400
500
600
700
800
Deformation ($\mu\epsilon$)

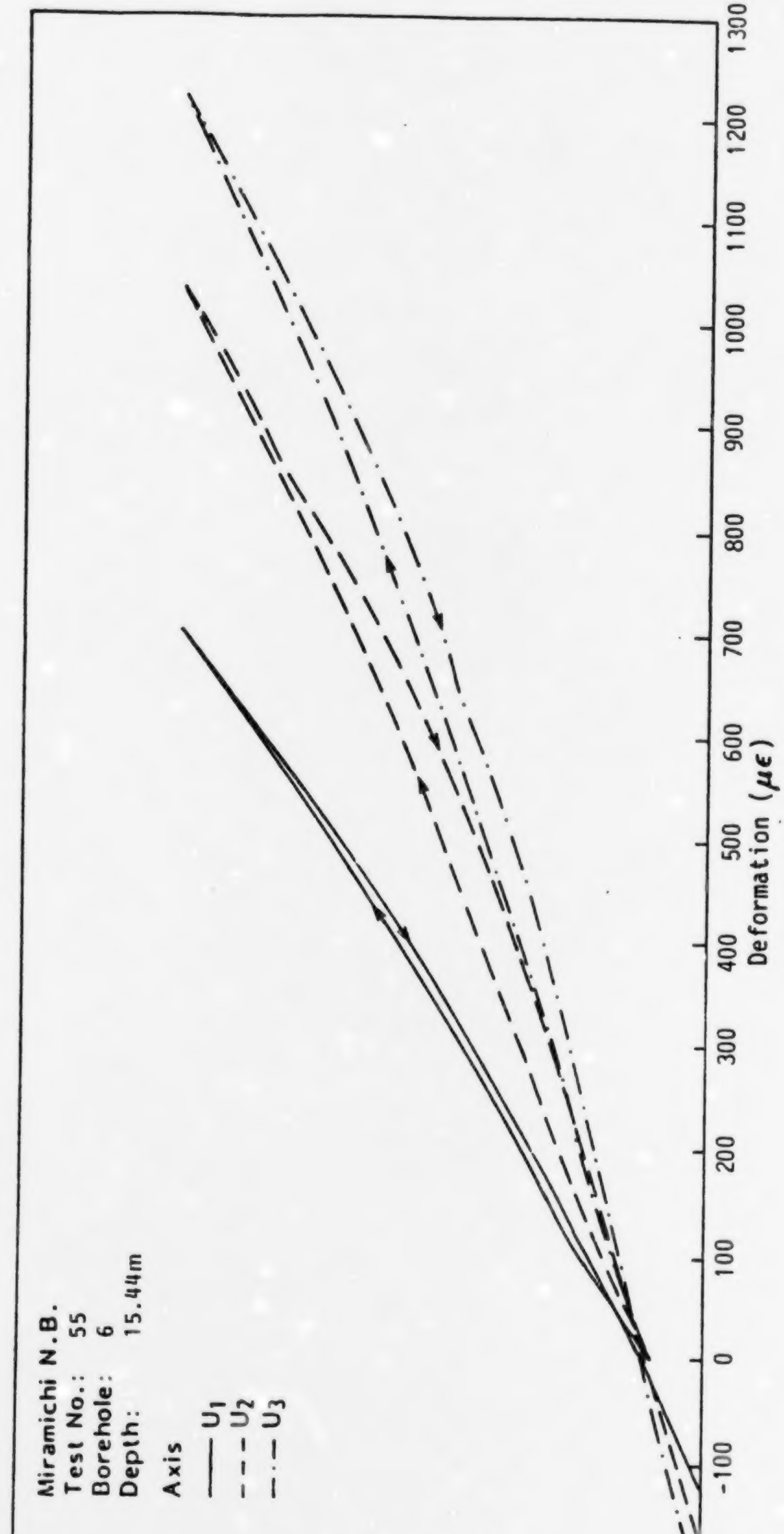
Miramichi N.B.
Test No.: 55
Borehole: 6
Depth: 15.44m
Axis
—— U_1
– – – U_2
–·–·– U_3
Load (MPa)
0
1
2
3
4
5
6
7
8
9
10
11
12
13
Deformation ($\mu\epsilon$)
-200
-100
0
100
200
300
400
500
600
700
800
900
1000
1100
1200
1300

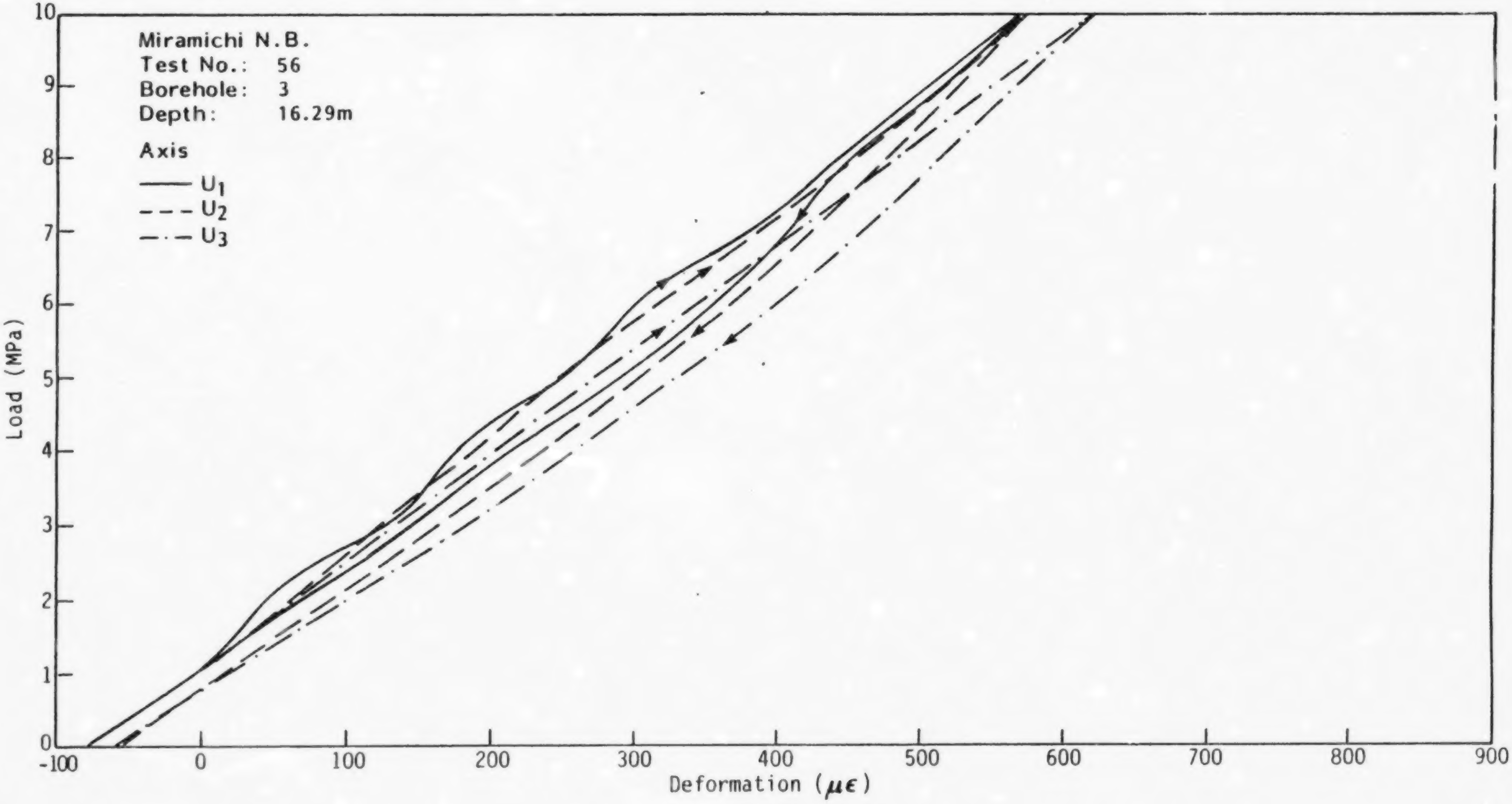
Miramichi N.B.
Test No.: 56
Borehole: 3
Depth: 16.29m
Axis
U1
U2
U3
Load (MPa)
0
1
2
3
4
5
6
7
8
9
10
-100
0
100
200
300
400
500
600
700
800
900
Deformation (με)

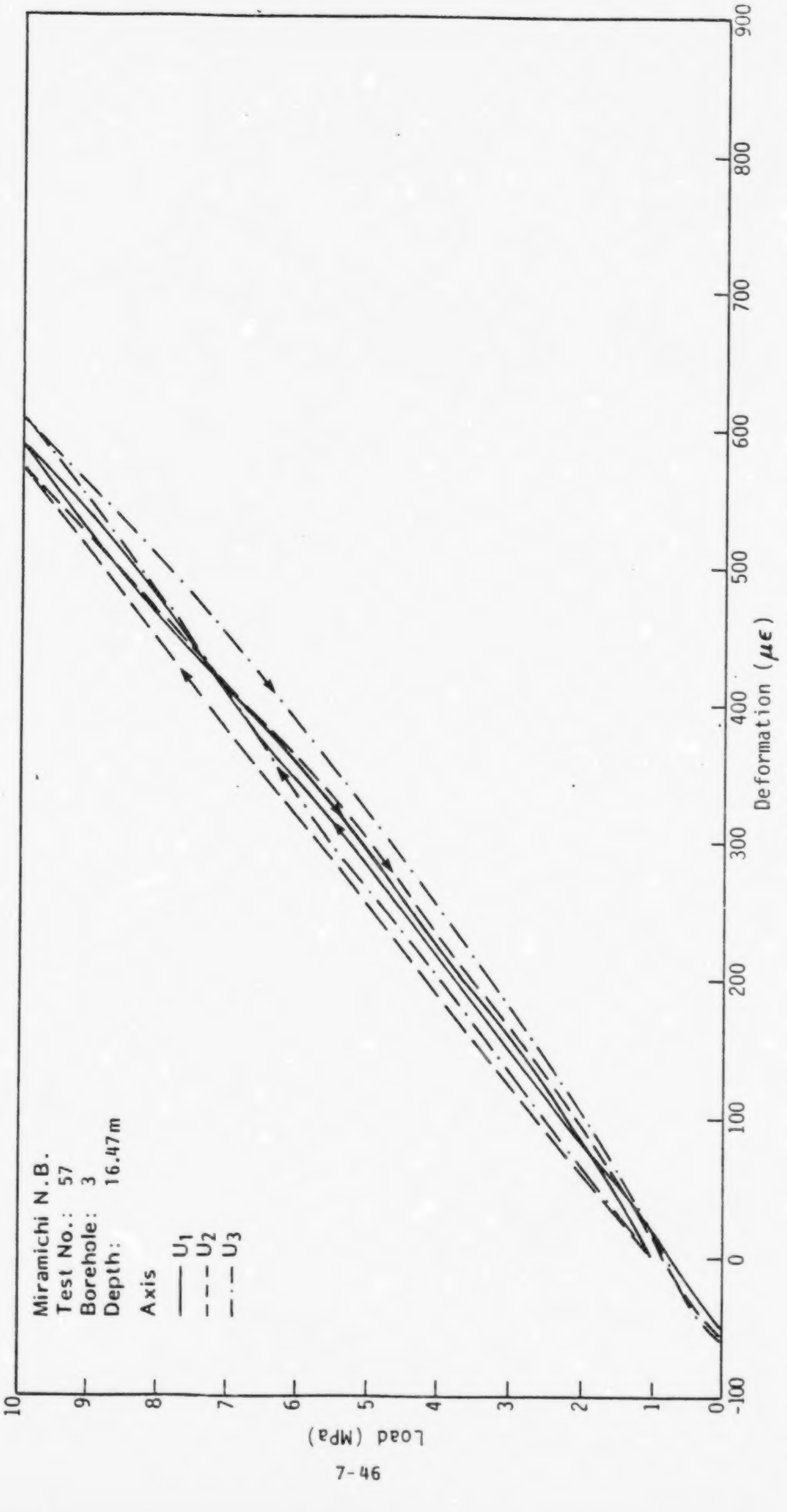
Miramichi N.B.
Test No.: 57
Borehole: 3
Depth: 16.47m
Axis
—— U_1
– – – U_2
–·– U_3
Load (MPa)
0
1
2
3
4
5
6
7
8
9
10
Deformation ($\mu\epsilon$)
-100
0
100
200
300
400
500
600
700
800
900

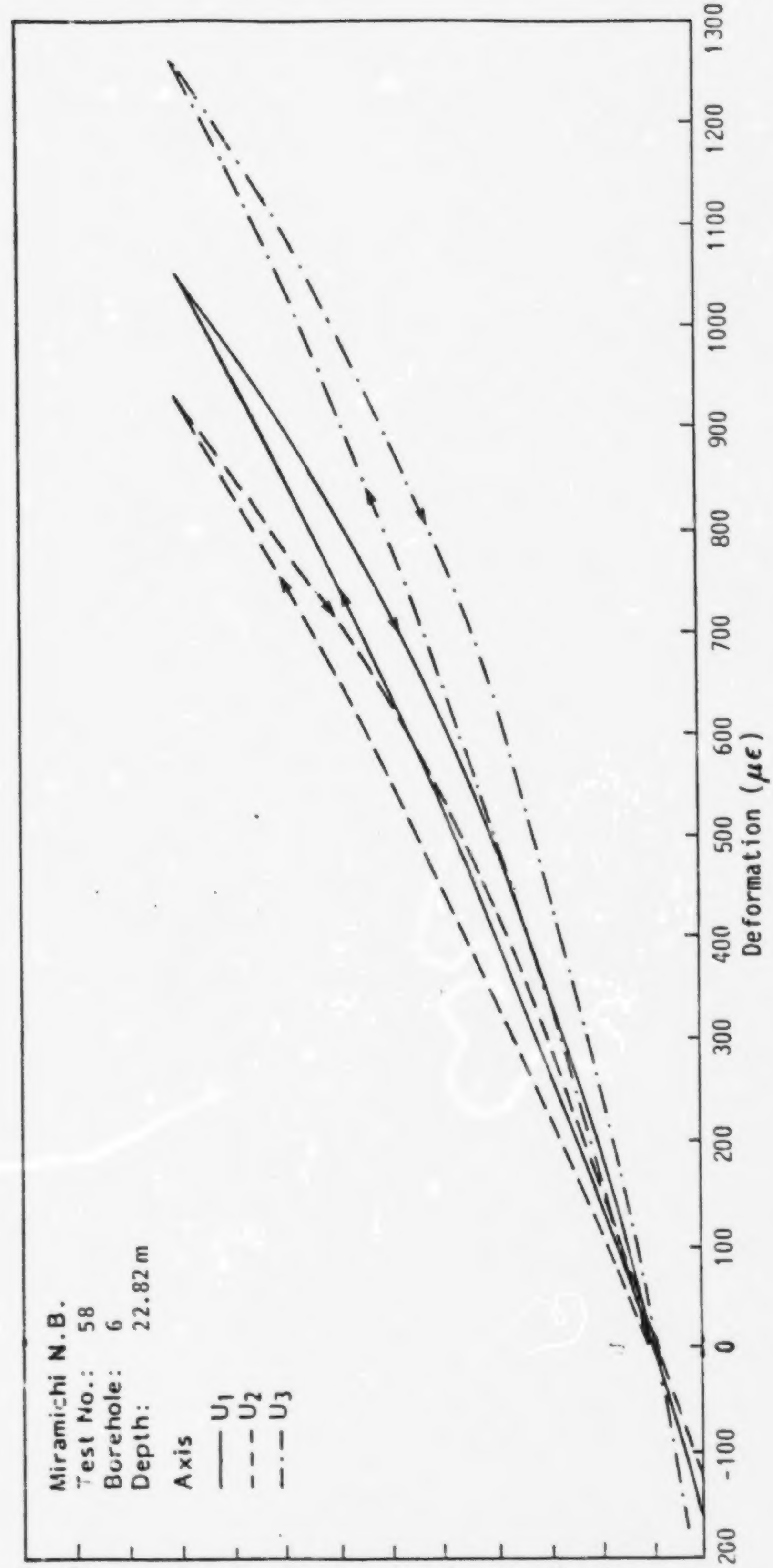
Miramichi N.B.
Test No.: 58
Borehole: 6
Depth: 22.82 m
Axis
—— U_1
– – – U_2
–·–·– U_3
Load (MPa)
0
1
2
3
4
5
6
7
8
9
10
11
12
13
Deformation ($\mu\epsilon$)
-200
-100
0
100
200
300
400
500
600
700
800
900
1000
1100
1200
1300

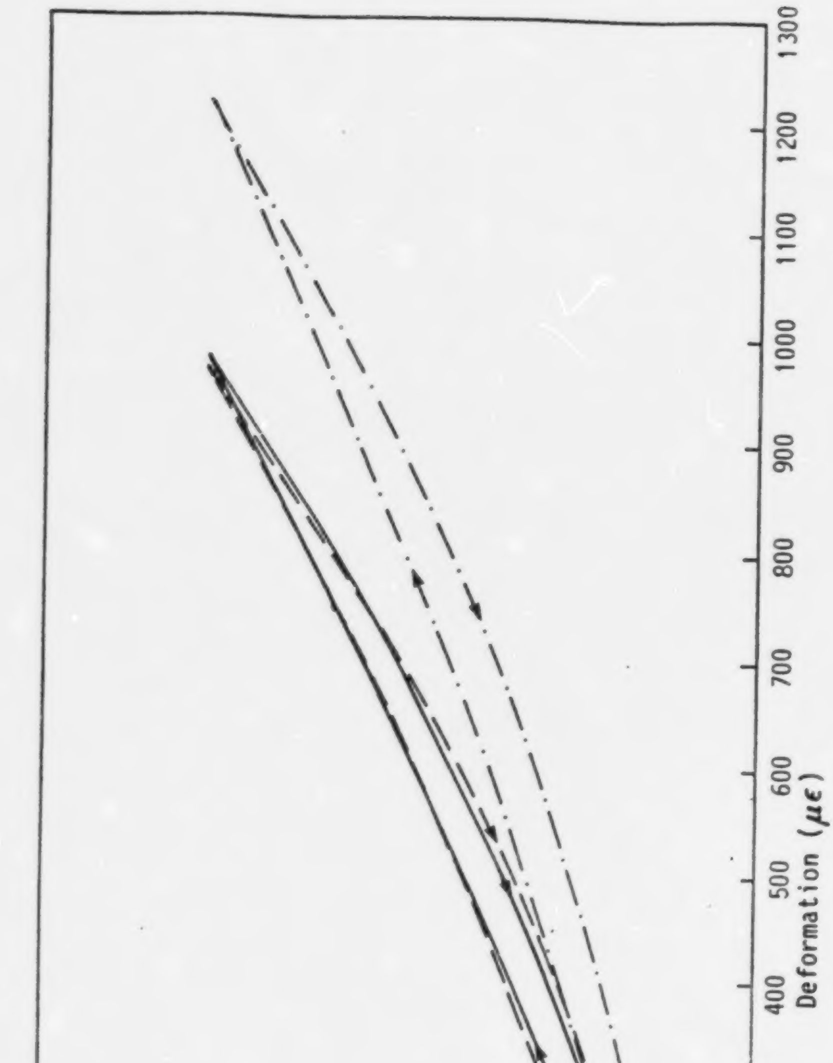
Miramichi N.B.
Test No.: 59
Borehole: 6
Depth: 23.18m
Axis
U1
U2
U3
Load (MPa)
0
1
2
3
4
5
6
7
8
9
10
11
12
13
Deformation (με)
-200
-100
0
100
200
300
400
500
600
700
800
900
1000
1100
1200
1300

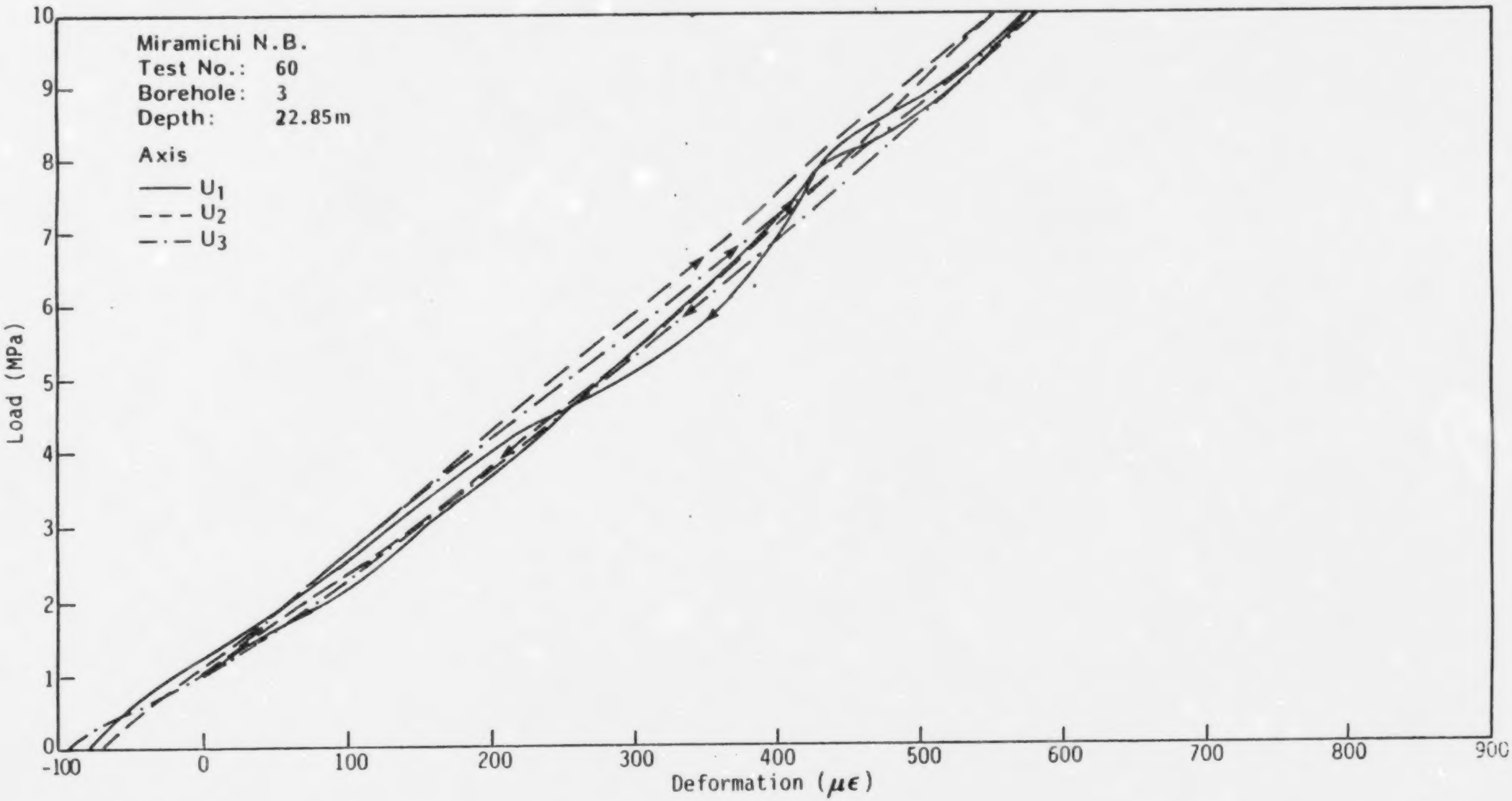
Miramichi N.B.
Test No.: 60
Borehole: 3
Depth: 22.85m
Axis
—— U_1
- - - U_2
-·- U_3
Load (MPa)
0
1
2
3
4
5
6
7
8
9
10
Deformation ($\mu\epsilon$)
-100
0
100
200
300
400
500
600
700
800
900

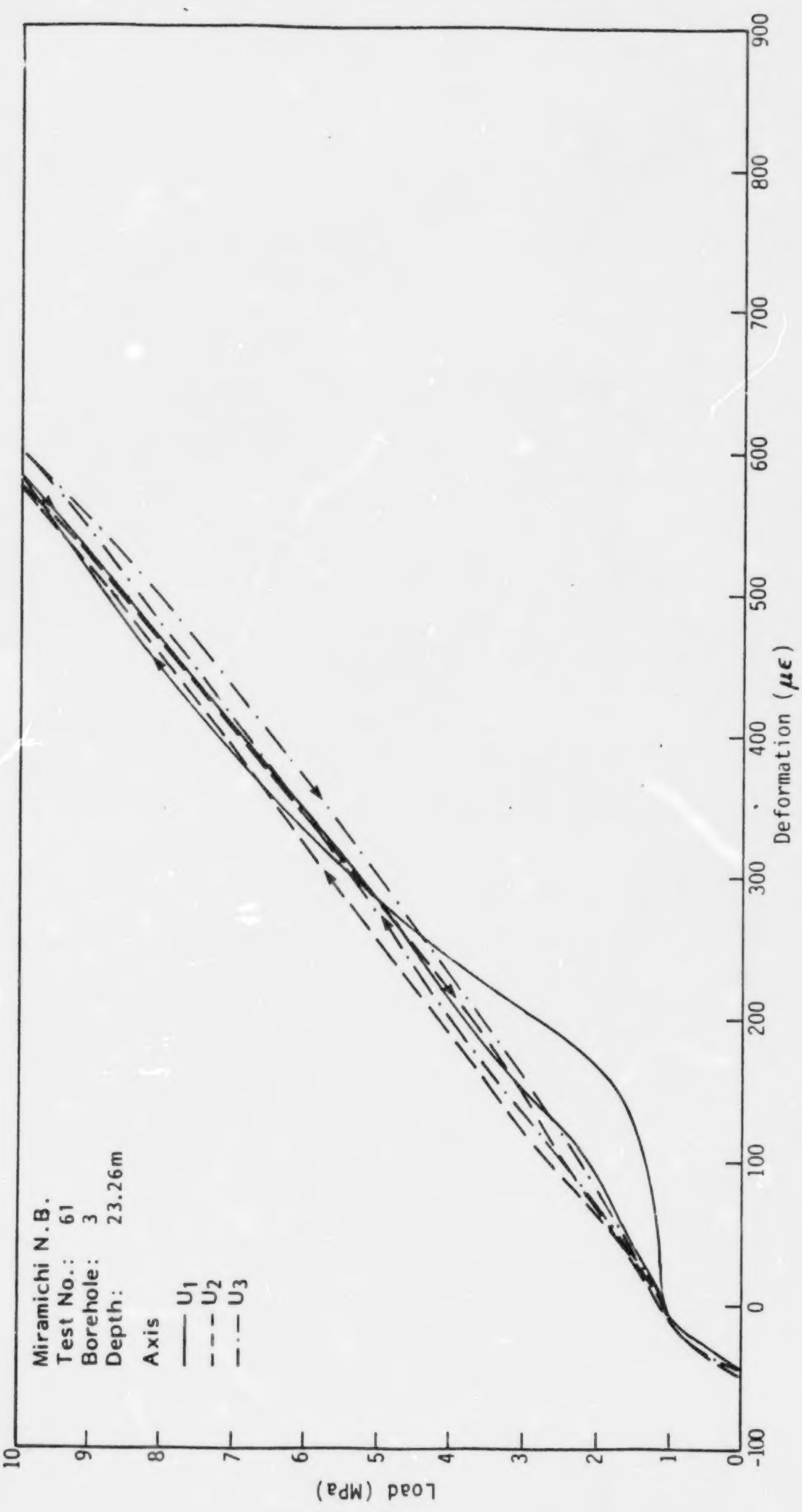
Miramichi N.B.
Test No.: 61
Borehole: 3
Depth: 23.26m
Axis
—— U_1
- - - U_2
-·-·- U_3
Load (MPa)
0
1
2
3
4
5
6
7
8
9
10
Deformation ($\mu\epsilon$)
-100
0
100
200
300
400
500
600
700
800
900

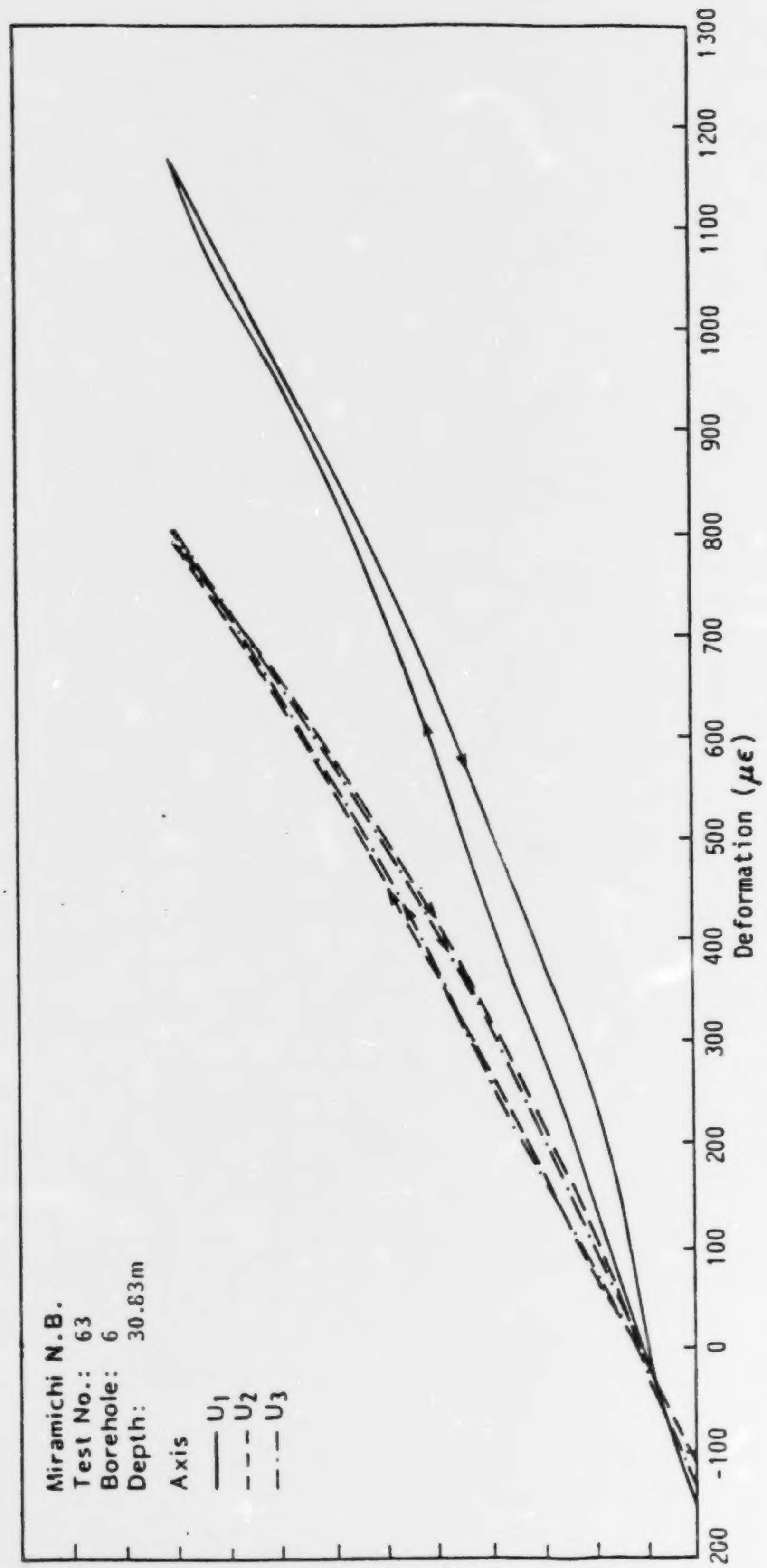
Miramichi N.B.
Test No.: 63
Borehole: 6
Depth: 30.83m
Axis
U_1
U_2
U_3
Load (MPa)
0
1
2
3
4
5
6
7
8
9
10
11
12
13
Deformation ($\mu\epsilon$)
-200
-100
0
100
200
300
400
500
600
700
800
900
1000
1100
1200
1300

APPENDIX 8

ROCKBURST PHOTOGRAPHIC RECORD

Crack Measurements

After the first sequence of rockbursts on the main outcrop occurred on May 20 six locations were chosen for crack measurements in order to determine the rate of crack growth. Only a very rough estimate of this could be made because the only measurement means available was a ruler with gradations of 1.0mm. The measurements do show some change with time. The locations of the measurement points are shown on the main outcrop plan (Figure 20).

The measurements show that there is a detectable change in crack dimensions with time although some of the cracks exhibited closure. This closure may be related to surface thermal effects or actual rock movement. Location 6 is the main pop up on the rock outcrop and it could be seen that it grew slightly after the second series of rockbursts. No measurements were made immediately before the first series of rockbursts and so it is not possible to determine their effect on the main pop up.

Measurements were made on a twice daily basis after the first set of rockbursts but no gradual changes were detected. After the second series of bursts, measurements were rechecked and only the height of the pop up in area 7 had changed. Figures 8-1 to 8-12 show the rock fragmentation due to some of the rockbursts. Figures 8-13 to 8-15 show the two rock pop ups. A bulging of a rock layer was found in area 3 on the main outcrop man (Figure 20) and is shown in Figures 8-16 and 8-17.

CRACK FORMATION TIMES AND WIDTHS ON THE MAIN MIRAMICHI OUTCROP

	Area Number* Location of Crack	Date	Time	Opening Width
Crack .dths in Area #1	1	20/5/84	17:00	6mm
		20/5/84	19:30	15mm
		21/5/84	18:00	15mm
	2	20/5/84	17:00	5mm
		20/5/84	18:30	7mm
		20/5/84	19:30	7mm
		21/5/84	18:00	5mm
	3	20/5/84	17:00	4mm
		20/5/84	18:30	3mm
		20/5/84	19:30	3mm
		21/5/84	18:00	3mm
	Hairline Crack 90° to 3	20/5/84	17:00	1mm
		20/5/84	18:30	1mm
		20/5/84	19:30	1mm
		21/5/84	18:00	1mm
	4	20/5/84	17:00	5mm
		20/5/84	18:30	6mm
		20/5/84	19:30	6mm
		21/5/84	18:00	6mm
	5 (Height of Pop Up)	20/5/84	17:00	50mm
		20/5/84	18:30	40mm
		20/5/84	19:30	40mm
		21/5/84	18:00	42mm
	6 (Height of Pop Up)	20/5/84	17:00	200mm
		20/5/84	18:30	200mm
		20/5/84	19:30	200mm
		21/5/84	18:00	200mm
		26/5/84	17:10	221mm
	7 (Width of Crack at Pop Up Crest)	20/5/84	17:00	7mm
		20/5/84	18:30	7mm
		20/5/84	19:30	7mm
		21/5/84	18:00	8mm
		26/5/84	17:10	7mm

*Refer to Figure 20 in the main report.

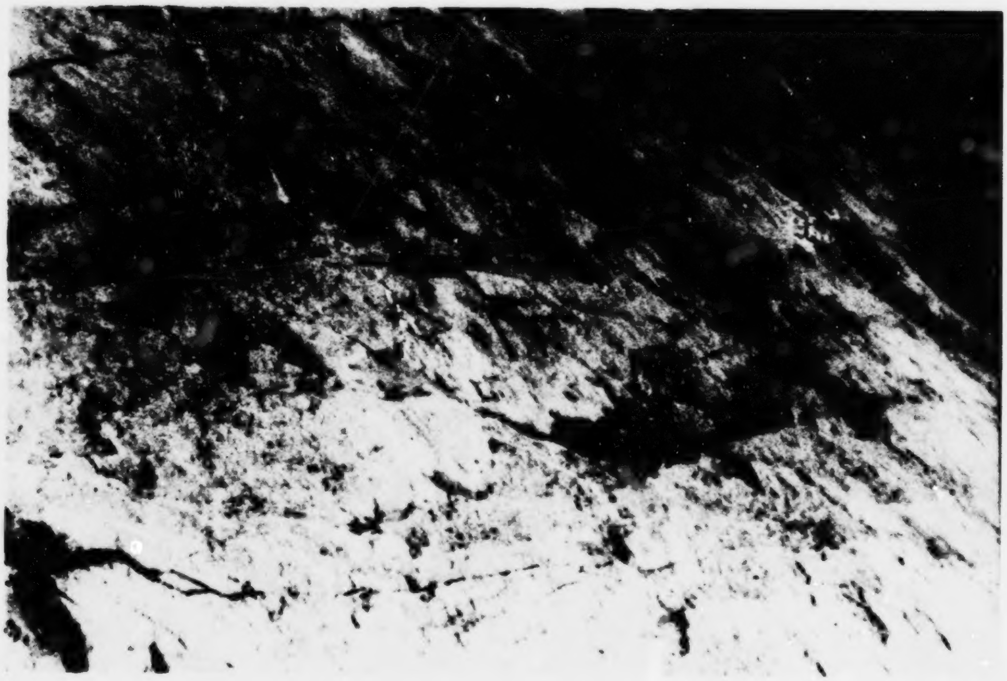

FIGURE 8-1
AREA OF ROCKBURST NOS. 1,4,5 AND 8

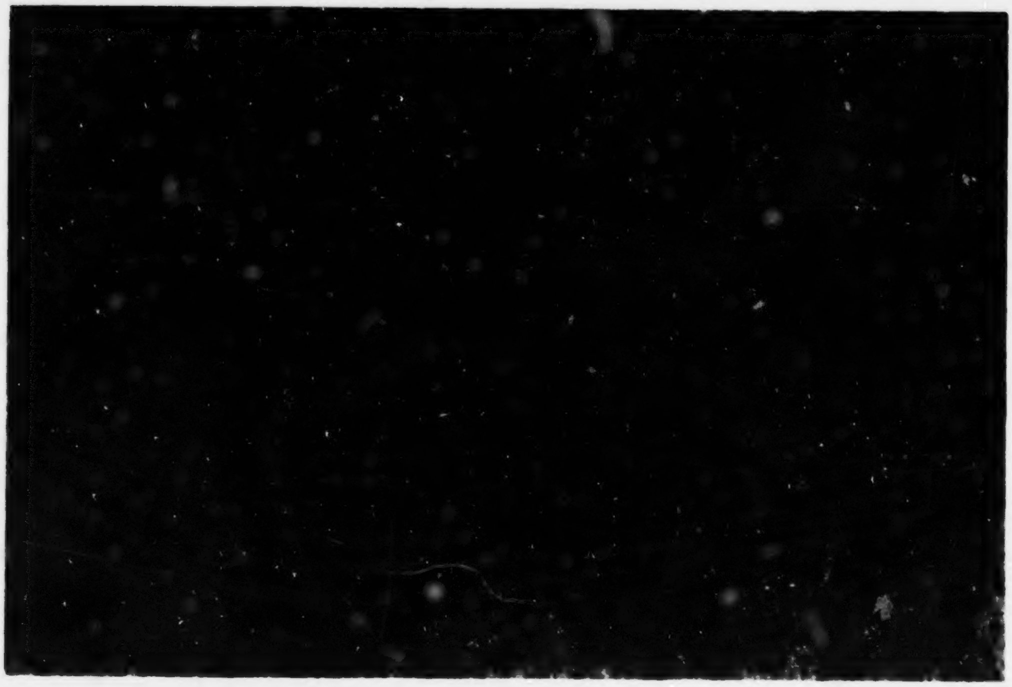

FIGURE 8-2
MAIN FRACTURE IN AREA OF ROCKBURST NOS. 1,4,5 AND 8

FIGURE 8-3

DETAIL OF MAIN FRACTURE IN AREA OF ROCKBURSTS NOS.1,4,5 AND 8 - MEASUREMENT POINT NO.1

FIGURE 8-4

FRACTURES RESULTING FROM ROCKBURST NO.2

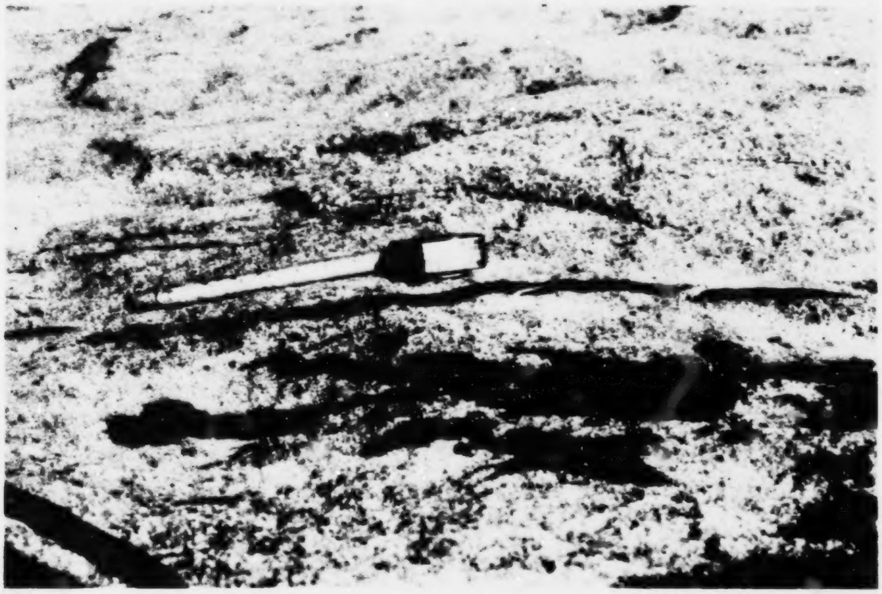

FIGURE 8-5
CLOSEUP OF ROCKBURST NO.2 FRACTURE

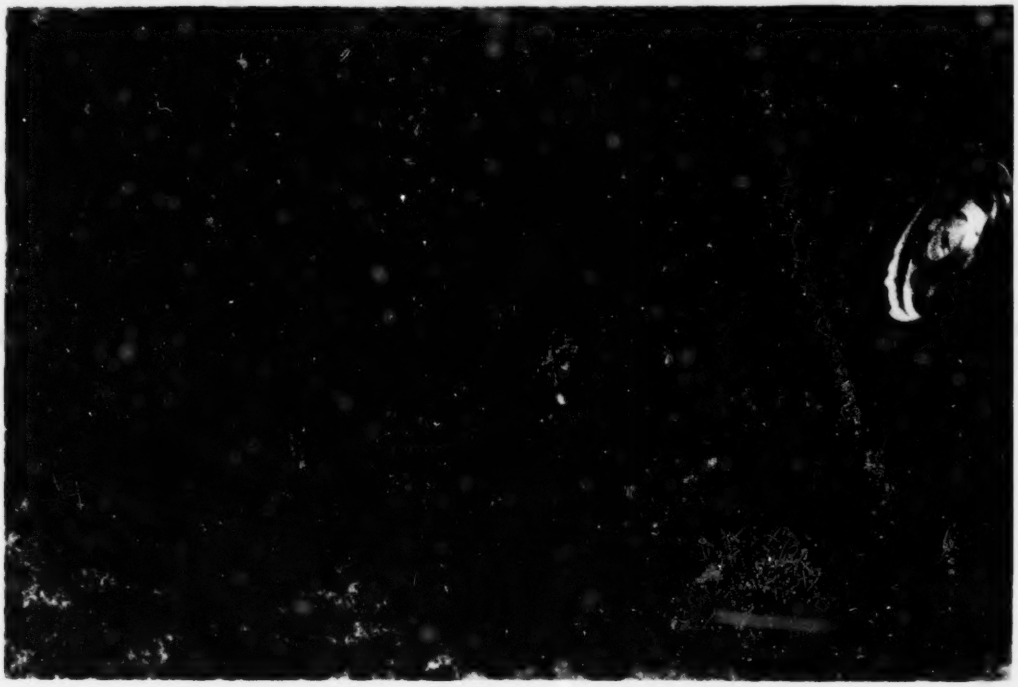

FIGURE 8-6
ROCKBURST NO.3

FIGURE 8-7

ROCKBURSTS NOS.4 AND 8
NOTE: DATE INDICATES DATE OF PHOTOGRAPH

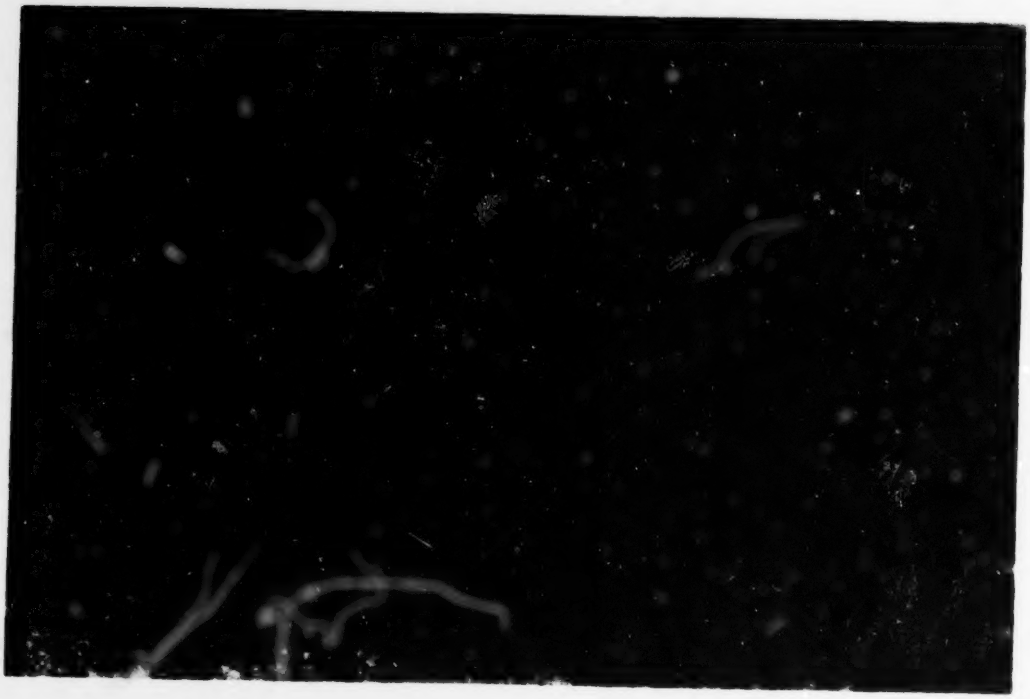

FIGURE 8-8

ROCKBURST NO.6

FIGURE 8-9
DETAIL OF ROCKBURST NO.6

FIGURE 8-10
DETAIL OF ROCKBURST NO.6

FIGURE 8-11
ROCKBURST NO.7

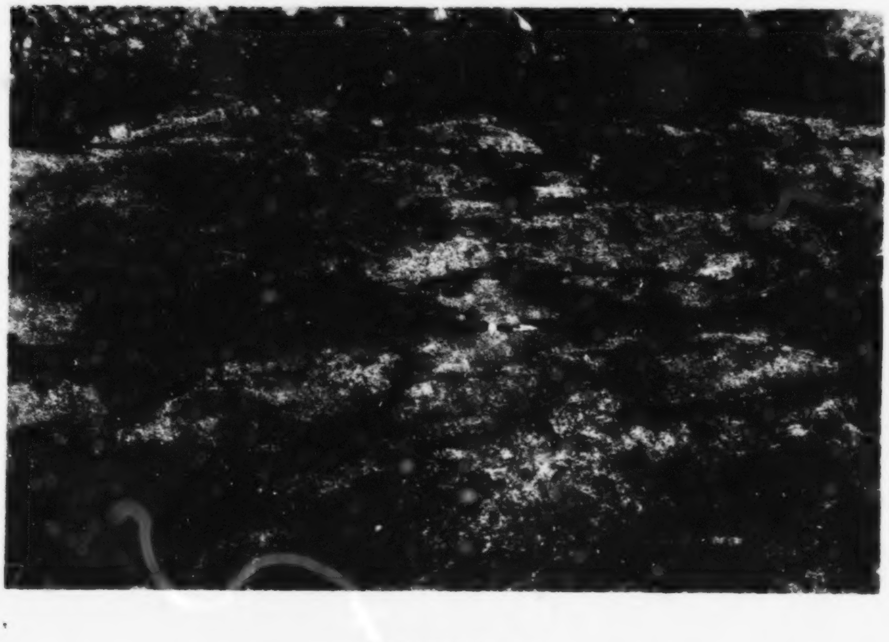

FIGURE 8-12
ROCKBURST NO.9

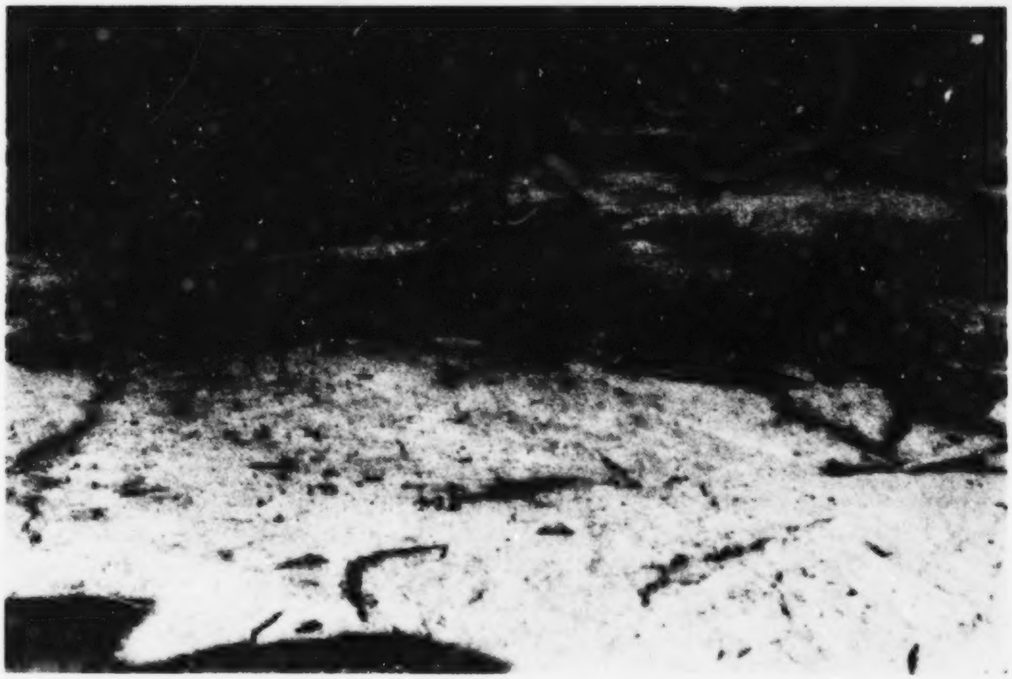

FIGURE 8-13
POP UP AREA 7

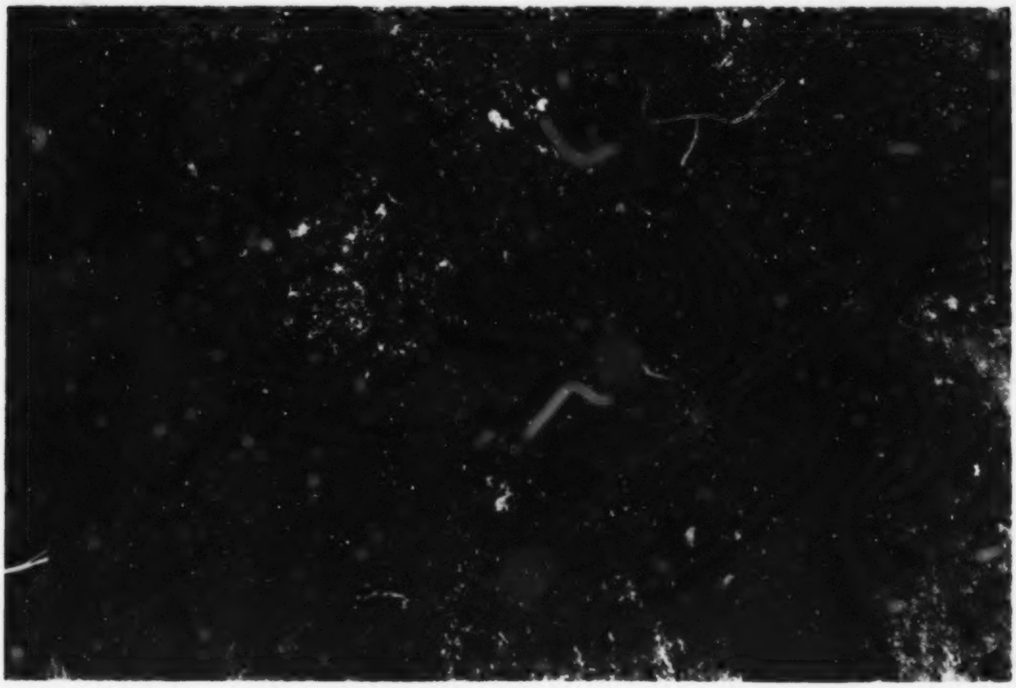

FIGURE 8-14
POP UP AREA 7

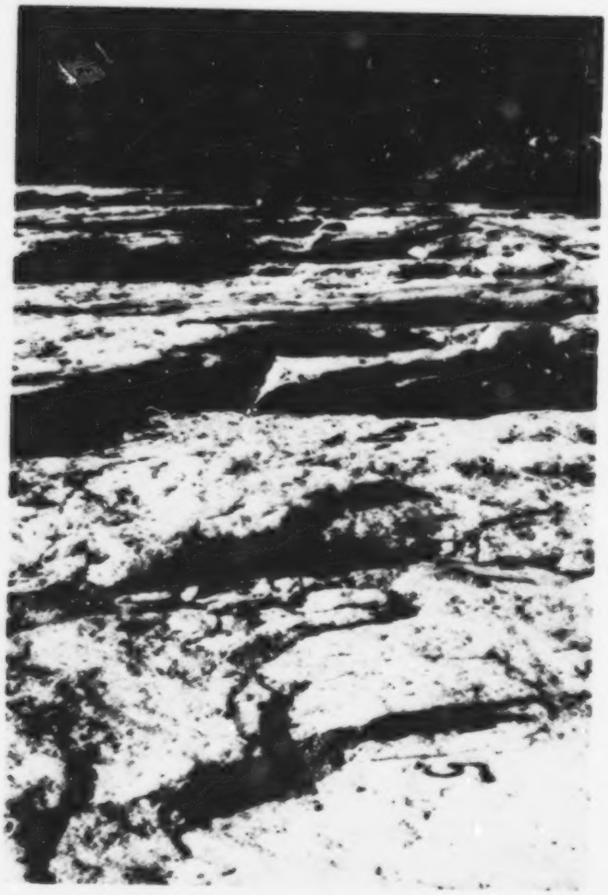

FIGURE 8-15
ROCK POP UP AREAS

FIGURE 8-16
ROCK BULGE AREA 3

FIGURE 8-17
DETAIL OF ROCK BULGE AREA 3

APPENDIX 9

PHOTOGRAPHIC RECORD OF CORE FROM INCLINED HOLES

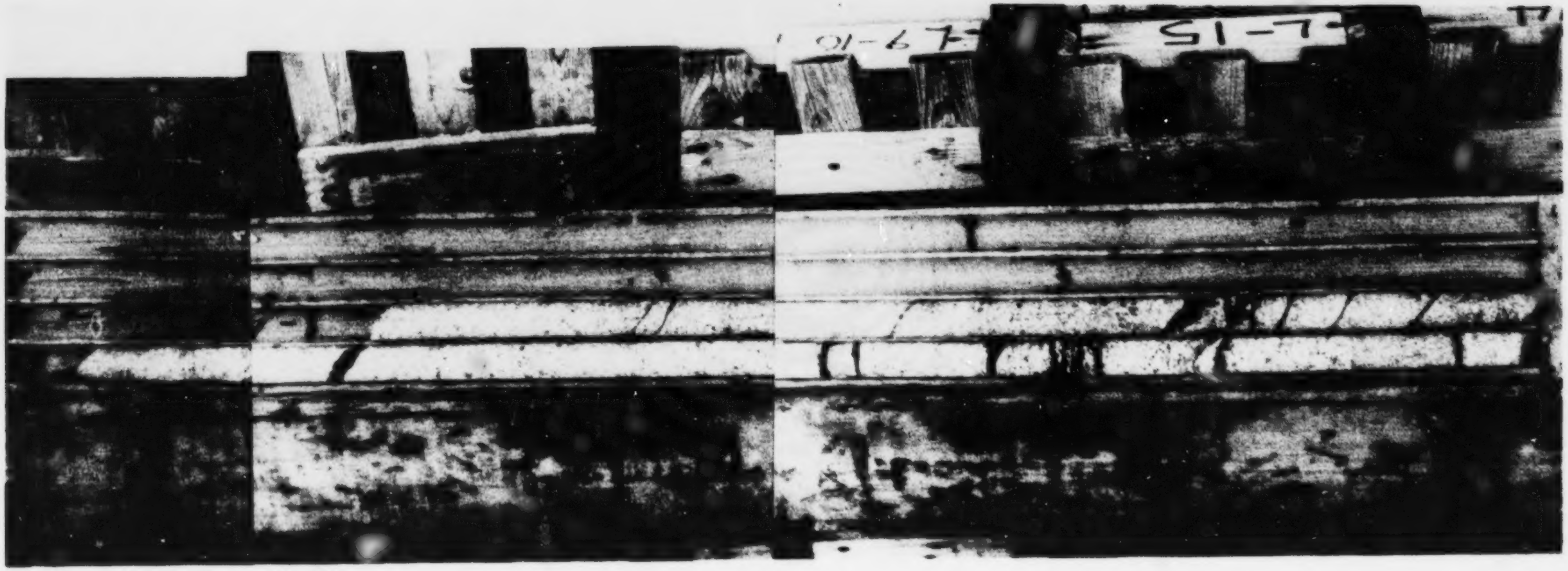

INCLINED HOLE NO. 1
(45° PLUNGE)

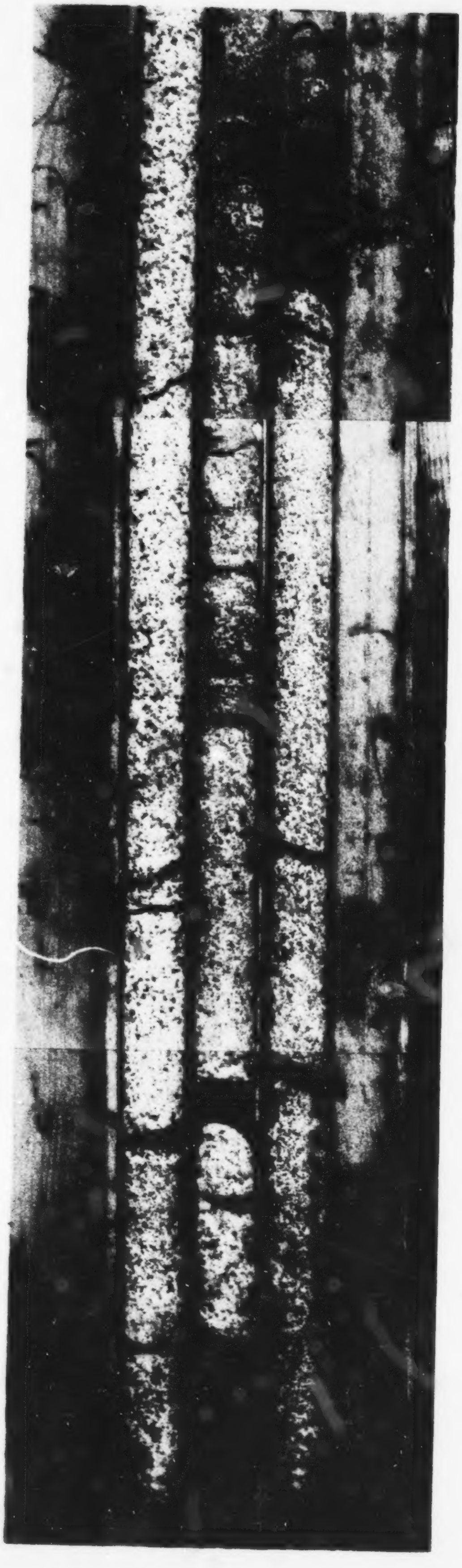

INCLINED HOLE NO. 2
(60° PLUNGE)

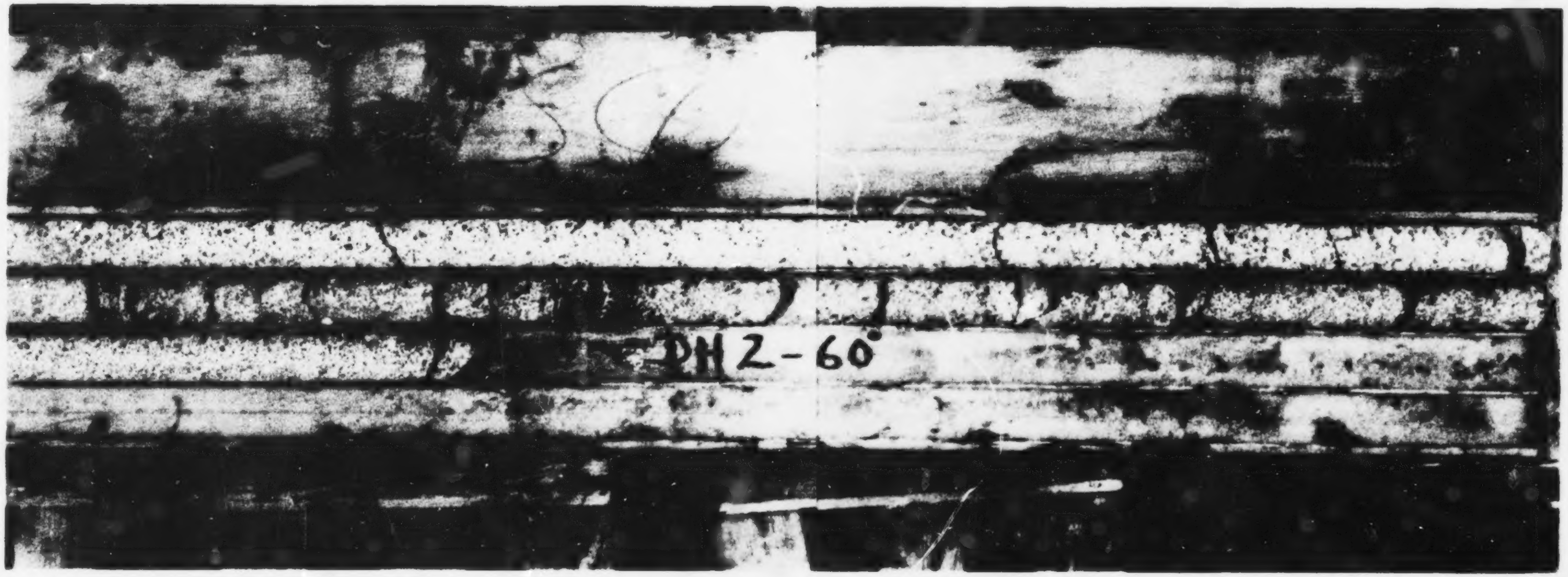

INCLINED HOLE NO. 2
(60° PLUNGE)

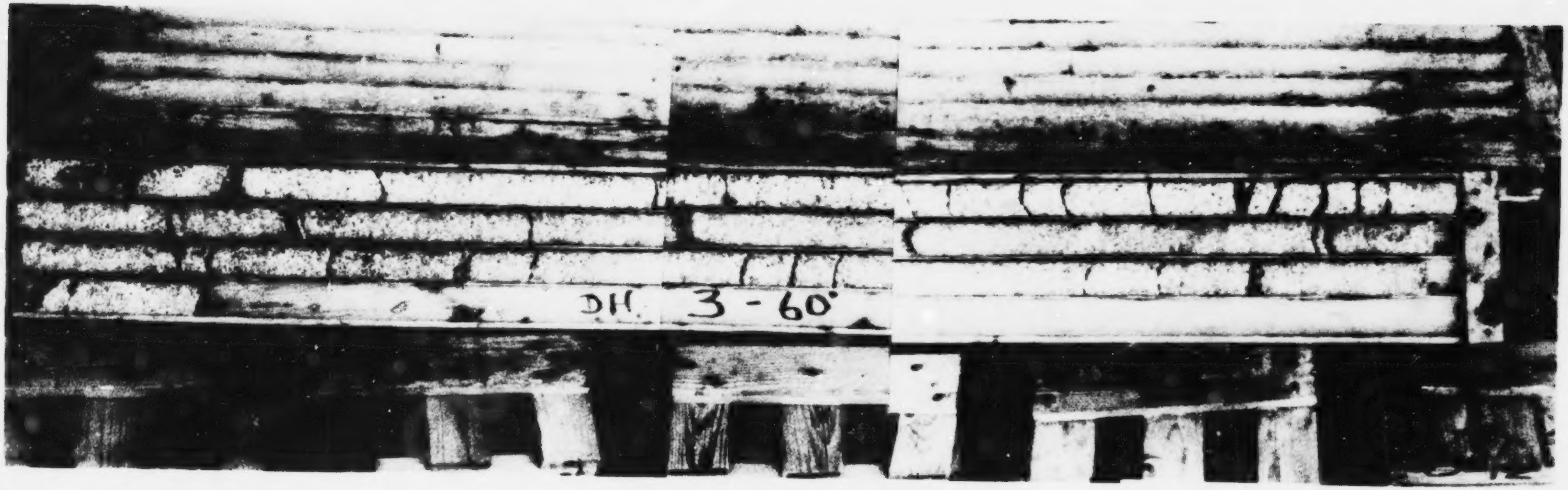

INCLINED HOLE NO. 3
(60° PLUNGE)

APPENDIX 10

BRUNSWICK MINING AND SMELTING BATHURST MINE STRESS DATA

Brunswick Mining and Smelting
Corporation Limited (N.P.L.)
Mining Division
P.O. Box 3000
Bathurst, New Brunswick E2A 3Z8

Tel: 506-546-6671
Twx: 610-243-4478

brunswick mining

[illegible]
[illegible] for NB.

6265-15

1983 12 15

Mr. John Adams
Energy, Mines and Resources Canada
1 Observatory Crescent
Ottawa, ON
K1A 0Y3

Dear Mr. Adams:

I have enclosed a summary of virgin stress measurements conducted in 1979 and 1982-83 at the Brunswick Mining and Smelting No. 12 Mine.

Because of the large amount of testing sites and resulting data (most testing results are considered invalid for various reasons), I have only included the average virgin stress values for three of our major mining horizons -- 1000 m level refers to 1000 meters below headframe elevation.

Basically, strain deformations are measured by overcoring a CSIRO Hollow Inclusion strain gauge, and stress values are back-calculated by assuming host rock properties. Because it is impossible to measure stress directly, average values are probably more applicable to any design criteria, and the principal stress values that I have sent you are the ones we currently use for computer (NFOLD) modelling.

Although I am submitting this information as a representative of Brunswick Mining and Smelting, overcoring results are supplied by Golder Associates, and should be acknowledged.

Sincerely,

Craig W. Pagel

Craig W. Pagel
Rock Mechanics Engineer

:d/79

TABLE 3

Virgin Stress Values at 475, 850 and 1000 m Level

Brunswick Mining & Smelting
#12 Mine

	Major Principal Stress			Intermediate Principal Stress			Minor Principal Stress		
	Magnitude (MPa)	Azimuth	Dip	Magnitude (MPa)	Azimuth	Dip	Magnitude (MPa)	Azimuth	Dip
1000 m	55	303	3	37	33	9	23	196	81
Ratio	2.4			1.6			1		
850 m	41	290	3	35	21	9	24	178	81
Ratio	1.7			1.5			1		
475 m	34	131	11	23	40	1	9	312	79
Ratio	3.8			2.5			1		

APPENDIX 11

GENERATION OF FIGURE 20a

During the in situ rock stress testing program, considerable cracking and spalling of the surface of the Indian Lake outcrop was observed. A levelling survey had been undertaken in 1983 by J. Chandra of New Brunswick Department of Natural Resources. This 5 m grid was relevelled by J. Chandra in 1984 to evaluate whether any vertical motions were observable on the outcrop.

A series of differential elevation values was calculated from the survey data and processed through the following SURFACE II computer analysis. The contours of surface deformation are presented in Figure 20.

```
******  SURFACE GRAPHICS SYSTEM ******                    DATE 04/11/85  TIME 16.45.20     PAGE    1

********** INPUT X-Y-Z DATA POINTS **********

THE NUMBER OF INPUT VARIABLES IS     6

X IS VARIABLE  2
Y IS VARIABLE  3
Z IS VARIABLE  6
IDENT. IS VARIABLE  1
NO VARIABLE SPECIFIED FOR MAP SYMBOL

THE VALUE        99.99000 WILL BE USED AS A CHECK FOR MISSING DATA

FORMAT OF DATA IS (F5.0,2F10.1,3F10.2)

THE NUMBER OF DATA POINTS TO BE READ IS   150

THE X-Y-Z DATA POINTS WILL BE READ FROM FILE  11

NO SUBSET SPECIFIED

******** END OF FILE ENCOUNTERED BEFORE ALL DATA POINTS READ
         ONLY   138 DATA POINTS FOUND ON INPUT FILE

         **************************************************

         THE X-MINIMUM OF X-Y-Z DATA IS          10.00000000
         THE X-MAXIMUM OF X-Y-Z DATA IS         115.00000000

         THE Y-MINIMUM OF X-Y-Z DATA IS             .00000000
         THE Y-MAXIMUM OF X-Y-Z DATA IS           35.00000000

         THE Z-MINIMUM OF X-Y-Z DATA IS           -.01000000
         THE Z-MAXIMUM OF X-Y-Z DATA IS            .10000000

            14 X-Y-Z DATA POINTS WERE FOUND TO HAVE MISSING DATA

           124 X-Y-Z DATA POINTS SAVED

         NO ROTATION OF AXIS
```

```
****** SURFACE GRAPHICS SYSTEM ******              DATE 04/11/85  TIME 16.45.31     PAGE    2

********** ECHO OF X-Y-Z DATA POINTS **********

                                                                                  MAP
SAMPLE  IDENTIFICATION         X              Y                 Z            SYMBOL
-----------------------------------------------------------------------------------------
   1          1.000000     107.300000     16.200000          .000000
   2         13.000000     115.000000     10.000000          .000000
   3         14.000000     115.000000     15.000000          .000000
   4         15.000000     115.000000     20.000000          .000000
   5         16.000000     115.000000     25.000000          .000000
   6         17.000000     115.000000     30.000000          .000000
   7         22.000000     110.000000      5.000000          .000000
   8         23.000000     110.000000     10.000000          .000000
   9         24.000000     110.000000     15.000000          .000000
  10         25.000000     110.000000     20.000000          .020000
  11         26.000000     110.000000     25.000000          .000000
  12         27.000000     110.000000     30.000000          .000000
  13         32.000000     105.000000      5.000000          .000000
  14         33.000000     105.000000     10.000000          .010000
  15         34.000000     105.000000     15.000000          .000000
  16         35.000000     105.000000     20.000000          .010000
  17         36.000000     105.000000     25.000000          .000000
  18         37.000000     105.000000     30.000000          .000000
  19         41.000000     100.000000       .000000          .000000
  20         42.000000     100.000000      5.000000          .000000
  21         43.000000     100.000000     10.000000        -.010000
  22         44.000000     100.000000     15.000000          .000000
  23         45.000000     100.000000     20.000000          .000000
  24         46.000000     100.000000     25.000000          .010000
  25         47.000000     100.000000     30.000000          .000000
  26         52.000000      95.000000      5.000000          .000000
  27         53.000000      95.000000     10.000000          .000000
  28         54.000000      95.000000     15.000000          .000000
  29         55.000000      95.000000     20.000000          .010000
  30         56.000000      95.000000     25.000000          .000000
  31         57.000000      95.000000     30.000000          .000000
  32         62.000000      90.000000      5.000000          .000000
  33         63.000000      90.000000     10.000000        -.010000
  34         64.000000      90.000000     15.000000          .000000
  35         65.000000      90.000000     20.000000          .020000
  36         66.000000      90.000000     25.000000        -.010000
  37         67.000000      90.000000     30.000000          .000000
  38         72.000000      85.000000      5.000000          .010000
  39         73.000000      85.000000     10.000000          .000000
  40         74.000000      85.000000     15.000000          .000000
  41         75.000000      85.000000     20.000000          .010000
  42         76.000000      85.000000     25.000000          .000000
  43         77.000000      85.000000     30.000000          .010000
  44         82.000000      80.000000      5.000000          .010000
  45         83.000000      80.000000     10.000000        -.010000
  46         84.000000      80.000000     15.000000          .000000
  47         85.000000      80.000000     20.000000          .020000
  48         86.000000      80.000000     25.000000          .010000
  49         87.000000      80.000000     30.000000          .010000
  50         92.000000      75.000000      5.000000          .000000
```

```
******  SURFACE GRAPHICS SYSTEM ******                 DATE 04/11/85  TIME 16.45.32     PAGE    3

********** ECHO OF X-Y-Z DATA POINTS **********

                                                                                        MAP
    SAMPLE  IDENTIFICATION          X               Y                Z        SYMBOL
---------------------------------------------------------------------------------------
      51          93.000000     75.000000      10.000000        -.010000
      52          94.000000     75.000000      15.000000         .020000
      53          95.000000     75.000000      20.000000         .000000
      54          96.000000     75.000000      25.000000         .000000
      55          97.000000     75.000000      30.000000         .000000
      56         103.000000     70.000000      10.000000        -.010000
      57         104.000000     70.000000      15.000000         .000000
      58         105.000000     70.000000      20.000000         .010000
      59         106.000000     70.000000      25.000000         .000000
      60         107.000000     70.000000      30.000000         .020000
      61         113.000000     65.000000      10.000000         .000000
      62         114.000000     65.000000      15.000000         .000000
      63         115.000000     65.000000      20.000000         .010000
      64         116.000000     65.000000      25.000000         .010000
      65         117.000000     65.000000      30.000000         .000000
      66         123.000000     60.000000       5.000000         .000000
      67         124.000000     60.000000      10.000000         .010000
      68         125.000000     60.000000      15.000000         .020000
      69         126.000000     60.000000      20.000000         .000000
      70         127.000000     60.000000      25.000000         .000000
      71         133.000000     55.000000      10.000000         .000000
      72         134.000000     55.000000      15.000000         .010000
      73         135.000000     55.000000      20.000000         .020000
      74         136.000000     55.000000      25.000000         .000000
      75         137.000000     55.000000      30.000000         .000000
      76         142.000000     50.000000       5.000000         .000000
      77         143.000000     50.000000      10.000000         .000000
      78         144.000000     50.000000      15.000000         .000000
      79         145.000000     50.000000      20.000000         .010000
      80         146.000000     50.000000      25.000000         .010000
      81         147.000000     50.000000      30.000000         .000000
      82         148.000000     50.000000      35.000000         .000000
      83         153.000000     45.000000      10.000000         .000000
      84         154.000000     45.000000      15.000000         .000000
      85         155.000000     45.000000      20.000000         .000000
      86         156.000000     45.000000      25.000000         .000000
      87         157.000000     45.000000      30.000000        -.010000
      88         163.000000     40.000000      10.000000         .000000
      89         164.000000     40.000000      15.000000         .050000
      90         165.000000     40.000000      20.000000         .010000
      91         166.000000     40.000000      25.000000         .010000
      92         167.000000     40.000000      30.000000         .000000
      93         173.000000     35.000000      10.000000         .020000
      94         174.000000     35.000000      15.000000         .030000
      95         175.000000     35.000000      20.000000         .030000
      96         176.000000     35.000000      25.000000         .010000
      97         177.000000     35.000000      30.000000         .000000
      98         183.000000     30.000000      10.000000         .010000
      99         184.000000     30.000000      15.000000         .010000
     100         185.000000     30.000000      20.000000         .000000
```

```
****** SURFACE GRAPHICS SYSTEM ******                DATE 04/11/85  TIME 16.45.32     PAGE    4

********** ECHO OF X-Y-Z DATA POINTS **********

                                                                              MAP
  SAMPLE  IDENTIFICATION        X              Y                Z            SYMBOL
------------------------------------------------------------------------------------
   101          186.000000     30.000000      25.000000        .010000
   102          187.000000     30.000000      30.000000        .010000
   103          193.000000     25.000000      10.000000        .000000
   104          194.000000     25.000000      15.000000        .030000
   105          195.000000     25.000000      20.000000        .010000
   106          196.000000     25.000000      25.000000        .010000
   107          197.000000     25.000000      30.000000        .010000
   108          203.000000     20.000000      10.000000        .000000
   109          204.000000     20.000000      15.000000        .020000
   110          205.000000     20.000000      20.000000       -.010000
   111          206.000000     20.000000      25.000000        .020000
   112          207.000000     20.000000      30.000000        .010000
   113          208.000000     20.000000      35.000000        .000000
   114          213.000000     15.000000      10.000000        .010000
   115          214.000000     15.000000      15.000000        .010000
   116          215.000000     15.000000      20.000000        .020000
   117          216.000000     15.000000      25.000000        .030000
   118          217.000000     15.000000      30.000000        .010000
   119          218.000000     15.000000      35.000000        .000000
   120          223.000000     10.000000      10.000000        .010000
   121          224.000000     10.000000      15.000000        .100000
   122          225.000000     10.000000      20.000000        .020000
   123          226.000000     10.000000      25.000000        .030000
   124          227.000000     10.000000      30.000000        .020000
```

```
****** SURFACE GRAPHICS SYSTEM ******                      DATE 04/11/85  TIME 16.45.32     PAGE    5

****** READ A SET OF OUTLINES ******

THE OUTLINES WILL BE READ FROM FILE  13

NUMBER OF OUTLINES IS      1

INPUT FORMAT IS (2F5.1)

OUTLINE    1 -- NUMBER OF POINTS IN OUTLINE IS     7  -- CODE =     1

THE X-MINIMUM OF OUTLINES IS            .00000000
THE X-MAXIMUM OF OUTLINES IS         115.00000000

THE Y-MINIMUM OF OUTLINES IS            .00000000
THE Y-MAXIMUM OF OUTLINES IS          35.00000000

****** ECHO OF OUTLINES ******

OUTLINE   1         CODE =   1

 (   1)     115.0000       .0000    (   2)     115.0000     35.0000    (   3)        .0000     35.0000
 (   4)        .0000      5.0000    (   5)      80.0000      5.0000    (   6)      80.0000       .0000
 (   7)     115.0000       .0000
```

```
****** SURFACE GRAPHICS SYSTEM ******                DATE 04/11/85  TIME 16.45.36     PAGE    6

********** GRID GENERATION **********

NUMBER OF X-Y-Z DATA POINTS IS   124

THE X-MINIMUM OF X-Y-Z DATA IS          10.00000000
THE X-MAXIMUM OF X-Y-Z DATA IS         115.00000000

THE Y-MINIMUM OF X-Y-Z DATA IS            .00000000
THE Y-MAXIMUM OF X-Y-Z DATA IS          35.00000000

THE Z-MINIMUM OF X-Y-Z DATA IS          -.01000000
THE Z-MAXIMUM OF X-Y-Z DATA IS           .10000000

NO X-Y-Z DATA POINTS FOUND OUTSIDE EXTREMES OF GRID MATRIX

***** GRID MATRIX PARAMETERS *****

THE X-VALUE AT LEFT   EDGE OF GRID MATRIX IS          -5.00000000
THE X-VALUE AT RIGHT  EDGE OF GRID MATRIX IS         120.00000000

THE Y-VALUE AT BOTTOM EDGE OF GRID MATRIX IS          -5.00000000
THE Y-VALUE AT TOP    EDGE OF GRID MATRIX IS          40.00000000

THE GRID MATRIX WILL HAVE  126 COLUMNS AND   46 ROWS

THE DISTANCE BETWEEN COLUMNS IS              1.00000
THE DISTANCE BETWEEN ROWS IS                 1.00000

SAMPLE DATA POINTS WILL BE RETAINED

DUPLICATE DATA POINTS WILL BE AVERAGED

NO DUPLICATE DATA POINTS FOUND

  124 X-Y-Z DATA POINTS WILL BE USED TO CALCULATE THE GRID MATRIX

THE GRID NODES WILL BE CALCULATED USING A WEIGHTED PROJECTION OF THE NEAREST DATA POINTS

SCALED INVERSE DISTANCE SQUARED WILL BE USED FOR THE WEIGHTING FUNCTION
```

```
****** SURFACE GRAPHICS SYSTEM ******                DATE 04/11/85  TIME 16.45.53     PAGE    7

****** SEARCH METHOD FOR PHASE 1 OF GRID ******

****** QUADRANT SEARCH ******

MAXIMUM NUMBER OF POINTS PER QUADRANT IS   2

MAXIMUM DISTANCE TO NEAREST SAMPLE DATA POINT IS          15.19971585

MAXIMUM SEARCH RADIUS IS          24.03286076

NUMBER OF QUADRANTS THAT MUST HAVE AT LEAST ONE DATA POINT IS   2

ORIENTATION OF QUADRANTS TO THE X-Y AXIS IS      .00 DEGREES

****** SEARCH METHOD FOR PHASE 2 OF GRID ******

****** QUADRANT SEARCH ******

MAXIMUM NUMBER OF POINTS PER QUADRANT IS   2

MAXIMUM DISTANCE TO NEAREST SAMPLE DATA POINT IS          15.19971585

MAXIMUM SEARCH RADIUS IS          24.03286076

NUMBER OF QUADRANTS THAT MUST HAVE AT LEAST ONE DATA POINT IS   2

ORIENTATION OF QUADRANTS TO THE X-Y AXIS IS      .00 DEGREES
```

```
****** SURFACE GRAPHICS SYSTEM ******            DATE 04/11/35  TIME 16.45.53     PAGE    8

******** REGIONAL LINEAR TREND ********

STATISTICAL ANALYSIS

SUM OF SQUARES TOTAL ******              .021039

SUM OF SQUARES REGRESSION *              .003320

SUM OF SQUARES DEVIATION **              .017718

MEAN SQUARES REGRESSION ***              .001660

MEAN SQUARES DEVIATION ****              .000146

GOODNESS OF FIT ***********              .157816

MULTIPLE CORRELATION ******              .397261

F TEST ********************            11.337075

FIRST DEGREE OF FREEDOM ***                    2

SECOND DEGREE OF FREEDOM **                  121


******** SOLUTION TO EQUATION ********

             .017757            -.000164            -.000043
```

```
****** SURFACE GRAPHICS SYSTEM ******                DATE 04/11/85  TIME 16.47.34     PAGE    9

********** ERROR ANALYSIS **********

THE NUMBER OF X-Y-Z DATA POINTS IS   124

THE X-MINIMUM OF THE X-Y-Z DATA POINTS IS          10.00000000
THE X-MAXIMUM OF THE X-Y-Z DATA POINTS IS         115.00000000

THE Y-MINIMUM OF THE X-Y-Z DATA POINTS IS            .00000000
THE Y-MAXIMUM OF THE X-Y-Z DATA POINTS IS          35.00000000

THE Z-MINIMUM OF THE X-Y-Z DATA POINTS IS           -.01000000
THE Z-MAXIMUM OF THE X-Y-Z DATA POINTS IS            .10000000

THE X-VALUE AT LEFT   EDGE OF GRID MATRIX IS          -5.00000000
THE X-VALUE AT RIGHT  EDGE OF GRID MATRIX IS         120.00000000

THE Y-VALUE AT BOTTOM EDGE OF GRID MATRIX IS          -5.00000000
THE Y-VALUE AT TOP    EDGE OF GRID MATRIX IS          40.00000000

THE Z-MINIMUM OF GRID MATRIX IS           -.01431774
THE Z-MAXIMUM OF GRID MATRIX IS            .10000000

THE GRID MATRIX HAS  126 COLUMNS AND   46 ROWS

THE GRID MATRIX HAS   449 MISSING VALUES

THE ERROR AT EACH X-Y-Z DATA POINT WILL BE PRINTED

THE CLASS INTERVAL WIDTH FOR THE HISTOGRAM IS            .00002000
```

```
****** SURFACE GRAPHICS SYSTEM ******              DATE 04/11/85  TIME 16.47.45     PAGE   10

********** ERROR ANALYSIS **********

STATISTIC                          ERROR        ABSOLUTE ERROR
--------------------------------------------------------------

MAXIMUM NEGATIVE ERROR            -.00018

MAXIMUM POSITIVE ERROR             .00000

MEAN ERROR                        -.00000             .00000

ROOT MEAN SQUARED ERROR            .00002             .00002

STANDARD DEVIATION                 .00002             .00002

VARIANCE                           .00000             .00000

PERCENT RELATIVE ERROR             .00016             .00016

SKEWNESS                        -10.90911           10.90911

KURTOSIS                        120.00830          120.00830

SUM OF SQUARES ERROR               .00000             .00000
--------------------------------------------------------------

NUMBER OF SAMPLES   122

SUM OF SQUARES Z          .02098
```

```
****** SURFACE GRAPHICS SYSTEM ******               DATE 04/11/85  TIME 16.47.45    PAGE  11
STATISTICS OF HISTOGRAM
NUMBER OF SAMPLES ****                    122
MINIMUM VALUE ********              -.00018427
MAXIMUM VALUE ********               .00000000
MEAN OF SAMPLES ******              -.00000151
STANDARD DEVIATION ***               .00001661
VARIANCE *************               .00000000
SKEWNESS *************            -10.90910506
KURTOSIS *************            120.00830460
CLASS INTERVAL WIDTH *               .00002000
******************************************************************************************
                         ***** HISTOGRAM FREQUENCY TABLE *****
CLASS            CLASS LIMITS              STD. CLASS LIMITS          COUNT        PERCENT
------------------------------------------------------------------------------------------
 -12       -.0002 TO    -.0002        -15.0468 TO   -13.8431            0              0
 -11       -.0002 TO    -.0002        -13.8431 TO   -12.6394            0              0
 -10       -.0002 TO    -.0002        -12.6394 TO   -11.4356            0              0
  -9       -.0002 TO    -.0002        -11.4356 TO   -10.2319            1              0
  -8       -.0002 TO    -.0001        -10.2319 TO    -9.0281            0              0
  -7       -.0001 TO    -.0001         -9.0281 TO    -7.8244            0              0
  -6       -.0001 TO    -.0001         -7.8244 TO    -6.6206            0              0
  -5       -.0001 TO    -.0001         -6.6206 TO    -5.4169            0              0
  -4       -.0001 TO    -.0001         -5.4169 TO    -4.2131            0              0
  -3       -.0001 TO    -.0000         -4.2131 TO    -3.0094            0              0
  -2       -.0000 TO    -.0000         -3.0094 TO    -1.8056            0              0
  -1       -.0000 TO    -.0000         -1.8056 TO     -.6019            0              0
   0       -.0000 TO     .0000          -.6019 TO      .6019          121             99
   1        .0000 TO     .0000           .6019 TO     1.8056            0              0
   2        .0000 TO     .0000          1.8056 TO     3.0094            0              0
   3        .0000 TO     .0001          3.0094 TO     4.2131            0              0
   4        .0001 TO     .0001          4.2131 TO     5.4169            0              0
   5        .0001 TO     .0001          5.4169 TO     6.6206            0              0
   6        .0001 TO     .0001          6.6206 TO     7.8244            0              0
   7        .0001 TO     .0001          7.8244 TO     9.0281            0              0
   8        .0001 TO     .0002          9.0281 TO    10.2319            0              0
   9        .0002 TO     .0002         10.2319 TO    11.4356            0              0
  10        .0002 TO     .0002         11.4356 TO    12.6394            0              0
  11        .0002 TO     .0002         12.6394 TO    13.8431            0              0
  12        .0002 TO     .0002         13.8431 TO    15.0468            0              0
```

```
        ****** SURFACE GRAPHICS SYSTEM ******               DATE 04/11/85  TIME 16.47.45     PAGE   12
                                           ***** HISTOGRAM OF ERROR DISTRIBUTION *****

            +-----------------------------------------------------------------------------------------------------+
156 TO  159 I                                                                                                     I
152 TO  155 I                                                                                                     I
148 TO  151 I                                                                                                     I
144 TO  147 I                                                                                                     I
140 TO  143 I                                                                                                     I
136 TO  139 I                                                                                                     I
132 TO  135 I                                                                                                     I
128 TO  131 I                                                                                                     I
124 TO  127 I                                                                                                     I
120 TO  123 I                                                 XXX                                                 I
116 TO  119 I                                                 XXX                                                 I
112 TO  115 I                                                 XXX                                                 I
108 TO  111 I                                                 XXX                                                 I
104 TO  107 I                                                 XXX                                                 I
100 TO  103 I                                                 XXX                                                 I
 96 TO   99 I                                                 XXX                                                 I
 92 TO   95 I                                                 XXX                                                 I
 88 TO   91 I                                                 XXX                                                 I
 84 TO   87 I                                                 XXX                                                 I
 80 TO   83 I                                                 XXX                                                 I
 76 TO   79 I                                                 XXX                                                 I
 72 TO   75 I                                                 XXX                                                 I
 68 TO   71 I                                                 XXX                                                 I
 64 TO   67 I                                                 XXX                                                 I
 60 TO   63 I                                                 XXX                                                 I
 56 TO   59 I                                                 XXX                                                 I
 52 TO   55 I                                                 XXX                                                 I
 48 TO   51 I                                                 XXX                                                 I
 44 TO   47 I                                                 XXX                                                 I
 40 TO   43 I                                                 XXX                                                 I
 36 TO   39 I                                                 XXX                                                 I
 32 TO   35 I                                                 XXX                                                 I
 28 TO   31 I                                                 XXX                                                 I
 24 TO   27 I                                                 XXX                                                 I
 20 TO   23 I                                                 XXX                                                 I
 16 TO   19 I                                                 XXX                                                 I
 12 TO   15 I                                                 XXX                                                 I
  8 TO   11 I                                                 XXX                                                 I
  4 TO    7 I                                                 XXX                                                 I
  0 TO    3 I XXX XXX XXX XXX XXX XXX XXX XXX XXX XXX XXX XXX XXX XXX XXX XXX XXX XXX XXX XXX XXX XXX XXX XXX XXX I
            +-----------------------------------------------------------------------------------------------------+
              -12 -11 -10  -9  -8  -7  -6  -5  -4  -3  -2  -1   0   1   2   3   4   5   6   7   8   9  10  11  12

            CLASS INTERVAL WIDTH =         .00002
```

```
****** SURFACE GRAPHICS SYSTEM ******                    DATE 04/11/85  TIME 16.47.46     PAGE   13

****************** SCATTER PLOT ******************

NUMBER OF OBSERVATIONS =   122

HORIZONTAL AXIS IS ORIGINAL Z VALUE
VERTICAL AXIS IS ESTIMATED Z VALUE

MINIMUM X VALUE =        -.01000
MAXIMUM X VALUE =         .10000

MINIMUM Y VALUE =        -.01000
MAXIMUM Y VALUE =         .10000

PLOT LIMITS ACROSS MAP ARE -- XMIN =        -.01000 TO XMAX =         .10000

PLOT LIMITS DOWN MAP ARE  --  YMIN =        -.01000 TO YMAX =         .10000

CORRELATION BETWEEN X AND Y =    1.00000


******** DEFINITION OF SYMBOLS ********

SYMBOL   VALUE    SYMBOL   VALUE    SYMBOL   VALUE    SYMBOL   VALUE    SYMBOL   VALUE    SYMBOL   VALUE
           0        6        6        C       12        I       18        O       24        U       30
  .        1        7        7        D       13        J       19        P       25        V       31
  2        2        8        8        E       14        K       20        Q       26        W       32
  3        3        9        9        F       15        L       21        R       27        X       33
  4        4        A       10        G       16        M       22        S       28        Y       34
  5        5        B       11        H       17        N       23        T       29        Z       35
  $      ALL VALUES GREATER THAN 35
```

```
****** SURFACE GRAPHICS SYSTEM ******              DATE 04/11/85  TIME 16.47.46     PAGE  14
```

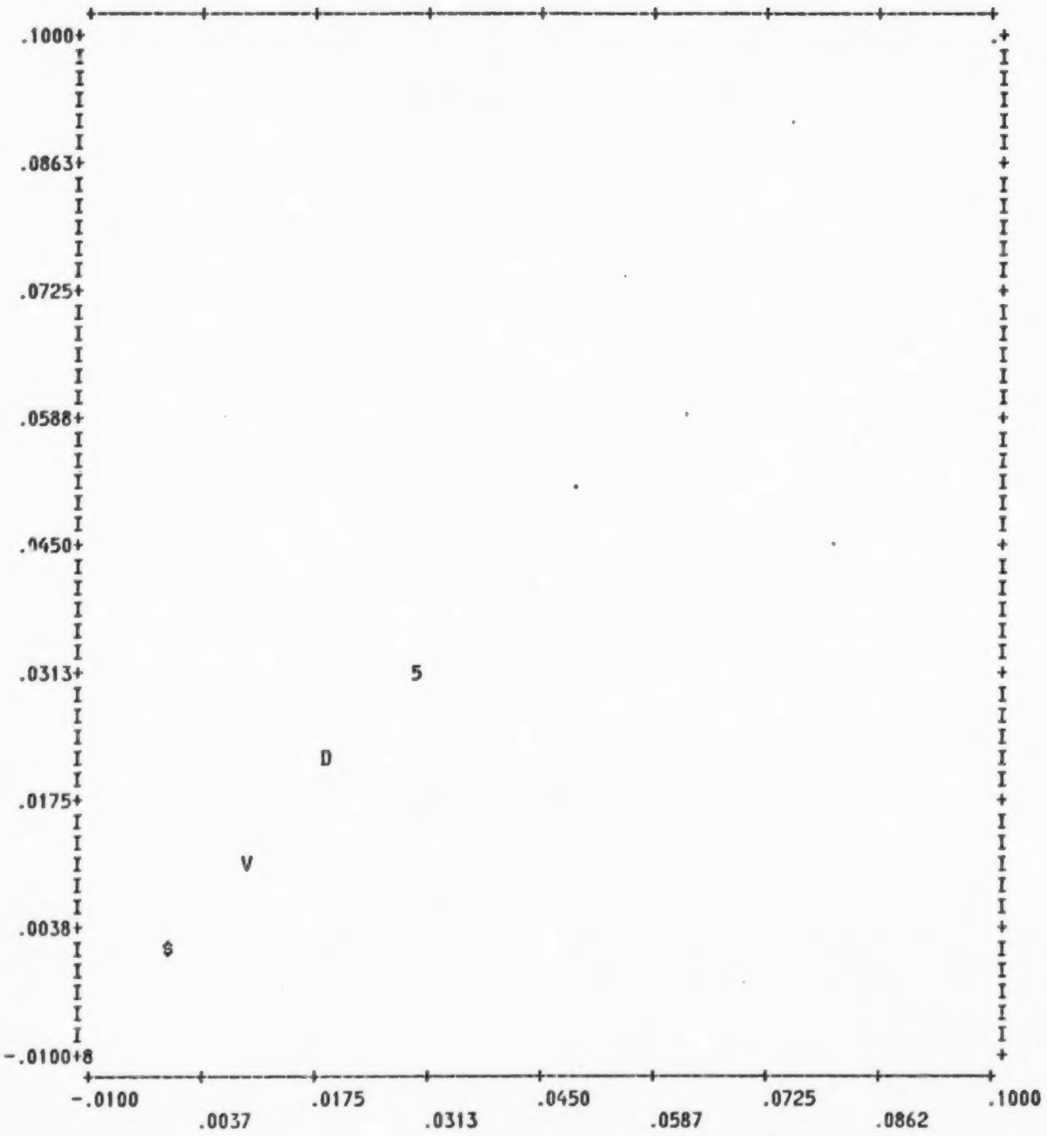

```
****** SURFACE GRAPHICS SYSTEM ******                DATE 04/11/85  TIME 16.47.46     PAGE   15

****************** SCATTER PLOT ******************

NUMBER OF OBSERVATIONS =   122

HORIZONTAL AXIS IS ORIGINAL Z VALUE
VERTICAL AXIS IS DIFFERENCE BETWEEN ORIGINAL AND ESTIMATED Z VALUE

MINIMUM X VALUE =          -.01000
MAXIMUM X VALUE =           .10000

MINIMUM Y VALUE =          -.00018
MAXIMUM Y VALUE =           .00000

PLOT LIMITS ACROSS MAP ARE -- XMIN =          -.01000 TO XMAX =          .10000

PLOT LIMITS DOWN MAP ARE  --  YMIN =          -.00018 TO YMAX =          .00000

CORRELATION BETWEEN X AND Y =      .04489


******** DEFINITION OF SYMBOLS ********

SYMBOL   VALUE    SYMBOL   VALUE    SYMBOL   VALUE    SYMBOL   VALUE    SYMBOL   VALUE    SYMBOL   VALUE
            0        6        6        C       12        I       18        O       24        U       30
  .         1        7        7        D       13        J       19        P       25        V       31
  2         2        8        8        E       14        K       20        Q       26        W       32
  3         3        9        9        F       15        L       21        R       27        X       33
  4         4        A       10        G       16        M       22        S       28        Y       34
  5         5        B       11        H       17        N       23        T       29        Z       35
  $       ALL VALUES GREATER THAN 35
```

****** SURFACE GRAPHICS SYSTEM ****** DATE 04/11/85 TIME 16.47.46 PAGE 16

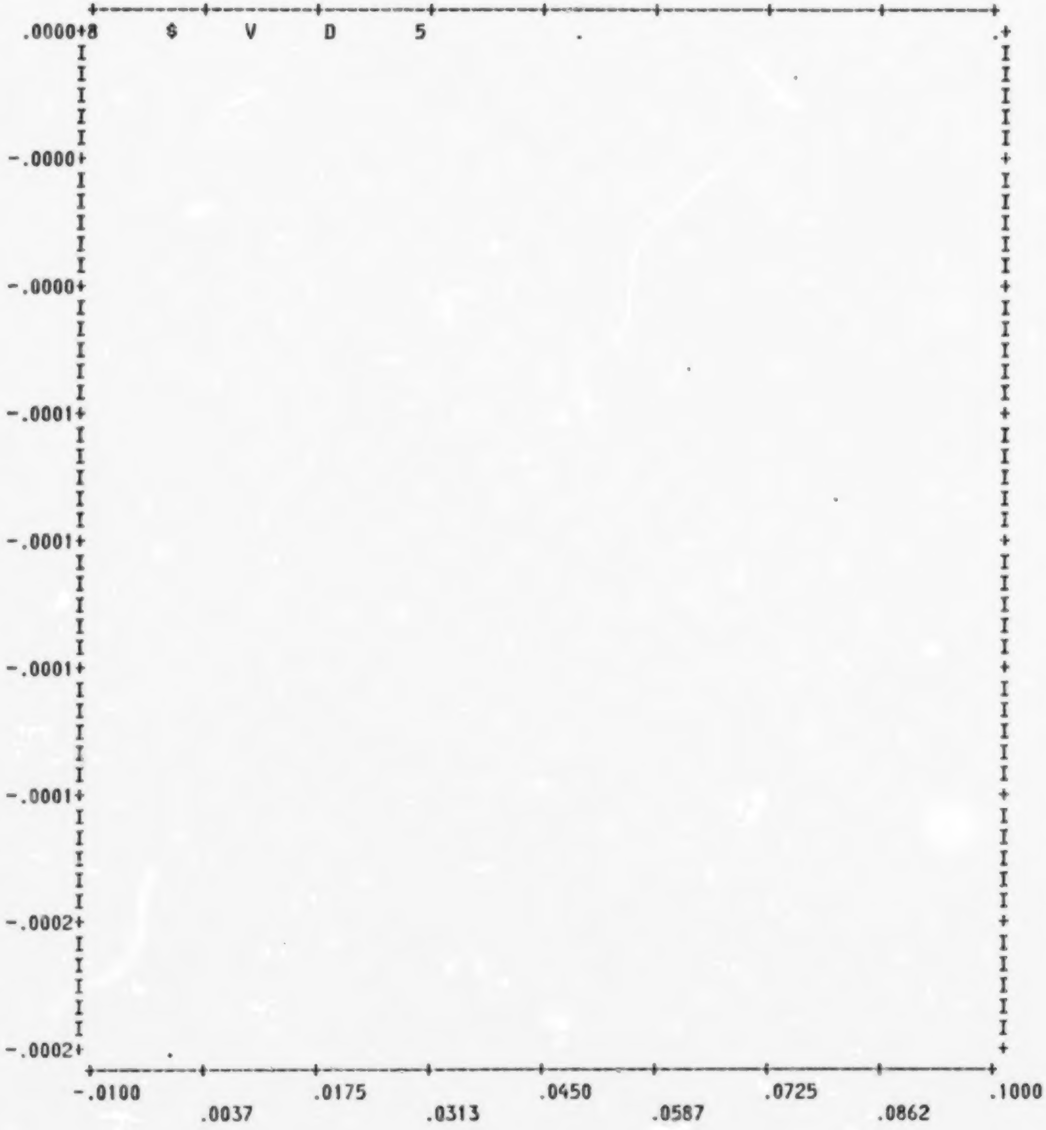

```
****** SURFACE GRAPHICS SYSTEM ******                  DATE 04/11/85  TIME 16.47.47     PAGE  17

****** ERROR ANALYSIS OF SAMPLE DATA POINTS ******

                                                                                              STANDARDIZED
 SAMPLE  IDENTIFICATION         X             Y              Z             Z-EST     DIFFERENCE    DIFFERENCE
---------------------------------------------------------------------------------------------------------------
    1          1.000000    107.300000     16.200000       .000000       .000184     -.000184    -11.000003 ***+
    2         13.000000    115.000000     10.000000       .000000       .000000      .000000       .090909
    3         14.000000    115.000000     15.000000       .000000       .000000      .000000       .090909
    4         15.000000    115.000000     20.000000       .000000       .000000      .000000       .090909
    5         16.000000    115.000000     25.000000       .000000       .000000      .000000       .090909
    7         22.000000    110.000000      5.000000       .000000       .000000      .000000       .090909
    8         23.000000    110.000000     10.000000       .000000       .000000      .000000       .090909
    9         24.000000    110.000000     15.000000       .000000       .000000      .000000       .090909
   10         25.000000    110.000000     20.000000       .020000       .020000      .000000       .090909
   11         26.000000    110.000000     25.000000       .000000       .000000      .000000       .090909
   12         27.000000    110.000000     30.000000       .000000       .000000      .000000       .090909
   13         32.000000    105.000000      5.000000       .000000       .000000      .000000       .090909
   14         33.000000    105.000000     10.000000       .010000       .010000      .000000       .090909
   15         34.000000    105.000000     15.000000       .000000       .000000      .000000       .090909
   16         35.000000    105.000000     20.000000       .010000       .010000      .000000       .090909
   17         36.000000    105.000000     25.000000       .000000       .000000      .000000       .090909
   18         37.000000    105.000000     30.000000       .000000       .000000      .000000       .090909
   19         41.000000    100.000000       .000000       .000000       .000000      .000000       .090909
   20         42.000000    100.000000      5.000000       .000000       .000000      .000000       .090909
   21         43.000000    100.000000     10.000000      -.010000      -.010000      .000000       .090909
   22         44.000000    100.000000     15.000000       .000000       .000000      .000000       .090909
   23         45.000000    100.000000     20.000000       .000000       .000000      .000000       .090909
   24         46.000000    100.000000     25.000000       .010000       .010000      .000000       .090909
   25         47.000000    100.000000     30.000000       .000000       .000000      .000000       .090909
   26         52.000000     95.000000      5.000000       .000000       .000000      .000000       .090909
   27         53.000000     95.000000     10.000000       .000000       .000000      .000000       .090909
   28         54.000000     95.000000     15.000000       .000000       .000000      .000000       .090909
   29         55.000000     95.000000     20.000000       .010000       .010000      .000000       .090909
   30         56.000000     95.000000     25.000000       .000000       .000000      .000000       .090909
   31         57.000000     95.000000     30.000000       .000000       .000000      .000000       .090909
   32         62.000000     90.000000      5.000000       .000000       .000000      .000000       .090909
   33         63.000000     90.000000     10.000000      -.010000      -.010000      .000000       .090909
   34         64.000000     90.000000     15.000000       .000000       .000000      .000000       .090909
   35         65.000000     90.000000     20.000000       .020000       .020000      .000000       .090909
   36         66.000000     90.000000     25.000000      -.010000      -.010000      .000000       .090909
   37         67.000000     90.000000     30.000000       .000000       .000000      .000000       .090909
   38         72.000000     85.000000      5.000000       .010000       .010000      .000000       .090909
   39         73.000000     85.000000     10.000000       .000000       .000000      .000000       .090909
   40         74.000000     85.000000     15.000000       .000000       .000000      .000000       .090909
   41         75.000000     85.000000     20.000000       .010000       .010000      .000000       .090909
   42         76.000000     85.000000     25.000000       .000000       .000000      .000000       .090909
   43         77.000000     85.000000     30.000000       .010000       .010000      .000000       .090909
   44         82.000000     80.000000      5.000000       .010000       .010000      .000000       .090909
   45         83.000000     80.000000     10.000000      -.010000      -.010000      .000000       .090909
   46         84.000000     80.000000     15.000000       .000000       .000000      .000000       .090909
   47         85.000000     80.000000     20.000000       .020000       .020000      .000000       .090909
   48         86.000000     80.000000     25.000000       .010000       .010000      .000000       .090909
   49         87.000000     80.000000     30.000000       .010000       .010000      .000000       .090909
   50         92.000000     75.000000      5.000000       .000000       .000000      .000000       .090909
   51         93.000000     75.000000     10.000000      -.010000      -.010000      .000000       .090909
```

```
****** SURFACE GRAPHICS SYSTEM ******                  DATE 04/11/85  TIME 16.47.48     PAGE   18

****** ERROR ANALYSIS OF SAMPLE DATA POINTS ******

                                                                                          STANDARDIZED
SAMPLE  IDENTIFICATION          X              Y              Z           Z-EST      DIFFERENCE    DIFFERENCE
-----------------------------------------------------------------------------------------------------------
  52       94.000000       75.000000      15.000000       .020000       .020000       .000000       .090909
  53       95.000000       75.000000      20.000000       .000000       .000000       .000000       .090909
  54       96.000000       75.000000      25.000000       .000000       .000000       .000000       .090909
  55       97.000000       75.000000      30.000000       .000000       .000000       .000000       .090909
  56      103.000000       70.000000      10.000000     -.010000      -.010000       .000000       .090909
  57      104.000000       70.000000      15.000000       .000000       .000000       .000000       .090909
  58      105.000000       70.000000      20.000000       .010000       .010000       .000000       .090909
  59      106.000000       70.000000      25.000000       .000000       .000000       .000000       .090909
  60      107.000000       70.000000      30.000000       .020000       .020000       .000000       .090909
  61      113.000000       65.000000      10.000000       .000000       .000000       .000000       .090909
  62      114.000000       65.000000      15.000000       .000000       .000000       .000000       .090909
  63      115.000000       65.000000      20.000000       .010000       .010000       .000000       .090909
  64      116.000000       65.000000      25.000000       .010000       .010000       .000000       .090909
  65      117.000000       65.000000      30.000000       .000000       .000000       .000000       .090909
  66      123.000000       60.000000       5.000000       .000000       .000000       .000000       .090909
  67      124.000000       60.000000      10.000000       .010000       .010000       .000000       .090909
  68      125.000000       60.000000      15.000000       .020000       .020000       .000000       .090909
  69      126.000000       60.000000      20.000000       .000000       .000000       .000000       .090909
  70      127.000000       60.000000      25.000000       .000000       .000000       .000000       .090909
  71      133.000000       55.000000      10.000000       .000000       .000000       .000000       .090909
  72      134.000000       55.000000      15.000000       .010000       .010000       .000000       .090909
  73      135.000000       55.000000      20.000000       .020000       .020000       .000000       .090909
  74      136.000000       55.000000      25.000000       .000000       .000000       .000000       .090909
  75      137.000000       55.000000      30.000000       .000000       .000000       .000000       .090909
  76      142.000000       50.000000       5.000000       .000000       .000000       .000000       .090909
  77      143.000000       50.000000      10.000000       .000000       .000000       .000000       .090909
  78      144.000000       50.000000      15.000000       .000000       .000000       .000000       .090909
  79      145.000000       50.000000      20.000000       .010000       .010000       .000000       .090909
  80      146.000000       50.000000      25.000000       .010000       .010000       .000000       .090909
  81      147.000000       50.000000      30.000000       .000000       .000000       .000000       .090909
  82      148.000000       50.000000      35.000000       .000000       .000000       .000000       .090909
  83      153.000000       45.000000      10.000000       .000000       .000000       .000000       .090909
  84      154.000000       45.000000      15.000000       .000000       .000000       .000000       .090909
  85      155.000000       45.000000      20.000000       .000000       .000000       .000000       .090909
  86      156.000000       45.000000      25.000000       .000000       .000000       .000000       .090909
  87      157.000000       45.000000      30.000000     -.010000      -.010000       .000000       .090909
  88      163.000000       40.000000      10.000000       .000000       .000000       .000000       .090909
  89      164.000000       40.000000      15.000000       .050000       .050000       .000000       .090909
  90      165.000000       40.000000      20.000000       .010000       .010000       .000000       .090909
  91      166.000000       40.000000      25.000000       .010000       .010000       .000000       .090909
  92      167.000000       40.000000      30.000000       .000000       .000000       .000000       .090909
  93      173.000000       35.000000      10.000000       .020000       .020000       .000000       .090909
  94      174.000000       35.000000      15.000000       .030000       .030000       .000000       .090909
  95      175.000000       35.000000      20.000000       .030000       .030000       .000000       .090909
  96      176.000000       35.000000      25.000000       .010000       .010000       .000000       .090909
  97      177.000000       35.000000      30.000000       .000000       .000000       .000000       .090909
  98      183.000000       30.000000      10.000000       .010000       .010000       .000000       .090909
  99      184.000000       30.000000      15.000000       .010000       .010000       .000000       .090909
 100      185.000000       30.000000      20.000000       .000000       .000000       .000000       .090909
 101      186.000000       30.000000      25.000000       .010000       .010000       .000000       .090909
```

```
****** SURFACE GRAPHICS SYSTEM ******                    DATE 04/11/85  TIME 16.47.48     PAGE   19

****** ERROR ANALYSIS OF SAMPLE DATA POINTS ******

 SAMPLE  IDENTIFICATION          X             Y             Z           Z-EST      DIFFERENCE   STANDARDIZED
                                                                                                  DIFFERENCE
----------------------------------------------------------------------------------------------------------------
  102        187.000000      30.000000     30.000000      .010000      .010000      .000000       .090909
  103        193.000000      25.000000     10.000000      .000000      .000000      .000000       .090909
  104        194.000000      25.000000     15.000000      .030000      .030000      .000000       .090909
  105        195.000000      25.000000     20.000000      .010000      .010000      .000000       .090909
  106        196.000000      25.000000     25.000000      .010000      .010000      .000000       .090909
  107        197.000000      25.000000     30.000000      .010000      .010000      .000000       .090909
  108        203.000000      20.000000     10.000000      .000000      .000000      .000000       .090909
  109        204.000000      20.000000     15.000000      .020000      .020000      .000000       .090909
  110        205.000000      20.000000     20.000000     -.010000     -.010000      .000000       .090909
  111        206.000000      20.000000     25.000000      .020000      .020000      .000000       .090909
  112        207.000000      20.000000     30.000000      .010000      .010000      .000000       .090909
  113        208.000000      20.000000     35.000000      .000000      .000000      .000000       .090909
  114        213.000000      15.000000     10.000000      .010000      .010000      .000000       .090909
  115        214.000000      15.000000     15.000000      .010000      .010000      .000000       .090909
  116        215.000000      15.000000     20.000000      .020000      .020000      .000000       .090909
  117        216.000000      15.000000     25.000000      .030000      .030000      .000000       .090909
  118        217.000000      15.000000     30.000000      .010000      .010000      .000000       .090909
  119        218.000000      15.000000     35.000000      .000000      .000000      .000000       .090909
  121        224.000000      10.000000     15.000000      .100000      .100000      .000000       .090909
  122        225.000000      10.000000     20.000000      .020000      .020000      .000000       .090909
  123        226.000000      10.000000     25.000000      .030000      .030000      .000000       .090909
  124        227.000000      10.000000     30.000000      .020000      .020000      .000000       .090909
```

```
****** SURFACE GRAPHICS SYSTEM ******              DATE 04/11/85  TIME 16.47.51     PAGE   20

****** BLANK OUT SPECIFIED AREA IN GRID MATRIX ******

THE GRID MATRIX HAS  126 COLUMNS AND    46 ROWS

THE X-MINIMUM OF GRID MATRIX IS          -5.00000000
THE X-MAXIMUM OF GRID MATRIX IS         120.00000000

THE Y-MINIMUM OF GRID MATRIX IS          -5.00000000
THE Y-MAXIMUM OF GRID MATRIX IS          40.00000000

THE Z-MINIMUM OF GRID MATRIX IS            -.01431774
THE Z-MAXIMUM OF GRID MATRIX IS             .10000000

THE GRID MATRIX HAS   449 MISSING VALUES

THE TOTAL NUMBER OF OUTLINES IS      1

THE NUMBER OF OUTLINES TO BE USED FOR BLANKING IS     1

THE Z-MINIMUM OF NEW GRID MATRIX IS            -.01135665
THE Z-MAXIMUM OF NEW GRID MATRIX IS             .10000000

THE NEW GRID MATRIX HAS  2221 MISSING VALUES
```

```
MIRAMICHI-INDIAN LAKE OUTCROP DEFORMATION                    DATE 04/11/85  TIME 16.47.58     PAGE   21

        ******** MAKE A CONTOUR MAP ********

        THE X-VALUE AT LEFT   EDGE OF GRID MATRIX IS           -5.00000000
        THE X-VALUE AT RIGHT  EDGE OF GRID MATRIX IS          120.00000000

        THE Y-VALUE AT BOTTOM EDGE OF GRID MATRIX IS           -5.00000000
        THE Y-VALUE AT TOP    EDGE OF GRID MATRIX IS           40.00000000

        THE Z-MINIMUM OF THE GRID MATRIX IS           -.01135665
        THE Z-MAXIMUM OF THE GRID MATRIX IS            .10000000

        THE GRID MATRIX HAS  126 COLUMNS AND   46 ROWS

        THE GRID MATRIX HAS  2221 MISSING VALUES

        THE X-VALUE AT LEFT   EDGE OF CONTOUR MAP IS           -5.00000000
        THE X-VALUE AT RIGHT  EDGE OF CONTOUR MAP IS          120.00000000

        THE Y-VALUE AT BOTTOM EDGE OF CONTOUR MAP IS           -5.00000000
        THE Y-VALUE AT TOP    EDGE OF CONTOUR MAP IS           40.00000000

        THE CONTOUR MAP WILL BE      49.21 INCHES WIDE BY      17.72 INCHES HIGH

        THE X-SCALE IS       2.5400 UNITS PER INCH
        THE Y-SCALE IS       2.5400 UNITS PER INCH

        ****** CONTOUR LEVELS AND ANNOTATION ******

        CONTOUR LEVELS WILL HAVE EQUAL SPACED INTERVALS

        THE REFERENCE CONTOUR LEVEL IS      -.02000

        THE INCREMENT BETWEEN EQUAL SPACED CONTOUR LEVELS IS       .00500

        THE MAXIMUM NUMBER OF CONTOUR LEVELS IS    27

        EVERY CONTOUR LEVEL WILL BE LABELED

        LABELS ON THE CONTOUR LINES WILL BE   .20 INCHES HIGH

        LABELS WILL BE PRINTED WITH  3 CHARACTER(S) TO THE RIGHT OF THE DECIMAL POINT

        LABELS WILL BE PRINTED A MINIMUM OF    19.69 INCHES APART

        EVERY    2ND CONTOUR LEVEL WILL BE DRAWN HEAVY
```

```
MIRAMICHI-INDIAN LAKE OUTCROP DEFORMATION                DATE 04/11/85  TIME 16.48.01     PAGE   22

        ****** CONTOUR PARAMETERS ******

        CONTOUR LINES WILL BE SMOOTHED BY PIECEWISE BESSEL INTERPOLATION

        DEPRESSION CONTOUR LINES WILL NOT BE ANNOTATED

        ****** BOX PARAMETERS ******

        TICK MARKS ALONG ALL EDGES OF BOX WILL BE LABELED

        THE NUMBER OF UNITS BETWEEN TICK MARKS ALONG X-AXIS IS         5.00000
        EVERY TICK MARK ALONG X-AXIS WILL BE LABLED

        THE NUMBER OF UNITS BETWEEN TICK MARKS ALONG Y-AXIS IS         5.00000
        EVERY TICK MARK ALONG Y-AXIS WILL BE LABELED

        REFERENCE VALUE FOR TICK MARKS AND LABELS ON X-AXIS IS          .00000
        REFERENCE VALUE FOR TICK MARKS AND LABELS ON Y-AXIS IS          .00000

        BOX LABELS WILL BE PRINTED WITHOUT A DECIMAL FRACTION

        LABELS AROUND BOX WILL BE      .30 INCHES HIGH
```

```
MIRAMICHI-INDIAN LAKE OUTCROP DEFORMATION                      DATE 04/11/85  TIME 16.51.27     PAGE   23
        ******** MAKE POSTING OF X-Y-Z DATA POINTS ********

        THE NUMBER OF X-Y-Z DATA POINTS IS   124

        THE X-MINIMUM OF THE X-Y-Z DATA POINTS IS          10.00000000
        THE X-MAXIMUM OF THE X-Y-Z DATA POINTS IS         115.00000000

        THE Y-MINIMUM OF THE X-Y-Z DATA POINTS IS            .00000000
        THE Y-MAXIMUM OF THE X-Y-Z DATA POINTS IS          35.00000000

        THE Z-MINIMUM OF THE X-Y-Z DATA POINTS IS           -.01000000
        THE Z-MAXIMUM OF THE X-Y-Z DATA POINTS IS            .10000000

        THE X-VALUE AT LEFT   EDGE OF POSTING IS           -5.00000000
        THE X-VALUE AT RIGHT  EDGE OF POSTING IS          120.00000000

        THE Y-VALUE AT BOTTOM EDGE OF POSTING IS           -5.00000000
        THE Y-VALUE AT TOP    EDGE OF POSTING IS           40.00000000

        THE POSTING WILL BE      49.21 INCHES WIDE BY      17.72 INCHES HIGH

        THE X-SCALE IS       2.5400 UNITS PER INCH
        THE Y-SCALE IS       2.5400 UNITS PER INCH

        ****** POST PARAMETERS ******

        POINTS WILL BE LABELED WITH IDENTIFICATION VARIABLE

        MAP SYMBOL WILL BE      .20 INCHES HIGH

        LABEL ON MAP SYMBOL WILL BE      .20 INCHES HIGH

        LABELS WILL BE PRINTED WITHOUT A DECIMAL FRACTION

        MAP SYMBOL  1 WILL BE USED FOR ALL DATA POINTS

        ****** BOX PARAMETERS ******

        TICK MARKS ALONG ALL EDGES OF BOX WILL BE LABELED

        THE NUMBER OF UNITS BETWEEN TICK MARKS ALONG X-AXIS IS         5.00000
        EVERY TICK MARK ALONG X-AXIS WILL BE LABLED

        THE NUMBER OF UNITS BETWEEN TICK MARKS ALONG Y-AXIS IS         5.00000
        EVERY TICK MARK ALONG Y-AXIS WILL BE LABELED

        REFERENCE VALUE FOR TICK MARKS AND LABELS ON X-AXIS IS          .00000
        REFERENCE VALUE FOR TICK MARKS AND LABELS ON Y-AXIS IS          .00000

        BOX LABELS WILL BE PRINTED WITHOUT A DECIMAL FRACTION

        LABELS AROUND BOX WILL BE      .30 INCHES HIGH
```